The University of Nottingham

UNITED KINGDOM · CHINA · MALAYSIA

Techno-economic and environmental assessment of CO_2 Utilisation processes for the production of Dimethyl ether and Olefins

Mohamed Abuagela Masaud Ahmed

Thesis submitted to the University of Nottingham for the degree of Doctor of Philosophy

July 2022

Acknowledgements

First and foremost, all praise and thanks are due to Allah the Almighty for all his countless blessings bestowed upon me and I emphasise all my prayers and sacrifices are for Him. The completion of this thesis would not have been possible without the help and the active support and advice I have received from the many individuals I have had the pleasure and privilege to work with.

I would like to express my special thanks and deepest appreciation to my supervisors, Dr. Ioanna Dimitriou and Dr. Jon McKechnie for their valuable support during my PhD and their immense knowledge and guidance throughout the research and thesis writing process.

I send my heartfelt thanks to my parents and siblings- Saif, Abdu, Adam and Reeman- for their constant support, love and encouragement during my study and my greatest gratitude goes towards their presence in my life.

Abstract

Decarbonising heavy industry, such as cement manufacturing, is now seen as essential to meet the climate change target of limiting global warming to 2°C since pre-industrial times. To achieve deep decarbonisation, carbon capture and storage (CCS) is required and, in areas where there is no storage capacity close by, the conversion of CO_2 to added-value products, like dimethyl ether (DME) and olefins, needs to be considered. In this study, the techno-economic performance and environmental impacts of carbon dioxide utilisation (CCU) systems are evaluated for indirect DME synthesis and methanol to olefins (MTO) using three alternative reforming routes: dry methane reforming, bi-reforming and tri-reforming. The CO_2 source is a cement manufacturing plant equipped with an oxyfuel CO_2 capture unit. The process scenarios are simulated in Aspen Plus V12 and integrated with MATLAB R2020b to allow for optimisation towards either minimising production costs or minimising environmental impact. The optimisation was completed using a simulated annealing hybrid function with pattern search and a genetic algorithm complete search. The CO_2 utilisation scenarios showed global warming potentials (GWP) ranging from 3.35 to 4.76 $tCO_2\text{-}eq{\cdot}t^{-1}$ DME and 2.74 to 4.19 $tCO_2\text{-}eq{\cdot}t^{-1}$ olefins; which is 16.34 - 41.12% and 7.51 - 86.48% lower than the conventional steam reforming process, respectively. The total production cost for the CCU scenarios ranged from \$819.32 to \$970.87 t^{-1} DME and \$1189.03 to \$1540.48 t^{-1} olefins; which is 3.24 - 22% and 11.03-43.85% higher than the conventional production process, respectively. For the MTO CCU scenarios this translates to a net loss of -\$749.65 to -\$362.97 t^{-1} olefins. Applying heat integration further reduced the GWP for the CCU scenarios to 2.2 – 3.27 $tCO_2\text{-}eq\ {\cdot}t^{-1}$ DME and 0.26 - 1.75 $tCO_2\text{-}eq{\cdot}t^{-1}$ olefins, where ADTRI-GWP displayed the lowest GWP for both the DME and MTO scenarios. This was 10.7 - 64.55% and 7.51 - 86.48% lower than the conventional steam reforming process, respectively. The total production cost was reduced to \$482.98 to 683.52 t^{-1} DME and \$857.87 to \$1083.06 t^{-1} olefins; whilst the total production cost of the conventional production process' decreased to \$417.78 t^{-1} DME and \$578.46 t^{-1} olefins. For the CCU-based scenarios, BI-OPEX displayed the lowest total production cost for both the DME and MTO scenarios. In the case of MTO production, the net profit or loss for the

CCU-based scenarios and the conventional production scenario ranged from -$288.64 to $100.85 t^{-1} olefins and $230.45 t^{-1} olefins, respectively. This was a significant improvement from the equivalent scenarios without heat integration. The cost of global warming potential reduction (CGWP) was introduced to determine the link between the difference in production cost and the GWP of CCU and conventional processes. The CGWP ranged from $93.69 to $581.23 and $156.12 to $2800.23 per tCO_2-eq for the DME CCU scenarios and MTO CCU scenarios, respectively. In both cases the production process using bi-reforming technology displayed the lowest CGWP. The effect of applying a carbon levy on natural gas (NG) used in the conventional production method was studied. For the CCU scenarios to achieve an equitable production cost to the conventional production method, a carbon levy of $94.49 to $385.13 t^{-1} NG and $160.71 to $655.32 t^{-1} NG is required for the DME CCU scenarios and MTO CCU scenarios, respectively. Overall, the results of this study indicate CCU processes utilising bi-reforming provided the highest commercial feasibility when compared to dry and tri-reforming technologies for the production of olefins and DME, whilst providing significant GWP reduction. It was also found that in order to minimise GWP, the use of adiabatic tri-reforming technology is preferred.

Table of Contents

List of Tables

List of Figures

Chapter 1 –Introduction

Term	Acronym
Greenhouse gas	GHG
Carbon capture and storage	CCS
Carbon capture and utilisation	CCU
Dimethyl ether	DME
Methanol to olefins	MTO
Life cycle assessment	LCA

1.0 Introduction

An exponential increase in greenhouse gas (GHG) over the last century has caused an unquestionable rise in global temperatures equating to around 0.84 °C above pre-industrial levels [1]. Significant issues arise due to the global warming that occurs in association to the release of GHG which may produce irreversible negative effects to the global ecosystem, as well as negative effects on the capability for society to operate due to disruption to various sectors such as agriculture, water supply and food security. The international community has considered and implemented a range of suitable policies to limit GHG emissions: promoting the use of renewable energy sources, improved regulation regarding energy efficiency and substitution of major GHG emitting fuels with alternative fuel sources with lower impacts [2]. However heavy industry processes, such as cement manufacturing, continue to emit large amount of CO_2 and other GHG emissions which will likely increase with the further industrialisation of developing countries, such as China and India.

Cement manufacturing is an emission-intensive industry generating an estimated 730kg CO_2 t^{-1} cement clinker produced [8] and accounting for approximately 5% of global CO_2 emissions [4]. Implementing emission reduction strategies, such as clinker substitution, utilising alternative fuels and optimising thermal efficiency could decrease CO_2 emissions from this industry to an estimated 540-590 kg CO_2 $tonne^{-1}$ cement clinker by 2050 [3] [4]. However, this is still significantly higher compared to the estimated 350-410 kg CO_2 t^{-1} cement clinker that is required to avoid runaway global warming [4] [5]. Therefore, it is essential that alternative solutions, such as carbon capture and storage (CCS) and carbon capture and utilisation (CCU), are implemented [6] [7].

CCS is used to reduce CO_2 emissions via an injection of the captured CO_2 underground [8] [9] [10]. Although CCS offers a significant potential to the reduction of global greenhouse gas emissions, there are technical and economic limitations for the large-scale application of CCS. Firstly, there are high energy penalties and capital expenditures associated with the capture and separation of the CO_2 from process flue gases, as well as high costs related to the transport

and storage of the CO_2. An alternative or synergistic solution is CCU. CCU allows for the offset of the costs related to the capture and transport of the CO_2 by converting the captured CO_2 to value-added products [11]. A range of viable CCU options are available, such as mineralisation, enhanced oil recovery and chemical or biological conversion to chemicals, fuels or materials [12] [13] [14].

A promising CCU option includes the production of syngas through a variety of reforming routes including dry-reforming, bi-reforming and tri-reforming [15] [16] [17]. Syngas is commonly used as an intermediate to multiple value-added products such as methanol, formaldehyde, Fischer-Tropsch fuels, dimethyl ether (DME) and olefins. DME offers a significant opportunity with a range of applications including aerosols, personal care products and chemicals, such as dimethyl sulfate and methyl acetate. DME can also be used as a diesel substitute due to the similarities in chemical properties and offers reduced NOx emissions, higher cetane numbers and significant decrease in particulate matter emission compared to diesel [18]. DME may be synthesised either directly from syngas in one step or indirectly via methanol dehydration, wherein which methanol is produced from the syngas as an intermediate [19]. Lower olefins including ethylene and propylene have significant global demand; 120 MT yr^{-1} and 180 MT yr^{-1} for propylene and ethylene respectively [20] [21]. Lower olefins may be produced through a methanol to olefins process. Due to the high global olefin demand the opportunity for CCU based olefins is substantial, in terms of the total captured CO_2 that may be incorporated. Although DME's demand as a fuel is focussed in the Asia-Pacific region, the properties of DME as a diesel substitute provides the opportunity for CCU-based DME to operate as an alternative low-carbon fuel.

This thesis aims to study the use of carbon capture and utilisation (CCU) to reduce the emissions of the cement industry and determine commercially feasible CCU options. A major factor limiting further adoption of CCU technologies is the uncertainty for investors and funding agencies including the effective reduction in GHG and long-term commercial feasibility. This uncertainty arises from the low level of maturity of many CCU pathways. Techno-economic feasibility studies are necessary to promote further progress

in CCU technologies and determine their commercial feasibility. Environmental impact studies are also essential to assess the potential reduction in GHG from the use of CCU technology. To this end, this thesis assesses and compares the techno-economic performance and global warming potential (GWP) of DME and olefins production from CO_2 utilisation processes which are based on three reforming technologies: dry methane reforming, bi-reforming and tri-reforming. The CCU scenarios are also compared with a conventional production case which is based on steam reforming. To provide a comprehensive assessment of key techno-economic and environmental indicators, process optimisation is conducted based on maximising commercial feasibility and GHG emissions reduction. This will help to identify the opportunities presented by CCU technologies in the cement industry for reducing the impact of climate change.

2.0 Research objectives

To meet the aim of the PhD the following objectives were identified:

- Objective one: Conduct preliminary screening of carbon capture technologies in the cement industry and their commercial feasibility.
    - Undertake a literature review on available carbon capture technologies including technology maturity, cost of capture and technical operations.

- Objective two: Conduct a preliminary screening of CCU technologies and their commercial feasibility.
    - Conduct a literature review on available CCU technologies and concepts.
    - Determine market demand of CCU products to ensure suitable scalability and commercial feasibility.

- Objective three: Complete a techno-economic assessment of CCU indirect dimethyl ether (DME) synthesis.

- Select suitable system boundary for conventional production and CCU scenarios studied.
- Model CCU indirect DME synthesis based on dry-, bi- and tri-reforming and conventional steam reforming.
- Optimise CCU indirect DME synthesis and conventional steam reforming scenarios towards minimising global warming potential.
- Optimise CCU indirect DME synthesis and conventional steam reforming scenarios towards minimising total production costs.
- Identify technical performance indicators for scenarios examined such as utility requirements and CO_2 conversion efficiency.
- Identify economic performance indicators such as capital costs and total production costs.
- Determine environmental impact through life cycle assessments (LCA) to provide the global warming potential for each scenario.
- Calculate cost of global warming potential reduction; comparing the incurred increase in production costs in comparison to conventional steam reforming indirect DME synthesis in relation to the amount of global warming potential reduced through substitution of product.

- Objective four: Complete a techno-economic assessment of CCU methanol to olefin (MTO) synthesis.
  - Select suitable system boundary for conventional production and CCU scenarios studied.
  - Model CCU MTO synthesis based on dry-, bi- and tri-reforming and conventional steam reforming based MTO synthesis.
  - Optimise of CCU MTO and conventional steam reforming based MTO synthesis towards minimising global warming potential.
  - Optimise CCU MTO synthesis and conventional steam reforming scenarios towards minimising total production costs.

- Identify technical performance indicators for scenarios examined such as utility requirements and CO_2 conversion efficiency.
- Identify economic performance indicators such as capital costs, total production costs and net profit or loss.
- Determine environmental impact through life cycle assessments (LCA) to provide the global warming potential for each scenario.
- Calculate cost of global warming potential reduction; comparing the incurred increase in production costs in comparison to conventional MTO synthesis in relation to the amount of global warming potential reduced through substitution of product.

- Objective five: Determine impact of policies for CCU technologies on commercial feasibility.
  - Identify current CCU policies and regulations.
  - Determine required carbon levy on natural gas and required premium pricing to achieve equal cost to conventional production.

3.0 Thesis design and structure

The chapters related to the techno-economic and environmental assessment of the CCU scenarios (Chapters 3 and 4) are undertaken in a modular approach where in which each chapter may be read as a standalone study. For each CCU pathway examined a literature review of the CCU product is provided in their respective chapters. This includes an analysis of relevant literature and an identification of current gaps in knowledge that are to be addressed by the study.

Chapter 2 provides a literature review of the cement industry and CCU technologies. In order to provide a contextual understanding of the project and the relevance and necessity of the research aim, background information on the cement manufacturing process and emission sources are supplied. This is emphasised through an outline of strategies available to reduce CO_2 in cement manufacturing and their limitations in achieving the emissions targets set for

cement production. An assessment of carbon capture technologies in literature is provided including technical and economic performance indicators and technology maturity. Furthermore, a review of relevant techno-economic assessments studies of CCU technologies is included.

Chapter 3 discusses the techno-economic and environmental assessment of DME production from CCU-based processes. An introduction to the study including relevance and related literature is given. A detailed literature review on DME is provided which includes an outline of the properties of DME and current uses. Furthermore, available DME production pathways and technologies are discussed including current conventional methods of production. The methodology employed is presented including an outline of the scenarios studied, the simulation and optimisation methodology as well as the techno-economic and environmental indicators. The techno-economic and environmental results are also provided, including material and utility usage and total production cost.

Chapter 4 follows a similar structure to Chapter 3. This chapter outlines the techno-economic and environmental assessment of olefins (e.g. ethylene, propylene) production from CCU-based processes Background information related to olefins including global demand, uses and current olefin production pathways are provided. Similarly to Chapter 3, the methodology used, results and conclusions of the study are given.

Chapter 5 provides a comparison between the two studied CCU pathways. The techno-economic and environmental indicators of the two CCU routes are compared and a study of applying policies and market assumptions are carried out.

Chapter 6 provides a summary of the main conclusions. Recommendations for future work in this area are also included in this chapter.

The Appendix contains supplementary information to the methodology and research conducted. The supplementary information for the methodology

applied in Chapter 3 and 4 including kinetic equations and parameters, and economic assumptions are provided. A summary of the MATLAB code deployed are also included.

References

[1] GISTEMP Team, "GISS Surface Temperature Analysis (GISTEMP)," NASA Goddard Institute for Space Studies, 2018. [Online]. Available: https://data.giss.nasa.gov/gistemp/. [Accessed 29 04 2018].

[2] European commison, "European strategic long-term vision for a prosperous, modern, competitive and climate neutral economy," 2018.

[3] M. Sanjuán, C. Andrade, P. Mora and A. Zaragoza, "Carbon Dioxide Uptake by Cement-Based Materials: A Spanish Case Study," *Applied Sciences,* vol. 10, no. 1, p. 339, 2020.

[4] D. Elzinga, S. Bennett, D. Best, K. Burnard, P. Cazzola, D. D'Ambrosio, J. Dulac, A. Fernandez Pales, C. Hood, M. LaFrance and e. al., Energy Technology Perspectives 2015: Mobilising Innovation to Accelerate Climate Action, Paris, France: International Energy Agency (IEA) Publications, 2015.

[5] B. Diczfalusy, M. Wrake, K. Breen, K. Burnard, K. Cheung, J. Chiavari, F. Cuenot, D. D'Ambrosio, J. Dulac, D. Elzinga, L. Fulton, A. Gawel, S. Heinen, O. Ito, H. Kaneko, A. Koerner, S. McCoy, L. Munuera, U. Remme, C. Tam and T. Trigg, Energy Technology Perspectives 2012: Pathways to a Clean Energy, Paris: International Energy Agency, 2012.

[6] Close, "Carbon Capture, Utilization and Storage.," *SETIS Magazine of the European Commission,* 2016.

[7] IEA, "Putting CO2 to Use," 2019.

[8] W. K. W. L. J. L. P. Z. R. B. A. S. T. M. P. Markewitz, *Energy Environ. Sci,* vol. 5, no. 6, pp. 7281-7305, 2012.

[9] *A Technical Basis for Carbon Dioxide Storage,* CO2 Capture Project, 2009.

[10] A. S. J. M. M. H. J. H. J. G. P. Zapp, "Overall environmental impacts of CCS technologies—A life cycle approach," *International Journal of Greenhouse Gas Control,* vol. 8, pp. 12-21, 2012.

[11] A. D. A. A. M. Aresta, "Catalysis for the valorization of exhaust carbon: from CO2 to chemicals, materials, and fuels. technological use of CO2," *Chemical reviews,* vol. 114, no. 3, pp. 1709-1742, 2014.

[12] J. B. R. W. S. K. P. S. H.H. Khoo, "Carbon capture and utilization: Preliminary life cycle CO2, energy, and cost results of potential mineral carbonation," *Energy Procedia,* vol. 4, pp. 2494-2501, 20122.

[13] W. G. S. M. P. Jaramillo, "Life Cycle Inventory of CO2 in an Enhanced Oil Recovery System," *Environmental Science and Technology,* vol. 43, no. 21, pp. 8027-8032, 2009.

[14] M. G. M. Aresta, "Life cycle analysis applied to the assessment of the environmental impact of alternative synthetic processes. The dimethylcarbonate case: part 1," *Journal of Cleaner Production,* vol. 7, no. 3, pp. 181-193, 1999.

[15] M. R. F. K. G.R. Moradi, "The effects of partial substitution of Ni by Zn in LaNiO3 perovskite catalyst for methane dry reforming," *Journal of CO2 Utilization,* vol. 6, pp. 7-11, 2014.

[16] J. P. S. S.-W. S. F. E.G. Mahoney, "The effects of Pt addition to supported Ni catalysts on dry (CO2) reforming of methane to syngas," *Journal of CO2 Utilization,* vol. 6, pp. 40-44, 2014.

[17] C. S. Y. C. C. C. T. J. S. O. U. O. H. D. S. D.-V. N. V. S. Z. A. Hamidah Abdullah, "Recent Advances in CO2 Bi-Reforming of Methane for Hydrogen and Syngas Productions," in *Chemo-Biological Systems for CO2 Utilization,* CRC Press, 2020, p. 27.

[18] U. H. J. W. M. W. J. e. a. Lee, "Well-to-Wheels Emissions of Greenhouse Gases and Air Pollutants of Dimethyl Ether from Natural Gas and Renewable Feedstocks in Comparison with Petroleum Gasoline and Diesel in the United States and Europe,," *SAE International Journal of Fuels and Lubricants,* vol. 9, no. 3, pp. 546-557, 2016.

[19] F. F.Yaripour, "Catalytic dehydration of methanol to dimethyl ether (DME) over solid-acid catalysts," *Catalysis Communications,* vol. 6, no. 2, pp. 147-152, 2005.

[20] Statista, "Propylene demand and capacity worldwide from 2015 to 2022," [Online]. Available: https://www.statista.com/statistics/1246689/propylene-demand-capacity-forecast-worldwide/. [Accessed 21 24 2022].

[21] Statista, "Ethylene demand and production capacity worldwide from 2015 to 2022," [Online]. Available: https://www.statista.com/statistics/1246694/ethylene-demand-capacity-forecast-worldwide/. [Accessed 24 Jan 2022].

[22] T. A. A. R. J. a. M. G. Boden, "Global, Regional,and National Fossil-Fuel CO2 Emissions, Carbon Dioxide Information Analysis Centre," Global, Regional,and National Fossil-Fuel CO2 Emissions, Carbon Dioxide Information Analysis Centre, [Online]. Available: https://cdiac.ess-dive.lbl.gov/trends/emis/meth_reg.html. [Accessed 22 May 2019].

[23] M. S. C. C. &. M. S. Imbabi, " Trends and developments in green cement and concrete technology," *International Journal of Sustainable Built Environment,* vol. 1, no. 2, pp. 194-216, 2012.

[24] S. Deolalkar, Designing Green cement plants, Elsevier, 2016.

[25] Cement Sustainability Initiative, "CO2 and Energy Accounting and Reporting Standard for the," 2005.

Chapter 2 – Literature Review

Term	Acronym
Carbon capture and storage	CCS
Monoethanolamine	MEA
Enhanced oil recovery	EOR
Carbon capture and utilisation	CCU
Adenosine diphosphate	ADP
Nicotinamide adenine dinucleotide phosphate	NADPH
Trios phosphate	TP
Technology Readiness Level	TRL
Dimethyl carbonate	DMC
Diphenyl carbonate	DPC
Dimethyl ether	DME
Formic acid	FA
Reverse water gas shift reaction	RWGS
Fischer-Tropsch	FT
Life-cycle assessment	LCA
Techno-economic assessments	TEA
Discounted pay pack period	DPBP
Operating expenditure	OPEX
Capital expenditure	CAPEX

1.0 Cement background

Cement is a material utilised as a binder. The cement when blended with water forms a plastic state capable of binding aggregates, either granulated or large solid bodies. This is through a process in which the cement paste first increases in rigidity, considered as the setting phase, followed by a progressive increase of the compressive strength of the cement paste, which is considered as the hardening phase [1]. Cement can be organic or inorganic depending on its composition, however the practical implementation of organic cements such as polymer-based cements are limited compared to inorganic cements due to the increased costs associated with their use [2].

Cement may be split into sub-classifications of hydraulic or non-hydraulic depending on its capability to harden under the presence of water.

In the case of hydraulic cements, the plastic paste formed by mixing the cement with water hardens via a hydration chemical reaction. The anhydrous cement and water, through the hydration reaction, form a hydrate formed with limited solubility in water. This provides a product that retains strength even underwater [3]. The general practise in naming of hydraulic cements is dependent on the prevailing hydraulic mineral used in its production for example Portland cement, sulphate cement and phosphate cement [1].

Non-hydraulic cements in contrast does not set in the presence of water but hardens via a reaction with carbon dioxide.

Although organic and non-hydraulic cements have their relevant uses dependant on conditions and requirements, most cements used in modern practise worldwide is Portland cement or a blended cement based upon Portland cement, or alternatively masonry-cement (Portland cement mixed with a plasticising material such as hydrated lime) [4].

1.1 Cement manufacturing process

Cement manufacturing is a complex and multi-step process with a range of specialised industry specific equipment. Although certain steps may differ in operation depending on the type of cement produced and the cement plant type, the production process for cement tend to operate through the following steps [5]:

1. Raw material extraction via quarrying: Calcareous deposits as well as other required materials, such as alumina and silica, are extracted via heavy duty machinery from quarries which tend to be located in close proximity to the cement plant.

2. Crushing: The extracted material is crushed to diameters of around 10 cm and transported to the cement plant.

3. Preparation of raw meal: Prior to use the raw materials undergoes a pre-homogenisation phase in which the raw materials are mixed to provide the required chemical composition. The homogenised material is further milled into a fine powder, "raw meal".

4. Preheating: The raw meal is preheated to temperatures greater than 900°C via a series of vertical cyclones prior to entering the kiln. This process allows a recovery of thermal energy and a decrease of utility usage.

5. Precalcining: During the production of cement calcination occurs where the primary raw material of calcium carbonate ($CaCO_3$), as limestone, is converted into calcium oxide, CaO, which is a major component of cement clinker. This process occurs in a precalciner, which is a combustion chamber below the preheater and above the kiln.

6. Clinker production: The meal exiting the precalciner is fed into the kiln. The kiln operates at temperature of around 1400 °C, where the kiln continuously rotates, and the extreme temperatures' initiates a range of chemical and physical reaction converting the meal into clinker. Further calcination occurs in the kiln.

7. Cooling and storage: The clinker exiting the kiln is of extreme temperatures which requires cooling. Rapid cooling of the clinker to around 100 ℃ is completed over a grate cooler (alternative coolers includes the planetary and rotary cooler), operating via a flow of combustion air over the clinker. Intermediate clinker storage is present to either transport the produced clinker for sale or transfer for further processing in the processing plant.

8. Blending: In order to convert the produced clinker into a final cement product, firstly the clinker is mixed with the required minerals. Other materials such as slag, fly ash and other materials maybe incorporated, replacing some of the clinker requirements to produce blended cements.

9. Grinding: The blended product is ground to a fine powder to produce the final cement product. Although historically ball mills have been used for this process, modern plants incorporate vertical mills or roller presses due the improved energy efficiency.

10. Storage: The final cement product is stored in cement silos prior to packaging or loading and transport to the end user.

1.2 Cement industry emissions

The main use for cement industrially is as a binder for construction materials. The cement is mixed with stone and sand to produce concrete. In terms of total volume, concrete is the most used manufactured product worldwide after clean water [6]. Concrete offers multiple benefits in terms of its physical properties; high strength, durability, fire resistance and resilience to flooding and corrosion; as well as it's the relatively cheap costs. Therefore, the employment of concrete is evident in nearly all infrastructures constructed; from homes and schools to industrial chemical and energy plants, therefore proving concrete and in consequence cement to be an essential and invaluable requirement for modern development.

In 2018 global cement production was estimated to be around 4.1 billion tonnes an increase of ~24% from 2010. Further to this the demand, production is expected to further increase by around 12%-23% by 2050. The main aspects fuelling the increased

demands is the continuous increase of global population in tandem with increased urbanisation globally, causing infrastructure requirements to continuously rise[1].

The cement industry represents a major emission intensive industry on the global scale emitting an estimated 750kg of CO_2 per tonne of cement produced [7], providing ~5% of global anthropogenic CO_2 emissions [8]. Therefore, cement plants are considered large industrial CO_2 sources providing significantly high CO_2 flue gas compositions that tend to range from 14-33%, in comparison to alternate CO_2 sources such as coal-fired power plants with 12-14% CO_2 flue gas composition and gas fired plants with 4%, cement plants offer a significant prospect for carbon capture [9].

1.2.1 Sources of emissions

The main sources of carbon dioxide released in the process of cement production is during the process of calcination and the process of combustion.

1.2.1.1 CO_2 emissions from calcination

The chemical decomposition that occurs during the process of converting limestone to lime is a major emitter of CO_2 during the cement production process. It is noted that the quantity of CO_2 emitted during the production is directly proportional to the lime content of the clinker. During the process of calcination each mole of $CaCO_3$ heated forms one mole of CaO and one mole of CO_2 [10],

$$CaCO_3 + heat \rightarrow CaO + CO_2.$$

1.2.1.2 Combustion of fuel

A major source of total released CO_2 is present in the process of combustion of fuel in the kiln and calciner in the clinkerisation process. During the production of cement clinker, heat is required to calcinate the raw feed in the precalciner, and in the kiln where sintering occurs at temperatures of around 1400°C in order to produce cement clinker. To produce the required temperatures, the combustion of fuel is required [10].

[1] A significant 26% increase in global population is expected by 2050 from 2018 (~7.6 billion to 9.6 billion) with an estimated urban population of 6.5 billion [176].

The total CO_2 released is dependent on the total amount of fuel combusted and the amount of carbon present within it. Although this is heavily dependent on the fuel employed, the fuel that tends to be used in practise is coal.

1.2.2 Strategies to reduce CO_2 emissions

In terms of the total CO_2 emissions produced during the production of cement around 60-70% of the total emissions is emitted during the calcination process, and approximately 65% of all combusted fuel is used to heat the kilns [11].

The main strategies implemented to reduce CO_2 emissions in the cement industry includes:

- Increase energy efficiency.
- Alternative fuels.
- Reduction of cement to clinker ratio.
- Use of alternative raw materials.

1.2.2.1 Increase energy efficiency

Incorporating state-of-the-art technologies in cement production offers significant opportunities for the reduction of the total energy requirements of cement production. Currently, the use of dry-process kilns (dry powdered raw material feed) is increasing in comparison to the traditional wet-process kilns (raw material slurry feed), due to the decrease in energy requirements as the moisture content of the raw material entered in to the kiln is lower than in the wet-process kilns, where energy demand is reduced due to the removal of the need to evaporate water [12]. An increase of dry-process kilns to 79% of clinker production in 2016 in comparison to 61% in 1990 is seen [13].

Operation of a cement plant with a dry-process kiln and the incorporation of a precalciner, multichannel burners and multistage cyclone preheaters are regarded to be the state-of-art technology present for clinker production, providing energy requirements of around 3 GJ/t clinker[2] [14]. Multichannel burners provide the opportunity for an optimal combustion environment to arise, whilst the use of a

[2] Current best available technology offers 3 GJ/t clinker (a dry process kiln with the presence of a precalciner and a six-stage cyclone preheater and multichannel burner).

precalciner and multistage heater allows for a heat integration dynamic to occur, allowing for the excess recovered process heat to be utilised in precalcination and drying of the raw meal. However, use of state-of-the-art technology in practise remains limited with only an estimated 64% of global cement plants using a precalciner [15].

Other than incorporating these technologies to new builds, capabilities to retrofit precalciners and multistage preheaters to current dry-process kilns are available. Alternative strategies for increasing energy efficiency includes improving combustion conditions in the kiln by operating with the usage of oxygen-enriched air or the addition of mineralisers to raw material, reducing the temperature at which clinker formation occurs and reducing viscosity. Further to this, the usage of grate coolers instead of rotary or planetary coolers provides the opportunity for a greater reduction in energy needs (estimated to be around 0.1-0.3 GJ/t clinker in combination with a precalciner) [14].

Electricity usage in the production of cement is present in a range of steps including the grinding of the cement and raw material and during the clinker production stage. The main two state-of-the-art technologies for grinding are high-pressure grinding rolls and vertical roller mills which offer significant electricity saving opportunities in comparison to ball mills[3]. The electricity usage for cement grinding is heavily dependent on the final product requirements; the greater the strength class of the final cement product, the greater fineness is required for the final cement powder [5].Implementing best available technology in the process of grinding and milling offers around 14% decrease in electricity consumption per tonne of cement produced [14].

Although a majority of the cement plants built in the past decade have been of up-to date technology, there remains significant wet and semi-dry cement production plants worldwide, especially in developing countries. It is predicted that the increased use of state-of-the-art technology, either through retrofit of current cement plants or new builds, will provide an estimated reduction of global average thermal energy

[3] High pressure grinding rolls offers a predicted 50% reduction in electricity consumption and vertical roller mills offers up to 70% reduction in electricity requirements compared to ball mills.

requirement from 3.5 GJ/t clinker (2014) to 3.1 GJ/ t clinker by 2050 allowing an estimated 12% reduction of direct CO_2 emissions from global cement production [14].

1.2.2.2 Alternative fuels

Current cement plants tend to use coal as the source for thermal energy, accounting for around 70% of the total global cement production thermal energy needs[4] [16]. Options for alternative fuels includes the use of waste product derivations such as biomass, industrial waste oils and solvents, tyres and plastic waste [17]. The reduction in the net CO_2 emissions using waste as a fuel is dependent on the biogenic fractions and the carbon content, in comparison to fossil fuels. However, using alternative fuels does not necessarily cause a direct reduction in emitted process CO_2 emissions, and in some cases, there is an increase. However, if the full life-cycle of the alternative fuel is considered a net decrease in CO_2 emissions may be seen, such as in the case of the use of biomass.

Multiple considerations are needed when integrating and selecting alternative fuels. Properties such as the calorific value, the moisture content and compositions of the alternative fuels are relevant, and they tend to have varying properties depending on the source. An example to this issue is municipal solid wastes which will differ in calorific value from source to source and in certain cases, even from the same source variations will occur. Further to this the combustion of certain alternative fuels produces exhausts with a range of undesirable fractions such as chlorine, dioxins and heavy metals. Therefore, it is imperative that a continuous supply source is identified with predictable properties that do not affect the process negatively [18].

The financial aspect of alternative fuel usage is also of importance, with the continuous increase of fossil fuel prices, deployment of alternative fuels tends to offer positive economic implications. Even with the capital costs requirements in the addition of pre-treatment, storage and handling needs for the alternative fuel of choice,

[4] Further to this oil and natural gas provides arounds 24% of the global thermal energy demand for the cement industry and biomass and other waste products provide around 5% of the total global energy demand for the cement industry.

this tends to be offset heavily by the decreased operational costs when compared to the use of coal [19].

A major positive is the fact that cement kilns offer great flexibility in the capability to implement alternative fuels with minimal modifications. However generally the minimum calorific value needs for the kiln tends to far exceed what is available from typical alternative fuel options[5] [20], therefore alternative fuels tend to be fired alongside fossil fuels. It is predicted that greater widespread use of alternative fuels can reduce around 24% of the direct CO_2 emissions globally from cement production by 2050 [14].

1.2.2.3 Reduction of clinker to cement ratio

Cement is composed of a blend of clinker and other additives. The composition on a mass basis of clinker in the cement is the clinker to cement ratio. A decrease in clinker to cement ratio produces a decrease in energy demand and direct process CO_2 emissions due to the calcination process. Other additives to the cement that may be used as a replacement to cement clinker includes fly ash, slag and pozzolanas [21].

A major aspect to consider in the production of blended cement is the fact that the blended cement produced must meet the regulations present in the region of production. Blended cement when compared to *Ordinary Portland Cement* may produce significantly differing practical feasibility in terms of durability and mechanical properties [1]. However, the major limitation for implementation of blended cement is the availability of the blending materials. Current global average clinker to cement ratio is determined to be around 0.65 however with a predicted continued increase in blended cement use a significant 7-8% reduction in clinker to cement ratio is estimated by 2050 [16].

1.2.2.4 Use of alternative raw materials

CO_2 emission reduction opportunity during the calcination process in cement production is limited. CO_2 emissions in cement production may be reduced by the

[5] Generally a minimum calorific value for the fuel to fire the kiln is 20 GJ/t fuel whilst a majority of the alternatives tend to be between 10-18 GJ/t [19].

incorporation of alternative materials that are waste such as recycled concrete and fibre concretes [19]. This reduces the CO_2 emissions as the decarbonation and associated CO_2 emissions has already been levied to the original process to create them. Limitations to implementing this is similar to the use of blended cements in terms of the availability of the raw material and ensuring final product quality.

1.2.3 Limitations to strategies of CO_2 emission reduction in cement production

Although the methods outlined offers opportunities in reducing the total global CO_2 emission from the cement industry, limitations are present in their implementation as is outlined in Table 2.1 below.

Table 2.1. Limitations to current conventional strategies for CO_2 emission reduction in the cement industry.

Increasing Energy efficiency*	• Heavy capital investment with careful planning and engineering.
Alternative fuels	• Availability of alternative fuel that provides the needs of the cement plant. • Regulations and legislations present regarding waste usage. • Possibility of harmful emissions from alternative fuel source use.
Clinker to cement ratio	• Availability of blending materials. • Market acceptance of blended cements; assumption in some cases that they are significantly inferior to Ordinary Portland Cement. • Standard specifications and regulations [a].
Alternative raw material	• Availability of raw material. • Technical expertise to produce suitable product with the use of the alternative raw material in cement production.

* Limited scope for further improvements in terms of reducing fuel consumption further, unless method to conduct clinkerisation at lower temperature found.

[a] As determined by local authorities, unless revision occurs.

It is of importance to realise in certain cases there is an interdependence between the varying CO_2 reduction strategies that may be incorporated. Although certain strategies may produce a net reduction in the direct and indirect CO_2 emissions related to cement production this may be offset by a reduction in the energy efficiency of the process. An example to this is the increased energy demand requirements that may occur in the reduction of clinker to cement ratio as per the fact that the substituted materials require calcination. Other examples include the use of alternative fuels, which tend to have a lower calorific content, increasing thermal energy demand for clinker production.

Even with current efforts to reduce CO_2 emissions from cement production, it is likely CO_2 emission will only be reduced from ~700 kg t^{-1} clinker to around 560 kg t^{-1} clinker by 2020 [19]. Although this a relevant and positive reduction of around 20%, this remains to be in excess of the targets set by the IPCC of 525kg CO_2 emissions t^{-1} clinker [22].

Therefore, it is of importance to investigate other strategies to reduce CO_2 emissions. An alternate strategy to reducing the total direct and indirect CO_2 emissions produced from the process is capturing the emitted CO_2 and minimising the amount that enters the atmosphere and becomes what is regarded as anthropogenic CO_2. Strategies that enable this includes carbon capture and storage (CCS), for which the waste CO_2 emitted from a point source is captured and transported to a storage site, in which the CO_2 is deposited at this site in a manner that will not allow it to enter the atmosphere. An alternate strategy to CCS is CCU for which as an alternative, the captured CO_2 is utilised as a raw material to produce a value-added product or service.

Prior to concluding the storage or utilisation aspect of CCS or CCU, there is a requirement for a capture of the CO_2. This capture process is conducted through a separation and purification of the CO_2 from the other constituents of the industrial waste gas stream.

2.0 Carbon Capture

Carbon capture in a cement production plant may occur via three type of carbon capture schemes:

1. Pre-combustion capture
2. Oxyfuel combustion
3. Post combustion

2.1 Pre-combustion capture

Pre-combustion capture is completed by treatment of a fossil fuel source via a gasification or reformation process. The fossil fuel source enters a gasifier with the addition of oxygen or air combined with steam, a syngas is produced through means of shift reactors. The CO that is constituent of the syngas is converted to CO_2, producing a stream of H_2 and CO_2. The CO_2 is separated from the stream and the H_2 is used as a fuel [23].

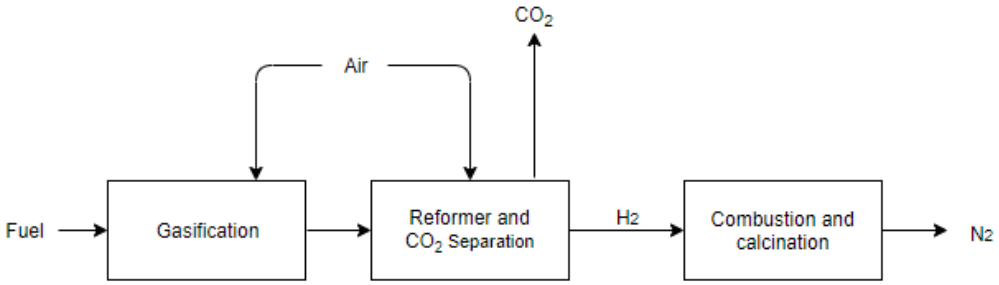

Figure 2.1. Block diagram for pre-combustion capture of CO_2 from a cement plant.

In terms of the cement production process, pre combustion capture offers limited value in terms of CO_2 capture as its potential is limited to only being capable of capturing CO_2 due to fuel combustion[6]. Therefore around 65% of the total CO_2 emissions that occurs due to the calcination process will remain unaffected. Moreover to this, pre-combustion technology presents further complications in terms of the significant change to the cement production process and kiln operation as per the fact adapting operations to utilising H_2 offers greater complexity[7]. Therefore, the use of pre-combustion technology is regarded as unfeasible.

[6] Energy and fuel combustion emissions in the cement production process represents only around 35% of the total cement production process CO_2 emissions.

[7] The explosive nature of H_2 makes it unusable by itself therefore there is a need for dilution with N_2 or steam prior to use.

2.2 Oxyfuel combustion

Oxyfuel capture systems use an oxygen rich environment- by limiting nitrogen concentrations- to combust the fuel. The oxygen rich environment is a product of a mix of CO_2 from a recycle stream from the flue gas and pure oxygen. The product of this combustion is a CO_2 gas stream composed from CO_2, H_2O and any other impurities that may be present. This final CO_2 gas stream in comparison to the initial non-capture system flue gas is of greater purity, increasing capture and compression efficiency.

The Oxyfuel capture systems equipment requirements includes[8] [24]:

- An air separation unit to extract oxygen from air prior to feeding it to the precalciner or kiln.
- A flue gas recirculation system, to circulate the CO_2 rich flue gas back to the precalciner or kiln; the main benefit of recirculating the flue gas is maintenance of a suitable flame temperature and combustion temperature control.
- A gas treatment plant to dry, purify and compress the captured CO_2 in preparation for transport.
- Oxygen requirements may be satisfied on-site via a cryogenic air separator.

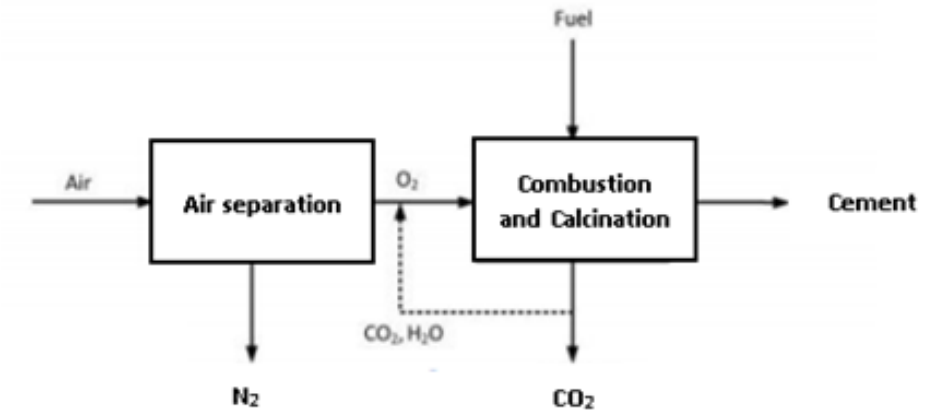

Figure 2.2. Block diagram for oxyfuel capture of CO_2 from a cement plant.

The oxyfuel capture system causes a modification in the operation of the cement production process. The system causes a change in the preheating requirements and kiln gas enthalpy, which may increase energy efficiency due to the oxygen rich environment. However, the air separation units and flue gas circulation systems tend

[8] It is of importance that sealing is implemented at all points including the kiln inlets and outlets.

to be extremely power intensive, incurring increases in energy and operating costs of approximately 45% [14].

Alternative oxy-fuel capture system operations are present, either partial oxy-fuel or full oxyfuel, depending on if it is applied in the precalciner only or also the kiln respectively. Partial oxy-fuel combustion produces CO_2 capture rates that are 55-75% whilst full oxy-fuel implementation allows CO_2 capture rates of 90-99% [25] [26] [15] [14].

2.3 Post combustion capture technologies

Post combustion capture in the cement industry operates by separating the generated CO_2 from the flue gases that have been generated due to fuel combustion or due to the calcination process. Due to the end-of-pipe technology aspect of most post combustion capture technologies it offers the ability for ease of retrofit to plants with minimal effect on plant operations. However, energy efficiency will decrease due to the increased energy demands related to the operation of the carbon capture system. Figure 2.3 provides a simplified block diagram for post combustion capture technology.

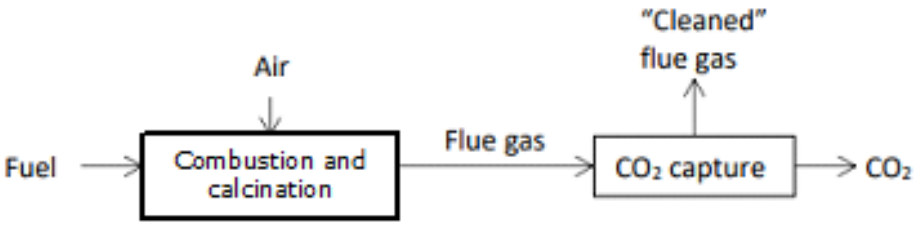

Figure 2.3. Block diagram for post combustion capture of CO_2 from a cement plant.

Post combustion capture technologies operate via a physical or chemical process to facilitate CO_2 extraction. Technologies available for the cement industry includes:

a) Chemical Absorption

The process of chemical absorption uses a liquid adsorbent. The flue gas for which CO_2 is to be extracted from is contacted onto the liquid adsorbent. The CO_2 saturated

sorbent is transferred to a stripping column in order to release the adsorbed CO_2 via means of heat and pressure reduction.

The main chemical sorbent implemented commercially are amine solvents mainly monoethanolamine (MEA). An example includes the Flour Daniel FG process which has been incorporated to over 23 plants worldwide, providing a capacity to treat up to around 320 tonnes of CO_2 daily [27]. Even with the prevalence of extensive experience and research regarding chemical absorptions there remains a high energy demand especially during the stripping phase of the process. This is because the partial pressure of the CO_2 that is present in the processed flue gases are generally low.

Although amine solvents have a high capacity for CO_2 adsorption, implementing these types of solvents produce high operating costs due to solvent losses[9] from evaporation, high solvent regeneration energy costs and corrosiveness. Therefore, alternative solvents for chemical absorption carbon capture systems have been researched and developed. An example to this is ionic liquids which in contrast to amine solvents provides greater capacities for CO_2 absorption, low corrosiveness and low vapour pressures. This also includes the benefit of reduced energy demands such as [bmim][Ac] ionic liquid , for which when compared to MEA use in carbon capture; a 16% reduction in energy requirements is seen [28]. Other promising alternatives to amine solvents includes piperazine[10], ammonia-based solvents and potassium carbonate sorbents [29] [30].

During the process of cement production only around 60% of the total heat provided and supplied is used in the calcination and clinker production phase. The excess heat has limited potential for recovery, and it is predicted that only around 15% of this may be recovered for use [15]. Therefore, a majority of the heat required for the chemical absorption capture system will need to be supplied either via steam or combined heat and power.

[9] Other losses occur due to degradation because of oxygen and other impurities such as SO_x and NO_x.

[10] Estimated 25-35% reduction in energy requirements compared to MEA (4 MJ/t CO_2 for MEA use vs 2.5 MJ/t CO_2).

b) Membrane separation

Membranes are materials that own the property of selective gas permeation through the material. In the presences of a pressure differential across the membrane, a flow of gas through the membrane is promoted allowing the membrane to act as a filter to produce a CO_2 rich permeate.

Although membranes do not have energy requirements in terms of regeneration, they have significant sensitivity to contaminants and high temperatures. Current strategies for membrane separation capture systems being explored is the use of membrane-assisted CO_2 liquefaction, via a combination of a single membrane unit for bulk separation and a CO_2 liquefaction train. These operate with a waste stream recycle that is mixed with the membrane system feed [31].

c) Mineralisation

The flue gas may be treated with a basic solution to produce minerals. A benefit to this system is the fact that the produced minerals offer two options of either sale as a valuable product or alternatively stored. An example to this is the Skymine process where in which the electrolysis of salt and water is used to produce chlorine, hydrogen and a sodium hydroxide solution [32]. The sodium hydroxide produced is reacted with the CO_2 present in the flue gas waste stream to produce sodium carbonate of high purity that has the capability for sale. Other benefits of this process are the extraction of other acidic components of the flue gas.

d) Adsorption

Adsorption follows a similar process to absorption, a solid layer and charcoal sieve is used to strip the CO_2 from the flue gas that is passed through, whilst allowing the rest of the gas to pass through. The fully loaded saturated solid layer is then replaced with a clean adsorption layer and the fully loaded layer is regenerated to remove the adsorbed CO_2.

e) Calcium looping

Calcium looping operates through a calcium oxide-based sorbent and the carbonation-calcination cycle that occurs due to the presence of an equilibrium between calcium carbonate, CO_2 and calcium oxide[11] [33],

$$CaCO_3 \rightleftharpoons CaO + CO_2,$$

and the variability in this equilibrium depending on the temperature and pressure [34].

The initial step is the carbonation step of the cycle where the CO_2 from the flue gas reacts with CaO as a sorbent to produce $CaCO_3$. This occurs in a fluidised bed combustor at temperatures of 650-850°C via an exothermic reaction[12]. The reverse calcination step of the cycle regenerates the CaO sorbent to produce a CO_2 rich gas stream. This occurs in a calcinator operating at temperatures of around 950°C [35].

With continuous use reduction and deterioration of sorbent occurs, therefore small amounts of fresh $CaCO_3$ needs to be added into the system to maintain sorbent activity. Positives of the calcium looping capture system is the fact that the purge for the deactivated CaO may be used as a substitute for raw materials in the clinker production process. This provides considerable saving in fuel requirements and consequently a reduction of CO_2 emissions[13].

2.4 Hybrid capture systems

Hybrid capture systems operate via the combination of the varying categories of capture methods in order to deliver improvements in energy efficiencies. An enhancement of the effectiveness of one technology is gained by producing optimal operational modes by the coupling with an alternate capture technology.

A feasible hybrid capture system may include a combination of an oxyfuel capture system with a post combustion capture system. The advantage of this combination

[11] Calcium oxide in the form of lime.
[12] Alternatively this carbonation step may occur in a carbonator located in the flue gas.
[13] This is due to reduced fuel use and a reduction of CO_2 emitted due to the calcination of $CaCO_3$ as some of the $CaCO_3$ in the raw meal is substituted with CaO as a raw material, therefore there will be less decomposition that will generate CO_2, and less heat required for calcination.

produces higher CO_2 concentrations in the flue gas due to the presence of oxygen enrichment and a lower dilution rate, due to nitrogen presence, this also in turn reduces the flowrates of the flue gas. This allows a reduction in the required post-combustion capture system size and energy requirements, as the sorbent needs in these systems decrease in higher CO_2 concentrations. Also, it may allow technologies such as membrane capture systems, which require high CO_2 concentrations, to be feasible, especially in relation to the fact that the energy requirements associated with their use tend to be significantly lower.

The main hybrid capture technology explored in relation to implementation in the cement industry is an oxy-fuel capture system combined with calcium looping. This is completed via the use of a circulating fluidised bed precalciner and a calcium looping system, where in which the calciner portion of the calcium looping system operates under oxy-combustion conditions [36].

2.5 Novel Technologies

Alternative strategies include direct separation. This process requires a re-engineering of the calciner with a specially designed steel vessel in order to indirectly heat the raw meal [37]. This allows pure CO_2 to be captured from what is released due to the calcination process. This is done because the exhaust gases of the process are kept separate. A benefit of this system is that energy costs[14] and capital cost requirements in comparison to other capture technologies are reduced. Although this does not allow the capture of all CO_2 emissions related to cement production, in combination with other capture technologies which are capable of capturing fuel usage related CO_2 emissions, a high total CO_2 capture rate may be achieved.

2.6 Technology limitations for carbon capture technology in cement manufacturing

Ironically the incorporation of a carbon capture system to a cement plant increases CO_2 emissions due to the energy penalty incurred due to their operation, and in turn an increase in fuel usage which produces indirect CO_2 emissions. This also influences the economics of the process in terms of capital and operating cost requirements

[14] Majority of energy costs due to heat losses in equipment and compression and transport of captured CO_2.

incurred, not only due to the increased fuel consumption but in some cases, the significant down time required to retrofit the plant with the necessary infrastructure or repurchase of equipment. Further to this certain carbon capture systems change the inherent process of cement production, which may affect the quality of the final product. Therefore, an element of importance in regard to carbon capture technologies is the complexity of the system and the modification requirements for installation when deployed in a retrofit capacity.

The main issues present for each technology in relation to what incurs the increased complexity and costs is outlined in Table 2.1

Table 2.1. Technological considerations required for the implementation of a carbon capture system to a cement plant *[38] [24] [39]*.

	Oxyfuel		Post combustion capture			Alternative
	Oxyfuel	**Partial Oxyfuel**	**Chemical Absorption**	**Membrane**	**Calcium looping**	**Direct capture**
Mode of operation	Combustion in oxygen enriched air produces CO_2 rich exhaust (Applied in kiln and precalciner).	Combustion in oxygen enriched air produces CO_2 rich exhaust (Applied in precalciner only).	Flue gas is passed through and contacted with solvent that absorbs CO_2. CO_2 released from solvent by heat in successive vessel.	Membrane used for selective gas capture to increase flue gas CO_2 concentrations.	CO_2 captured via a carbonation-calcination cycle.	Direct capture of CO_2 from calcination process, via separation of exhaust flows and calcination process products.
Modification to plant required[a]	Modification of clinker cooler and kiln burner and calciner.	Modification of calciner and installation of preheater.	Minimal and minor modifications including extra fans in preheater.	No modifications required.	Modification of calciner and/or kiln in order to integrate calcium looping system. Possible integration of calcium looping waste product for plant raw material.	Modification of calciner.
Effects on product	May produce variations in product quality[b].	No effect.	No effect.	No effect	May have effect on clinker quality[b].	Unknown.
Energy penalty sources	High energy requirements for separating air into constituent elements in air separation unit.		Low partial pressure of CO_2. Solvent losses and high energy requirements for regenerations.		Energy requirements related to regeneration that occurs via carbonation process.	Heat losses through equipment.
Other issues			Equipment corrosion. Emissions related to solvent degradation. High solvent cost	Sensitivity to minor components in flue gas to membrane performance. High costs and electricity demand for compression equipment.		

[a] Does not include additional equipment requirements, only modification required to a conventional cement plant.

[b] Although no changes seen when examined on a lab scale, due to the nature of the processes there may be an effect on a commercial scale.

An important factor for the selection and implementation of a carbon capture system either in a retrofit capacity or a new build includes the economics of the plant, the maturity and complexity of the technology to be incorporated and the actual capabilities of the capture system to capture CO_2.

However, the factor of greatest importance in terms of carbon capture implementation is the economics. This includes the initial investment requirements in terms of the capital cost, which is heavily dependent on funding and budgeting restrictions of the relevant parties. Further to this the operating costs and economic policies associated with the capture of the CO_2 such as carbon tax or tax credits, need to be factored.

Another important factor is the technical specifications of the systems, in terms of estimated CO_2 capture rates. It can be assumed that the greater the capture rate the more effective the technology, however this is not always the case as this only accounts for direct process related CO_2 emissions. In general, in order to capture and process the CO_2, significant energy requirements are incurred, in terms of electricity and heating, which dependent on the source of electricity and heating may produce significant indirect CO_2 emissions that offsets the reduction in anthropogenic emissions captured. Therefore, it is of greater importance to identify the actual CO_2 avoided and further to this the equivalent specific CO_2 avoided.

Table 2.2 below provides a brief summary of key technical and economic elements in relation to prominent and promising carbon capture technologies that may be implemented in the cement industry.

Table 2.2.Carbon capture technologies for the cement industry: technology comparison.

	Oxyfuel		Post combustion capture				Alternative
	Oxyfuel [25] [26] [40]	**Partial Oxyfuel** [15]	**Amine Absorption** [25] [40]	**Chilled Ammonia** [25] [40]	**Membrane-assisted CO_2 liquefaction** [25] [40]	**Calcium looping** [25] [26] [40]	**Hybrid**
Estimated capture rate	90%*	65%	95%[c]	90%	90%	94%	95%
Estimated CO_2 avoided	82%	56%	64%	78%	78%	90%	89%
Capital cost of New build $ (Retrofit)	332 M for 1 Mtpa (128 M)	275 M for 1 Mtpa (85 M)	290 M for 1 Mtpa (75 M)	366M for 1 Mtpa (154 M)	466 M for 1 Mtpa (255 M)	431 M for 1 Mtpa (214 M)	451 M for 1 Mtpa (234 M)
TRL	4	6[a]	6[d]	4	4	6	4
	Lab-scale tests	1.3-2 tph pilot plant	Mobile capture unit using amine-based sorbent from 2013-2016	Lab scale tests	Lab scale tests	200 kW pilot plant	Lab scale tests
Benchmark costs[y] ($/ tCO_2)	42.4	53.7	80.2	66.2	83.5	52.4	58.6
Clinker cost[y] ($/ tclinker)	93	87.9	107.4	104.9	120	105.8	110.3
Equivalent specific CO_2 avoided[z] (tCO_2/tclinker)	719	402	558	640	687	797	1205

*Up to 95% seen in pilot plant, in some models 100% achieved.

[a] Further progress unlikely due to lack of commercial feasibility.

[a] Actual reduction in direct emissions estimated to be around 64%.

[y] Including capital cost requirements.

[z] The equivalent specific CO_2 avoided and estimated CO_2 avoided accounts for all indirect and direct emissions. They provide a greater indication to the overall reduction in CO_2 emissions due to the addition of the capture system.

Alternative factors to what is provided in Table 2.2 that require significant consideration for the retrofit of carbon capture systems to cement plants is the time

associated with the shutdown of the plant in order to implement the change, the current and required plant footprint, the management of the required fuel and steam and the suitability of local power grid for increased load.

The time required to implement the retrofit of a capture system is of importance as the shutdown costs may incur significant losses that will cause further negative implications in regard to the costs associated with the capture system. This is mainly, not only because of the loss of production, but also due to the significant fixed costs cement plant tend to have, where in which an estimated 40% of total operation costs are related to fixed costs, for example a 1Mtpa clinker plant tends to have significant fixed costs of $3 M per month [38]. The shutdown time will be determined by the type of system implemented, for example an end-of-pipe technology will produce significantly decreased shutdown time requirements, as the new capture system may be pre-constructed and then connected to the exhaust of the cement plant.

In regard to space, there needs to be multiple considerations including if there is sufficient space to accommodate the new capture units, either for the additional units required or a modification or replacement of current units [41]. Other considerations are the availability of space in proximity to the exhaust sources, namely the preheater and kiln in the cement plant, as it is preferable that it is close in order to allow for minimal losses to occur and minimise piping and pumping requirements. Dependant on the mode of transport for the captured CO_2, an availability of an intermediate storage facility is of great importance [41].

Contingent on the employed capture system, the water supply and treatment and electricity and stream supply need to be suitable, as in some cases a significant increase in fuel supply is required, therefore suitable storage and handling facilities for the fuel is needed [41].

3.0 Carbon capture and storage (CCS)

CCS technologies decrease anthropogenic CO_2 via the capture and storage of the CO_2. CCS is concluded via four steps: the initial capture of the CO_2, the compression of the CO_2 into either a liquid or dense gas, the transportation of the CO_2 from the capture

location to the storage location and the segregation of the captured CO_2 from the atmosphere. CCS as a means of CO_2 emissions reductions is expected to provide a 20% reduction in CO_2 emissions over the next century [42].

Transportation of the captured CO_2 may be done via pipelines systems that have been used for natural gas and oil. The captured CO_2 may be either injected directly into geological formations or alternatively transformed into a mineral carbonate form and stored. Although the process of inserting CO_2 into geological formations has been conducted extensively for a variety of purposes, including enhanced oil recovery (EOR), the concept of a commercial CCS system remains limited. Options for CO_2 storage may be split into two categories:

a) Geological storage: CO_2 is injected into a porous sedimentary formation at depths that exceed around 1km, either under supercritical conditions or in the form of a compressed liquid and gas. In order to allow the permanent sequestering of the CO_2 injected a range of trapping mechanisms are present dependent on the formation type. These include the trapping of the CO_2 under an impermeable caprock formation or a dissolution or absorption of the CO_2 with in situ formation fluid or organic matter. Options for geological formations includes the use of depleted oil and gas reservoirs, saline formations and coal formations [43].

b) Ocean storage: Captured CO_2 may be stored on the deep seafloor at depths that are greater than around 3500m. The captured CO_2 may be either injected directly into the deep ocean or through the fertilisation of the ocean with nutrients that promote CO_2 to be drawn down from the atmosphere [44].

It is noted that CO_2 utilisation opportunities are present that may also be regarded as CCS technologies including EOR and coal-bed methane recovery and mineral carbonation.

Limitations to CCS options remain, including the risk of leakages through various pathways including through natural faults and fractures or manmade wells or diffusion through caprock, decreasing the effectiveness of the CCS process as well as causing a risk on the local geology and ecosystem. This is further coupled with the high costs

that tends to be associated with the process, especially due to the capture process. In order to allow an offset on the economic issues associated with the implementation of carbon capture and CCS, CCU technologies may be employed.

4.0 Carbon capture and utilisation (CCU) technologies

The main goal of CCU technologies is to integrate the captured CO_2 as a raw material into a range of industrial production processes, either directly or succeeding a chemical transformation. This will produce a twofold benefit, the production of valuable products and the emulation of a natural carbon cycle or at least a partway closing of the industrial carbon cycle. Other beneficial outcomes of CCU technologies are the potential to reduce resource consumption, creating an extension of resource lifetime.

4.1 Carbon dioxide

The main limitation of CCU technologies is the stability of CO_2[15] as a molecule, causing it to be considered as inert. Therefore, CO_2 is present at the bottom of the potential well, and since it represents the greatest oxidation state of carbon it remains as the lowest energy state for all binary neutral species containing carbon. Therefore, it is essential that for CO_2 to participate in chemical reactions and create products of higher energetic value, with a decrease from the initial +4 oxidation state of CO_2, significant energy expenditure is required. Alternatively due to the electron deficiency of the carbon atom an affinity to nucleophiles and electrophilic aromatic directing groups is created. This allows CO_2 to be considered as an anhydrous carbonic acid capable of reacting with basic compounds with favourable energetics. This is done via an exothermic process to produce carbonates, where CO_2 is integrated with its full moiety into the compound. The free energies of formation for C1 molecules are outlined in Table 2.1.

Table 2.1.Free energies of formation for C1 molecules

Species	C Formal Oxidation State	ΔG_f (kJ mol^{-1})
$CH_{4(g)}$	−4	−50.75
$CH_3OH_{(l)}$	−2	−166.1

[15] CO_2 has a $\Delta G°_f$ of −396 kJ/mol.

Species	C Formal Oxidation State	ΔG_f (kJ mol^{-1})
C	0	0
$HCOOH_{(l)}$	+2	−345.09
$CO_{(g)}$	+2	−137.15
$CO_{2(g)}$	+4	−394.01

This allows the reactions relevant to CO_2 to be split into two main categories [45]:

a) Low energy processes

Processes where the carbon atom in CO_2 maintains it's +4 oxidation state or is lowered by a maximum of 1 unit. In most of these cases the whole CO_2 moiety is attached to the other reactant. In order to complete this process CO_2 is reacted with electron-rich molecules[16] under mild conditions. Products of these reactions includes urea, polyols, carboxylates and linear esters.

b) High energy processes

Processes where the carbon atom in CO_2 decreases in oxidation state by at least two units below its initial +4 oxidation state: examples to these forms includes HCOOH, CO, H_2C, CH_3OH, CH_4 and other similar compounds. In order to complete this process energy input is required and concluded via range of manifestations: electrons (electrochemical reduction), hydrogen (hydrogenation), metals (reaction with group 1 metals), and radiation (breakdown of CO_2 molecule into CO and ½ O_2 at a high energy).

Therefore in order to enable the chemical transformation of CO_2, two strategies may be employed: an input of energy or the use of a highly reactive chemical species.

Regarding the use of energy in order to provide the requirements for overcoming the thermodynamic needs, it needs to be considered that this may produce significant

[16] Example of electron rich molecules includes H_2O,olefins,diens and alkynes.

reduction in savings in terms of the environmental benefits gained due to CCU implementations or mitigate it completely. Thus, it is essential that a suitable chemical catalyst is employed when considering the development of a feasible CCU technology. This will aid the process to be of greater energy efficiency. Consequently, research and advancements of catalysis tends to be a pivotal aspect of CCU technologies.

4.2 CO_2 Conversion pathways

A range of conversions pathways may be employed depending on the source of the required energy to conduct the reaction:

1. Thermocatalytic: where thermal energy is provided to allow the reaction to occur in the presence of a catalyst.
2. Electrochemical: where in which energy is provided in the form of electrons; mainly occurring in an electrochemical cell.
3. Photochemical: where in which solar energy is used to provide thermal or electrical energy.
4. Biochemical: where in which a living organism or an enzyme is used to produce the CO_2-based product.

4.2.1 Thermocatalytic

In terms of CCU technologies the main options include: the direct hydrogenation of CO_2 to the required fuel product or the reduction of the CO_2 to carbon monoxide followed by conversion to fuel. For both options, in order to conduct these reactions a reducing agent is needed to allow for CO_2 activation, usually in the form of gaseous hydrogen.

4.2.1.1 Direct thermocatalytic processes

The main challenge in the direct thermocatalytic synthesis of fuels from CO_2 is the identification of a suitable catalyst to convert CO_2 to a valuable product, with low enough kinetic requirements and minimal energy requirements. The main factors that need to be examined is commercial feasibility of the catalysts in terms of costs and the capability for the catalyst to reduce energy demands to a level that allows the process to aid in emission reduction, whilst providing suitable yields. The products that may

be produced via the direct hydrogenation of CO_2 includes methane, methanol and formic acid and may employ a homogenous and heterogeneous catalysts.

4.2.1.2 Indirect thermocatalytic processes

The alternative two-step process for CO_2 to fuel conversion is done by an initial hydrogenation of CO_2 to carbon monoxide through a conversion of H_2O and CO_2 to syngas[17]. This is advantageous as it is significantly easier to convert the CO_2 to CO and H_2O to H_2 than it is to produce fuels by the direct CO_2 hydrogenation processes. The secondary step usually follows a conventional fuel production method that incorporates syngas as part of its production process such as the Fischer-Tröpsch technologies that converts syngas to liquid fuels,

$$(2n+1)\ H_2 + n\ CO \rightarrow C_nH_{2n+2} + n\ H_2O.$$

4.2.2 Electrochemical Reduction

A multitude of laboratory and pilot scale studies regarding the electrochemical reduction of CO_2 have been conducted and demonstrated the capability to produce a range of products proceeding via a range of pathways[18]. Products that may be produced vary in state, including gaseous products such as carbon monoxide, methane and ethylene or liquid products such as formic acid, methanol, ethanol and propanol. Table 2.2 outlines the seven key CO_2 electrochemical reduction products and their corresponding electrochemical half-cell reactions.

Table 2.2.Electrochemical half-cell reactions for CO_2 *[46] [47] [48]*.

Half-Cell rlectrochemical reactions	Potential (V vs SHE)
$CO_{2(g)} + 2H^+ + 2e^- \leftrightarrow CO_{2(g)} + H_2O_{(l)}$	-0.106
$CO_{2(g)} + 2H^+ + 2e^- \leftrightarrow HCOOH_{(l)}$	-0.25
$CO_{2(g)} + 6H^+ + 6e^- \leftrightarrow CH_3OH_{(l)} + H_2O_{(l)}$	0.016
$CO_{2(g)} + 8H^+ + 8e^- \leftrightarrow CH_{4(g)} + 2H_2O_{(l)}$	0.169
$2CO_{2(g)} + 12H^+ + 12e^- \leftrightarrow C_2H_{4(g)} + 4H_2O_{(l)}$	0.065

[17] Syngas is a H_2/CO Mixture.

[18] The electrochemical reduction of CO_2 has been found to proceed via a range of reduction pathways from two-,four-,six-,eight-,twelve- and eighteen- reduction pathways.

$$2CO_{2(g)} + 12H^+ + 12e^- \leftrightarrow C_2H_5OH_{(l)} + 3H_2O_{(l)} \quad 0.085$$

$$3CO_{2(g)} + 18H^+ + 18e^- \leftrightarrow C_3H_7OH_{(l)} + 5H_2O_{(l)} \quad 0.095$$

$$2H^+ + 2e^- \leftrightarrow H_{2(g)} \quad 0.000$$

For the electrochemical reduction process the product is reliant on varying the selectivity of the process via a range of factors including the selected electro catalyst, the applied potential, the solvent and the pH of electrolytes present. Although the process of electrochemical reduction of CO_2 offers multiple benefits -including the capabilities to operate the systems at ambient pressures and temperatures; the simple and modular nature of the technology that allows ease of scale-up - a range of limitations for the process remains. The electrochemical reduction of CO_2 on most electrodes requires large overvoltage's which cause decreased conversion rates, mainly due to the competing hydrogen evolution that may occur[19].

The process of the electrochemical reduction of CO_2 is completed via an input of electricity to an electrolyser that consists of an anode, a cathode and an electrolyte which provides the medium to allow the movement of charge between the electrodes. The applied potential produces and drives CO_2 reduction kinetics to occur at the cathode whilst water oxidation occurs at the anode.

The electric potential supplied produces molecular oxygen, protons and electrons at the anode:

$$H_2O \rightarrow \frac{1}{2}O_2 + 2H^+.$$

The electrons produced flows to the cathode, where they may combine with protons during movement through the cathodic and anodic compartment separator of the electrochemical cell. This produces hydrogen or in the case of CO_2 a reduction product as is outlined in Table 2.2.

The pH provides significant effects on the distribution of CO_2 and other forms of oxidised carbon, where in which an increased pH causes decreased CO_2 concentration.

[19] It is to be noted that if the CO_2 reduction occurs in an aqueous environment, a hydrogen evolution reaction occurs in tandem which is undesirable as it is in competition with the desired CO_2 reduction reaction and generally occurs favourably. This is due to the fact that the redox potentials are similar in aqueous electrolytes [175].

This is due to the conversion of CO_2 into HCO_3^- and CO_3^{2-} through the reaction with hydroxyl anions.

Theoretically the CO_2 reduction process occurs by the formation of a carbon dioxide radical anion intermediate, however there is a lack of conclusiveness to this theory, as per the alternate views on the possibilities for CO_2 molecule presence in aqueous solutions systems. However, this proves as a suitable explanation to the high over potential requirements. As there is a necessity for a high potential to conduct a single electron reduction of CO_2 into a carbon dioxide anion radical, occurring via the reorganisation of the initial linear molecule into a bent anion radical [49]:

$$CO_2 + e^- \rightarrow CO_2^{\cdot -}.$$

The formation of this intermediate is the main cause of significant over potential requirements and in most cases regarded as the rate determining step. The CO_2^- radical anion may in turn be reduced further to form ·COOH via a pronation of an oxygen molecule, where further reduction occurs into CO followed by release from the electrode surface. Alternative pathways for the radical anion intermediate include a reduction to HCOO· via a pronation of the carbon atom in the presence of high over potentials[20]. The $HCOO^-$ is then further reduced to form formate, $HCOO^-$. Due to this a majority of CO_2 electrochemical reduction processes either yield CO or formate as a product. However in some cases the formed CO may be further reduced to other hydrocarbon products, hypothesised to be through a combination of H addition, C-O bond scission and C-C bond coupling [50].

Current research on electrochemical reduction of CO_2 evaluates a range of homogeneous and heterogonous catalysts in order to maximise CO_2 reduction whilst minimising the competing proton reduction processes, through the increase of electron transfer and improvement of the chemical kinetics of the required reduction process. This includes increasing knowledge on electrode selection and how this may impact production rates and process stability in terms of chemical and thermal stability.

[20] The protons that are present in the electrolyte and the carbon dioxide molecules compete for the electrons present, for which there is a greater preference for proton reduction for a majority of compounds over CO2 reduction in aqueous electrolytes unless high over potentials are present.

Requirements for suitable electrode selection and electrocatalysts ideally produces a match for the redox potential of the electron transfer with the required chemical reaction, in order to produce reduced overvoltage requirements[21].

4.2.3 Photochemical

Photochemical reduction exploits solar energy[22] in order to reduce the CO_2 using the energy of the incident light. This may be introduced either thermally with the focus of the light on to a high temperature reactor or with the use of catalysts, homogeneously or heterogeneously, in a solution or solid semiconductor, allowing the light to be absorbed and the creation of electrical energy. Research has mainly focused on semiconductor catalysts as favourable electron transfer kinetics occurs with their use.

The synthesis of chemical and fuels from a CO_2 raw material using a semiconductor catalyst operates under the irradiation of light to start a photocatalytic process. Semiconductor materials used as a photocatalyst form band gaps composed of the energy region that is present in between an empty conduction band and an occupied valence band [51].

When exposed to light radiation electrons are excited, allowing a migration of these electrons from the fully occupied valence band at a specific energy level to a higher energy level empty conduction band. This produces several holes in the valence band equitable to the number of migrating electrons [52]. If the energy of the photon absorbed is greater than or equal to that of the band gaps, an electron pair and hole is formed per absorbed photon[23],

$$\text{Photocatalyst} \rightarrow h\nu\ e^- + h^+.$$

Alternatively, the charge carrier may recombine at the surface or in the bulk prior to react with any adsorbed species, causing it to release energy as heat or light,

[21] Electrode performance is dependent on the efficiency of the interactions that occur between ionic, electronic and gas phases. The region for which these three phases co-exist forms a reaction site that is regarded as the triple phase boundary. It is noted that the larger this area the greater the electrode efficiency.
[22] Although solar light is the main source alternate light sources may be used.
[23] A presentation for the formation of electron–hole pairs where e^-, hν and h^+ represents the conduction band electron, photon energy and hole in the valence band, respectively.

$$e^- + h^+ \rightarrow \text{heat}.$$

The occurrence of recombination is counterproductive as it produces losses in free charge carriers and in turn a loss of energy due to the energy release. The dominance of either the recombination process or adsorptions depends mainly on the relative ratio between released electron lifetime and recombination rate, which is reliant on a range of structural properties and factors such as surface properties, dimensions and crystallinity [53].

After the electrons migrate to the required surface adsorption onto an active surface occurs, followed by a surface redox reaction through an electrochemical process. This happens because the excited electrons and formed holes are capable of driving and promoting differing half reactions: the electrons allows for the reduction of CO_2 whilst the holes oxidise water to molecular water [54].

The reduction potential for the excited electrons is equal to the energy level of the conduction band, whilst the energy level of the valence band denotes to the oxidation capabilities of the holes formed. This in turn concludes the ability for the semiconductor to complete oxidations or reductions. Further to this the redox potential of the absorbed species, as well as the energy of the band gap, provides the probability and rate of charge transfer for the electrons and holes. Therefore, for an electron to be donated to a vacant hole, the redox potential of a donor needs to be above that of the valence band whilst the acceptor needs to be below that of the conduction band. Furthermore the band gap of the semiconductor needs to be sufficiently large in order to accommodate the large over potential requirements for CO_2 reduction, whilst not being overly large in order to maximise utilisation of the solar spectrum. An example includes TiO_2 which features a band gap of 3.2ev [55], limiting its photon absorption capabilities to the ultraviolet domain[24] [56].

[24] The ultraviolet domain accounts for less than 5% of the total solar spectrum.

Although significant progression to the photochemical reduction of CO_2 has occurred, major limitations for commercial feasibility is present especially in terms of the efficiency of the process. Current photochemical systems incorporate excessively large energy requirements relative to the quantity of CO_2 reduced, also a majority of current systems requires expensive and rare noble metals in order to conduct the process.

4.2.4 Biological pathway

The use of the natural capabilities for microorganisms to automatically capture and convert CO_2 into useful chemical products and fuels proves a major avenue for CCU. These biological pathways may occur via two routes, either via photosynthesis or in a non-photosynthetic approach.

4.2.4.1 Photosynthetic approach

Photosynthesis is the process in which a biological system, in the presence of sunlight, converts CO_2 and water into carbohydrate molecules, therefore it can be regarded that these biological systems derive their energy from the reduction of CO_2,

$$6CO_2 + 6H_2O \xrightarrow{Photosynthesis} C_6H_{12}O_6 + 6O_2.$$

The energy produced from this process drives the carbon fixation[25] pathways which may occur via six autotrophic carbon fixation pathways and for most systems through oxygen-based photosynthesis.

Oxygen-based photosynthesis occurs via the utilisation of chlorophyll over two steps [57]:

1. Water disassociation

Water is regarded as an electron donor and is disassociated into electrons, protons and free oxygen molecule,

[25] Carbon fixation is the process in which carbon monoxide is converted to other organic compounds via a biological organism.

$$2H_2O \rightarrow 4e^- + 4H^+ + O_2.$$

This is done using the energy harnessed from the sunlight to allow for the oxidation of water to oxygen as well as the production of adenosine triphosphate (ATP) from adenosine diphosphate (ADP) and inorganic phosphate (P_i) ,

$$ADP + P_i \rightleftharpoons ATP + H_2O$$

and the reduction of nicotinamide adenine dinucleotide phosphate ($NADP^+$),

$$NADP^+ + 2e^- + 2H^+ \rightleftharpoons NADPH + H^+,$$

to produce NADPH to be used as an electron source.

2. Carbon fixation

The ATP and NADPH is consumed to allow for the conversion of carbon dioxide into sugars, for example trios phosphate (TP),

$$3CO_2 + 6NADPH + 6H^+ + 9ATP + 5H_2O \rightarrow TP + 6NADP^+ + 9ADP + 8P_i.$$[26]

For example, for the production of formaldehyde, the carbon fixation process can be summarised to

$$CO_2 + 4e^- + 4H^+ \rightarrow CH_2O + H_2O.$$

A major benefit of the use of these biological systems is the flexibility of these systems regarding feedstock requirements and environment, also biological systems tend to be able to operate at low CO_2 concentrations and in the presence of impurities that may be present in common industrial exhaust. However, it remains that photosynthesis is inefficient, considering it is estimated on average only 3-6% of total solar radiation is incorporated [58]. Nonetheless it may be regarded that the greater

[26] The formula for inorganic phosphate (P_i) is $HOPO_3^{2-} + 2H^+$. Formulas for triose and TP are $C_2H_3O_2$-CH_2OH and $C_2H_3O_2$-$CH_2OPO_3^{2-} + 2H^+$

the size of the biological system, the greater the energy needs for structure maintenance and growth, therefore smaller biological systems are more suitable to allow improved photosynthetic efficiencies. Research on biological photosynthetic CCU is focussed mainly on algae. Algae refers to any prokaryotic (cyanobacteria) or eukaryotic (green algae) microorganism that allows for cultivation [59]. The main product for these biological pathways is algal biofuel, however other chemicals may be produced[27]. Proteins are also produced that may be incorporated into human and animal consumption.

Regarding the low photosynthesis efficiency, current strategies researched and developed includes the design and development of current bioreactors by maximising light exposure over a large volume or surface area. Algae tend to have a limited rate of carbon dioxide fixation and conversion, therefore as a result algal cultivation is extremely land and water intensive in order to improve the CO_2 fixation rate[28]. To allow for this on a commercial scale open ponds are the main option as a photobioreactor.

It is noted that although a range of target fuels and chemical products may be produced from current naturally occurring cyanobacteria, manipulations of the genetic materials of these organisms may allow alternative target molecules to be produced. It is of importance that significant knowledge to the capabilities for inserting desired genetic material via gene integrations without impeding on essential cell functions is present. Other than genetic engineering of cyanobacteria, metabolic engineering is required as well to increase production rates. Regarding the genetic manipulation of green algae, knowledge in this area is lower than that of what is present for bacteria due to challenges including difficult genome insertion and gene silencing. Nonetheless genetic modification for green algae has been conducted in order to increase the photosynthetic efficiency and optimisation of carbon uptake and incorporation [60].

4.2.4.2 Non-photosynthetic approach

[27] These chemicals include a variety of food additives, commodities, and specialized chemicals.
[28] Theoretically, to capture all CO_2 from a 10 kiloton/day power plant a 25-37 acres of cultivation is required [107] .

Non-photosynthetic biological pathways use autotrophic organism to consume carbon monoxide, hydrogen and carbon dioxide to produce a range of carbon molecule-based products. An advantage of non-photosynthetic synthesis over photosynthetic processes is the greater diversity in reaction pathways and growth rates. Furthermore, greater efficiencies may be achieved as the bottleneck of photosynthesis efficiency is avoided. Non-photosynthetic systems provides greater productivity and capacity for continuous cultivation.

Multiple non-photosynthetic pathways are present including:

1. Light independent CO_2 fixation

Chemolithotrophs such as acetogens can develop their energy needs via a combination of the oxidation of reduced inorganic compounds and CO_2, to allow light-independent CO_2 fixation to occur [61]. This is advantageous as issues related to production using photosynthesis are eliminated such as cell shading. However, there may be greater complexity in terms of the cultivation process, as per the fact that two inputs are required instead of only one.

2. Two-stage integrated

An alternative approach to producing a specific target chemical is the use of the carbon provided from acetogon CO_2 fixation. As an example, it has been demonstrated that the acetogen Moorella theromacetica converts aerobically CO_2 into acetic acid, this is followed by a second stage where in which the acetic acid is further converted into lipids via the use of Yarrowia lipolytica [62]. As certain products may not be produced anaerobically, a two-stage bioreactor process coupling the non-photosynthetic fixation of CO_2 with an acetate-dependent production, aerobic products may be produced.

3. Bioelectrochemical process

An avenue of great value is the implementation of artificial photosynthesis in which a similar setup to electrochemical reduction of CO_2 is deployed, where electron generation occurs at the anode and microorganisms at the cathode conduct the

reduction of CO_2 under anaerobic conditions. This is done to avoid oxygen reduction and the depletion of electrons, furthermore this avoids the production of toxic by-products such as H_2O_2 [63].

Alternative methods are present dependent on the means of electron transfer, either direct electron transfer from electrode to microorganism or indirect electron transfer via electron donors. The direct electron transfer approach requires a reversal to the function of the electrotrophs of the microorganism[29], to instead drive electrons into the cell [63]. This allows a linking of the reduction process that occurs intercellular with a supply of extracellular electrons, therefore promoting biosynthetic pathways that are capable of producing valuable fuels and chemicals through electricity. In terms of the indirect electron transfer route, options for electron donors includes a variety of suitably electrochemically synthesised electron donors including H_2 and formate[30]. Electron donors such as H_2 and formate provides advantages in terms of their low redox potential and the capability to provide favourable thermodynamics for the reduction of CO_2.

4.3 Factors affecting the viability of CCU technologies

The commercial feasibility of CCU technologies are affected by a range of factors including:

a) The technology maturity: Prior to a CCU technology becoming viable, sufficient maturity of the technology is required. This may be addressed via a range of tools that may start from an initial theoretical or lab scale demonstration of the underlying mechanics to a pilot scale demonstration plant; that may aid the provision of proof to commercial feasibility. The main tool implemented to analyse the technology maturity of a variety of technologies is the use of Technology Readiness Level (TRL); an initial

[29] Typically, electrotrophs transfer electrons out of the cell through conduit cytochromes and their transporters.
[30] However, formate is generally considered in greater regards for this process as it is favourable. This is because H_2 tends to have low solubility, low mass transfer rate and high combustibility, whilst formate has high solubility and high mass transfer rate into the cell. Although formate provides product recovery issues and degradation of the anode. Therefore as a solution formate needs to be consumed at the same rate as it is produced.

assessment of the technology elements allows a classification from a scale of 1 to 9 [64].

b) Environmental feasibility: A key factor that is of importance in the implementation of CCU technologies is the capability to reduce anthropogenic greenhouse gas emissions. Therefore, it is of importance that an environmental assessment is conducted. However, it is noted that CCU technologies offers alternative routes for climate change mitigation which may not be apparent with a standalone environmental assessment of the CCU technology. Alternate climate mitigation routes include the substitution of a product with reduced global warming impact, therefore a comparison with the conventional production technology may be required.

c) Economic feasibility: An essential aspect of commercial feasibility for a CCU technology is sufficient economics to drive key stakeholders to implement the technology, therefore sufficient profitability is required, especially when compared to alternate conventional production technologies. These may be affected by political regulation and other factors that aid in promoting the use of the alternate CCU technology, such as the existence of a carbon tax for CO_2 emissions. Economic assessments of CCU technologies are key for the determination of economic feasibility and tend to be implemented with a technical assessment to provide a comprehensive techno-economic assessment.

d) Product market demand: Even if a CCU technology offers significant advantages in all the latter factors, feasibility is greatly limited if the demand of the product is small as it restricts the total implementation of the CCU technology and produces inadequate captured CO_2 incorporation.

4.4 Current status of CO_2 use

Although CO_2 is considered to be a renewable C1 feedstock, as it is of low toxicity, extremely abundant and cheap, there remains limited large scale industrial processes that incorporate CO_2 as a raw material. However, there remains a demand for CO_2, albeit relatively low, equitable to an estimated total of 222 million tonnes per year.

However, a majority of the current demand of CO_2 is supplied via naturally derived CO_2, with a limited amount obtained from anthropogenic sources, estimated to be around only 40 Mt per year. In regard to the chemical industry, an estimated 180 Mt of CO_2 is used, where in which the greatest proportion of 144 M tonnes of CO_2 is used to produce 155 million tonnes of Urea [65]. Table 2.3 below outlines the estimated market for CCU options.

Table 2.3. Estimates of markets for CO_2 utilisation (2013), adapted Aresta, Dibenedetto et al. (2013) *[65]*.

Process	Industrial volume of production per year (kt)	Global CO2 Use (kt)	Lifetime of storage
Direct Use		42,400	
Beverage carbonation	2900	2900	Days to years
Food packaging	8200	8200	Days to years
Industrial gas	6300	6300	Months
Oil and Gas Recovery	7-23% of oil reserve, <5% of gas reserve	25000	Permanent
Materials and Chemical		167515	
Urea	155,000	114000	Months
Inorganic carbonates	200,000	50000	Decades to permanent
Formaldehyde	21,000	3500	Months
Polycarbonates	4000	10	Decades
Carbonates	200	5	Months
Fuels		12510	
Methanol	50,000	8000	Months
Dimethyl ether	11,400	3000	Months
Tertiary butyl methyl ether	30.00	1500	Months
Algae to biodiesel	5	10	Months
Total		222,425	

a Whilst EOR offers the potential of permanent storage, most of the CO_2 used for EOR is currently not stored

[x] The main sources of CO2 for current demand includes natural wells, by-products of alternative chemicals produced e.g. Hydrogen and sodium Phosphate and fermentation off-gases.

The current main processes that incorporate CO_2 as a feedstock's includes urea, inorganic carbonates[31], methanol and salicylic acid[32]. However, there is a prospect of commercial feasibility for a range of alternative products.

4.5 Direct Utilisation of CO_2

Current applications of direct utilisation of CO_2 are plentiful and it is considered as the usage of CO_2 without the occurrence of a chemical transformation. This occurs in varying industries and products such as fire extinguishers, dry ice and greenhouse fertilisers, however the major industrial direct utilisation source is enhanced oil recovery (EOR).

4.5.1 Enhanced oil recovery

EOR has been implemented from the 1970s to allow for an increased oil yield. EOR is conducted via a pumping of CO_2 and other compounds, such as Nitrogen and surfactants, into oil aquifers. A significantly increased amount of oil recovery is achievable compared to primary and secondary recovery; an estimated extraction rate of 30-60% using EOR in comparison to 20-40% via primary and secondary [66]. The CO_2 dissolves in oil to reduce the surface tension between the oil and water, this displaces the oil from the bedrock spaces it is trapped in, whilst reducing oil viscosity. Although captured CO_2 is suitable for the purpose of EOR, current strategies implement natural CO_2 that is available at a low cost and high purity. Therefore limited economic incentives are present to using captured CO_2 instead.

4.6 Synthesis based CCU

Synthesis based CO_2 utilisation technologies may be split into three categories, depending on the product targeted from each synthesis route:

1. Chemicals
2. Fuels

[31] The main inorganic carbonate product being sodium carbonate produced via the Solvay process at an estimated 52 Million tonnes.
[32] Salyscilic acid is produced via the Kolve-Schmitt process

3. Polymers and materials

4.6.1 Chemicals

Theoretically a large variety of chemicals may be produced utilising CO_2 as a feedstock, however a majority have restricted commercial feasibility due to limitations including market potential and capability for production on an industrial scale.

4.6.1.1 Urea

As noted previously urea is considered to be the major CO_2 transformation product and incorporates a majority of the global CO_2 demand. The production of urea is conducted via a two-step process: liquid ammonia and dry ice (solidified CO_2) via an exothermic reaction producing ammonium carbonate; the ammonium carbonate undergoes an endothermic decomposition and dehydration to produce the final product urea. This is an exothermic process that does not require the use of a catalyst[33]. The synthesis route is illustrated in Scheme 1.

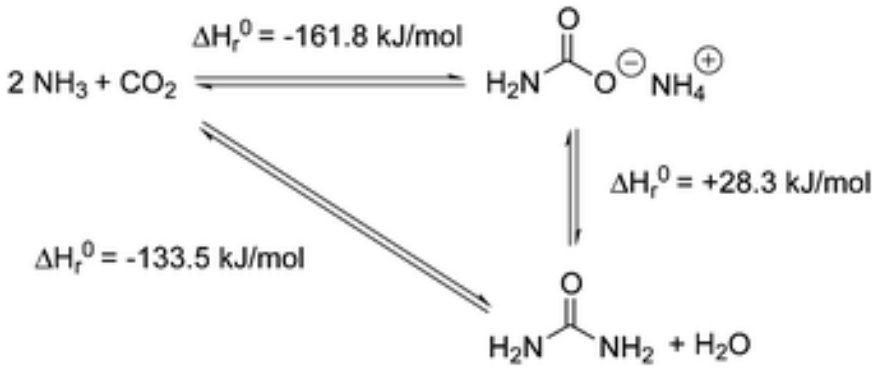

Scheme 1. Urea synthesis

Most of the produced urea is for use in fertiliser production[34], due to its high nitrogen content and low cost per unit of nitrogen. Further to this, it is used to synthesise a range of polymers[35]. However, the implication of urea production in terms of climate mitigation is negligible due to a range of factors. The current methods of producing urea is well established and when comparing the use of captured CO_2 as a feedstock for this process in comparison to conventional CO_2 sources, the economic feasibility

[33] This process is the Habber-bosch urea process.
[34] It is estimated to be that around 80% of urea produced is used for fertiliser production
[35] Urea based polymers include Urea-formaldehyde and urea-melamine-formaldehyde (resin and adhesive).

is limited as current means of production has significantly lower costs than what may be achieved via the use of captured CO_2. Also the storage of the CO_2 within urea is very short as CO_2 is re-released into the atmosphere during fertiliser use, additionally N_2O emissions are also present[36] . Therefore, accounting for these factors and the current saturation of the market, urea is a poor option as a CCU technology [67].

4.6.1.2 Ethylene

Ethylene is produced in extremely high volumes of over 150 million tonnes per year [68], and is used as a commodity chemical to synthesise a range of chemicals or to produce polymers. Currently ethylene globally is produced from fossil fuel derived precursors.

Ethylene may be produced through the thermocatalysis of CO_2 via hydrogenation,

$$2CO_2 + 6H_2 \rightarrow C_2H_4 + 4H_2O.$$

Current research has found that an iron catalyst allows for a significant 65% selectivity for ethylene and light olefin production from CO_2 hydrogenation. Issues remain in the fact that CO_2 conversion remains low and alternate low-value chemicals are also produced such as CO and methane. To allow this process to be viable significant catalyst performance improvements is needed [69] [70].

Electrochemical reduction of CO_2 using a copper catalyst to produce ethylene is a feasible alternative. Current research has explored the use of varying carbon nanostructures and operating conditions to allow for ethylene production, however progress in ethylene selectivity greater than 40% has been limited due to competing reactions such as the reaction of CO_2 with the base present to produce bicarbonate. Strategies explored includes optimisation of CO_2 diffusion to the catalyst active sites, by introducing polymer-based gas diffusion layers around the reaction surface. This produces hydrophobic and conductive supports, which has allowed an increase of faradaic efficiencies for ethylene to around 60% at rates between 160-250 mA cm^{-2} [71] [72]. Further to this ethanol at faradaic efficiencies of 10-30 % is produced as a

[36] Fertilisers are the main source for N_2O emissions accounting for around a third of global anthropogenic N_2O emissions.

by-product, this may allow greater economic feasibility for the process as ethanol is also regarded as a valuable commodity. Furthermore, the fact that the produced ethylene and ethanol are of differing phases- ethylene is produced as a gas and ethanol as a liquid- aids separation of the products. However, the ethanol will need to be extracted from the electrolyte which may be complex.

Limitations that remain for this process are related to the stability of the catalyst especially in relation to issues related to catalyst degradation. Therefore, greater exploration of suitable catalysts and catalyst structures is needed, especially in the fact that significant operation hours ,even on a lab scale, has not been demonstrated.

4.6.1.3 Dimethyl carbonates

Dimethyl carbonate (DMC) is a linear carbonate used as a solvent and a methylation agent. Further uses have been developed including the synthesis of polycarbonates due to its chemical properties and its non-toxicity. It may be incorporated as an oxygenate for the transport of fuel when blended with gasoline [73]. The current scale of production for dimethyl carbonate is around 90 kt annually [74]. Current conventional means of dimethyl carbonate productions includes either the transesterification of ethylene carbonate or propylene carbonate and methanol; or the use of CO, methanol and O_2.

CCU based DMC may be produced through the thermocatalytic reaction of CO_2 with methanol [75],

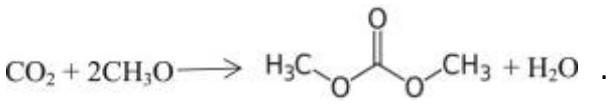

Homogonous catalysts based on tin and heterogenous catalysts based on ceria-zirconia oxide have been developed for this process. However current limitations caused, due to the thermodynamics of the system, includes the low yield ranging from 1-5% at standard reaction conditions, 160-180 C and 90-300 atm CO_2 [76]. To allow this system to be commercially feasible alternativee catalysts needs to be developed and a

suitable strategy for water removal is required to drive the equilibrium and increase DMC yield.

Alternate strategies for DMC production is the alcoholysis of urea. This involves the reaction of urea with methanol to produce DMC and ammonia. The ammonia may be converted into urea via captured CO_2 [77]. This process is of greater viability due to the lack of a water by-product, therefore there is a reduction in process and purification complexity. However, it was found that the by-product ammonia may remain attached to the catalyst causing deactivation and catalyst dissolution. Research has aimed to determined alternate catalysts and improve catalyst performance and yields of up to 50% have been reported. Catalysts explored includes metal oxides and organotin derivatives.

4.6.1.4 Diphenyl carbonate

Diphenyl carbonate (DPC) is used as a raw material for the synthesis of polycarbonates, due to the versatility offered in terms of its chemical properties and its ability to act as a phenylating and methoxycarbonylating agent. Global production for DPC is estimated to be around 250kt per year [78]. Current industrial methods to synthesise DPC includes the reaction of phenol and phosgene, in the presence of bases or the transesterification of DMC. The major limitation of the phosgene-based route is the toxicity of the phosgene.

Asahei Kasei has developed a two-step process where in which di-n-butylcarbonate is initially produced from a reaction between CO_2 and n-butanol, followed by a production of DPC and n-butanol which is recycled. A validation pilot plant was constructed in Urashiki, Okayama with a 1000 tonne/yr production rate, it has been operated for over 1000 hours to validate stability and operability [79]. DPC production from phenol and CO_2 is also possible, however issues for this process are similar to the issues present for DMC production using methanol and CO_2. Shell in 2011 opened a 500 tonne per year pilot plant using a phenol and CO_2 reaction to produce DPC; to counteract the issues propylene oxide is used to remove the water produced [80]. This produces propylene glycol as a by-product. However continued progress for commercial feasibility for this process has not been explored.

4.6.1.5 Carboxylic acids

Carboxylic acids and their derivatives represent commodity chemicals used in a variety of implementations including as a reagent, a solvent and in order to produce polymers. Carboxylic acids industrially are mainly produced either through carbonylation reactions or the oxidation of hydrocarbons, usually from a petrochemical feedstock. A key step for the synthesis of carboxylic acid using CO_2 as a feedstock involves the insertion of CO_2 into a C-H group, which would be beneficial in terms of bypassing the oxidation requirements. However, CO_2 insertion is regarded as thermodynamically unfavoured. Therefore, to allow for reductive carboxylation to occur thermocatalytic operations with strong reducing agents, such as bases, or separation of carboxylic acid as it is formed is required. Furthermore C-H bond activation require a strong oxidant. A range of specific carboxylic acids have been targeted in research:

a) Acrylic acid and methacrylic acid

Acrylic acid and methacrylic acid are used for the synthesis of polymers, carbon fiber and water superabsorbers, with an estimated total global production of around 5.8 million tonnes for acrylic acid. Acrylic acid and methacrylic acid may be synthesised through the carboxylation of ethylene or propylene respectively with CO_2 [81]. To alleviate the issues related to process thermodynamics, a stepwise approach is conducted with an initial carboxylate formation followed by a protonation. Initial studies on catalysis use a Ni catalyst to allow for an understanding of catalysis mechanism. The reagents are coupled with the Ni catalyst centre to allow the protolytic liberation of the required product. This allowed developments to proceed to allow repeated Ni catalyst use and the demonstration of direct carboxylation in the presence of a base to produce an acrylic acid salt. Current progress on synthesis methods includes the use of a Pd and Ni catalysts in the presence of a base and Zn^0 promoter to convert ethylene and CO_2 into acrylate [82] [83]. To allow for adoption, catalyst performance improvements is necessary and a minimisation of Zn^0 and base requirements.

b) Oxalate and Oxalic Acid

Oxalate and Oxalic acid are used for cleaning applications and dye fixation and is produced at a scale of around 120,000 tonnes per year. Normally these are synthesised through the oxidative carbonylation of alcohols with CO and O_2 to produce diesters. These diesters are subsequently hydrolysed with acid to produce oxalic acid [84]. It is noted that this process is difficult therefore if a process that allows the production of oxalic acid through CO_2 is determined oxalic acid demand may increase as it is a suitable feedstock for a range of chemicals. An example includes the synthesis of monoethylene glycol from dimethyl oxalate, in which monoethylene glycol is currently synthesised from CO and H_2, however the esterification of oxalic acid may be a suitable alternative. Twardowski et al demonstrated the synthesis of ethylene glycol from the electrochemical conversion of CO_2 into oxalic acid, followed by the esterification of oxalic acid to ethylene glycol at a rate of 2.4 tonnes per year [85].Alternatives methods researched is the use of mononuclear and binuclear copper complexes for electrochemical reduction of CO_2 to oxalic acid [86] [87], however greater understanding of reaction mechanics is required to improve selectivity and overpotential needs.

4.6.2 Fuels

Fossil fuels are regarded as the primary energy source in current global infrastructure and provides a variety of key raw materials required by the chemical industry. Additionally, the global fuel markets are around two orders of magnitudes greater than that of the chemical market, therefore the production of fuels from CO_2 may be determined to be a valuable goal for CCU. As discussed previously the fact that CO_2 is at the lowest energy state for all binary neutral species containing carbon and the goal in producing fuels is the manufacture of energy releasing combustible products, significant energy input requirements are present. Due to this factor only a few target molecules are viable as outlined in Table 2.4. These viable products include syngas, methanol, formic acid and methane.

Table 2.4. CO_2 reduction reactions to liquid or gaseous carbon-based fuel (the redox potential $\Delta E°$ and Gibbs free energy of reaction $\Delta G°$ values are for at 298 K) *[88]*

Reaction	$\Delta E°$/V	$\Delta G°$/kJ mol^{-1}
$H_2O \rightarrow H_2 + ½\ O_2$	1.23	56.7
$CO_2 + H_2 \rightarrow HCOOH$	—	5.1
$CO_2 + H_2O \rightarrow HCOOH + ½\ O_2$	1.34	61.8
$CO_2 + H_2 \rightarrow CO + H_2O$ [a]	—	4.6
$CO_2 \rightarrow CO + ½O_2$	1.33	61.3
$CO_2 + 3H_2 \rightarrow CH_3OH + H_2O$	—	−4.1
$CO_2 + 2H_2O \rightarrow CH_3OH + 3/2\ O_2$	1.20	166
$CO_2 + 4H_2 \rightarrow CH_4 + 2\ H_2O$	—	−31.3
$CO_2 + 2H_2O \rightarrow CH_4 + 2O_2$	1.06	195

4.6.2.1 Methanol

Methanol is a major target product for CCU implementation due to the large global demand, it is predicted that global demand will exceed 95 million metric tonnes by 2021 [89]. Furthermore, methanol may be converted to other valuable commodities such as gasoline, olefins and dimethyl ether, for which developments may promote further increase in demand. Methanol is typically synthesised using syngas produced from steam methane reforming using fossil fuel sources. The typical approach explored in regards to CCU and methanol production is through the indirect thermocatalytic processes, involving the hydrogenation of CO_2 via reforming processes.

Direct thermocatalytic methanol production involving the direct hydrogenation of CO_2 is also another suitable pathway for methanol production,

$$CO_2 + 3H_2 \rightarrow CH_3OH + H_2O.$$

In order to accommodate this process, catalyst and reaction development has been extensive. However limitations still remain in regard to the high-pressure requirements needed to attain suitable production rates and selectivity, due to the presence of the

reverse water-gas-shift reaction. This occurs because the formation of methanol is exothermic coupled with the presence of a reduction of molecular weight for carbon containing molecules. Therefore, an improvement in thermodynamics requires a decrease in temperature and an increase in pressure for improved selectivity. However, a decrease in temperature is not suitable due to the low reactivity of CO_2, therefore high temperatures are required for suitable conversion [90]. Furthermore, the reverse water-gas-shift reaction is an undesirable reaction in this case as it reduces yield via H_2 consumption.

A major limitation for commercial feasibility for this process is the H_2 requirements which produces increased costs for methanol production in comparison to conventional fossil fuel-based methods (0.08 $/kg via conventional fossil fuel-based methods; 0.3 $/kg on a best-case scenario using hydrogen from water electrolysis [91]). Nonetheless currently two pilot plants for direct CO_2 hydrogenation to methanol are present: The Mitsui Chemical Company in Japan producing approximately 100 tons of methanol annually and the Carbon recycling international in Iceland producing around 4000 tons of methanol annually [92] [93]. However, it is to be noted that this is due to specific circumstances that allow for economic viability[37].

Further issues to the direct CO_2 hydrogenation for methanol production than what is outlined above is the fact that produced water causes catalyst inhibition and deactivation, therefore in terms of industrial commercial feasibility there is currently no satisfactory catalyst available. This is further compounded by the fact that the understanding of the mechanism for CO_2 hydrogenation remains not fully developed. Current trends for CO_2 hydrogenation operate via a ternary Cu-Zn-Al Oxide catalyst that was originally developed for CO hydrogenation, at temperatures of 464-523 K and pressure of 5.0-10.0 MPa [94]. However there remains limited capabilities for this catalyst to hydrogenate pure CO_2. In general, current catalysts used for CO_2 hydrogenation tends to be modified catalyst used for CO hydrogenation to methanol. Therefore, there is continued research on catalysts that provides suitable selectivity,

[37] Mitsui Chemical Company: The CO_2 and H_2 is a waste product generated in an adjacent petrochemical facility. Carbon Recycling International: The plant uses geothermal energy to produce hydrogen and uses the CO_2 captured from the geothermal power plants flue gas.

conversion and minimal deactivation. An example for researched catalysts are the use of transition metal carbides, such as MO_2C and Fe_3C [95] [96]. Other factors that may provide significant progress is variations of reactor design, as an example it was determined that a two-stage catalyst bed system provided significant performance improvements over its single bed counterpart. If a sufficiently efficient catalyst is developed improvements on the commercial feasibility may be focussed upon such as cost, sustainability considerations and scale-up. Although heterogeneous and homogenous catalysts have been explored for methanol production, it is of greater likeliness that a homogenous catalyst is more appropriate for large-scale methanol production, however heterogeneous catalyst systems may be relevant for small scale systems such as portable devices.

Another option explored for methanol production is the electrochemical reduction of CO_2. Although a majority of current research regarded methanol as a by-product at selectivity's below 15 percent [97], it was found that a molybdenum-bismuth bimetallic chalcogenide electro catalyst may produce methanol at a faradaic efficiency that exceed 70 percent [98]. However, an exploration of current status of electrochemical reduction determined that it is unlikely that methanol via an electrochemical CCU process is to be viable unless it is produced from the initial reduction of CO_2 to CO followed by CO conversion into methanol.

4.6.2.2 Dimethyl ether

Dimethyl ether (DME) is a derivative of methanol that may be used as an alternative to conventional diesel [92]. Current progress includes the development of a plant that produces 100 tons per day of DME by the Korea Gas Corporation [99], operating via the direct tri-reforming from methane, CO_2, O_2 and H_2O into syngas followed by DME formation. However, this current technology is currently economically unviable.

Conventional strategies for DME production are the dehydration of methanol or via syngas. Therefore research and development in CCU technologies for methanol production may offer significant progress to DME production.

4.6.2.3 Formic Acid

A majority of the value for Formic acid (FA) is its capabilities to operate as a reducing agent combined with its acidity. This factor stimulates the demand for formic acid in a range of industries including pharmaceuticals, food and the textile industry, providing an estimated global demand of 700 kt $year^{-1}$ with an estimated average annual growth of around 3.6% [100]. Further to this, in terms of alternate formic acid uses, a greater interest is present in the capability of using FA as a hydrogen storage component to form as a source of chemical energy storage [101].Conventional means of FA synthesis operates via the hydrolysis of methyl formate through a two-step process: an initial carbonylation of methanol to methyl formate, followed by a hydrolysis of the methyl formate into methanol and FA.

Although, the direct thermocatalytic pathway to formic acid synthesis is unfavourable thermodynamically, especially if the reactants are initially gaseous, the process becomes exergonic under aqueous conditions. The process is done through the hydrogenation of CO_2 in the presence of a suitable catalyst and other strategies, including either the deprotonation of FA using a base as outlined in Scheme 2 or a removal of FA as it is formed, to drive the reaction.

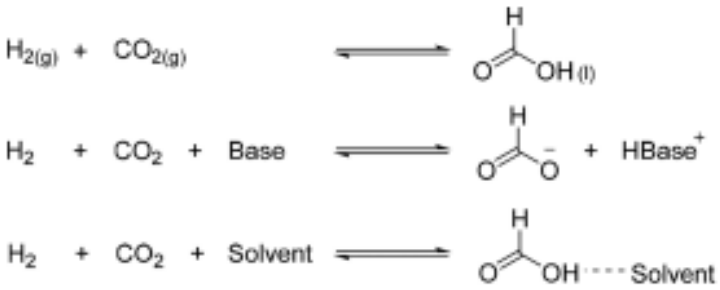

Scheme 2. Theremocatalytic synthesis of formic acid from CO_2.

While a majority of the catalysts have significant productivity, they generally only operate in the presence of a base which increases costs due to reduced atom economy. Current research remains bench scale and includes processes such as CO_2 hydrogenation into FA, with the use of a ruthenium and phosphino based catalysts, and a production of a FA–amine adduct. This is followed by a reactive distillation separate to output to the required FA product. This is mainly due to the presence of challenges regarded the current processes cost efficiency and complexity which may be avoided through: (i) the exploration of alternate catalyst systems that provides a suitable production efficiency whilst not requiring the presence of a base, (ii) improvement in separation technology and process for FA recovery from the reaction

medium and (iii) the option for an alternate cheaper ligand for homogenous catalysis stability.

Alternative strategies developed includes the electrochemical reduction of CO_2 into FA. Examples includes the electrocatalytic reduction of CO_2 into FA: via a tin-based catalyst, at a faradaic efficiencies ranging from 80-95%, at moderate to high over potentials in either a three electrode electrochemical cell or a liquid electrolyte based electrolysis flow cells, operating at a rate of 200 mA/cm^2; via a palladium nanoparticle electrode at a faradaic efficiency of >90% at over potentials <200 mV. However the periodic regeneration of the palladium is required due to trace CO by-product poisoning; using a three-compartment electrolyser with a cation-anion exchange membrane at a faradaic efficiency of 94% at a rate of 200 mA/cm^2 [102] [103]. Current developments for the electrochemical pathway for FA production include the electrochemical reduction of CO_2 to FA and formate salt by the Mantra Venture Group, at a pilot plant located at the Lafarge cement plant in Richmond, Canada capable of converting 100kg of CO_2 a day [104]. To further develop these processes challenges that needs to be overcome includes the improvement of the separation technology for FA; in terms of energy efficiency and the improvement of catalyst and electrode stability and durability.

Photochemical approaches have also been explored, but the production rate for FA is too low, and therefore there is no viability for this pathway for FA production [105].

4.6.2.4 Methane

Methane holds great value in terms of its use as a fuel and in the production of syngas. Currently the major source of methane is as a natural gas and there are limited methane synthesis routes. However, methane synthesis is still possible either via the electrochemical reduction of CO_2 or the Sabatier reaction operated via a nickel catalyst,

$$CO_2 + 4H_2 \rightarrow CH_4 + 2H_2O.$$

However due to the abundance of methane derived from natural gas and in turn the low cost; it is extremely unlikely that any process focussing on methane synthesis from CO_2 is to be commercially feasible.

4.6.2.5 Carbon monoxide

Carbon monoxide is regarded as a major and important feedstock for syngas which is used in the synthesis of many chemicals and fuels. The typical approach for syngas production is the partial oxidation of methane via a platinum catalyst, steam reforming of methane in the presence of a nickel catalyst, or the gasification and partial oxidation of coal at extremely high temperatures.

In terms of CCU, the main purpose for syngas production is for the indirect thermocatalytic production of relevant products. In order to produce syngas a range of options are present, including the use of a reverse water gas shift reaction (RWGS), the alternate forward water gas shift reaction[38] and a range of possible dry, bi- and tri-reforming processes.

The reverse water gas shift reaction is currently mainly implemented to adjust CO, H_2 and CO_2 ratios in syngas,

$$CO_2 + H_2 \longrightarrow CO + H_2O.$$

The reverse water gas shift reaction may operate in the presence of a heterogeneous catalyst at high temperatures of around 500°C to favour the RWGS reaction [106]. Strategies such as continuous product removal and high CO_2 and H_2 concentrations are employed to drive conversion. Various options for catalyst for the RWGS have been researched and includes platinum-,copper- and iron-based catalysts. However issues are still present including undesired methane by-product formation. Other strategies explored is the use of a fluidised bed reactor instead of a fixed bed reactor to improve conversion. In order to provide commercial viability, fundamental advancements are required including the finding of lower temperature catalysts and the capabilities to combine separation with the reverse water gas shift reactors [107]. However, the commercial feasibility of using RWGS for CO production is unlikely, due to the significant advancement and progress of alternate routes.

[38] Forward water gas shift reactions are mainly employed to produce hydrogen from fossil fuels

Dry methane reforming occurs through a strongly endothermic reaction of methane and CO_2 over a noble metal or nickel-based catalyst. Due to the stability of the CH_4 and CO_2 molecules and the high dissociation energies associated with these molecules, extremely high temperatures of 800-1000°C are used [108]. Alternative catalysts investigated for use in this process includes activated carbon,

$$CH_4 + CO_2 \rightarrow 2CO + 2H_2.$$

Bi reforming is the process in which syngas is formed via a combination of steam reforming and dry reforming at temperatures ranging between 800-1000°C [109].

$$2CH_4 + 2H_2O \rightarrow 2CO + 6H_2$$
$$CH_4 + CO_2 \rightarrow 2CO + 2H_2$$
$$3CH_4 + 2H_2O + CO_2 \rightarrow 4CO + 8H_2$$

Scheme 3.Bi reforming process.

Tri-reforming occurs via a combination of the dry reforming process, steam reforming and the exothermic oxidation of methane at temperatures ranging between 800-1000°C [110].

$$CH_4 + CO_2 \rightarrow 2CO + H_2$$
$$CH_4 + H_2O \rightarrow CO + 3H_2$$
$$CH_4 + \frac{1}{2}O_2 \rightarrow CO + 2H_2$$
$$CH_4 + 2O_2 \rightarrow CO_2 + 2H_2O$$

Scheme 4.Tri-reforming process.

The usage of the syngas is heavily dependent on the H_2/CO ratio. Examples includes a ratio of 1.0 which may be used in the synthesis of long chain hydrocarbons or oxygenated chemical compounds and fuels such as acetic acid, in addition to this the desirable H_2/CO value for methanol production and Fischer-Tröpsch technologies is ~2.0. If the produced syngas does not have the desired ratios an additional water-gas shift reaction step may be incorporated to provide adjustments via the reaction of CO with H_2O to produce CO_2 and H_2.

A major issue in regard to reforming processes for syngas production that limits effective industrial implementation and commercialisation is the occurrence of carbon formation, particularly in the presence of elevated pressures [59]. The main mechanics of this is outlined via the Boudouard reaction which is favoured thermodynamically at temperatures below 900°C.

$$CH_4 \rightarrow C + 2H_2$$

$$2CO \rightarrow C + CO_2$$

Scheme 5. Boudouard reaction.

The carbon formation causes sintering and in turn a rapid deactivation of the catalyst, especially if using conventional reforming catalysts. Although these effects may be minimised via the operation at temperatures greater than 900°C, this cause alternate issues such as catalyst stability.

Carbon monoxide may also be produced via the electrochemical conversion of CO_2 to CO and oxygen. Although there is currently no knowledge of a catalyst that is capable in the direct thermochemical reduction of CO_2 into CO, electrochemical processes have been developed. These may occur at high temperature (T>700°C) in a solid oxide electrolysis cell (SOEC) or at low temperatures (T <200°C) using a solution phase or gas diffusion electrolysis cell.

a) High temperature electrolysis in SOEC

SOECS are monolithic electrolysis systems composed from two electrodes separated by a solid oxide-conducting electrolyte [111]. In order to electrochemically convert CO_2 into CO a simultaneous co-reduction of H_2O and CO_2 occurs, where the cathode CO_2 is reduced into CO as well as O_2^- which migrate through the electrolyte to the anode in order to be oxidised to O_2, and at the anode H_2O is reduced to produce H_2.

$$H_2O \rightarrow H_2 + \frac{1}{2}O_2$$

$$CO_2 \rightarrow CO + + \frac{1}{2}O_2$$

Scheme 6. Electrolysis reactions at anode and cathode.

A high temperature of 700-900°C is required in order to achieve sufficient oxide conductivity through the electrolyte. During normal operation this temperature is provided and maintained via joule heating due to the internal resistance present within the cell, although this produces an energy penalty, the need for external heating is abated.

Current research provides a positive outlook for the SOEC technology due the capabilities for researched SOECs to produce CO product at high purities,>99%, and operate at high current densities, ranging from 0.2 to 2 Acm^{-2}, at high energy efficiencies >95%. Furthermore, stable CO_2 electrolysis at current densities of up to 0.5 Acm^{-2} with small cell voltages has been observed over several hundred hours, however degradation is found to be significant at higher current densities [111] [112]. Considerations for alternative electrodes and electrolytes has been explored. The electrolyte selected requires a good oxide conductivity coupled with low electron conductivity, furthermore it needs to be stable at a range of operating conditions whilst having a similar thermal expansion coefficient to the electrodes used. Examples for electrolytes studied is ceria, lanthanum gallate and zirconia, with dopants to increase ion conductivity. Nonetheless, Haldor Topsoe has developed and sell commercial SOECs capable of producing CO onsite at a purity of 99 to 99.999% with a requirement of 6-8 kWh per cubic meter of CO [113]. A commercial system with a 12 $Nm^3\ h^{-1}$ capacity is operating at Gas innovations in Texas since 2016 [114]. Even though commercial feasibility has been demonstrated improvements to SOECs are still required to increase adoption including the developing of alternate electrodes with greater stability at high current densities, research into alternate electrolyte capable in providing high oxide conductivity at lower temperatures and a greater tolerance to impurities in the cell.

b) Low temperature electrolysis

Significant research for low temperature systems to electrochemically reduce CO_2 to CO has been conducted. Currently developed systems typically provide rates of 2-10 mA/cm^2 and faradaic efficiencies of 95-98% in a range of standard three electrode or H-type cells with a variety of electrolytes [115] [116].

With the use of silver catalysts or supported gold catalysts and a flowing liquid electrolyte high CO production rate may be achieved, ranging from 150-450 mA/cm^2 with faradaic efficiencies of 60-98% [117]. Jeanty et al researched the use of 10 cm^2 and 100 cm^2 gas diffusion electrodes with a silver catalyst cathode and an IrO_2 catalyst anode with a flowing liquid electrolyte. The cells operated for 200 hours at a rate of 150 mA/cm^2 with a faradaic efficiency for CO of 60% [118]. Haas et al also explored a hybrid system using this technology to produce an artificial photosynthesis process. A faradaic efficiency of 100% was achieved via the coupling of a 10cm^2 CO_2 to CO electrolyser to a fermentation process, to allow the formed CO to combine with unreacted CO_2 to produce butanol and hexanol [119]. Although this technology provides performance capabilities that prove it to be viable, issues still exist in the use of gas diffusion electrodes and their use in the presence of alkaline electrolytes. In order to maximise current density and faradaic efficiency the CO_2 feed flow rate is in extreme excess to the CO_2 reduction rate, producing a dilute product stream. Furthermore losses in CO_2 are exhibited due to the gas diffusion at the electrode, as it may react with OH^- ions to form a carbonate precipitate on the electrode or the carbonate may migrate to the anode and release CO_2 into the O_2 stream. The scale of this issue depends on a range of factors including the electrode used, the flowrates and pressures as well as the electrolyte. Therefore to allow for commercial feasibility, challenges that need to be addressed include the improvement of CO_2 conversion rates by minimising CO_2 losses to the electrolyte, sufficient catalyst and electrode stability and durability and a reduction of the energy requirement for the process.

c) Alternative electrolysis systems

Intermediate temperature CO_2 electrolysis processes operating at temperatures ranging between 200-500°C have also been developed. Alternative electrolyser configurations have been developed. Kutz et al explored the use of an anion conductive membrane-based electrolyser with a silver cathode catalyst. It was found that CO production rates from 100-200 mA/cm^2 may be sustained for over 1000 hours. The membrane electrolyte reduced CO_2 loss and electrolyte degradation [120].

Liu et al compared various electrolysis systems for CO production from CO including: a flowing liquid-electrolyte for CO production coupled with a polymer electrolyte for H_2 production; and the co-electrolysis of CO_2 and H_2O in a single anion exchange membrane electrolyser [121]. It was found that both systems were capable of producing CO at rates suitable for large scale industrial requirements (100 mA/cm^2)

4.6.2.6 The Fischer-Tropsch process

The Fischer-Tropsch (FT) process for the conversion of CO and H_2 into liquid fuels has been commercialised on a large scale extensively, however an alternative approach for the process involves the direct use of CO_2 for the FT Process. It is understood that this process operates through an initial reverse water-gas-shift reaction reaction followed by a consecutive CO hydrogenation with H_2 to form hydrocarbons through the conventional FT reaction mechanism,

$$nCO_2 + (2n+1)H_2 \rightarrow C_nO_{2n+2} + 2n\ H_2O$$
$$nCO + (2n+1)H_2 \rightarrow C_nO_{2n+2} + n\ H_2O$$

Scheme 7. Fischer-Tropsch reaction scheme from CO_2 and CO.

Limitations of the direct FT process from CO_2 is the low CO concentrations during operations. This produces a greater distribution of light hydrocarbons, that are unsuitable for liquid fuels, due to lack of chain growth occurring. Iron-based catalysts that are suitable for the reverse water-gas-shift reaction and the FT process have been researched. This includes the incorporation of transition metal promoters to the iron-based catalyst to improve the product distribution. Alternative catalyst systems using SiO_2 supports have been developed to allow for increased process performance [122]. Demonstration plants by Sunfire in Germany producing 3 tonnes per year of liquid fuel through this process have been constructed [123]; Ineratec has also operated a pilot plant producing liquid fuel at 200 litres per year in Finland [124]. To allow for development on this process a greater understanding of reaction mechanism is required, allowing for improved catalyst and reactor design.

4.6.3 Polymers and materials

4.6.3.1 Polymers

A promising avenue for CCU and general fixation of CO_2 is incorporating CO_2 into polymer productions. Current usages for polymers are varied and wide from constructing of toys to the insulation of electrical wiring and this is further emphasised by the annual global production that far exceed 200 million tonnes [125]. Current productions for most polymers are produced using a petroleum feedstock.

Polymers from CCU may be produced directly or indirectly from monomers such as methanol, ethylene and DMC. However, polymers and methods capable of constructing the macromolecule with only CO_2 as a sufficient C1 source are preferable.

Polycarbonates and polyether carbonates are typically produced via the reaction of phosgene with 1,2 diols however a synthesis route in which CO_2 is catalytically copolymerised with epoxides is available [126],

Various heterogenous and homogenous catalysts have been researched in order to allow for the selective formation of polycarbonates instead of cyclic carbonates to produce a variety of co-monomers including vinyl oxide, propylene oxide and ethylene oxide. However homogeneous catalysts have been preferred as they allow for higher selectivity. Examples includes a variety of zinc derivates such as mono- and di-nuclear zinc phenoxides and β-diiminates, however the catalyst that has shown greatest effectiveness is the use of metal salen complexes [126] [127].

Various companies are attempting to commercialise alternating carbonates such as aliphatic polycarbonates produced via the reaction of CO_2 with epoxides. Examples to this includes Econic which manufactures and sells polycarbonates that contain up to 50% CO_2 by weight, where in which the general length and number of branches of the polymer is adjusted and altered to be suitable for the required applications; Econic has opened a demonstration plant for polyol production in Runcorn, UK [128]. Novomer, which has been acquired by Saudia Aramco, also produces alternating carbonates to be used as a polyol feed to produce polyurethanes and for other general polymer

applications [129]. A limitation of polycarbonates is the sensitivity of high CO_2 content polymers to water causing it to decompose into cyclic carbonates. To stabilise these polymers additives are incorporated which entails the use of a capping reagent to convert hydroxyl groups from terminal to inert, therefore minimising the backbiting effect that converts these to cyclic carbonates. SK energy has also built a production plant in Korea to produce polycarbonates from CO_2 and propylene oxide; to increase the materials mechanical stability colaminates combined with polypropylene films are introduced [130]. Furthermore, BASF has explored the copolymerisation of CO_2 and cyclohexane oxide for the purpose of blending with polylactides [131].

Commercialisation activities of polyether carbonates produced from a CO_2 feed has also been conducted. Covestro opened in 2016 a plant in Dormagen, Germany with a 5000 tonne per year capacity for the production of polyether carbonate polyols. In order to produce the required polyols a reaction of CO_2 with propylene oxide in the presence of a zinc-based catalyst is used. The produced polyols are incorporated in the production of polyurethanes for the purpose of foam mattresses. This CO_2 required is supplied from a neighbouring ammonia plant; it is estimated it is incorporated at around 20% wt% of the total polyol produced from the plant. A major factor for applicability of polyether carbonate polyol production via CO_2 is the large market of around 7.5 mill tonnes per year, therefore if it is implemented at a 20% wt average CO_2 content, there is a possibility for 1.6 million tonnes per year of CO_2 to be incorporated [132].

For further adoption and commercialisation, stable catalysts that are capable in being industrially feasible for a greater range of epoxides is required to produces a wider range of polymers. The capability to produce copolymers via the use of alternate monomers should be further explored. These may be developed by gaining a greater understanding on catalyst factors and properties that affect the properties of the polymer produced. Greater knowledge in copolymerisation with renewable forms of epoxides is also of importance.

4.6.3.2 Mineral carbonation

Mineral carbonation occurs via the chemical reaction between CO_2, as a liquid or in a solution, with alkaline solids in the form of a metal oxide. These alkaline solids tend

to be magnesium or calcium rich and generally are sourced from natural formations such as in silicate minerals, such as serpentines and basalt [133]. The process of mineral carbonations offers significant advantages in terms of the knowledge present in the reaction mechanisms involved and the existence of a market for mineral carbonates in the construction industry. Furthermore, the capability for the process to sequester a significant amount of CO_2 in a stable form for a long time (decades to centuries), as well as the low energy requirements for the carbonation due to the favourable thermodynamics, are advantageous.

Carbonates are mainly used to produce cement and concrete as well as applications in the pharmaceutical industry [134]. The construction materials industry provides a positive outlook for mineral carbonation processes due to the large market offered, over 50 billion tonnes of material is produced annually [135]. This is further promoted by the increased demand for "green" construction materials.

The process of mineral carbonation may occur in a single or multistep process depending on the alkaline solid used, which may occur readily at ambient temperature and pressure conditions. Carbonation processes occur through the dissolution-precipitation reactions. The CO_2 is solubilised into a liquid phase and dissolution occurs to the main reacting metal species present in the alkaline solid. This is followed with a precipitation of the resultant carbonate mineral from a supersaturated solution. During the direct carbonation process the dissolution and precipitation process occurs simultaneously and is achieved by the presence of a high pressure in a dry or aqueous medium [136]. The alternate multistep processes happen through the initial dissolution step followed by a hydration reaction that converts the metal species to a hydroxide form. The final carbonation is completed with the reaction of CO_2 with the hydroxide form [136]. The advantage of this alternate process is the fact that the exothermic nature of the carbonation reaction allows the full process to be self-sufficient in terms of heating requirements [137],

$$\text{Metal oxide} + CO_2 \rightarrow \text{Metal carbonate} + \text{heat}.$$

Commercialisation and research of mineral carbonation processes in the construction industry is focussed on both the binding agent and the aggregates with over 20

companies engaged in this sector. Variations of the processes includes either the direct utilisation of the captured CO_2 or the combination with other feedstock's such as brine, alkaline-based waste products and minerals [138]. Blue planet implements industrial waste to produce a synthetic $CaCO_3$ layer over a recycled aggregate substrate with the capability to use low purity CO_2 sources which will allow the avoidance of the need for energy intensive capture processes [139]. Alternatively Carbon8 has produced a system that uses air pollution control residues that is reacted with pure CO_2, this processes has reached significant commercialisation with a production rate of 65 kT aggregate per year in the site at Brandon with a second plant commissioned in 2016 [140]. CarbonCure implements the injection of pure CO_2 into a concrete mix to react with any unreacted calcium present, this process offers advantages in terms of providing increased strength compared to conventional concrete mixes. Full-scale commercialisation is available for this technology with it being installed into a variety of concrete plants [141]. Solidia Technologies offers a technology that reacts silicate with pure CO_2 to be used during the cement production processes [142].

Although the use of mineral carbonation has advantages in terms of the total CO_2 sequestering prospective, the market potential may be limited due to the nature of the cement and aggregate market; the cement and aggregate market tends to be a low-margin market with a trend for homogenous standardisation [138]. Therefore, large-scale adoption and commercialisation is difficult. As well as the presence of regulations and standards that tend to even differ jurisdictionally. The difficulty in incorporating new construction material to construction material standards and regulations poses further difficulty. Further issues are present in the significant energy expenditure requirements needed to prepare the alkaline reactants such as the need for high-temperature activation. Further developments for the mineral carbonation process that will allow increased market adoption and commercialisation includes the capability to integrate mineral carbonation technologies with carbon capture technologies, to allow for greater process efficiencies, and an assessment of regulatory methods that allows innovative technologies to be adopted whilst ensuring safety and quality requirements.

4.7 Environmental assessment of CCU technologies

In order to provide a sufficient and comprehensive environmental assessment for a CCU technology the system boundary for consideration should incorporate the source of the captured CO_2. Due to the variety in the possible CO_2 sources and the variance in the concentration of the CO_2 available in the emissions of the source, the CO_2 source is a significant factor. This is because prior to incorporating the CO_2 in the CCU technology, there is a need for the capture of the CO_2. There are differences in the energy requirements depending on the capture technology used and the requirements for processing and removal of other impurities in the flue gas that are detrimental to the CCU technology.

The main tool used for the assessment of the environmental effects of a system is the use of a life-cycle assessment (LCA) [143]. LCA assessments may be conducted through two alternate approaches: attributional and consequential:

a) Attributional LCA: provides the potential environmental impacts related to a system e.g. a product over its life cycle on a cradle-to-grave scale; including the upstream regarding the supply chain and the downstream concerning the use and end-of-life value chain [143].
b) Consequential LCA: assesses the net difference in environmental impacts due to a change. This incorporates market mechanisms and disruptions in current supply chains [143].

CCU technologies provides variation and changes in environmental impacts via various mechanisms depending on the product. This is mainly a factor of the total lifetime of the products lifecycle, as some products only delays the emission of the captured CO_2 whilst others sequester the captured CO_2 for long periods ranging from decades to even longer. Therefore, a consideration for a suitable time-scale for the environmental assessment is required, furthermore especially in the case of short-term delay of emission the main mechanism for climate change mitigation present is displacement of chemicals and products with greater environmental impact. To allow for all climate mitigation mechanisms to be accounted for, a comparison with a business-as-usual approach is required. However dependent on the scope of the study

alternate scenarios may be explored such as variations in the electricity source and the impact of policies such as carbon tax.

5.0 The potentials of CCU technologies: a review of CCU technology techno-economics

A systematic review of academic literature in reference to techno-economic studies of CCU technologies have been analysed to provide a comparison of techno-economic indicators for available CCU technologies.

A variety of CCU technologies were considered to provide estimates for key economic parameters such as OPEX, CAPEX and total cost of production, as well as key technological parameters such as utility requirements and CO_2 conversion rates.

5.1 Selection of Data

An extensive review of available literature is conducted to determine suitable sources from academic literature and grey literature. Sources are classified based upon the product produced, the nature of the process, such as if it utilises an electrochemical process or a thermocatalytic process and if it is a direct or indirect method of production. In techno-economic assessments of CCU technologies there exists a degree of variations in the system boundaries of the process, where in some cases the CCU element is combined with the source of the CO_2 and the carbon capture system. Therefore literature that combines the techno-economic data of the CCU technology with carbon capture technology and CO_2 source is omitted. This will aid in providing a standalone analysis of the CCU technology.

5.2 Techno-economic assessments

Techno-economic assessments (TEA) provide a comprehension of the potential commercial feasibility of CCU technologies to allow a justification of their viability for further research and development. TEA combine engineering and process operation factors via a suitable model to examine the economics of the process and determine the viability of the process. To conduct an accurate and comprehensive

TEA, a significant understanding of the process assessed is required: to allow for the development of an accurate mass and energy balance for the process in terms of the overall process and on a per-unit level. However, the low level of technological maturity for CCU systems hinders the accuracy of the process modelling process.

The values used for economic assessments are impacted by a variety of parameters dependant on the assumptions used, such as fuel prices, capital costs and the assumed plant lifetime. Therefore, to minimise the variability of the technical and economic parameters of CCU technologies there is a requirement for standardisation:

1. System Boundary: the system boundary was limited to the CCU production plant when applicable with a removal of CO_2 transport and capture costs as this is heavily dependent on the captured CO_2 source. A system boundary that incorporates the electricity and heating supply is used.
2. Functional Unit: all technological and financial parameters are standardised to a functional unit of per tonne of CCU product.
3. Operating expenditure (OPEX): a conversion of costs was conducted to the value of $\$_{2018}$ utilising an assumed annual inflation rate of 1.91% [1] and annual currency exchange rates [2].
4. Capital expenditure (CAPEX): an extrapolation of costs to $\$_{2018}$ based upon the CEPC index was used with the use of annual currency exchange rates when required [2].

To allow for a comparison of the CCU technologies other technological parameters are introduced, including the CO_2 efficiency representing the amount of CO_2 feed that is transformed into a final product through the whole production process, this is represented as a percentage of the total CO_2 feed that enters the system and calculated by

$$CO_2\ efficiency = \frac{(Total\ CO_2\ feed - direct\ process\ CO_2\ emmisions)}{Total\ CO_2\ feed}.$$

It is seen from CCU technology techno-economic assessments tend to operate under the assumption of zero CO_2 emission in heating and electricity supply, however in terms of a commercial industrial setting this assumption may not be valid and limits the accounting of utility usage. For example, a process with a high $CO_2\ efficiency$ and extremely high utility requirements may be unjustifiably assumed to be of greater value for anthropogenic CO_2 mitigation purposes than an alternate process with the opposing properties. Therefore, an accounting of indirect CO_2 emissions is determined by utilising factors for electricity and heating requirements: a factor of 0.508tCO_2/MWh for electricity [1] and 0.02tCO_2/MWh for steam [2]. This in turn allows the $Total\ CO_2\ efficiency$ to be determined which is calculated via

$$Total\ CO_2\ efficiency = \frac{(Total\ CO_2\ feed - direct\ process\ CO_2\ emmisions - indirect\ CO_2\ emmisions)}{Total\ CO_2\ feed}.$$

A secondary functional unit is introduced to allow for a comparison between technologies with different CCU products. The goal of CCU technology implementation is considered with the functional unit, *Profit/tCO_2 incorporated* with the inclusion of an estimated cost of \$40 tCO_2^{-1}.

TEA assessments have been conducted for a variety of studies related to a range of CCU products.

5.2.1 Methanol

Studies related to the techno-economics for the synthesis of methanol from CO_2 are numerous, especially in relation to methanol synthesis via hydrogenation. This is likely due to the high technology maturity for CCU-based methanol synthesis with the presence of commercial scale plants in operation. Alternate routes to the hydrogenation CCU-based methanol synthesis routes where in which technoeconomics have been explored includes: the photochemical synthesis of methanol [144], methanol synthesis via a syngas intermediate produced via mixed dry and steam reforming [145], electrolysis [146], via a syngas intermediate produced via dry reforming [147] and the direct synthesis of methanol from CO_2 via a rWGS mechanism [148].

5.2.2 Polyols

Polyols act as an intermediate for the formation of polymers and offers a suitable product for CO_2 utilisation as in comparison to alternative CCU options, the CO_2 remains in the end-product polymer for a long period of time. The main polyol synthesis route that tends to be explored is the synthesis of polyetherenecarbone polyols that act as an intermediate for the production of polyurethanes, which may be used for a variety of uses such as bedding and footwear [149]. A range of academic and commercial research and development for this process has been conducted, however TEA of this synthesis route remains limited. Fernández-Dacosta et al conducted a comparative analysis for the implementation of carbon capture technology to a hydrogen production plant, producing hydrogen via steam methane reforming [150]. To allow for a comparative analysis three cases were produced: a reference system incorporating a H_2 production plant with no capture system and a conventional polyol production plant, a H_2 production plant with a carbon capture system with the captured CO_2 used for CCS; and a H_2 production plant with a carbon capture system with the captured CO_2 being incorporated into the production of polyols and the remaining CO_2 used for CCS. It was noted in regard to the CCU-based polyol production system the factor of greatest significance to the commercial feasibility and profitability of the process is the propylene oxide price. However, an important factor is the fact that propylene oxide is also a feedstock for the conventional production of polyols. Furthermore, propylene oxide is used to a larger degree in the conventional based polyol, therefore increased propylene oxide price further enhances the economic advantages provided via the use of CCU-based polyols.

CCU-based polyol synthesis may be included in alternate configurations to produce a multi-product CO_2 utilisation system. Fernández-Dacosta et al conducted an assessment of the use of a multi-product CCU and CCUS system in order to provide an analysis of this concept [151]. Similarly, to the former study, in order to conduct this comparative assessment, the CO_2 source chosen was a H_2 production plant. Various cases representing a range of reference and explored configurations were studied: the CCU-based formation of DME and polyols in parallel with an initial conversion of captured CO_2 to DME synthesis followed by a re-capture of the released CO_2 to be used for polyol synthesis. This is compared with two reference systems

where in which in the first no carbon capture is used with conventional fossil-fuel based production of DME and polyols and an alternative where conventional DME and polyol production is combined with CCS. The analysis determined that there exists no conclusive difference between the profitability and environmental impact of the cascade or parallel systems due to produced variations that occur on a units level that produces a compensator effect on a system level.

5.2.3 Electrochemical reduction

A range of products may be achieved through the electrochemical reduction of CO_2. Jouny et al produced a technoeconomic assessment for a range of CO_2 products including n-propanol, formic acid, carbon monoxide, ethanol, ethylene and ethanol [146]. Prior to further assessment, historical trends in the performance of electrolysis systems towards a range of electrolysis-based CO_2 reduction products were analysed. This was based upon faradaic and energy efficiencies achieved in relation to the current density present. A greater focus was placed upon heterogenous catalyst-based systems due to catalyst robustness exhibited in comparison to the homogenous alternative. This allowed for an outline of catalytic performance in terms of the electrochemical reduction of CO_2. However limitations were present in terms of the available data towards long term stability due to the tendency for the data analysed pertaining to short time-scale studies. The collated data provided an estimated mass balance based upon the faradaic efficiencies, to conduct a production rate of 100 tonnes of CCU product per day at a current density of 200 mA/cm^2. Although a range of electrolyser configurations have been researched, the technoeconomic assessment used an alkaline water electrolyser system stack as a representative model for the technoeconomic assessment. The technoeconomic study concluded that the only profitable products that may be achieved through the electrochemical reduction of CO_2 are simple products of low order such as formic acid and carbon monoxide, however higher order alcohols such as ethanol and propanol may be promising alternatives if suitable electrochemical performance benchmarks are achieved.

5.2.4 Formic Acid

Multiple routes are available for formic acid synthesis through use of a CO_2 raw material ranging from homogenous and heterogeneous catalysis to photochemical and

electrochemical reduction [152]. TEA related to CCU-based formic acid production remains limited. Perez et al conducted an assessment of formic acid synthesis from captured CO_2 and hydrogen through the homogenous catalysis, via a ruthenium hydroxide catalyst [153] based upon the patent by Schaub et al [154]. A plant producing 12 kt formic acid at a concentration of 85% wt was compared to a conventional formic acid plant, to determine the commercial feasibility of the CCU-based formic acid production plant. It was found that although CO_2 emissions was reduced significantly in comparison to the conventional process, the operating costs and the profitability of the plant was significantly hampered. A cost of production for formic acid of €1524 per tonne formic acid was seen for the CCU plant in comparison to a €475 per tonne formic acid for the conventional plant.

Aldaco et al assessed the environmental and technoeconomic differences between the use of an electrochemical reduction based formic acid production method with conventional synthesis coupled with CCS, utilising a 500 MW coal combustion plant [155]. A 350 kt per year formic acid production rate was assumed. In contrast to the study conducted by Jouney et al, the commercial feasibility of the system was found to be negative with a production cost of around $1100 per tonne formic acid. It was determined that although the CCS system provided greater reduction in CO_2 emissions, the economics of the CCU system was favourable due to the offset of costs via the sale of the formic acid product.

5.2.5 FT Fuels

Zhang et al considered two alternate methods for CO_2 gas to liquid conversion to produce FT synthetic oil and light olefins [156]. A reforming process using a typical FT synthesis process coupled with a RWGS reaction is used in both processes. However there is difference in the use of a reformer: the first modelled process introduced the CO_2 feed to a natural gas feed to produce a syngas mixture via a mixture of dry-reforming and steam reforming followed by the reforming process in the F-T synthesis unit. The second modelled process introduces the CO_2 feed directly into the F-T synthesis unit. It was found that both processes allow for significant profitability allowing for a discounted pay pack period(DPBP) of 8.75 and 8.96 years respectively,

with plant scale having a significant impact on the process; decreasing production rate for the first option from 40,000 barrels per day to 22,915 increases the DPBP by 55.5%.

Dimitriou et al. studied four alternative processes for the CCU based production of FT fuel that all incorporate the anaerobic digestion of sewage sludge, a capture of CO_2 from the produced biogas via MEA, the use of a combined heat and power generation unit, the production of syngas via a RWGS process using a pressure swing adsorption system and a FT synthesis unit [157]. It was found that the scenarios studies displayed limited commercial feasibility due to significant production costs ranging from £15.8–29.6 per litre of liquid fuels. This was largely due to the significant expenditure required in order to produce the required hydrogen. It was noted that although the base case produced 1 t/d liquid fuel at a capital investment of £30M, an increase of scale to 1670 t/d with an increase of total capital investment to £1.34 billion reduced costs significantly down to £1.2/l which remains above the cost of conventional fuels.

Schmidt et al. compared multiple options for the power to liquid production of aviation fuel [158]. Two alternative synthesis pathways were selected, a methanol intermediate and F-T. A high and low temperature electrolysis process for each synthesis route was analysed. Further to this for two alternative capture sources and technologies were explored: direct CO_2 capture from the air and from exhaust emissions. It was found that the F-T synthesis from captured CO_2 supplied from a concentrated source, a high temperature electrolysis unit provides significantly increased CO_2 conversion efficiencies and reduced production costs more than low temperature electrolysis. However, production costs remain high in comparison to conventional fuels.

5.2.6 DME and DMC

Michailos et al provided a techno-economic assessment for a novel power to DME plant producing DME via a combined CO_2 hydrogenation and methanol dehydration process [159]. The system boundary used included the CO_2 capture from a cement plant, electrolysis based H_2 generation and the DME synthesis process. Although the process provided a CO_2 to DME conversion rate of 82.3%, an energy expenditure of 18.05 MWh per tonne DME was required, providing an energy efficiency of 44.4%. The operating expenditures was dominated by the electricity costs related to the

electrolyser unit used for H_2 production, therefore it was noted that the commercial feasibility in terms of producing a positive NPV is extremely improbable.

Kongpanna et al conducted a study on four CO_2 based processes to produce dimethyl carbonate [160]. It was found that the most significant process in terms of performance and economics was the ethylene carbonate intermediate based route, allowing for a 58.6% reduction in global warming potential when compared to the conventional BAYER process. The benefit of this process is further emphasised by the avoidance of the use of phosgene, allowing for a 99,9% reduction in human toxicity-carcinogenic potential.

5.2.7 Butanol

Phytonix has developed a technology for the production of bio-butanol and bio-octanol through the use of photosynthetic bacteria, using a CO_2 feedstock. It is reported that expected production costs for the production of n-butanol is estimated to be $1.95 per gallon [161].

Other biological based butanol production processes have been studied. Nilsson et al explored the techno-economics of a a hybrid process combining an initial fermentation of CO_2 with the catalytic reduction of succinic acid [162]. It was found that the process is not commercially feasible due to the high costs present in the production of succinic acid by the fermentation section. Yang et al explored the manipulation and engineering of clostridium cellulovorans to produce n-butanol and ethanol from lignocellulosic biomass at an estimated production cost of around $2.25 per gallon [163].

5.2.8 OME

OME_{3-5} may be introduced as part of a diesel blend in order to provide an alternate fuel for the purposes of heavy-duty transportation. Zimmermann et al produced a technoeconomic assessment of a plant producing OME_{3-5} as well as other by products including methanol, formaldehyde, methanol, trioxane and methylal [164]. As a basis for the technoeconomic assessment a combination of the technology introduced from studies by Michailos et al. and Schmitz et al. was used [165] [166]. It was found that although the production of OME_{3-5} allows for an alternate fuel that can reduce environmental impact of heavy-duty transportation, there is a reliance on the

availability of a suitable supply of low cost and emission methanol, hydrogen and electricity. Furthermore in terms of economics, the current cost of renewable electricity does not allow for a profitable process, however continued reduction in renewable costs may allow the process to become competitive.

5.2.9 Ethylene Glycol

Ethylene glycol forms as an essential raw material to produce polyester. Although current production method relies upon fossil fuel-based synthesis via the hydration of ethylene oxide. However this relies on the supply of ethylene where in which demand is high, due to the increase of the polyester industry. Yang et al produced a detailed technoeconomic assessment for the production of ethylene glycol via the use of coal and CO_2 [167]. To allow an enhancement of the CO_2 emission reduction and reduce resource requirements, technologies such as mixed steam and dry reforming and a coke oven gas are used. It was found in comparison to the conventional ethylene glycol process direct CO_2 emissions was reduced by 94.05%, the viability of this process is further emphasised by the reduced production costs of 9.72% in comparison to the conventional production route.

5.2.10 Ethanol

Atsonios et al explored two routes for ethanol synthesis from a CO_2 feedstock: ethanol from a RWGS reaction and ethanol synthesis using a DME intermediate [168]. It was found that the DME intermediate process provided a higher thermal efficiency due to the decreased heating demands in comparison to the RWGS system. The DME based ethanol process provided an 18% reduction in ethanol production costs in comparison to the RWGS system.

5.3 Summary of techno-economic assessment

Table 2.1.Summary of technical assessment for CCU technologies in literature.

Product	Method	Conversion factor	Direct CO_2 emission (t)	CO_2 efficiency (%)	Net Electricity use (MwH/t product)	Heating requirements (MWh/t product)	Cooling requirements (MWh/t product)	Byproducts	Indirect CO_2	Total CO_2 efficiency (%)
Polyol	Thermocatalysis [150]	0.23t CO_2 and 0.81t Propelene Oxide and 0.02 Glycerol and 0.01t Monopropelene per t Polyol	0.106	68.45	0.01	0.017	0.04	-	0.00949	65.63
Poly(oxymethylene) dimethyl ethers	Methanol synthesis [164]	1.84t CO_2 and 0.25t H_2 per t OME	0.142	92.30	13.61	2.44	1.22	1.49t O_2	7.55	-315.57
Olefins and synthesis fuels	Through RWGS of CO_2 [156]	1.416t CO_2 and 1.07t Methane and 4.61 H_2O per 0.36t Olefins and 1.076 tonnes synthetic oil	0.19	86.30	1.62 per t Olefins , 0.54 MWh per t Synthetic Oil	8.4 MWh per t Olefins, 2.81 MWh per t Oil	13.57 MWH per t Olefins,4.54 MWH per t Oil	-	1.00	15.77

Product	Method	Conversion factor	Direct CO_2 emission (t)	CO_2 efficiency (%)	Net Electricity use (MwH/t product)	Heating requirements (MWh/t product)	Cooling requirements (MWh/t product)	Byproducts	Indirect CO_2	Total CO_2 efficiency (%)
	CO_2 to CO through Dry reforming/steam reforming [156]	1.416t CO_2 and 1.07t Methane and 4.61t H_2O per 0.36t Olefins and 1.091 tonnes Synthetic oil	0.205	85.50	1.6 per t Olefins,0.53 per t Oil	9.85 MWh per t Olefins,3.25 MWH per t oil	13.96 MWH per t Olefins,4.61 MWH per t Oil	-	1.11	7.02
n-propanol	Electrolysis of CO_2 [146]	2.499t CO_2 per t n-propanol	0	100.00	14	-	-		7.11	-184.59
Methanol	CO_2 to CO through Dry reforming w/ steam reforming S/C=1/5 [145]	0.48t CO_2 and 0.39 Methane and 0.75t Steam per t Methanol	0.0924	88.90	0.09	1.85	0.46		0.525	-28.68
	Thermocatalysis [169]	1.46t CO_2 and 0.2t H_2 per t Methanol	0.09	93.84	0.169	0.439	0.862	Oxygen 1.57 t/t methanol	0.2	80.16
	CO_2 to CO through Dry reforming [147]	1.862t CO2 and 1.77t Methane per t Methanol	1.84	1	0.68	-	-	-	0.345	-17.37

Product	Method	Conversion factor	Direct CO_2 emission (t)	CO_2 efficiency (%)	Net Electricity use (MwH/t product)	Heating requirements (MWh/t product)	Cooling requirements (MWh/t product)	Byproducts	Indirect CO_2	Total CO_2 efficiency (%)
	CO_2 to CO Through RWGS [148]	1.74t CO_2 and 0.19t H_2 per t Methanol	0.25	85.4	5.41			1.54t O2	2.75	-57.95
	Electrolysis [146]	1.2495t CO_2 per t Methanol	0	100.00	8.4	-	-		4.27	-241.5
Formic Acid	Thermocatalysis [153]	0.834t CO_2 and 0.595 H_2O	0.166	80.10	4.05	2.78	2.96	Oxygen 0.477 t/t formic acid	2.78	-253
	Electrolysis [146]	0.99925t CO_2 per t FA 0.957 CO_2 and 0.593 H_2O per t FA	0	100.00	24.63	-17.22	-	0.37 O_2	1.016	-1.68
Ethylene Glycol	CO_2 to CO via coal gasification [167]	0.7816t Coal per t Ethylene glycol	0.15	57.63	-	-	-	-	0	80.81
Ethylene	Electrolysis [146]	3.24975t CO_2 per t Ethylene	0	100	19.25	-	-		9.78	-200.92
Ethanol	CO_2 to CO Through RWGS [14]	2.3t CO_2 and 0.32t H_2 per t Ethanol	0.44	81.10	0.5	3.36	-	0.38t Methanol and 0.31t	1.12	32.18

Product	Method	Conversion factor	Direct CO_2 emission (t)	CO_2 efficiency (%)	Net Electricity use (MwH/t product)	Heating requirements (MWh/t product)	Cooling requirements (MWh/t product)	Byproducts	Indirect CO_2	Total CO_2 efficiency (%)
								Propanol and 2.52 O_2 per t Ethanol		
	Indirect through Dimethyl ester intermediate [14]	1.89t CO_2 and 0.26t H_2 per t Ethanol	0.038	98	0.54	1.7	-	1.16t DME and 2.04t O_2 per t Ethanol	0.71	60.16
	Electrolysis [146]	2.00025t CO_2 per t Ethanol	0	100.00	11.5	-	-		5.84	-192.06
DME	CO_2 to CO Through rWGS [159]	2.05t CO_2 and 0.28t H_2 per t DME	0.36	82.30	17.11	0.904	2.22	2.25 O_2	8.93	-335.6
Dimethyl carbonate	Indirect through Ethylene carbonate intermediate [160]	0.536t CO_2 and 0.487 t Ethylene Oxide and 0.71t Methanol per t DMC	0.049	90.86	-	18.2	13.14	Ethylene Glycol 0.69 t/t DMC	4.72	-789.26
	Thermocatalysis [160]	0.94t CO_2 and 0.65t Methanol	0	100	0.69	13.61	6.4	-	3.88	-312.58

Product	Method	Conversion factor	Direct CO_2 emission (t)	CO_2 efficiency (%)	Net Electricity use (MwH/t product)	Heating requirements (MWh/t product)	Cooling requirements (MWh/t product)	Byproducts	Indirect CO_2	Total CO_2 efficiency (%)
CO	Electrolysis [146]	1.995t CO_2 per t CO	0	100.00	3.25	-	-		1.65	17.24
Butanol	Bioreactor [161]	2.64t CO_2 and 2.47t H_2O per t Butanol	0.71	91.27	-	-	-		0	73.11

Although in some cases such as n-propanol synthesis through the electrolysis of CO_2 a positive value for $CO_2\ efficiency$ is seen when not considering indirect emissions , incorporating indirect emissions decreases efficiency significantly as outlined by the negative $Total\ CO_2\ efficiency$ value. This concludes the importance of considering all sources of emissions, direct and indirect, to provide a valid assessment of a CCU technologies effectiveness. It is to be noted that CCU technologies generally do not tend to retain the capture carbon for extremely long periods and may be considered as a short term sequestering process. Although some CCU technologies such as the production of polyols may produce a long period of CO_2 emission storage that may be considered permanent, the main outlook for CCU in terms of abatement of anthropogenic CO_2 is the substitution of products with a product of decreased environmental impact. The tendency for CCU technologies to produce reduced environmental impacts in comparison to conventional means of producing the same product is mainly due to the displacement of reactant and intermediates or substitution of fossil fuels with less impacting alternatives.

Therefore, it is of importance to consider the manner in which the CCU technology reduces CO_2 emissions by accounting for the time period the CO_2 is sequestered into the CCU product and if applicable applying a comparison with alternate conventional production methods for the product. A comparison with conventional production methods will provide the reduction of CO_2 emissions due to substitution by determining the variance between the CO_2 emissions produced between the two systems. Furthermore to conclude the real net benefit of the implementation of CCU technologies the use of cradle-to-gate analysis or for increased accuracy cradle-to-grave environmental assessments with methodologies such as LCA are required. Also, a selection of a suitable system boundary is required as for example the carbon capture source and carbon capture system method will also provide impact to the environmental benefits of the CCU technologies due to the increased energy demands associated with carbon capture systems.

Table 2.2.Summary of economic assessment for CCU technologies in literature.

Product	Method	CAPEX ($/t product)	OPEX ($/t product)	Production cost ($/t product)	Product cost ($/t product) [19] [20] [21] [22]	Total By-product value ($/t product)	Profit ($/t product)	Profit per tCO_2 incorporated ($/t CO_2)
Polyol	Thermocatalysis [150]	5.48	1355.96	1361.33	1933.61	-	572.17	2487.7
Poly(oxymethylene) dimethyl ethers	Methanol synthesis [164]	67.65	1705.03	1765.79	1000	250.29	-522.39	-307.59
Olefins and synthesis fuels	Through RWGS of CO_2 [156]	1.47	6.48	7.95	8.63	-	0.68	0.60
	CO_2 to CO through Dry reforming/steam reforming* [156]	1.50	6.39	7.89		-	0.74	0.67
n-propanol	Electrolysis of CO_2 [146]	41.43	692	733.43	1430	-	656.57	262.73
Methanol	Thermocatalysis [169]	28.02	751.72	433	360	263.73	150.73	109.94
	CO_2 to CO through Dry reforming [147]	34.70	136.26	170.96		-	189.04	8592.73
	CO_2 to CO Through RWGS [148]	217.53	188.50	406.03		258.69	212.66	142.73
	Electrolysis [146]	28.86	451	479.86		-	-159.86	-127.94
	CO_2 to CO through Dry reforming/steam reforming [145]	25.61	302.79	326.43		-	33.57	86.61
Formic Acid	Thermocatalysis [153]	83.28	1755.24	1838.52	740	80.13	-1018.39	-1524.54
	Electrolysis [146]	14.71	264	278.71			421.29	421.61

Product	Method	CAPEX ($/t product)	OPEX ($/t product)	Production cost ($/t product)	Product cost ($/t product) [19] [20] [21] [22]	Total By-product value ($/t product)	Profit ($/t product)	Profit per tCO_2 incorporated ($/t CO_2)
Ethylene Glycol	CO_2 to CO via coal gasification [167]	47	567.96	614.96	764		109.04	534.45
Ethylene	Electrolysis [146]	52.86	781	833.86	1300		426.14	131.13
Ethanol	CO_2 to CO Through RWGS [168]	1013.15	1260.13	2273.28	1000	1003.41	-269.98	-144.70
	Indirect through Dimethyl ester intermediate [168]	565.64	1231.17	1796.81			-796.81	-430.24
	Electrolysis [146]	36.71	573	609.71			350.29	175.1231
DME	CO_2 to CO Through RWGS [159]	462	1703	2130	495.92		-1674.08	-100011
Dimethyl carbonate	Indirect through Ethylene carbonate intermediate [160]	214.88	843.46	1058.34	685	828	454.66	933.59
	Thermocatalysis [160]	123.21	1284.63	1407.84			-722.84	-769.98
CO	Electrolysis [146]	17.29	137	154.29	600		405.71	203.36
Butanol	Bioreactor [161]	40.76	271.74	312.5	1500		1147.5	594.44

*Natural gas price adjusted to 2018 value due to significant discrepancy to what was assumed in study $6/MMBTU vs $2.4/MMBTU.

The system with the greatest amount of input in regards to techno-economic assessments was methanol production by thermocatalysis [170] [169] [171] [168] [172] [173] with production costs varying between $207.83-$960.42/t methanol. The variability of the production costs emphasises the importance and outlines variances dependent on the complexity of the simulation methodology and the assumption used such as location of the plant and electricity cost. D.Belloti et al provided an analysis of a methanol production plant in China, Germany and Italy and due to significant price differences presented in the electricity costs of the three locations ranging from $11.17/MWh electricity in China to $50.28/MWh electricity in Germany a variance in methanol production costs of $207.83 - 726.28/t methanol was seen [169].

A multitude of CCU systems use hydrogen as a feed, wherein which for all techno-economic assessments studied an electrolyser system was used. This was done in order to allow the utilisation of zero emission electricity sources such as solar and wind power. This produces increased costs due to the capital expenditure for the electrolyser unit. However, a positive of the electrolysis unit is the production of an O_2 byproduct, which in some cases offsets losses, and in some cases allows the production process to be considered profitable.

Alternatively conventional steam reforming-based hydrogen may be used. Although this may reduce the environmental benefits achieved from using electrolysis based H_2, this will increase process profitability and may retain reductions in anthropogenic CO_2 emissions via product substitution, when comparing with conventional production methods.

References

[1] G. Bye, Portland cement: Composition, production and properties, 1999.

[2] I. Soroka, Portland Cement Paste and Concrete, 1979.

[3] H. M. J. R. A. L. A. N. G. W. S. J. S. S. K. L. S. J. J. T. effrey W Bullard, "Mechanisms of cement hydration," *Cement and concrete research,* vol. 41, no. 12, pp. 1208-1223, 2011.

[4] M. A. Benvenuto, Industrial Chemistry, Berlin, Germany: De Gruyter.

[5] C. T. C. H. a. T. H. H. Alsop, Cement Plant Operations Handbook : For Dry Process Plants.5th ed., Dorking, 2007.

[6] J. M. Crow, "The concrete conundrum," *Chemistry World,* pp. 62-66, March 2008.

[7] M. S. C. C. &. M. S. Imbabi, " Trends and developments in green cement and concrete technology," *International Journal of Sustainable Built Environment,* vol. 1, no. 2, pp. 194-216, 2012.

[8] T. A. A. R. J. a. M. G. Boden, "Global, Regional,and National Fossil-Fuel CO2 Emissions, Carbon Dioxide Information Analysis Centre," Global, Regional,and National Fossil-Fuel CO2 Emissions, Carbon Dioxide Information Analysis Centre, [Online]. Available: https://cdiac.ess-dive.lbl.gov/trends/emis/meth_reg.html. [Accessed 22 May 2019].

[9] O. M. E. O. Adina Bosoaga, "CO2 capture technologies for cement industry," *Energy Procedia* , vol. 1, pp. 133-140, 2009.

[10] W. Kurdowski, Cement and Concrete Chemistry, 2014.

[11] S. Dep, a and lar, Designing Green Cement plants, Elsevier, 2016.

[12] A. Boateng, Rotary Kilns, Butterworth-Heinemann, 2015.

[13] UN Climate Change, "Austalia NIR," 2018.

[14] European Cement Research Academy and Cement Sustainability Initiative, "Development of State of the Art Techniques in Cement Manufacturing: Trying to Look Ahead," Düsseldorf and Geneva, 2017.

[15] K. Koring, V. Hoenig, H. Hoppe, J. Horsch, C. Suchak, V. Klevenz and B. Emberger, "Deployment of CCS in the Cement Industry," IEAGHG, Cheltenham, UK, 2013/10.

[16] IEA, "Technology Roadmap:Low-Carbon Transition in the Cement Industry," 2018.

[17] R. U.Kääntee, "Cement manufacturing using alternative fuels and the advantages of process modelling," *Fuel Processing Technology,* vol. 85, no. 4, pp. 293-301, 2004.

[18] A. U.-. B. Eugeniusz Mokrzycki, "Alternative fuels for the cement industry," *Applied Energy,* vol. 74, no. 1-2, pp. 95-100, 2003.

[19] S. Deolalkar, Designing Green cement plants, Elsevier, 2016.

[20] M. ,. M.Schneider, "Sustainable cement production—present and future," *Cement and Concrete Research,* vol. 41, no. 7, pp. 642-650, 2011.

[21] M. L. Peter Hewlett, Lea's Chemistry of Cement and Concrete, 2018.

[22] Cement Sustainability Initiative, "CO2 and Energy Accounting and Reporting Standard for the," 2005.

[23] IEA, "CO2 capture in the cement industry," 2008.

[24] R. S. F. H. M. S. Francisco Carrasco-Maldonado, "Oxy-fuel combustion technology for cement production – State of the art research and technology development," *International Journal of Greenhouse Gas Control,* vol. 45, pp. 189-199, 2016.

[25] M. &. O. G. S. &. D. L. E. &. P.-C. J.-F. &. J. A. &. B. D. &. F. C. &. R. M. &. R. S. &. A. R. &. H. H. &. S. D. &. M. M. &. G. Voldsund, "Comparison of Technologies for CO2 Capture from Cement Production—Part 1: Technical Evaluation.," *Energies,* 2019.

[26] Y. A.Rolfe, "Technical and environmental study of calcium carbonate looping versus oxy-fuel options for low CO2 emission cement plants," *International Journal of Greenhouse Gas Control,* vol. 75, pp. 85-97, 2018.

[27] C. M.T.Sander, "The Fluor Daniel® econamine FG process: Past experience and present day focus," *Energy Conversion and Management,* Vols. 5-8, p. 33, 1992.

[28] A. L.Gomez-Coma, "Carbon dioxide capture by [emim][Ac] ionic liquid in a polysulfone hollow fiber membrane contactor," *International Journal of Greenhouse Gas Control,* vol. 52, pp. 401-409, 2016.

[29] K. k. C. H. Y. T. Ruize Lua, "CO2 capture using piperazine-promoted, aqueous ammonia solution: Rate-based modelling and process simulation," *International Journal of Greenhouse Gas Control,* vol. 65, pp. 65-75, 2017.

[30] A. K. F. A. G. A. Rahul R. Bhosale, "CO2 Capture Using Aqueous Potassium Carbonate Promoted by Ethylaminoethanol: A Kinetic Study," *IECR,* 2016.

[31] F. V. O. G. B. A. RichardBouma, "Membrane-assisted CO2 Liquefaction: Performance Modelling of CO2 Capture from Flue Gas in Cement Production," *Energy Procedia,* vol. 114, pp. 72-80, 2017.

[32] D. Perilli, "The Skyonic SkyMine: The future of cement plant carbon capture?," *Global Cement Magazine,* vol. 5, pp. 8-12, 2015.

[33] B. J.C.Abanades, "Emerging CO2 capture systems," *International Journal of Greenhouse Gas Control,* vol. 40, p. 126=166, 2015.

[34] J. C. A. E. J. A. M. J. B. S. B. N. M. D. J. R. F. M.-C. F. R. G. J. P. H. R. S. H. P. H. e. a. Matthew E. Boot-Handford, "Carbon capture and storage update," *Energy Environ. Sci,* vol. 7, pp. 130-189, 2014.

[35] D. C. L. L. M. Luis M. Romeo, "Reduction of greenhouse gas emissions by integration of cement plants, power plants, and CO2 capture systems," *Greenhouse Gases: Science and Technology,* vol. 1, no. 1, 2011.

[36] †. M. a. J. C. A. Nuria Rodríguez, "CO2 Capture from Cement Plants Using Oxyfired Precalcination and/or Calcium Looping," *Environ. Sci. Technol.* , vol. 46, pp. 2460-2466, 2012.

[37] Leilac, "PUBLIC LEILAC FEED SUMMARY REPORT," 2017.

[38] D. L. F. a. P. F. Thomas Hills, "Carbon Capture in the Cement Industry: Technologies, Progress, and," *Environ. Sci. Technol.,,* vol. 50, no. 1, p. 368–377, 2016.

[39] M. V. S. F. R. S. H. C. Kristin Jordal, "CEMCAP – Making CO2 Capture Retrofittable to Cement Plants," *Energy Procedia,* vol. 114, pp. 6175-6180, 2017.

[40] C. o. T. f. C. C. f. C. P. 2. C. Analysis, "Stefania Osk Gardarsdottir ,Edoardo De Lena, Matteo Romano,Simon Roussanaly, Mari Voldsund, José-Francisco Pérez-Calvo,David Berstad,Chau Fu,Rahul Anantharaman,Daniel Sutter,Mateo Gazzani,Marco Mazzotti,Giovanni Cinti," *Energies,* 2019.

[41] J. L. Xi Liang, "Assessing the value of retrofitting cement plants for carbon capture: A case study of a cement plant in Guangdong, China," *Energy Conversion and Management,* vol. 64, pp. 454-465, 2012.

[42] B. D. d. C. H. L. M. M. L. Metz, "Special report on carbon dioxide capture and storage," Cambridge University Press,, Cambridge, UK, 2005.

[43] R. G. R. R. R. Arshad Raza, "Significant aspects of carbon capture and storage – A review," *Petroleum,* 2018.

[44] SteveGoldthorpe, "Potential for Very Deep Ocean Storage of CO2 Without Ocean Acidification: A Discussion Paper," *Energy Procedia,* vol. 114, pp. 5417-5429, 2017.

[45] T. M Aresta, "Carbon dioxide utilisation in the chemical industry," *Energy Conversion and Management,* vol. 38, pp. S373-S378, 1997.

[46] T. M. T. F. H. Zhenyu Sun, "Fundamentals and Challenges of Electrochemical CO2 Reduction Using Two-Dimensional Materials," *Chem,* vol. 3, no. 4, pp. 560-587, 2017.

[47] D. Lide, CRC Handbook, BocaRaton, Florida: CRC Press, 2003.

[48] D. Lange's, Handbook of Chemistry, NewYork: McGraw-Hi, 1979.

[49] L. B. K. Chandrasekaran, "In-situ spectroscopic investigation of adsorbed intermediate radicals in electrochemical reactions: CO2− on platinum," *Surf. Sci.,* vol. 185, pp. 405-514, 1987.

[50] N. M.Gattrell, "A review of the aqueous electrochemical reduction of CO2 to hydrocarbons at copper," *Journal of Electroanalytical Chemistry,* vol. 594, no. 1, pp. 1-19, 2006.

[51] L. O. Z. L. K. Koci, "Photocatalytic reduction of CO2 over TiO2 based catalysts," *Chem. Papers,* vol. 62, no. 1, pp. 1-9, 2008.

[52] B. H. U. Akpan, "Parameters affecting the photocatalytic degradation of dyes using TiO2-based photocatalysts: a review," *J. Hazard. Mater.,* vol. 170, no. 2, pp. 520-529, 2009.

[53] C. H. A. R. O. Carp, "Photoinduced reactivity of titanium dioxide," *Prog. Solid State Chem.,* vol. 32, no. 1-2, pp. 33-177, 2004.

[54] M. M.-V. Oluwafunmilola Ola, "Review of material design and reactor engineering on TiO2 photocatalysis for CO2 reduction," *Journal of Photochemistry and Photobiology C: Photochemistry Reviews,* vol. 24, pp. 16-42, 2015.

[55] M. M. R. R. O. Hamidah Abdullah, "Modified TiO2 photocatalyst for CO2 photocatalytic reduction: An overview," *Journal of CO2 Utilization,* vol. 22, pp. 15-32, 2017.

[56] M. L. F. D. S. C. P. K. Bhupendra Kumar, "Photochemical and Photoelectrochemical Reduction of CO2," *Annual Review of Physical Chemistry,* vol. 63, pp. 541-569, 2012.

[57] B. B. Buchanan, "Carbon dioxide assimilation in oxygenic and anoxygenic photosynthesis," *Photosynthesis Research,* vol. 33, pp. 147-162, 1992.

[58] I. Zelitch, "Improving the efficiency of photosynthesis," *Science,* vol. 188, pp. 626-633, 1975.

[59] M. J. M. a. K. F. Mikkelsen, "The teraton challenge. A review of fixation and transformation of carbon dioxide.," *Energy & Environmental Science,* vol. 3, pp. 43-81, 2010.

[60] D. B. J. C. Z. a. H. C. Wu-Scharf, "Transgene and transposon silencing in Chlamydomonas reinhardtii by a DEAH-box RNA helicase," *Science,* vol. 290, pp. 1159-1162, 2000.

[61] D. P. Kelly, "Introduction to the chemolithotropihc bacteria," in *The Prokaryotes*, Berlin, Heidelberg., Springer, 1981.

[62] P. S. C. A. K. B. W. H. L. D. E. a. G. S. Hu, "Integrated bioprocess for conversion of gaseous substrates to liquids," *Proceedings of the National Academy of Sciences of the United States of America,* vol. 113, pp. 3773-3778, 2016.

[63] D. R. a. K. P. N. Lovley, "Electrobiocommodities: Powering microbial production of fuels and commodity chemicals from carbon dioixde with electricity.," *Current Opinion in Biotechnology,* vol. 24, pp. 385-390, 2013.

[64] EARTO, " The TRL scale as a Research & Innovation Policy Tool".

[65] D. A. A. A. Aresta M, "The changing paradigm in CO2 utilization," *Journal of CO2 Utilization,* 2013.

[66] A. A.-K. S. Kokal, "Enhanced Oil Recovery: Challenges and Opportunities," EXPEC Advanced Research Centre, Saudi Aramco, 2010.

[67] D. J. P. Styring, "Carbon Capture and Utilisation in the green economy," Centre for low carbon futures 2050, 2011.

[68] Research and Markets, "The Ethylene Technology Report 2016 - Research and Markets," 2016.

[69] R. N. K. C. S. a. P. P. Satthawong, "Light olefin synthesis from CO2 hydrogenation over K-promoted Fe–Co bimetallic catalysts," *Catalysis Today,* vol. 251, pp. 34-40, 2015.

[70] J. Z. Y. Q. Z. W. D. a. Y. W. Wang, "Synthesis of lower olefins by hydrogenation of carbon dioxide over supported iron catalysts," *Catalysis Today,* vol. 215, pp. 186-193, 2013.

[71] T. T. H. S. V. S. M. T. T. F. J. T. A. I. F. P. J. A. K. a. A. A. G. Hoang, "Nanoporous copper–silver alloys by additive-controlled electrodeposition for the selective electroreduction of CO2 to ethylene and ethanol," *Journal of the American Chemical Society,* vol. 140, no. 17, pp. 5791-5797, 2018.

[72] C.-T. T. B. M. G. K. A. S. C. M. G. F. P. G. d. A. A. K. J. P. E. P. D. L. O. S. B. C. Z. R. Q.-B. Y. P. D. S. a. E. H. S. Dinh, "CO2 electroreduction to ethylene via hydroxide-mediated copper catalysis at an abrupt interface," *Science,* vol. 360, no. 6390, pp. 783-787, 2018.

[73] J. H. P.-S. C. H.-K. Sang-Hyun Pyo, "Dimethyl carbonate as a green chemical," *Current Opinion in Green and Sustainable Chemistry,* vol. 5, pp. 61-66, 2017.

[74] J. N. S. X. Z. N. Z. F. X. W. W. a. Y. S. Ma, " A short review of catalysis for CO2 conversion.," *Catalysis Today,* vol. 148, no. 3, pp. 221-231, 2009.

[75] Y. P. L. L. Z. X. Aixue Li, "Synthesis of dimethyl carbonate from methanol and CO2 over Fe–Zr mixed oxides," *Journal of CO2 Utilization,* vol. 19, pp. 33-39, 2017.

[76] A. H. A. A. C. a. H. K. Tamboli, "Catalytic developments in the direct dimethyl carbonate synthesis from carbon dioxide and methanol," *Chemical Engineering Journal* , vol. 332, pp. 530-544, 2017.

[77] K. a. V. C. S. Shukla, "Synthesis of organic carbonates from alcoholysis of urea: A review," *Catalysis Reviews,* vol. 59, no. 1, 2017.

[78] J. X. M. a. S. W. Gong, "Phosgene-free approaches to catalytic synthesis of diphenyl carbonate and its intermediates.," *Applied Catalysis,* vol. 316, no. 1, pp. 1-21, 2007.

[79] Asahi Kasei Corp., "Demonstration of validation plant for DRC process to produce DPC, a monomer of PC," 07 August 2017. [Online]. Available: https://www.asahi-kasei.co.jp/asahi/en/news/2017/e170807.html. [Accessed 02 March 2019].

[80] A. H. Tullo, "Shell To Scale Up Diphenyl Carbonate," C&En, 19 December 2011. [Online]. Available: https://cen.acs.org/articles/89/i51/Shell-Scale-Diphenyl-Carbonate.html. [Accessed 02 May 2019].

[81] M. Limbach, " Chapter Four: Acrylates from alkenes and CO2, the stuff that dreams are made of.," in *Advances in Organometallic Chemistry*, New York, Academic Press, 2015, pp. 174-202.

[82] C. E. A. P. G. Y. B. S. a. D. V. Hendriksen, "Catalytic formation of acrylate from carbon dioxide and ethene.," *Chemistry—A European Journal,* vol. 20, no. 38, pp. 12037-12040, 2014.

[83] S. C. E. N. H. T. K. I. J. P. A. A. G. S. A. S. F. R. P. H. a. M. L. Stieber, "crylate formation from CO2 and ethylene: Catalysis with palladium and mechanistic insight," *Chemical Communications,* vol. 51, no. 54, pp. 10907-10909, 2015.

[84] J. Y. L. F. H. a. J. Z. Qiao, "A review of catalysts for the electroreduction of carbon dioxide to produce low-carbon fuels," *Chemical Society Reviews,* vol. 43, no. 2, pp. 631-675, 2014.

[85] Z. E. B. C. J. J. K. K. T. K. A. K. R. P. A. B. N. S. G. L. a. T. J. K. wardowski, "Method and system for production of oxalic acid and oxalic acid reduction products". 2016.

[86] R. P. B. M. L. A. L. S. a. E. B. Angamuthu, "Electrocatalytic CO2 conversion to oxalate by a copper complex," *Science,* vol. 327, no. 5693, pp. 313-315, 2010.

[87] U. R. F. R. F. a. A. W. M. Pokharel, "Reduction of carbon dioxide to oxalate by a binuclear copper complex," *Nature Communications,* vol. 5, 2014.

[88] N. &. B. A. &. H. J. &. G. A. &. J. G. &. S. A. C. &. K. W. C. &. S. N. &. F. P. &. M. D. N. Florin, "An overview of CO 2 capture technologies," *Energy & Environmental Science,* vol. 3, pp. 1645-1669, 2010.

[89] I. Markit, Interviewee, *Global Methanol Demand Growth Driven by Methanol to Olefins as Chinese Thirst for Chemical Supply Grows*. [Interview]. 12 June 2017.

[90] A. A. B. A. U. A. V. B. T. A. W. M. M. J. G. a. F. K. Álvarez, "Challenges in the greener production of formates/formic acid, methanol, and DME by heterogeneously catalyzed CO2 hydrogenation processes," *Chemical Reviews* , vol. 117, no. 14, pp. 9804-9838, 2017.

[91] M. D. A. &. A. A. Aresta, "Catalysis for the valorization of exhaust carbon," *Chemical Reviews,* vol. 114, no. 3, pp. 1709-1742, 2015.

[92] E. A. G. C. J.-L. D. a. S. P. Quadrelli, "Carbon dioxide recycling: Emerging large-scale technologies with industrial potential," *ChemSusChem,* vol. 4, no. 9, pp. 1194-1215, 2011.

[93] J. S. W. K. B. a. W. L. Klankermayer, "Selective catalytic synthesis using the combination of carbon dioxide and hydrogen: Catalytic chess at the interface of energy and chemistry.," *Angewandte Chemie International Edition,* vol. 55, no. 26, pp. 7296-7343, 2016.

[94] I. M.-C. L. G. Fierro, "Effect of Pd on Cu-Zn Catalysts for the Hydrogenation of CO2 to Methanol: Stabilization of Cu Metal Against CO2 Oxidation," *Catalysis Letters,* vol. 79, no. 1-4, pp. 165-170, 2002.

[95] G. W. W. Han Han, "High selective synthesis of methanol from CO2 over Mo2C@NSC," *Journal of the Taiwan Institute of Chemical Engineers,* vol. 95, pp. 112-118, 2019.

[96] P. L. D. J. S. S. D. S. M. G. W. a. J. G. C. José A. Rodriguez*, "Hydrogenation of CO2 to Methanol: Importance of Metal–Oxide and Metal–Carbide Interfaces in the Activation of CO2," *ACS Catal,* vol. 5, no. 11, p. 6696–6706, 2015.

[97] C. M. R. a. J.-M. S. Costentin, "Catalysis of the electrochemical reduction of carbon dioxide," *Chemical Society Reviews* , vol. 42, no. 6, pp. 2423-2436, 2013.

[98] X. Q. Z. X. K. H. L. Q. Q. Z. Z. a. B. H. Sun, "Molybdenum-bismuth bimetallic chalcogenide nanosheets for highly efficient electrocatalytic reduction of carbon dioxide to methanol," *Angewandte Chemie International Edition,* vol. 55, no. 23, pp. 6771-6775, 2016.

[99] Green Car Congress, "Korea Gas to build 300,000 tpy DME plant; one-step process," 09 February 2011. [Online]. Available: https://www.greencarcongress.com/2011/02/kogas-20110209.html. [Accessed 05 May 2019].

[100] Markets and Markets, "Formic acid market by types (grades of 85 %, 94 %, 99 % and others) by Application (Agriculture, leather & textile, rubber, chemical & pharmaceuticals, & others) & byGeography – Global trends, Forecasts to 2019," May 2014. [Online]. Available: https://www.marketsandmarkets.com/Market-Reports/formic-acid-Market-69868960.html.. [Accessed 02 May 2019].

[101] M. G. a. G. Laurenczy, "Formic acid as a hydrogen source—Recent developments and future trends.," *Energy Environ. Sci,* vol. 5, p. 8171–8181, 2012.

[102] J. Y. L. F. H. a. J. Z. Qiao, "A review of catalysts for the electroreduction of carbon dioxide to produce low-carbon fuels," *Chemical Society Reviews,* vol. 43, no. 2, pp. 631-675, 2014.

[103] B. V. A. J. P. B. S. K. T. Q. N. M. S. a. J. M. S. Kumar, "Reduced SnO2 porous nanowires with a high density of grain boundaries as catalysts for efficient electrochemical CO2 into HCOOH conversion.," *Angewandte Chemie International Edition,* vol. 56, no. 13, pp. 3645-3649, 2017.

[104] "Mantra Venture Group announces strategy for 2010," PRNewswire, 13 Janurary 2010. [Online]. Available: Mantra Venture Group announces strategy for 2010. [Accessed 02 May 2019].

[105] J. L. M. F. B. J. E. P. I. Y. H. I. C. F. J. E. P. T. Z. K. L. J. G. Y. Y. T. W. S. E. A. a. A. B. B. White, "Light-driven heterogeneous reduction of carbon dioxide: Photocatalysts and photoelectrodes," *Chemical Reviews,* vol. 115, no. 23, pp. 12888-12935, 2015.

[106] W. S. W. X. M. a. J. G. Wang, "Recent advances in catalytic hydrogenation of carbon dioxide," *Chemical Society Reviews 40,* vol. 40, no. 7, pp. 3703-3727, 2011.

[107] "Gaseous Carbon Waste Streams Utilization Status and Research Needs," NAP, 2019.

[108] G. L.Guczi, "Methane dry reforming with CO2: A study on surface carbon species," *Applied Catalysis A: General,* vol. 375, no. 2, pp. 236-246, 2010.

[109] A. G. M. C. a. G. K. S. P. George A. Olah, "Bi-reforming of Methane from Any Source with Steam and Carbon Dioxide Exclusively to Metgas (CO–2H2) for Methanol and Hydrocarbon Synthesis," *J. Am. Chem. Soc,* vol. 135, no. 2, p. 648–650, 2013.

[110] W. C.-S. J.-H. C.-C. L.-S. B. Seung-Ho Lee, "Tri-reforming of CH4 using CO2 for production of synthesis gas to dimethyl ether," *Catalysis Today,* vol. 87, no. 1-4, pp. 133-137, 2003.

[111] S. D. S. H. J. A. H. a. M. B. M. Ebbesen, "High temperature electrolysis in alkaline cells, solid proton conducting cells, and solid oxide cells," *Chemical Reviews* , vol. 114, no. 21, pp. 10697-10734, 2014.

[112] S. D. a. M. M. Ebbesen, "Electrolysis of carbon dioxide in solid oxide electrolysis cells," *Journal of Power Sources,* vol. 193, no. 1, pp. 349-358, 2009.

[113] Haldor Topsoe, [Online]. Available: https://www.topsoe.com/processes/carbon-monoxide/site-carbon-monoxide. [Accessed 02 May 2019].

[114] C. C. M. a. P. B. Mittal, "Small-scale CO from CO2 using electrolysis," *Chemical Engineering World,* vol. 52, no. 3, pp. 44-46, 2017.

[115] H. Y.-W. C. A. B. F. S. C. S. B. I. S. N. J. D. I. Z. H. S. J. K. K. E. A. S. J. C. Y. J. R. a. B. R. C. Mistry, "Enhanced carbon dioxide electroreduction to carbon monoxide over defect-rich plasma-activated silver catalysts," *Angewandte Chemie International Edition,* vol. 56, no. 38, pp. 11394-11398, 2017.

[116] S. R. K. K. B. S. D. M. G. a. G. S. Neubauer, "Overpotentials and Faraday efficiencies in CO2 electrocatalysis–the impact of 1-ethyl-3-methylimidazolium trifluoromethanesulfonate," *dvanced Energy Materials,* vol. 6, no. 9, 2016.

[117] S. Y. H. C. K. W. H. S. L. H.-R. M. J. A. A. G. T. F. N. N. a. P. J. A. K. Verma, "Insights into the low overpotential electroreduction of CO2 to CO on a supported gold catalyst in an alkaline flow electrolyzer," *ACS Energy Letters ,* vol. 3, no. 1, pp. 193-198, 2018.

[118] P. C. S. E. M. K. W.-F. O. H. a. M. F. Jeanty, "Upscaling and continuous operation of electrochemical CO2 to CO conversion in aqueous solutions on silver gas diffusion electrodes," *Journal of CO2 Utilization,* vol. 24, no. 454-462, 2018.

[119] T. R. K. R. W. M. D. a. G. S. Haas, "Technical photosynthesis involving CO2 electrolysis and fermentation," *Nature Catalysis,* vol. 1, no. 1, pp. 32-39, 2018.

[120] R. B. Q. C. H. Y. S. D. S. Z. L. a. M. I. R. Kutz, "Sustainion imidazolium functionalized polymers for carbon dioxide electrolysis.," *Energy Technology,* vol. 5, no. 6, pp. 929-936, 2017.

[121] Z. R. I. M. Q. C. R. K. H. Y. K. L. M. K. S. L. a. D. R. L. Liu, "Electrochemical generation of syngas from water and carbon dioxide at industrially important rate," *Journal of CO2 Utilization ,* vol. 15, pp. 50-56, 2016.

[122] K. L. C. Z. ,. V. C. ,. Z. ,. Y. Y. L. Qiang Chang, "XAFS Studies of Fe−SiO2 Fischer-Tropsch Catalyst During Activation in CO, H2, and Synthesis Gas," *ChemCatChem,* vol. 11, no. 8, 2019.

[123] Sunfire, [Online]. Available: https://www.sunfire.de. [Accessed 02 May 2019].

[124] INERATEC, [Online]. Available: https://ineratec.de/en/home/. [Accessed 02 May 2019].

[125] "The world of plastics, in numbers," The Conversation, 09 Auguest 2018. [Online]. Available: http://theconversation.com/the-world-of-plastics-in-numbers-100291. [Accessed 02 May 2019].

[126] S. J. a. D. J. D. Poland, "A quest for polycarbonates provided via sustainable epoxide/CO2 copolymerization processes," *Green Chemistry,* vol. 19, no. 21, pp. 4990-5011, 2017.

[127] Y. X. S. S. L. G. R. X. W. a. F. W. Qin, "Recent advances in carbon dioxide based copolymers," *Journal of CO2 Utilization 11(Supplement C),* pp. 3-9, 2015.

[128] "Econic," [Online]. Available: http://econic-technologies.com/. [Accessed 02 May 2019].

[129] "Novomer," [Online]. Available: https://www.novomer.com/. [Accessed 02 May 2019].

[130] SK Energy, [Online]. Available: http://eng.skenergy.com/. [Accessed 02 May 2019].

[131] D. J. D. a. S. J. Wilsona, "What's new with CO2? Recent advances in its copolymerization with oxiranes," *Green Chemistry,* no. 10, 2012.

[132] Covestro, [Online]. Available: https://www.covestro.com. [Accessed 02 May 2019].

[133] E. H. S. R. G. a. J. M. Oelkers, "Mineral carbonation of CO2," *Elements,* pp. 4(5):333-337, 2008.

[134] National Center for Biotechnology Information, "COMPOUND SUMMARY:Calcium carbonate," PubChem Database, [Online]. Available: https://pubchem.ncbi.nlm.nih.gov/compound/10112. [Accessed 30 April 2019].

[135] The Freedonia Group, "GLOBAL DEMAND FOR CONSTRUCTION AGGREGATES TO EXCEED 48 BILLION METRIC TONS IN 2015," ConcreteConstruction, 09 February 2012. [Online]. Available: https://www.concreteconstruction.net/business/global-demand-for-construction-aggregates-to-exceed-48-billion-metric-tons-in-2015_o. [Accessed 30 April 2019].

[136] W. Huijgen, "Carbon Dioxide Sequestration by Mineral Carbonation," Energy Research Centre of the Netherlands, Wageningen University, The Netherlands , 2007.

[137] J. B. R. W. S. K. P. S. H.H. Khoo, "Carbon capture and utilization: preliminary life cycle CO2, energy,and cost results of potential mineral carbonation," *Energy Proc.,* vol. 4, pp. 2494-2501, 2011.

[138] R. A. J. F. C. S. M. D. Sandalow, "Carbon Dioxide Utilization (CO2U) ICEF Roadmap 2.0," Lawrence Livermore National Laboratory, 2017.

[139] BluePlanet, "BluePlanet," [Online]. Available: http://www.blueplanet-ltd.com/. [Accessed 30 April 2019].

[140] Carbon8, "Carbon8," [Online]. Available: http://c8s.co.uk/. [Accessed 30 April 2019].

[141] Carbon Cure, "Carbon Cure," [Online]. Available: https://www.carboncure.com/. [Accessed 30 April 2019].

[142] SolidaTech, "SolidaTech," [Online]. Available: https://solidiatech.com/. [Accessed 30 April 2019].

[143] JRC -IEA, "ILCD handbook—International reference life cycle data system (ILCD) handbook - general guide for life cycle assessment - detailed guidance," European Commission - Joint Research Centre - Institute for Environment and Sustainability, Luxembourg, 2010.

[144] C. A. H. T. A. J. D. E. D. J. E. M. E. B. S. T. M. Jiyong Kim, "Methanol production from CO2 using solar-thermal energy: process development and techno-economic analysis," *Energy Environ. Sci.,* , vol. 4, pp. 3122-3132, 2011.

[145] J. K. R. G. H. Zhang C, "Carbon dioxide utilization in a gas-to-methanol process combined with CO2/Steam-mixed reforming: Techno-economic analysis," *Fuel,* vol. 190, pp. 303-311, 2017.

[146] W. L. F. J. Matthew Jouny, "General Techno-Economic Analysis of CO2 Electrolysis Systems," *Ind. Eng. Chem. Res.*, vol. 57, no. 6, p. 2165–2177, 2018.

[147] S. S. S. B. D. C. V. N. K. Mondal, "Dry reforming of methane to syngas: a potential alternative process for value added chemicals - a techno-economic perspective," *Environ Sci Pollut Res,* vol. 23, pp. 22267-22273, 2016.

[148] P. B.Anicic, "Comparison between two methods of methanol production from carbon dioxide," *Energy,* vol. 77, pp. 279-289, 2014.

[149] Econic, "UK'S FIRST CARBON CAPTURE UTILISATION DEMONSTRATION PLANT OPENS ITS DOORS," 06 March 2018. [Online]. Available: http://econic-technologies.com/news/uk-first-ccu-demo-plant/. [Accessed 08 May 2019].

[150] F.-D. C. D. S. M. C. G. R. P. D. A. A, "Prospective techno-economic and environmental assessment of carbon capture at a refinery and CO2 utilisation in polyol synthesis," *Journal of CO2 Utilization,* vol. 21, pp. 405-422, 2017.

[151] F.-D. C. V. A, "Closing carbon cycles: Evaluating the performance of multi-product CO2 utilisation and storage configurations in a refinery," *Journal of CO2 Utilization,* vol. 23, pp. 12-142, Journal of CO2 Utilization.

[152] "Formic Acid Manufacture: Carbon Dioxid eUtilization Alternatives," *applied sciences,* 2018.

[153] J. C. S. A. B. T. Mar Pérez-Fortes, "Methanol synthesis using captured CO2 as raw material:Techno-economic and environmental assessment," *Applied Energy,* vol. 161, pp. 718-732, 2016.

[154] F. D. P. R. M. K. Schaub T, "Process for preparing formic acid by reaction of carbon dioxide with hydrogen". United States Patent 8791297 B2, 2014.

[155] I. B. M. L. R. D.-R. I. E. Rubén Aldaco, "Bringing value to the chemical industry from capture, storage and use of CO2: A dynamic LCA of formic acid production," *Science of The Total Environment,* vol. 663, pp. 738-753, 2019.

[156] K.-W. J. ,. R. G. Y.-J. L. ,. S. C. K. Chundong Zhang, " Efficient utilization of carbon dioxide in gas-to-liquids process: Processsimulation and techno-economic analysis," *Fuel,* vol. 157, pp. 285-291, 2015.

[157] P. G.-G. R. H. E. R. M. C.-F. A. A. a. R. W. K. A. Ioanna Dimitriou, "Carbon dioxide utilisation for production of transport fuels: process and economic analysis," *Energy and Environmental Science,* no. 6, 2015.

[158] P. Schmidt, "Power-to-Liquids potentials and perspectives for future supply of renewable aviation fuel," German Environment Agency, 2016.

[159] S. &. M. S. &. S. V. &. S. G. &. S. P. Michailos, "Dimethyl ether synthesis via captured CO2 hydrogenation within the power to liquids concept: A techno-economic assessment.," *Energy Conversion and Management,* vol. 184, pp. 262-276, 2019.

[160] P. &. P. V. &. G. R. &. A. S. Kongpanna, "Techno-economic evaluation of different CO2-based processes for dimethyl carbonate production.," *Chemical Engineering Research and Design.,* vol. 93, pp. 496-610, 2015.

[161] Phytonix, *Dark Cycle Efficient & Low-Cost Production of Butanol from Carbon Dioxide, Water & Sunlight,* 2015 BIO World Congress on Industrial Biotechnology, Montreal, Canada.

[162] F. B. M. H. L. W. R. A. B. Robert Nilsson, "Techno-economics of carbon preserving butanol production using a combined fermentative and catalytic approach," *Bioresource technology,* vol. 161, pp. 263-269, 2014.

[163] S.-T. Yang, *Engineering Clostridia for n-Butanol Production from Lignocellulosic Biomass and CO2,* Ohio State University, 2017.

[164] R. S. G. O. A. S. M. Arno Zimmermann, "OME Worked Example for the tea guidlines for co2 utilization," CO2Chem Media and Publishing Ltd, 2019.

[165] J. B. E. S. H. H. N. Schmitz, *Fuel,* vol. 185, pp. 67-72, 2016.

[166] K. A. P. S. S. Michailos, "Techno-Economic Assessment of Methanol Synthesis via CO2 hydrogenation," Sheffield, UK, 2018.

[167] X. L. Z. W. H. a. D. Z. Qingchun Yang, "Efficient Utilization of CO2 in a Coal to Ethylene Glycol Process Integrated with Dry/Steam-Mixed Reforming: Conceptual Design and Technoeconomic Analysis," *ACS Sustainable Chem. Eng,* vol. 7, pp. 3496-3510, 2019.

[168] P. K. ,. E. Atsonios K., "Thermocatalytic CO 2 hydrogenation for methanol and ethanol production: Process improvements," *International Journal of Hydrogen Energy,* vol. 41, no. 2, pp. 792-806, 2016.

[169] R. M. L. Bellotti D, "Economic feasibility of methanol synthesis as a method for CO 2 reduction and energy storage," *Energy Procedia,* 2019.

[170] J. S. A. B. E. T. M. Pérez-Fortes, "Methanol synthesis using captured CO2 as raw material: techno-economic and environmental assessment," *Appl Energy,* vol. 161, pp. 718-732, 2016.

[171] P. K. K. E. Atsonios K., "Investigation of technical and economic aspects for methanol production through CO 2 hydrogenation," *International Journal of Hydrogen Energy,* 2016.

[172] C. C. Szima S., "Improving methanol synthesis from carbon-free H 2 and captured CO 2 : A techno-economic and environmental evaluation," *Journal of CO2 Utilization,* vol. 24, pp. 555-563, 2018.

[173] T. P. D. Anicic B., "Comparison between two methods of methanol production from carbon dioxide," *Energy,* vol. 77, pp. 279-289, 2014.

[174] R. G. M.Hornberger, "Calcium Looping for CO2 Capture in Cement Plants – Pilot Scale Test," *Energy Procedia,* vol. 114, pp. 6171-6174, 2017.

[175] Y. Hori, "Electrochemical CO2 Reduction on Metal Electrodes," in *Modern Aspects of Electrochemistry*, New York, Springer, 2008, pp. 88-189.

[176] "World Population Forecast (2020-2050)," [Online]. Available: https://www.worldometers.info/world-population/#table-forecast. [Accessed 22 March 2019].

Chapter 3 – Techno-economic and Environmental assessment of CCU indirect DME synthesis

Term	Acronym
Greenhouse gas	GHG
Carbon capture and storage	CCS
Carbon capture and utilisation	CCU
Dimethyl ether	DME
Global warming potential	GWP
Redlich-Kwong-Soave	RK
Non-random two-liquid	NRTL
Water gas shift	WGS
Dry methane reforming	DMR
Total capital investment	TCI
Total direct costs	TDC
Total indirect costs	TIC
Fixed capital investment	FCI
Working capital	WC
Total capital investment	TCI
Fixed cost of production	FCP
Operating supervision	OS
Annual maintenance and repair costs	AMR
Variable costs of production	VCP
Annual capital repayment	ACR

capital expenditure	CAPEX
Life cycle assessments	LCA
Component object model	COM
Mixed integer non-linear programming	MILP
Mesh adaptive search	MADS
Aspen Energy Analyzer	AEA
Cost of global warming potential reduction	CGWP
Minimum fuel selling price	MFSP
Liquified petroleum gas	LPG

1.0 Introduction and gaps in knowledge

A promising carbon capture and utilisation (CCU) option includes the production of dimethyl ether (DME) through dry-reforming, bi-reforming and tri-reforming to produce a syngas intermediate [1] [2] [3]. DME has multiple applications including aerosols, personal care products and as a diesel substitute. The available synthesis routes for DME includes a one-step direct synthesis from syngas or an indirect route through methanol dehydration, with a methanol intermediate produced from syngas as an intermediate [4].

Several techno-economic studies have been carried out on DME production via the direct and indirect route implementing a variety of feed stocks including natural gas, biomass and shale gas. Schakel et al. conducted a techno-environmental study on direct DME synthesis via dry methane reforming with natural gas and captured CO_2 from a hydrogen production unit. It was found that CO_2 avoidance is limited to 9% due to significant utility demands for heating and direct CO_2 formation [5]. Sensitivity analyses were performed to investigate the effect of a few process conditions on the technical performance of the process (e.g. DME production rate). Uddin et al. conducted a techno-economic and uncertainty analysis of an indirect DME production plant from syngas produced via bi-reforming of captured CO_2 from an ammonia plant or landfill, DME production costs were estimated at \$0.87/gal for the ammonia plant and \$0.91/gal for the landfill scenario [6]. None of these two studies carried out process optimisation, focusing instead on deterministic calculations of costs and environmental impacts and thus potentially overestimating these two important parameters.

Model-based process optimisations of DME synthesis based on sustainability and economics metrics have mainly focused on the indirect DME process. Asadi et al. conducted a multi-objective optimisation of the conventional indirect DME production process decreasing GWP by a factor of 10 whilst decreasing the return

on investment by 6% [7]. The study only focused on the DME synthesis step and thus did not consider the methanol production process. Mevawala et al. carried out a techno-economic optimisation of the DME synthesis process via the direct and indirect route from shale gas. It was found that after optimisation, the breakeven DME price for the direct and indirect DME synthesis process decreased by 9.52% and 0.48% respectively [8].

The aforementioned publications which conducted techno-economic optimisations of the indirect DME production process have either limited the system boundary to the DME production section or incorporated alternative syngas sources, such as shale gas rather than syngas from reforming technologies using captured CO_2 as a feed. Furthermore, limited techno-economic and environmental performance data is available in the literature for CO_2 utilisation pathways to indirect DME production, including dry methane reforming and tri-reforming.

2.0 DME background

DME is a highly flammable, non-toxic, colourless gas under ambient conditions. It is an organic compound with the chemical formula CH_3-O-CH_3 and is the simplest ether. DME has similar physical properties to liquified petroleum gases. DME has good storage properties as it has a vapor pressure of 6 bar at room temperature. It may be easily stored as a liquid at low pressures [a].

Table 3.1. Physical properties of dimethyl ether.

Chemical Formula	CH_3OCH_3
Molecular weight (g mol^{-1})	46.07
Density (g cm^{-3})	0.661
Normal Melting point (°C)	-141
Normal boiling point (°C)	-24.9
Vapour pressure (bar)	1.5
Solubility in water (g dm^{-3})	71 at 20 °C

Due to increasing oil prices due to oil embargos and increased supply of natural gas in the seventies and eighties, significant research was done regarding the conversion to liquid fuels. Amoco (BP), developed a range of technologies producing conventional and novel fuels and fuel additives including DME.

Further collaboration between Amoco, Haldor Topsoe and Navistar International corp identified methanol dehydration as a possible route for DME synthesis and DME as a diesel alternative. Haldor Topsoe further developed the methanol dehydration route for DME manufacturing. A partnership between Amoco and General Electric Co. (GE) proved DME's validity as a gas turbine fuel [9].

2.1 DME uses and applications

DME has a range of applications including as a diesel substitute, as a liquefied petroleum gas (LPG) substitute and as a propellent. DME can also be used as an intermediate to various chemicals such as dimethyl sulfate, methyl acetate, acetic acid, olefins and gasoline.

2.1.1 DME as a refrigerant and propellent

DME is used as a refrigerant and high-grade propellent for a range of end-user products such as home and personal care items and pharmaceuticals. This is due to the several advantages it has such as its high stability, low odor and low toxicity. DME is recommended as an environmentally friendly alternative to aerosols and refrigerants such as chlorofluorocarbons, as in comparison it has a lower GWP and zero ozone depletion potential.

DME is designated R-E170 in ANSI/ASHRAE and may be used in refrigerant blends such as with ammonia, CO_2 and propene. Adamson reported that DME has favourable properties as a substitute for R12 in small systems [10]. Zharov et al studied the use of a DME and CO_2 refrigeration mixture for air conditioning systems. It was found that a max DME concentration of 8.3% is suitable prior to the mixture becoming unsafe due to excessive flammability [11].

2.1.2 DME as a fuel

Due to concerns regarding energy security and environmental impact, DME has been identified as an alternative fuel to diesel in compression ignition. DME provides improved combustion efficiency in comparison to diesel due to the significant C-O bond presence (~34.8 wt.% oxygen content) [12]. The improved combustion efficiency and the decreased flame temperature requirements for DME, provides reduced NOx emissions. The oxygen promotes complete combustion, reducing carbon monoxide and unburnt carbon emissions. Furthermore, the oxygen reduces the air requirement for combustion, further reducing NOx emissions [13]. DME decreases soot and particulate emissions significantly, as there is an absence of C-C bonds in DME and a lower ignition delay when compared to diesel. This is of relevance as internal combustion engines are a major source of air pollution, accounting for 30% of all air pollution [14].

Table 3.2. DME and diesel properties comparison as a fuel.

Properties	DME	Diesel fuel
Chemical formula	CH_3-O-CH_3	-
Molar mass (g mol^{-1})	46	170
Oxygen content (% w/w)	34.8	0
Carbon to hydrogen ratio	0.337	0.516
Cetane number[a]	55-66	40-50
Lower heating value (MJ kg^{-1})	27.6	42.5
Viscosity (cP)	0.15	2
Density (kg m^{-3})	660	831
Auto-ignition temperature (K)	508	523
Boiling point (K)	248.1	450-643
Stoichiometric air-fuel mass ratio	8.9	14.6

[a] For compression ignition engines, the cetane number provides a measure of the self-ignition properties of the fuel.

The lower bond energy of C-O compared to C-H increases the ease of breaking the bonds, this allows DME to have a shorter ignition delay and a higher cetane number compared to diesel.

However, when compared to diesel an 80% increased volume of DME is required for a similar energy output due to the significantly lower LHV. Furthermore, DME's low viscosity and reduced lubrication properties, increases the risk of fuel leakage and wear to fuel injection system parts [15].

Table 3.3. Advantages and disadvantages of DME in comparison to diesel as a fuel

Advantages	Disadvantages
High oxygen content	Lower LHV-larger fuel tank
High cetane number	Low viscosity
Quick evaporation of liquid phase DME when injected into the engine cylinder	Lower boiling point- pressurised system to maintain liquid state
Non-corrosive	Lower modulus of elasticity

2.1.3 DME for LPG

DME may be used as a liquefied petroleum gas (LPG) substitute. DME is blended with LPG for domestic applications such as cooking and heating at percentages of up to 25 vol%. However, at blending levels below 20 vol% current infrastructure may be used with little to no modifications. The greatest demand for DME/LPG blends is in the Asia Pacific region, especially China, due to rising oil prices and the desire to reduce reliance on imported oil and LPG.

DME has similar physical properties to LPG therefore storage and transport infrastructure for LPG do not require adjusting.

2.2 DME synthesis routes

DME may be synthesised from a range of feedstocks including natural gas, coal and carbon dioxide. Coal or biomass is converted to syngas through gasification.

DME may be synthesised either directly from syngas in one step or indirectly via methanol dehydration, wherein which methanol is produced from the syngas as an intermediate [4].

The indirect process concludes through an initial methanol synthesis step,

$$CO + 2H_2 \leftrightarrow CH_3OH \qquad \textit{Eqn.M1}$$

$$CO_2 + 3H_2 \leftrightarrow CH_3OH + H_2O \qquad \textit{Eqn.M2}$$

$$CO_2 + H_2 \leftrightarrow CO + H_2O \qquad \textit{Eqn.RWGS}$$

followed by a dehydration reaction.

$$2CH_3OH \leftrightarrow CH_3OCH_3 + H_2O \qquad \textit{Eqn.DME}$$

To allow for this a hybrid bifunctional catalyst of a mechanically mixed and pelletised typical metallic methanol synthesis catalyst (Cu-based) and a typical acidic methanol dehydration catalyst (e,g γ-Al_2O_3) is used .

$$CO + 2H_2 \leftrightarrow CH_3OH \qquad \textit{Eqn.M1}$$

$$CO_2 + 3H_2 \leftrightarrow CH_3OH + H_2O \qquad \textit{Eqn.M2}$$

$$CO_2 + H_2 \leftrightarrow CO + H_2O \qquad \textit{Eqn.RWGS}$$

$$2CH_3OH \leftrightarrow CH_3OCH_3 + H_2O \qquad \textit{Eqn.DME}$$

The direct DME synthesis route offers advantages in maximising hydrogenation through the shifting of the thermodynamic equilibrium favourably due to the continuous removal of methanol from the system. The direct synthesis process has been developed by multiple companies such as Haldor-Topsoe, J.F.E and Air product, however none have reached commercial viability. Industrial application is limited as the single step process separation complexity and costs are significantly increased due to the gases that need to be separated and catalyst deactivation consideration. The γ-alumina is deactivated easily due to water which in turn blocks

the methanol dehydration active sites. Further research and development have focussed upon incorporating less hydrophilic materials for the acidic element such as zeolites including HZSM-5 and silicoaluminophosphates (SAPOs) [16] [17]. In order to allow them to be suitable replacements for γ-alumina, to minimise coke formation there is a requirement for high site density and moderate acidity.

Two alternative synthesis routes are used for direct DME synthesis, *DrctDME1 and DrctDME2*:

$$3CO + 3H_2 \leftrightarrow CH_3OCH_3 + CO_2 \qquad \textit{Eqn.DrctDME1}$$

$$2CO + 4H_2 \leftrightarrow CH_3OCH_3 + H_2O \qquad \textit{Eqn.DrctDME2}$$

The JFE direct synthesis reaction implements *DrctDME1*. *DrctDME1* synthesises DME through a combination of methanol synthesis, methanol dehydration, and a water gas shift reaction. The Haldo Topsoe direct DME synthesis route follows *DrctDME2*. *DrctDME2* synthesises DME through a combination of methanol synthesis and methanol dehydration.

3.0 Study outline

This work aims to assess and compare the techno-economic performance and global warming potential (GWP) of CO_2 utilisation processes for scenarios based on three reforming technologies: dry methane reforming, bi-reforming and tri-reforming, which is compared to the use of steam reforming as the conventional technology of indirect DME production. CO_2 captured from a cement manufacturing plant is used as the source of CO_2 for the reforming processes. Each reforming technology is optimised towards minimisation of operating costs and GWP and further improved through heat integration and heat exchanger network optimisation. The scenarios considered are shown in Table 3.4.

Table 3.4. Table outlining list of indirect DME production scenarios represented in this study.

Scenario	Reforming technology	Optimisation target
SR	Steam reforming	Operating Costs
DR-OPEX	Dry-reforming	Operating Costs
DR-GWP	Dry-reforming	GWP
BR-OPEX	Bi-reforming	Operating Costs
BR-GWP	Bi-reforming	GWP
ADTRI-OPEX	Adiabatic tri-reforming	Operating Costs
ADTRI-GWP	Adiabatic tri-reforming	GWP
ISOTRI-OPEX	Isothermal tri-reforming	Operating Costs
ISOTRI-GWP	Isothermal tri-reforming	GWP

4.0 Methodology

Modelling and simulation of the scenarios examined are developed on Aspen Plus V12, the commercial simulation software developed by Aspen Tech, to allow for the calculations of mass and energy balances. Due to the robust nature of the software, it is widely deployed in chemical engineering related industries and research in the process of the design and optimisation of chemical plants [18]. Optimisation has been completed using MATLAB R2020b and the actxserver function to link Aspen Plus to MATLAB. Heat integration has been carried out using the Aspen Energy Analyser. Based on the optimised simulation results, the production costs of DME have been calculated including the contribution of the capital and operating costs on the total cost of production. Sensitivity and uncertainty analysis have been completed on significant parameters affecting the economics of the process, such as capital expenditure and CO_2 feedstock costs.

4.1 System boundaries

The main aim of this work is to provide an assessment of the economics and the environmental impact of the implementation of carbon dioxide utilisation

technologies in a cement manufacturing plant including the costs and GWP of the capture, compression and transport of CO_2 .Therefore, it is of great importance that suitable system boundaries that align with research goals are set to allow for an appropriate assessment of the techno-economic and environmental factors of a process. Figure 3.1 shows the system boundary implemented for the CCU and conventional DME production options. To ease comparisons between the different process scenarios considered, the system boundary was limited to the indirect DME production process, which incorporates methanol synthesis and DME synthesis as separate processing steps. The CO_2 exiting from the CCU plant is not captured and is emitted to the environment.

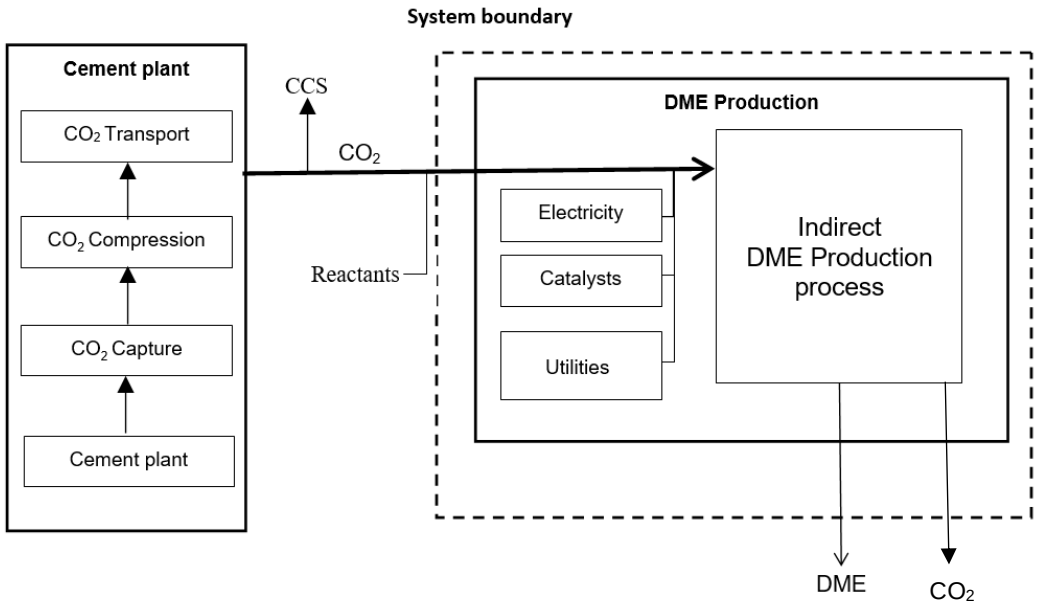

Figure 3.1. System boundary for the CCU and conventional production scenarios. The CO_2 feed is only present in the CCU scenarios.

4.2 Plant location and scale

The plant location is a significant factor regarding the economics of a process due to the variance in costs depending on the region and country the plant is located. Several factors are affected by plant location including the cost of materials, labour costs; duties and taxes; transportation costs and equipment costs. Furthermore, the

design and engineering of the plant is affected by the plant location due to need to adhere to local regulations that may affect design complexity and plant sizing that is compatible with market supply and demand. For this study it was assumed the plant is located in the United Kingdom.

A suitable plant scale is required to allow for results that are of relevance to real-world industrial applications therefore it is of importance an appropriate production rate is chosen. Due to the variability in the CCU processes examined and the need to provide a comparison between them, the cement plant is used as a basis for the production scale as it is the common factor between the CCU processes. The cement plant was assumed to operate at a production rate indicative of a reference European cement plant which is 1,000,000 tonnes of clinker produced annually (or approximately 3000 tonnes per day) [18]. This production rate provides the amount of CO_2 that is released and captured. The CCU plant assumes an estimated 10% usage of the captured CO_2 as a raw material, to account for . Due to this the selected capture technology is significant. A range of factors are of importance in selecting a suitable carbon capture technology, including the technology maturity, the efficiency of the capture operation and the costs of the capture process. In order to provide a conventional process of comparable production scale for comparison, the sizing was based upon the upper and lower bounds outlined in section 4.10.3.

Gardarsdottir et al carried out a study where they compared different carbon capture technologies retrofitted to a cement plant including MEA and chilled ammonia-based absorption, oxyfuel, calcium looping and membrane-assisted CO_2 liquification [19]. They found that the oxyfuel capture unit provided the lowest capture cost reducing process GWP by 719 kg CO_2-eq per tonne clinker. Therefore, for this study, it was assumed that CCU processes use 9900 kg hr^{-1} of CO_2 captured from an oxyfuel capture unit with costs and process characteristics based on the work by Gardarsdottir et al. A summary of key plant characteristics is shown in Table 3.5.

Table 3.5. Cement plant location, capacity, and captured CO_2 data.

Plant location	United Kingdom
Production capacity (Mtonnes clinker yr^{-1})	1
Annual operating hours (hours)	8000
CO_2 capture technology	Oxyfuel
Clinker produced (tonne hr^{-1}) [19]	125
CO_2 captured (tonne hr^{-1}) [19]	99
Captured CO_2 to CCU (%)	10

4.3 Process outline

As shown in Figure 3.2, the process scenarios modelled include the reforming section either via steam-, dry-, bi- or tri- reforming with an initial input of captured CO_2 from the cement plant and other required reactants. The syngas produced from the reforming process passes to the methanol synthesis section which acts as an intermediate for DME synthesised further downstream.

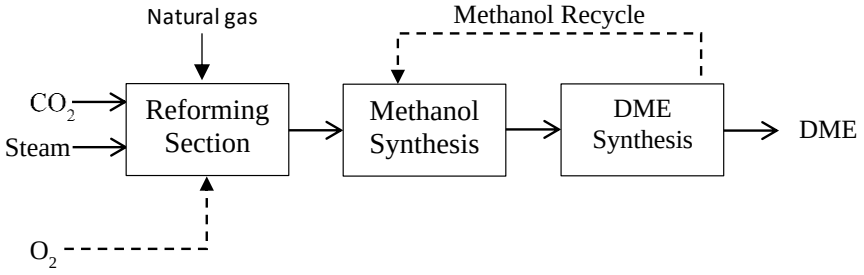

Figure 3.2. Block flow diagram of the reforming process for indirect DME production from CO_2 captured from a cement plant. The O_2 feed stream is only present in the tri-reforming scenarios.

4.4 Modelling assumptions

All scenarios have been modelled in steady-state using the sequential modular mode within Aspen Plus V12. The Broyden method was used for the convergence of tear

streams, design specifications and recycles. To determine the physical and thermodynamic properties of streams and individual components, the Redlich-Kwong-Soave (RK) model with the Modified Huron-Vidal Second Order mixing rule (MHV2) was used for high pressure streams (>10bar) [20]. For all other streams, the non-random two-liquid (NRTL) model with the RK equation of state for estimating vapour phase properties was used [20] .

Compressor and gas turbine mechanical and isentropic efficiencies are 100% and 71.5% respectively whilst pumps are set at 70% pump efficiency and 80% driver efficiency. Isentropic efficiencies for high, medium and low-pressure steam turbines are 92%, 94% and 88% respectively [21]. A minimum approach temperature difference of 10 °C was implemented for all heat transfer in the processes.

A summary of key units operating conditions and simulation assumptions are shown in Table 3.6.

Table 3.6. Summary of key units' operating conditions and simulation assumptions

	Feedstocks
NG feed	NG pipeline system; 25 bar, 40 °C [22]; 88.71 mol% CH_4, 6.93 mol% C_2H_6, 1.25 mol% C_3H_8, 0.28 mol% n-C_4H_{10}, 0.05 mol% n-C_5H_{12}, 0.02 mol% n-C_6H_{14}, 0.82 mol% N_2, and 1.94 mol% CO_2 [23]
Steam feed	42 bar, 350 °C

Make up water feed	1 bar, 25 °C
Oxygen feed (tri-reforming)	80 bar, 25 °C; Air cryogenic separation [24]
	Reforming section
Pre-reformer	Gibbs reactor; Adiabatic; Catalyst: $Ni/MgAl_2O$ [25]
Reformer	Plug flow reactor; Number of tubes:439; Reactor length: 10m; Reactor tube diameter:0.1m
Gas shift unit	Gibbs reactor; Adiabatic; Catalyst: Fe_2O_3/Cr_2O_3 [26]
	Methanol synthesis section
Methanol reactors	Four plug flow reactors in parallel; Adiabatic; Inlet temperature:250 °C;

	Inlet pressure:60 bar;
	Reactor length:2.6 m;
	Reactor diameter:10m;
	Catalyst: $CuO/ZnO/Al_2O_3$ [27]
Methanol recovery unit	RadFrac equilibrium column;
	Condenser pressure: 1.36 bar;
	Pressure drop: 0.34 bar;
	Reflux ratio: 1.26;
	No. of stages:52;
	Feed stage:27
	DME synthesis section
DME synthesis reactor	Plug flow reactor;
	Adiabatic;
	Number of tubes:2000;
	Reactor length: 10m;
	Reactor tube diameter: 0.05m;
	Catalyst: γ-Al_2O_3 [28]
DME purification unit	RadFrac equilibrium column;
	Condenser temperature: 35 °C;
	Condenser pressure: 10 bar

Reflux ratio: 8;

No. of stages: 80;

Feed stage:40

4.5 Syngas production

The conversion of the feed to syngas is completed in the reforming section shown in Figure 3.3. An initial pre-reforming of the natural gas feed is carried out utilising steam, where the output is mixed with the CO_2 feed (and oxygen for the tri-reforming scenarios only). If further adjustment of syngas composition was needed, a water gas shift reactor (WGS) was included.

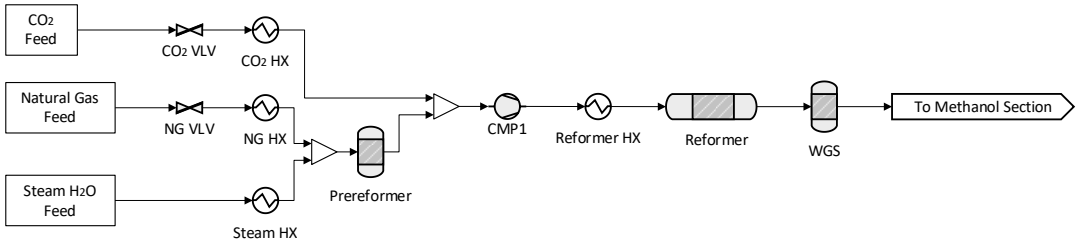

Figure 3.3. Flowsheet of reforming section.

4.5.1 Pre-reformer

Pipeline natural gas does not only contain methane but also significant amounts of higher hydrocarbons such as ethane, butane and pentane [23]. Therefore, an initial pre-reforming step is employed to convert the natural gas feed composed of a range of hydrocarbons to a methane rich product.

The implementation of the pre-reformer provides advantages in terms of reduced capital costs due to reduction in reformer size requirements and in turn allowing for a reduction in utility requirements [29]. Furthermore, a pre-reformer reduces the risk of carbon formation occurring in the primary reformer and increases plant feed

composition flexibility. The pre-reformer operates at a temperature range of 350 to 650 °C as an adiabatic steam reformer via a nickel-based catalyst [30]. For simulating the pre-reformer, a Gibbs reactor operating at chemical equilibrium under adiabatic conditions was used.

4.5.2 Reforming

The reforming technologies considered and modelled in this study include steam methane, dry-, bi- and tri- reforming. These are described in the following sections.

4.5.2.1 Steam methane reforming

The catalytic steam reforming of methane is the most commonly used reforming technology in industry for the production of syngas. Natural gas mixed with steam is converted to CO, CO_2 and H_2 via a set of endothermic, irreversible reactions over the catalyst pellets:

$$CH_4 + H_2O \leftrightarrow CO + 3H_2 \qquad \textit{Eqn.SMR1}$$

$$CH_4 + 2H_2O \leftrightarrow CO_2 + 4H_2 \qquad \textit{Eqn.SMR2}$$

$$CO + H_2O \leftrightarrow CO_2 + H_2 \qquad \textit{Eqn.SMR3}$$

In this study optimisation for the steam reforming scenario was based upon typical operating pressure and temperature, which range from 5-40 bar and 700-1000 °C respectively, using a Ni/Al_2O_3 based catalyst [31]. To allow for an increased conversion of natural gas, a significant amount of steam is introduced at a steam-to-carbon molar ratio of 3 to 5. The steam reformer model in this work implements the reaction kinetics developed by Xu and Froment shown in Appendix 1 [32].

4.5.2.2 Dry reforming

Dry methane reforming (DMR) involves the reaction of methane with CO_2 to produce syngas:

$$CH_4 + CO_2 \leftrightarrow 2CO + 2H_2 \qquad \textit{Eqn.DMR}$$

The main limitation for the large-scale implementation of dry reforming is the significant catalyst deactivation occurring due to carbon deposition, especially at lower reaction temperatures. The major source of carbon deposition in this process is the occurrence of methane decomposition and the Boudouard reaction. To minimise these, the DMR reactor temperature is typically maintained at 800-1000 °C. Common catalysts used in DMR are based upon Ni, where a coupling with noble metals is preferred to reduce carbon deposition [33]. This study has used the kinetics developed by Zhang et al over a bi-metallic Ni-CO/Al-Mg-O catalyst coupled with the kinetics for the reverse water gas shift reaction by Richardson et al, as shown in Appendix 1 [34] [35].

4.5.2.3 Bi-reforming

Bi-reforming combines the process of dry and steam reforming of methane with the following reactions taking place in the reformer:

$$CH_4 + CO_2 \leftrightarrow 2CO + 2H_2 \qquad \textit{Eqn.BR1}$$
$$CH_4 + H_2O \leftrightarrow CO + 3H_2 \qquad \textit{Eqn.BR2}$$
$$CH_4 + 2H_2O \leftrightarrow CO_2 + 4H_2 \qquad \textit{Eqn.BR3}$$
$$CO + H_2O \leftrightarrow CO_2 + H_2 \qquad \textit{Eqn.BR4}$$

The major advantage of this reforming technology compared to steam or dry methane reforming in an isolated manner is the capability to reduce carbon

deposition on the catalyst due to the decomposition of methane and the Boudourd reactions as discussed above [36].

Furthermore, catalyst stability is further enhanced via the presence of two oxidising agents such as CO_2 and H_2 and the capability to achieve the required H_2/CO ratio for downstream production processes via feedstock composition manipulation, therefore reducing the need for extra units. Bi-reforming typically occurs at temperatures ranging from 800-1100 °C and pressures of 5-30 atm. The kinetics developed by Park et al and based on a Ni-CeO_2/$MgAl_2O_4$ catalyst have been used to model the bio-reforming reactor in Aspen Plus, shown in Appendix 1 [37].

4.5.2.4 Tri reforming

The tri-reforming process combines the endothermic process of steam and dry reforming with the exothermic nature of partial oxidation:

$$CH_4 + H_2O \leftrightarrow CO + 3H_2 \qquad \textit{Eqn.TR1}$$

$$CH_4 + 2O_2 \leftrightarrow CO_2 + 2H_2O \qquad \textit{Eqn.TR2}$$

$$CH_4 + 2H_2O \leftrightarrow CO_2 + 4H_2 \qquad \textit{Eqn.TR3}$$

$$CO + H_2O \leftrightarrow CO_2 + H_2 \qquad \textit{Eqn.TR4}$$

Similarly to bi-reforming, the synergy of the individual reforming pathways limits the catalyst deactivation thus increasing catalyst life and process efficiency. The inclusion of oxygen greatly increases energy efficiency due to the heat released from the exothermic oxidation reaction and limits carbon formation. The tri-reforming reactor model in this study used the kinetic models developed by Xu and Froment [32] as well as Trimm and lam [38], for a Ni-based catalyst, as shown in Appendix 1.

4.5.3 Water gas shift

When the syngas produced from the reforming unit does not meet the optimal stoichiometric requirements for further synthesis, a high temperature water-gas shift unit has been employed. The high temperature gas shift (300-500 °C) is preferential to the low temperature shift process (180-280 °C) since the latter is used to achieve low CO content syngas which is unsuitable for further conversion to methanol [39].

The water gas shift unit was simulated as a Gibbs reactor in Aspen Plus operating at chemical equilibrium under adiabatic conditions, and optimised within the temperature range of 300-500 °C. The equilibrium of the water gas shift reaction,

$$CO + H_2O \leftrightarrow CO_2 + H_2, \qquad Eqn.WGS$$

is independent of pressure and is determined by the reaction temperature.

4.6 Methanol synthesis

The syngas feed is catalytically converted through the direct hydrogenation of CO and CO_2 to produce methanol according to the following reactions:

$$CO + 2H_2 \leftrightarrow CH_3OH \qquad Eqn.M1$$

$$CO_2 + 3H_2 \leftrightarrow CH_3OH + H_2O \qquad Eqn.M2$$

The reverse water gas shift reaction also takes place during methanol synthesis:

$$CO_2 + H_2 \leftrightarrow CO + H_2O \qquad Eqn.RWGS$$

Due to the presence of reversible exothermic reactions in the methanol synthesis process, conversion rates are limited through thermodynamic and chemical

equilibrium consideration. Although the RWGS reaction is endothermic due to the significance of *Eqn.M1* and *Eqn.M2* and their exothermic nature and molecule reduction in transfer from the reactant to product side, increased conversion to methanol is favourable using a low temperature and high pressure. Typical industrial methanol reactors implement a copper-zinc based catalyst, operating at temperatures ranging between 200-300 °C and pressures of 50-100 bar, to achieve a selectivity greater than 99.5%.

The methanol production model developed in this study was based on the ICI technology which accounts for approximately 60% of global methanol production [40]. The ICI-synetix technology uses a multi-bed direct-cooled adiabatic quench reactor configuration. The syngas feed is split into four fractions which are fed into the synthesis reactor into four alternate catalyst beds with successive cold quench gas to provide temperature control [41]. The reactors are operated adiabatically as there is a linear relationship between temperature and conversion for the exothermic methanol synthesis reactions, therefore suitable reactor and catalyst bed sizing is needed to allow each synthesis step to reach equilibrium. Temperature control is of importance to reduce catalyst damage due to increased temperatures and to increase equilibrium conversion. Furthermore, the stoichiometric ratio, S is adjusted to approximately 2.1 to maximise methanol synthesis [42]:

$$S = \frac{n_{H_2} - n_{CO_2}}{n_{CO} - n_{CO_2}} \qquad \textit{Eqn.1}$$

where n_i, is the number of moles of component i present in the methanol reactor feed. In this study, a fixed reactor inlet temperature of 250 °C and pressure of 60 bar was used using the kinetics over a commercial $CuO/ZnO/Al_2O_3$ catalyst developed by Skrzypek et al [27]. Figure 3.6 outlines the flowsheet for the methanol synthesis section.

Figure 3.4. Flowsheet for methanol synthesis section.

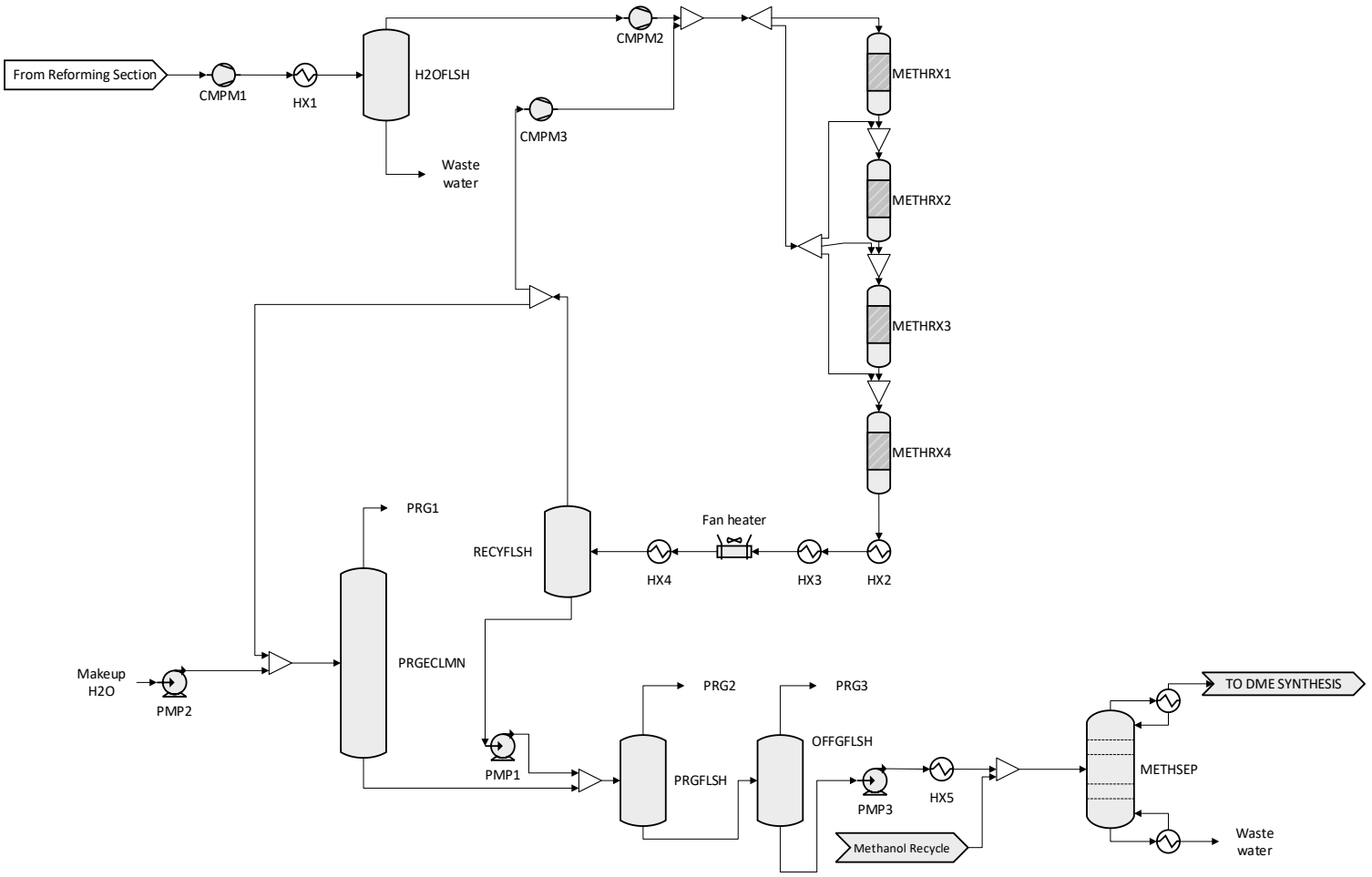

4.7 DME synthesis

The DME synthesis model in this study was based on Turton et al [43]. The process flow diagram of the DME processing step is shown in Figure 3.5 below.

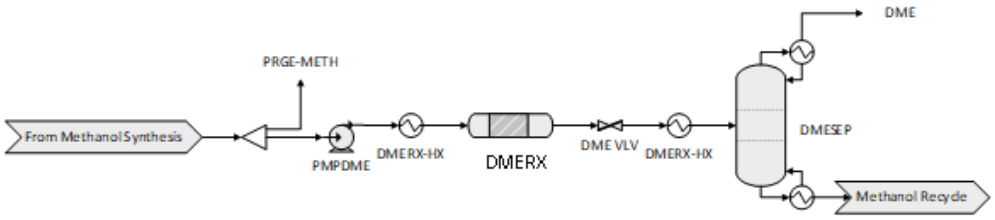

Figure 3.5. Flowsheet for DME synthesis section.

Purified methanol is pumped into a heat exchanger to increase the feed to the required reactor inlet pressure and temperature. In the DME reactor methanol dehydration occurs as an exothermic reversible reaction to produce the required DME through a fixed-bed reactor.

The reactor operates adiabatically through a gas phase reaction using a γ-Al_2O_3 catalyst at temperatures ranging from 160-360 °C and pressures ranging from 1-50 bar. The γ-Al_2O_3 is suitable due to high DME selectivity and high mechanical stability and resistance [44].In this study the kinetics parameters for methanol dehydration used was from Mollavali et al coupled with the equilibrium constant from Diep et al [28] [45]. The reactor effluent is depressurised to 10 bar and then cooled and condensed to a temperature of 125 °C prior to being sent to the distillation column. The distillation column allows for the DME to be separated to the required ASTM specification outlined in Table 3.7.

Table 3.7. ASTM specifications for DME *[46]*.

Property	Requirement
Dimethyl Ether, mass%, min	98.5
Methanol, mass %, max	0.05
Water, mass%, max	0.03
Vapor pressure, max	7.58 bar at 37.8 °C

The column bottoms containing methanol and water is recycled back to the methanol purification column included in the methanol synthesis section.

4.8 Economic assessment

Purchased equipment costs were estimated through the Aspen Icarus database within Aspen Plus V12, by an initial sizing estimate and mapping of all equipment. Pumps were mapped as single stage centrifugal pumps and compressors as horizontal centrifugal compressors.

Table 3.8. Key economic parameters.

Plant economic life (years)	20
Annual operating hours (hours)	8000
Base year	2019
Interest rate (%)	10

The total capital investment (TCI) for each scenario were then calculated from the purchased equipment cost using the factorial estimation method by Peters et al [47] for a fluid processing plant as outlined in Table 3.9.

Table 3.9. Cost factors used for economic analysis.

Cost component	Factor as a fraction of delivered equipment cost
Direct costs	
Purchased equipment, PC	1
Purchased equipment installation	0.47
Instrumentation & Controls(installed)	0.36
Piping (installed)	0.68
Electrical systems (installed)	0.11
Buildings (including services)	0.18
Yard improvements	0.10
Service facilities (installed)	0.70
Total direct costs (TDC)	3.60
Indirect costs	
Engineering and supervision	0.33
Construction expenses	0.41
Legal expenses	0.04
Contractor's fee	0.22
Contingency	0.44
Total indirect costs (TIC)	1.44
Fixed capital investment (FCI) = TDC + TIC	**5.04**
Working capital (WC)	0.89
Total capital investment (TCI) = FCI + WC	5.93

The fixed cost of production (FCP) accounting for all costs independent of plant productivity includes salaries, maintenance, insurance and property tax costs and

was determined through assumptions related to required operating labour and factors of the fixed capital investment. The annual maintenance and repair costs were assumed to be 6% of the TCI and includes maintenance labour costs which represents 40% of the annual maintenance and repair costs. Annual insurance and property tax including regulatory fees were assumed to be 3% of the TCI. Labour costs were based upon the assumption of number of employees, assuming 3 operators per shift and 3 shifts per day, at a cost of $34 per operating hour with operating supervision costs representing an estimated 15% of operating labour costs. Costs related to administrative and other support labour were estimated to represent an estimated 20% of operating labour, supervision, and maintenance costs. Other general plant overheads represent 60% of the operating labour, supervision, and maintenance costs. A summary of the FCP parameters is shown in Table 3.10.

Table 3.10. Fixed costs of production parameters and basis for calculation for economic analysis.

Fixed costs parameters	
Labour costs	
Operators per shift	3
Shifts per day	3
Operator wage	$\$34\ hr^{-1}$
Operating supervision (OS)	15% of total operating labour cost (OLC)
Other fixed costs	
Annual maintenance and repair costs (AMR)	6% of TCI
Operating supplies	15% of AMR
Laboratory charges	15% of AMR
Property tax	2% of FCI
Insurance	1% of FCI
Plant overheads	60% of (OLC+OS+AMR)
Administration and support labour costs	20% of (OLC+OS+AMR)

The variable costs of production (VCP) are affected by the production rate of the plant and the process conditions selected and includes all raw materials costs, utility

usage, waste streams disposal requirements and any other consumables such as catalysts. The VCP was determined based upon process simulation mass and energy balance results. The price inflation of equipment and raw materials were not considered for the ease of comparison between the evaluated process scenarios. Similarly, government subsidies and by-product revenues were excluded from the economic analysis. Costs related to material and utility are available in Appendix 1.

The annual capital repayment (ACR) was calculated to determine the annual payments required to pay back the loan used to provide the TCI for plant construction and set-up:

$$ACR = \frac{TCI \times r(1+r)^y}{(1+r)^y - 1} \qquad \textit{Eqn.2}$$

where r is the interest rate and y is the plants economic life [48].

The capital expenditure per tonne of DME produced (CAPEX) was calculated from the total FCP and the ACR:

$$CAPEX = \frac{ACR + FCP}{\dot{m}_{DME,out} \times OH} \qquad \textit{Eqn.3}$$

where $\dot{m}_{DME,out}$ is the mass flowrate ($t{\cdot}hr^{-1}$) of DME produced and OH is the annual operating hours.

The total production cost (TPC) per tonne of DME was calculated by:

$$TPC = CAPEX + \frac{VCP}{\dot{m}_{DME,out} \times OH} \qquad \textit{Eqn.4}$$

where VCP is the total annual variable costs of production accounting for all costs related to raw materials and utility.

4.9 Environmental assessment

In order to assess the effectiveness of the CCU scenarios in reducing CO_2 emissions, an environmental assessment is required. Life cycle assessments (LCA) is a methodology based upon ISO 14044:2016 criteria and guidelines to the application of life cycle thinking in the assessment of environmental impacts of products and processes accounting for the complete life cycle.

To conduct an LCA, three steps are followed:

- Outlining the goal and scope of the project
- Inventory analysis collating the required data from mass and energy balances and evaluation of the environmental impacts due to the process's life cycle.
- An interpretation of the results in relation to the research objectives.

The benefit of an LCA is the fact that a quantifiable and comprehensive outline of the environmental impacts of the process is provided, accounting for all process inputs and outputs and translating them to suitable and comprehensible environmental impact categories. Since a major objective of a CCU process is the reduction of CO_2 emissions, the environmental impact assessed in this study is GWP which quantifies the environmental impact of greenhouse gases and their effect on global warming. Other environmental impacts like ozone depletion and terrestrial acidification are not considered here.

The completion of a comprehensive LCA requires the capability to identify impacts from raw material requirements and associated utility needs. Determining specifically the impacts of each of these process inputs would limit the effectivity of an LCA due to the time-consuming nature of conducting an LCA via this route.

Therefore. the 'Ecoinvent database' lifecycle inventory dataset was used which includes previously completed LCA studies of common materials and utilities. For materials not available in the 'Ecoinvent database' such as the CO_2 and O_2 feed, LCA data was extracted from previous literature.

Some of the assumptions of relevance to the LCA conducted includes:

- Environmental impacts related to plant construction are not considered.
- Environmental impacts in relation to catalyst production are considered negligible.
- GWP for the CO_2 feed was taken from the data for oxyfuel carbon capture for a cement plant from Gardarsdottir et al [19].
- Environmental impact data for utilities used natural gas and oxygen were taken from the 'Ecoinvent database'.

4.10 Process optimisation

In order to carry out the process optimisation for each CCU scenario, the procedure outlined in Figure 3.6 was used.

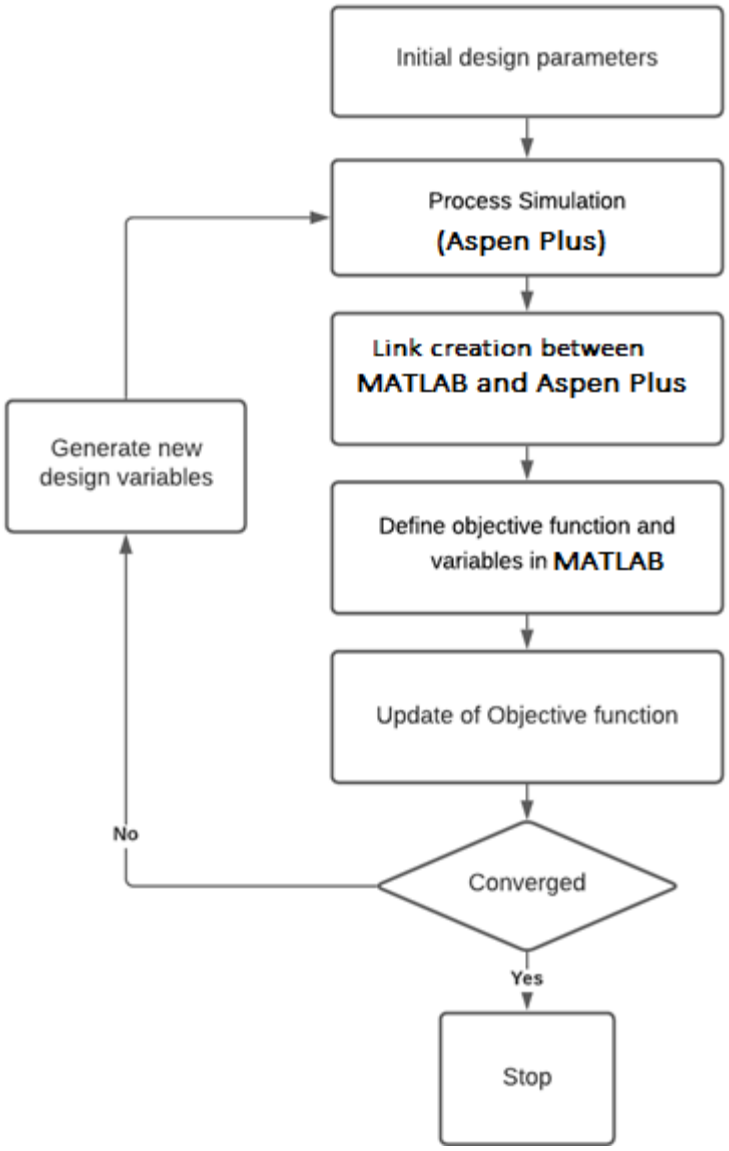

Figure 3.6. General flowsheet for the optimisation strategy in MATLAB and Aspen Plus V12.

With each optimisation iteration the objective function was calculated, allowing each variable to be adjusted for the next iterations until the minimum was achieved for the objective function. In order to link and allow communication and data exchange to occur between Aspen Plus and MATLAB, a component object model (COM) server was created via the actxserver function [49]. The objective functions were calculated within Aspen Plus through a FORTRAN calculator block.

Optimisation of the overall process was performed towards two targets: (i) Minimising total variable operating costs per tonne of DME produced (ii)Minimising GWP per tonne of DME produced. To this end, two objective functions have been produced and used in this work: J (cost minimisation) and S (GWP minimisation).

4.10.1 Objective function J (cost minimisation)

The objective function, J, of minimising total variable operating costs, T_{OC}, per tonne of DME produced, $F_{DME,out}$, is provided below

$$MIN: J = \frac{T_{OC}}{F_{DME,out}}$$

where, the total variable operating costs, T_{OC}, are calculated as the sum of the total utilities cost, U_{cost}, and raw materials costs, RM_{cost}:

$$T_{OC} = RM_{cost} + U_{cost}$$

4.10.2 Objective function S (GWP minimisation)

The objective function used for the minimising of GWP incorporates all GWP variations derived from the feedstock, raw materials, the utility requirements of the system and the greenhouse gases exiting from plant exit streams including purge streams. GWP values for all feed streams, except for O_2 and CO_2 as outlined in section 4.9, and utilities were extracted from the 'Ecoinvent database' whilst the GWP of the exit streams were determined through the calculation of the GWP for each greenhouse gas present in the purge streams, namely hydrogen, CO_2 and methane.

The total GWP, T_{GWP}, is calculated from the sum of all sources outlined above:

$$T_{GWP} = \sum^{l} F_l \, i_{GWP,l} + \sum^{n} P_n \, i_{GWP,n} + \sum^{m} U_m \, i_{GWP,m}$$

where $i_{GWP,l}$ is the GWP per unit of l, F_l is the raw material requirements of l per tonne DME produced, P_n is the total amount of greenhouse gas n that exits the purge per tonne DME produced and U_m is the utility m required per tonne DME produced.

The objective function for minimising global warming potential per tonne of DME produced, S, is given below:

$$Min: S = \frac{T_{GWP}}{F_{DME,out}}$$

4.10.3 Decision variables

The decision variables were selected within suitable ranges for the operation of the plant as shown in Table 3.11.

Table 3.11. Decision variables including lower and upper bounds used for optimisation.

Decision variable	Lower bound	Upper bound
Reformer heat exchanger temperature (°C)	800	1000
Reformer heat exchanger pressure (bar)	1	30
Natural gas heat exchanger temperature (°C)[a]	250	650
Natural gas heat exchanger pressure (bar)	1	30
Pre-reformer temperature (°C)	350	650
Pre-reformer pressure (bar)	1	30
DME reactor heat exchanger temperature (°C)	160	360
DME reactor heat exchanger pressure (bar)	1	50
Reformer exit stream ratio into water gas shift unit[b]	0	1
Natural gas feed mass flow ($tonnes.hr^{-1}$)	7	25
Steam feed mass flow ($tonnes.hr^{-1}$)	10	80
Oxygen feed mass flow ($tonnes.hr^{-1}$)[c]	1	20
Methanol recycle purge ratio (%)[d]	1	10

[a] For adiabatic tri-reforming, exit temperature of reformer restricted to less than 1050 °C to limit catalyst deactivation.

[b] Water gas shift bypass option implemented via a splitter.

[c] For tri-reforming cases.

[d] Prior to the DME synthesis section a purge for a portion of the recycled methanol is present.

4.10.4 Optimisation algorithm

The objective functions and process synthesis models represents a mixed integer non-linear programming model (MILP), therefore to ensure a global optimum was achieved a stochastic meta-heuristic algorithm approach was implemented.

Although a deterministic method allows greater reliability in achieving a global optimum, it offers limited robustness due to the requirement of assumptions that may not be guaranteed for the simulation model such as the presence of function continuity and convexity [50]. Alternatively, stochastic approaches provide greater robustness since the algorithms focus on a search of the solution over the entire feasible region [51]. Although in theory stochastic optimisation techniques require infinite iterations to achieve convergence to the global optimum, in practise a convergence to an acceptable global optimum is achieved quickly. To further guarantee a convergence to a global optimum, a simulated annealing algorithm was selected in this study. This implemented a hybrid function including a pattern search with a complete poll through a mesh adaptive search (MADS) Positive basis Np1 algorithm and a complete search using the genetic algorithm at intervals of 10 iterations.

4.11 Heat integration

All scenarios were modelled and optimised as described in the previous sections and then exported to the Aspen Energy Analyzer (AEA) for heat integration and heat exchanger network optimisation. A minimum approach temperature of 10 °C was selected to carry out the heat integration. Resultant optimisation iterations were checked for infeasibility (e.g. temperature crosses) and their capability to fulfil all required energy requirements as well as operational practicality. The heat integration of the optimised scenarios was carried out to minimise total costs, including capital investment and operating costs. The heat exchanger network providing the lowest operating and annualised costs was selected from all suitable iterations provided by AEA.

5.0 Results

5.1 Technical performance indicators

The mass and energy balances of the optimised scenarios calculated in Aspen Plus allow us to determine the overall CO_2 conversion for each CCU scenario as follows:

$$Overall\ CO_2 conversion\ (\%) = \frac{\dot{m}_{CO_2,in} - \dot{m}_{CO_2,out}}{\dot{m}_{CO_2,in}},$$

where $\dot{m}_{CO_2,in}$ is the mass flowrate ($t \cdot hr^{-1}$) of CO_2 in the process feed stream coming from the cement CO_2 capture plant and $\dot{m}_{CO_2,out}$ is the mass flowrate of CO_2 ($t \cdot hr^{-1}$) in the output streams.

Additionally, the DME conversion is calculated to determine the amount of DME produced per t of feed CO_2:

$$DME\ conversion\ factor = \frac{\dot{m}_{DME,out}}{\dot{m}_{CO_2,in}}.$$

5.1.1 Technical performance before heat integration

Table 3.12 shows key technical performance indicators for the CCU based DME production scenarios. CO_2 conversion ranges from -4.7% to 86.16% for all six CCU scenarios. All dry and bi-reforming scenarios offer significantly higher overall CO_2 conversion compared to the tri-reforming designs. For example, BI-OPEX has a CO_2 conversion of 86.16% whilst CO_2 conversion is only 10.02% for ADTRI-GWP. In the case of ISOTRI-OPEX, a net increase of 4.7% in CO_2 emissions is seen, this is due to a) the partial oxidation reaction (*Eqn.TR2)* taking place in the tri-reformer and producing additional CO_2 in the tri-reforming designs and b) the increased

natural gas feed requirements of the tri-reforming scenarios, increasing the total quantity of reactant natural gas that will produce CO_2. For example, the natural gas feed for ISOTRI-OPEX is 20.08% greater than for BI-OPEX.

The DME conversion factor of the tri-reforming scenarios is greater than the dry and bi-reforming scenarios with ISOTRI-OPEX having the highest DME conversion factor at 3.03 t DME·t^{-1} CO_2. The primary reason for this is that the DME production rate tend to be greater for the tri-reforming scenarios, due to the increased total feed with the addition of oxygen.

The DME conversion factor of the scenarios optimised towards minimising costs was 4.08 to 42.25% greater than for the scenarios optimised towards minimising GWP. This is because optimising towards GWP minimisation maximised the amount of CO_2 required per tonne DME, as the CO_2 feed was a source of net decrease in GWP. For example, CO_2 demand for DR-GWP was 31.37% higher than DR-OPEX.

Table 3.12. Technical performance indicators for CCU scenarios studied before heat integration.

		Conventional	Dry reforming		Bi-reforming		Adiabatic Tri-reforming		Isothermal Tri-reforming	
		SR	DR-OPEX	DR-GWP	BI-OPEX	BI-GWP	ADTRI-OPEX	ADTRI-GWP	ISOTRI-OPEX	ISOTRI-GWP
CO_2 Feed	$t \cdot t^{-1}$ ***DME***	-	0.51	0.67	0.51	0.67	0.49	0.51	0.33	0.47
Natural gas Feed	$t \cdot t^{-1}$ ***DME***	0.69	0.77	0.76	0.77	0.76	1.05	0.95	0.95	0.93
Steam water Feed	$t \cdot t^{-1}$ ***DME***	0.85	0.95	0.98	0.95	0.98	0.73	0.75	0.56	0.69
Make-up water	$t \cdot t^{-1}$ ***DME***	1.46	1.63	2.14	1.63	2.13	1.58	1.63	1.05	1.49
O_2 Feed	$t \cdot t^{-1}$ ***DME***	-	-	-	-	-	0.83	0.76	0.64	0.64
DME production rate	$t \cdot hr^{-1}$	20.08	20.16	15.37	20.07	15.26	22.91	20.08	31.10	22.05
Heating requirements	$GJ \cdot t^{-1}$ ***DME***	23.19	27.80	27.79	27.78	27.99	20.75	19.82	19.29	19.82
Cooling Requirements	$GJ \cdot t^{-1}$ ***DME***	18.58	22.30	22.69	22.26	22.90	25.98	24.35	22.50	23.47
Electricity requirements	$kWh \cdot t^{-1}$ ***DME***	487.1	583.34	689.78	583.45	692.40	688.52	747.05	585.94	715.53
CO_2 conversion	*%*	-	86.12	70.10	86.16	70.09	7.77	10.02	-4.70	10.02
DME conversion factor	$tDME \cdot t^{-1}\ CO_2$	-	1.96	1.49	1.96	1.49	2.04	1.96	3.03	2.13

Heating utility requirements range from 19.29 to 27.99 $GJ \cdot t^{-1}$ DME produced for the CCU scenarios. Heating utility usage is similar for the dry and bi-reforming scenarios ranging from 27.78 to 27.99 $GJ \cdot t^{-1}$ DME. In comparison, the tri-forming scenarios have lower heating requirements by 33.88% to 45.1%, ranging from 19.29 to 20.75 $GJ \cdot t^{-1}$ DME. The lower heating utility requirements of the tri-reforming processes are due to the exothermic nature of the partial oxidation reaction (*Eqn.TR2)* which provides a portion of the required heating requirements in the reformer. The conventional scenario has lower heating requirements than the dry and bi-reforming scenarios due to the reduced total feed quantity that needs to be heated in the SR scenario. However, the heating requirements of the conventional scenario is still greater than that for the cases of tri-reforming.

Electricity requirements range from 487.1 to 747.05 $kWh \cdot t^{-1}$ DME. Optimising towards GWP in comparison to operating expenditure increases electricity usage by 8.5% to 22.12%. The electricity requirements correlate with the total feed requirements, as it is mainly used for the pumps and compressors.

As shown in Figure 3.9, in the case of SR and dry- and bi-reforming a significant portion of the heating utility is the natural gas representing 54.88% to 55.92% of the total heating utility requirements. In contrast, the tri-reforming scenarios show a lower portion of the total heating utility from natural gas, providing 36.57% to 39.23% of the total heating utility requirements. Natural gas for heating is mainly used in the pre-reformer and reformer and the exothermic reaction of tri-reforming provides a portion of the required heating in the reformer.

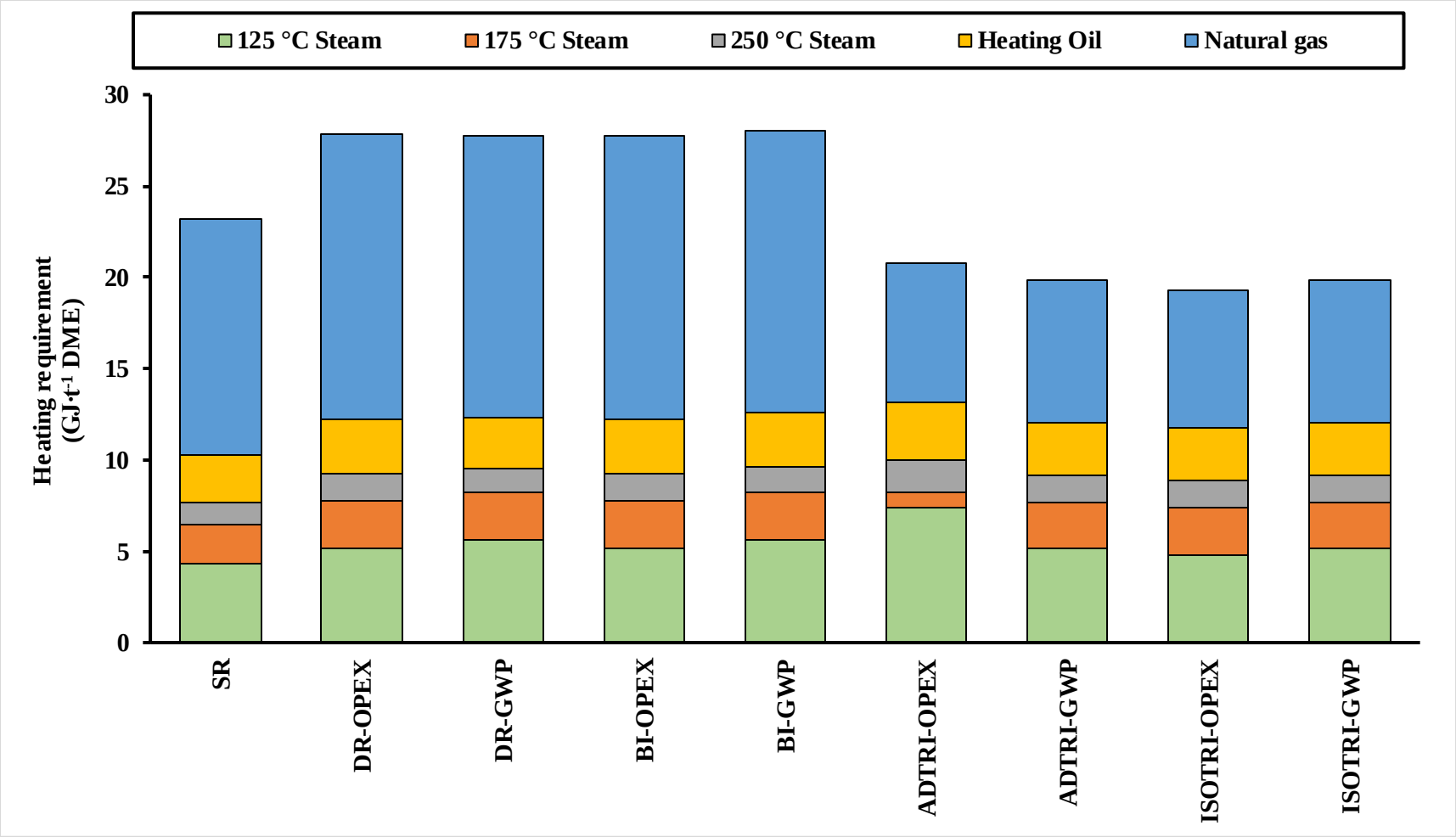

Figure 3.7. Heating utility breakdown for CCU scenarios optimised before heat integration.

5.1.2 Technical performance after heat integration

Table 3.13 and Figure 3.8 show a significant decrease in utility requirements after heat integration. The heating utility requirements range from 0.51 to 5.28 GJ t^{-1} DME for the CCU scenarios studied. Even though prior to heat integration the heating utility for the dry and bi-reforming processes are significantly lower than the tri-reforming processes, after heat integration the opposite occurs. The main factor affecting this is the lower available utility for heat integration in the case of tri-reforming, as it is an exothermic process.

Table 3.13. Technical performance indicators for CCU scenarios studied after heat integration.

		Conventional	Dry reforming		Bi-reforming		Adiabatic Tri-reforming		Isothermal Tri-reforming	
		SR	DR-OPEX	DR-GWP	BI-OPEX	BI-GWP	ADTRI-OPEX	ADTRI-GWP	ISOTRI-OPEX	ISOTRI-GWP
CO_2 Feed	$t \cdot t^{-1}$ *DME*	-	0.51	0.67	0.51	0.67	0.49	0.51	0.33	0.47
Natural gas Feed	$t \cdot t^{-1}$ *DME*	0.69	0.77	0.76	0.77	0.76	1.05	0.95	0.95	0.93
Steam water Feed	$t \cdot t^{-1}$ *DME*	0.85	0.95	0.98	0.95	0.98	0.73	0.75	0.56	0.69
Make-up water	$t \cdot t^{-1}$ *DME*	1.46	1.63	2.14	1.63	2.13	1.58	1.63	1.05	1.49
O_2 Feed	$t \cdot t^{-1}$ *DME*	-	-	-	-	-	0.83	0.76	0.64	0.64
DME production rate	$t \cdot hr^{-1}$	20.08	20.16	15.37	20.07	15.26	22.91	20.08	31.10	22.05
Heating requirements	$GJ \cdot t^{-1}$ *DME*	0.79	0.66	0.79	0.51	0.85	2.90	1.90	5.28	4.43
Cooling Requirements	$GJ \cdot t^{-1}$ *DME*	2.15	2.61	2.09	2.61	2.04	6.62	8.62	4.44	6.18
Electricity requirements	$kWh \cdot t^{-1}$ *DME*	487.1	583.34	689.78	583.45	692.40	688.52	747.05	585.94	715.53
CO_2 conversion	*%*	-	86.12	70.10	86.16	70.09	7.77	10.02	-4.70	10.02
DME conversion factor	$tDME \cdot t^{-1}$ CO_2	-	1.96	1.49	1.96	1.49	2.04	1.96	3.03	2.13

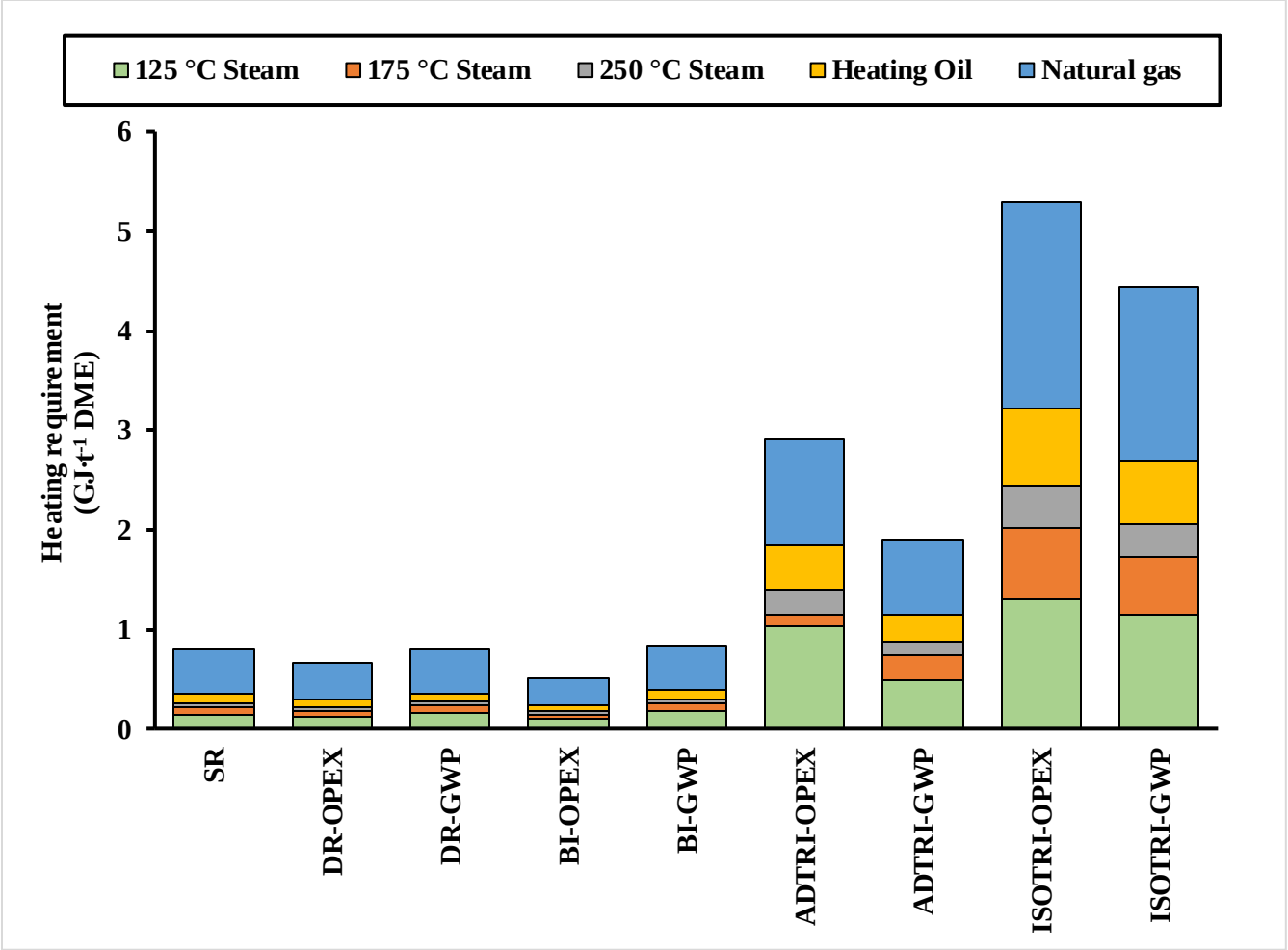

Figure 3.8. Heating utility breakdown for scenarios optimised after heat integration.

5.2 Economic performance indicators

5.2.1 Economics before heat integration

Table 3.14 provides a breakdown of the total production cost and other key economic performance parameters. The total production cost of the CCU scenarios range from **$**819.32 to **$**970.87 t^{-1} DME: 3.24% to 22% higher than the total production cost of conventional DME synthesis scenario. The tri-reforming options provide a lower production cost compared to the other CCU reforming technologies with ISOTRI-OPEX having the lowest production cost. This is due to decreased total utility cost and CAPEX in comparison to the other scenarios. The dry-reforming and bi-reforming CCU scenarios have comparable economics.

The greatest impact on total production cost for the conventional, dry- and bi-reforming scenarios is the utility costs. For the tri-reforming scenarios, material and utility costs have similar contributions to production cost. For example, total utility costs represent 51.03% of DR-OPEX's total production cost, whilst material and utility costs represent 42.66% and 41.9% respectively of ISOTRI-OPEX total production cost. CAPEX ranges from **$**126.42 and **$**188.05 t^{-1} DME and has a lower impact on total production cost in comparison to material and utility costs: representing 15.43% to 19.37% of the total production cost

Table 3.14. Key economic performance indicators before heat integration

	Conventional	Dry reforming		Bi-reforming		Adiabatic Tri-reforming		Isothermal Tri-reforming	
	SR	DR-OPEX	DR-GWP	BI-OPEX	BI-GWP	ADTRI-OPEX	ADTRI-GWP	ISOTRI-OPEX	ISOTRI-GWP
Purchased equipment cost (M$)	11.25	11.25	11.25	11.25	11.25	11.25	11.25	11.25	11.25
FCI (M$)	62.38	62.38	62.38	62.38	62.38	62.38	62.38	62.12	62.38
Working capital (M$)	11.02	11.02	11.02	11.02	11.02	11.02	11.02	10.97	11.02
CAPEX ($\cdot t^{-1}$ *DME)*	148.51	162.97	188.05	162.36	187.38	145.44	156.18	126.42	148.90
Total raw material cost ($\cdot t^{-1}$ *DME*)	247.19	296.42	356.57	296.08	318.15	361.86	358.37	349.56	348.25
Total utility cost ($\cdot t^{-1}$ *DME)*	397.91	478.76	426.10	476.62	465.33	308.26	355.75	343.34	362.24
Total utility and material cost ($\cdot t^{-1}$ *DME)*	645.10	775.18	782.67	772.70	783.48	670.12	714.12	692.90	710.49
Total production cost ($\cdot t^{-1}$ *DME)*	*793.61*	*938.15*	*970.72*	*935.07*	*970.87*	*815.56*	*870.30*	*819.32*	*859.39*

From Figure 3.9 it is seen that for all scenarios studied costs related to the natural gas feed is the source of the majority of the total material costs. For the CCU scenarios the natural gas feed represents an 83.11% to 92.2% of the total material cost for the CCU scenarios whilst providing a significant 99.01% of the total material cost for the SR scenario. The portion of total material cost due to the natural gas feed is lower in the tri-reforming scenarios than the dry and bi-reforming scenarios due to the introduction of the oxygen feed.

Figure 3.12 shows that natural gas used for heating was a majority of the total utility costs, providing 41.35 to 61.68% of the total utility costs.

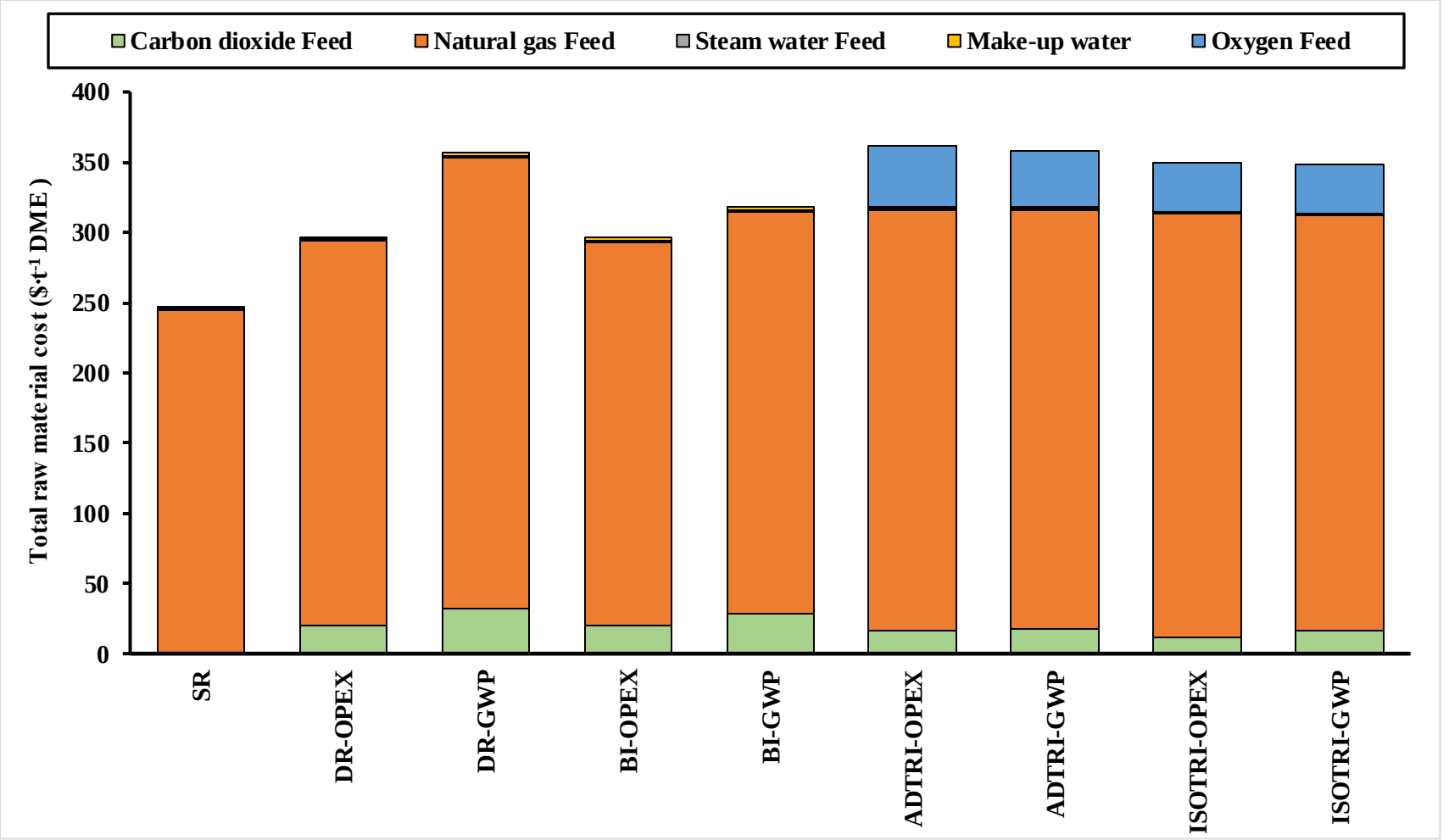

Figure 3.9. Breakdown of total raw material cost for scenarios studied before heat integration.

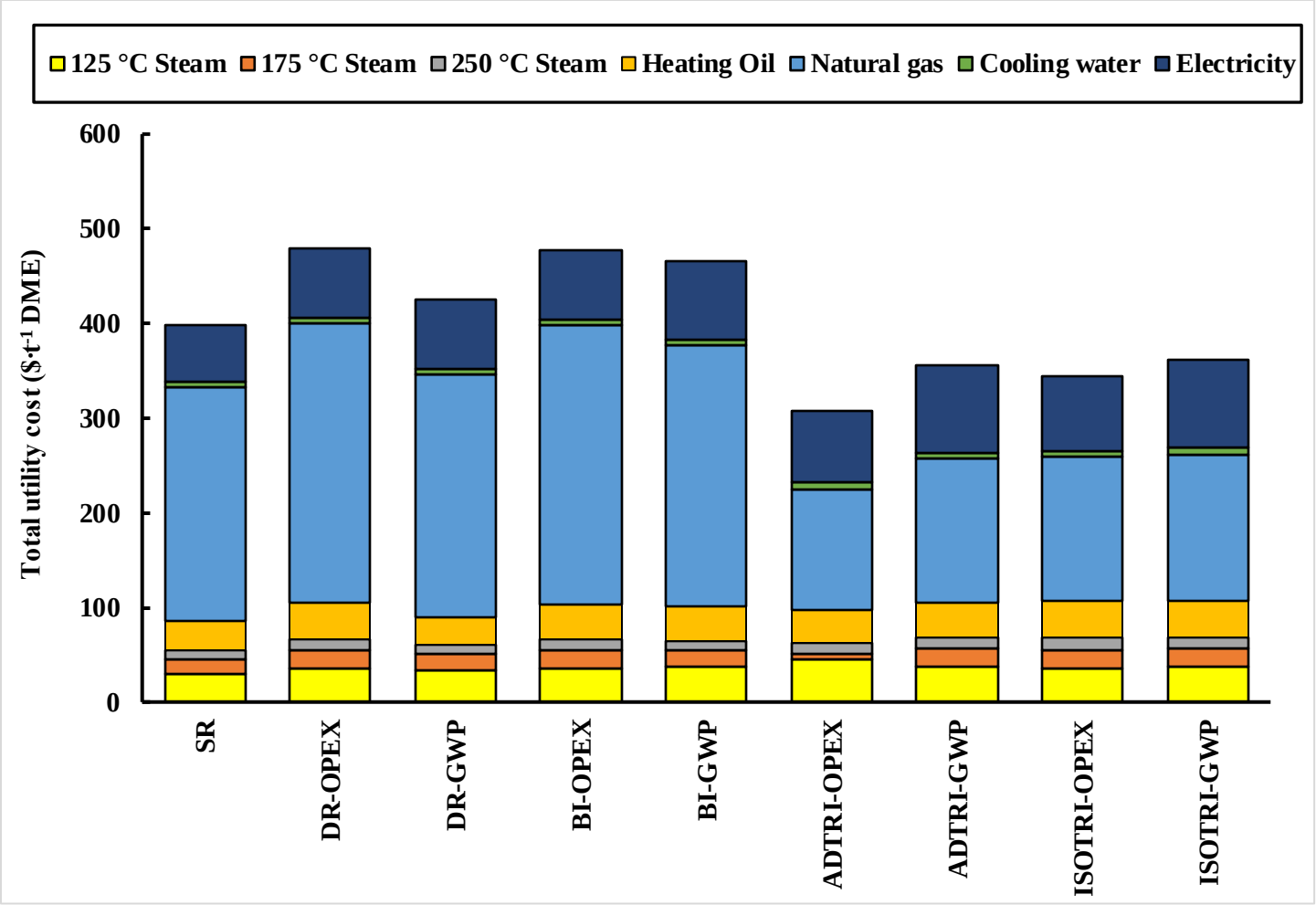

Figure 3.10. Breakdown of total utility costs for scenarios studied before heat integration.

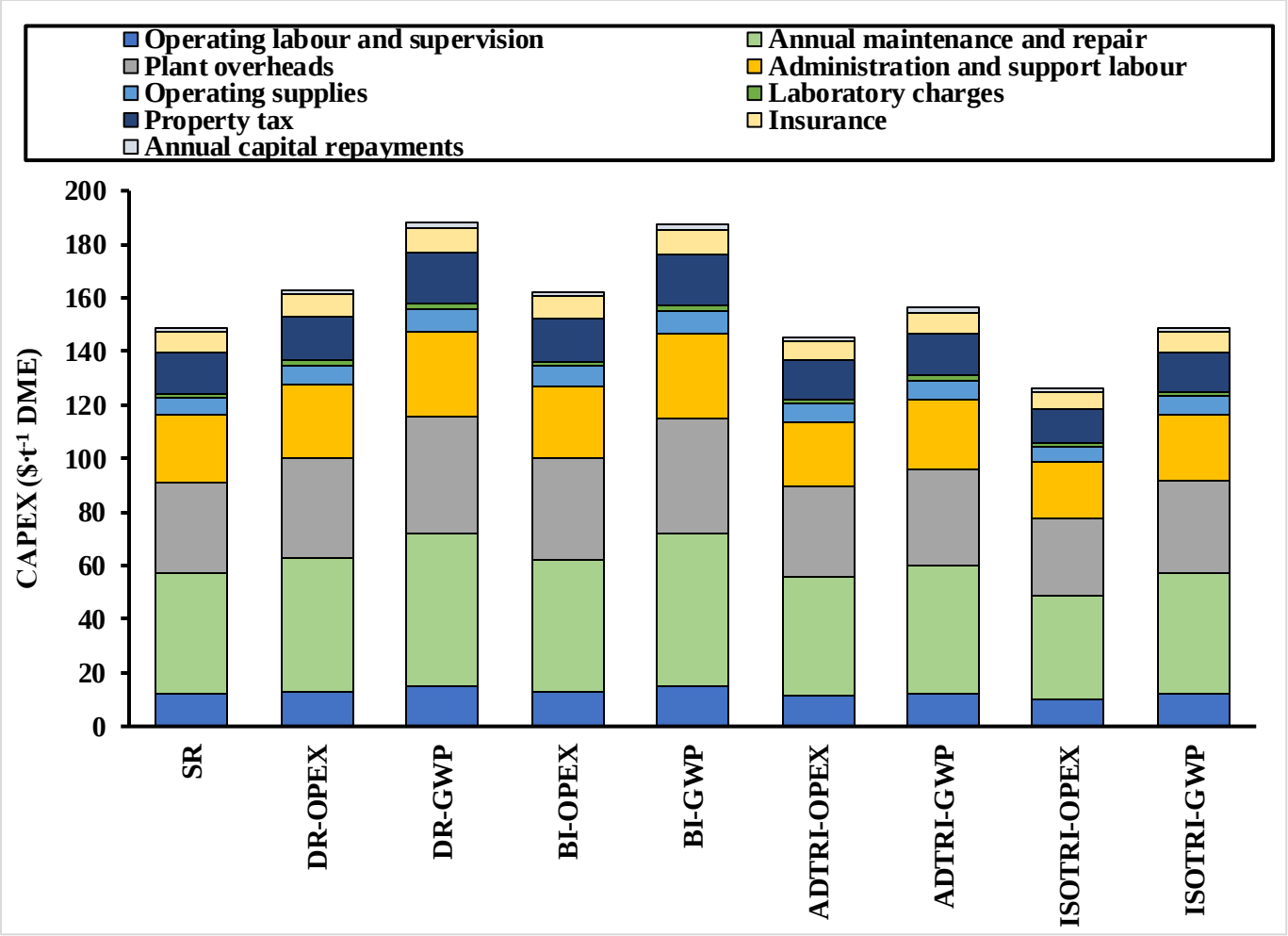

Figure 3.11. Breakdown of CAPEX for scenarios studied before heat integration.

5.2.2 Economics after heat integration

Table 3.15 and Figure 3.12 shows a significant decrease in total production cost is achieved after the optimisation of the utility usage of the processes by heat integration; an 18.76 to 48.35% decrease is seen. The bi-reforming and dry-reforming scenarios have a lower total production cost than the tri-reforming scenarios, even though prior to heat integration the tri-reforming processes displayed lower production cost. This is due to the reduced opportunity for heat integration in the case of tri-reforming and the higher utility costs. This can be seen in the lower reduction seen in total utility costs for the tri-reforming scenarios in comparison to the dry and bi-reforming scenarios. The total utility costs after heat integration were reduced by 80.58 to 81.68% for dry and bi-reforming scenarios, in comparison to a 56.75 to 61.67% reduction in total utility costs for tri-reforming scenarios.

Table 3.15. Key economic performance indicators after heat integration.

	Conventional	Dry reforming		Bi-reforming		Adiabatic Tri-reforming		Isothermal Tri-reforming	
	SR	DR-OPEX	DR-GWP	BI-OPEX	BI-GWP	ADTRI-OPEX	ADTRI-GWP	ISOTRI-OPEX	ISOTRI-GWP
Purchased equipment cost (M$)	7.40	7.13	7.64	6.90	7.64	12.95	13.45	11.45	10.79
FCI (M$)	41.03	39.52	42.34	38.25	42.34	71.79	74.57	63.25	59.82
Working capital (M$)	7.25	6.98	7.48	6.76	7.48	12.68	13.17	11.17	10.57
CAPEX ($\cdot t^{-1}$ *DME)*	97.68	103.25	127.63	99.56	127.18	167.39	186.71	128.72	142.79
Total material cost ($\cdot t^{-1}$ *DME*)	247.19	296.42	296.87	295.28	297.65	361.86	358.37	349.56	348.25
Total utility cost ($\cdot t^{-1}$ *DME)*	72.91	88.47	90.42	88.13	90.39	133.33	138.44	142.93	138.85
Total utility and material cost ($\cdot t^{-1}$ *DME)*	270.87	384.88	387.29	383.41	388.04	495.19	496.81	492.49	487.10
Total production cost ($\cdot t^{-1}$ *DME)*	417.78	488.14	514.92	482.98	515.22	662.58	683.52	621.21	629.89

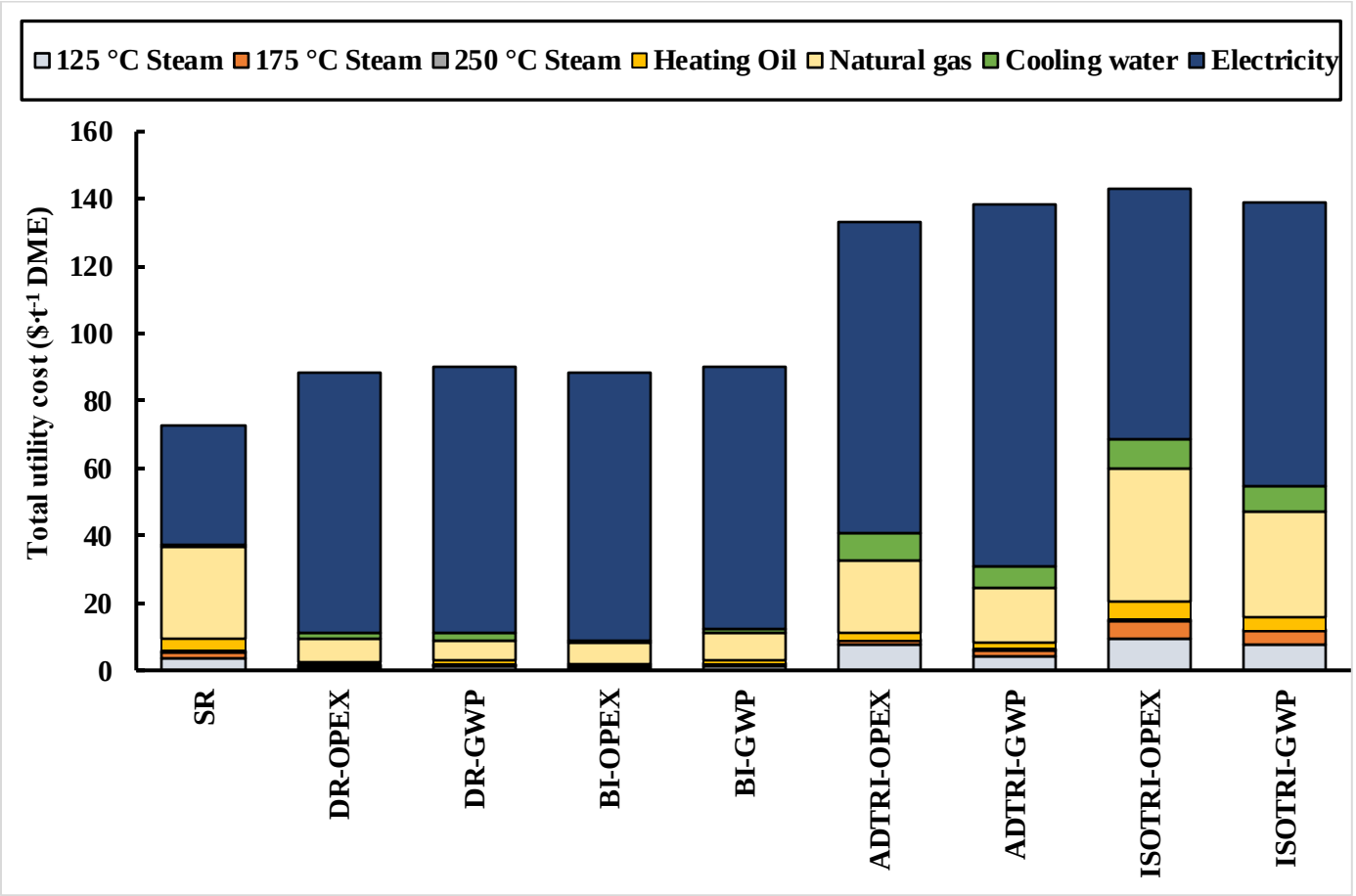

Figure 3.12. Heating utility breakdown for scenarios optimised after heat integration.

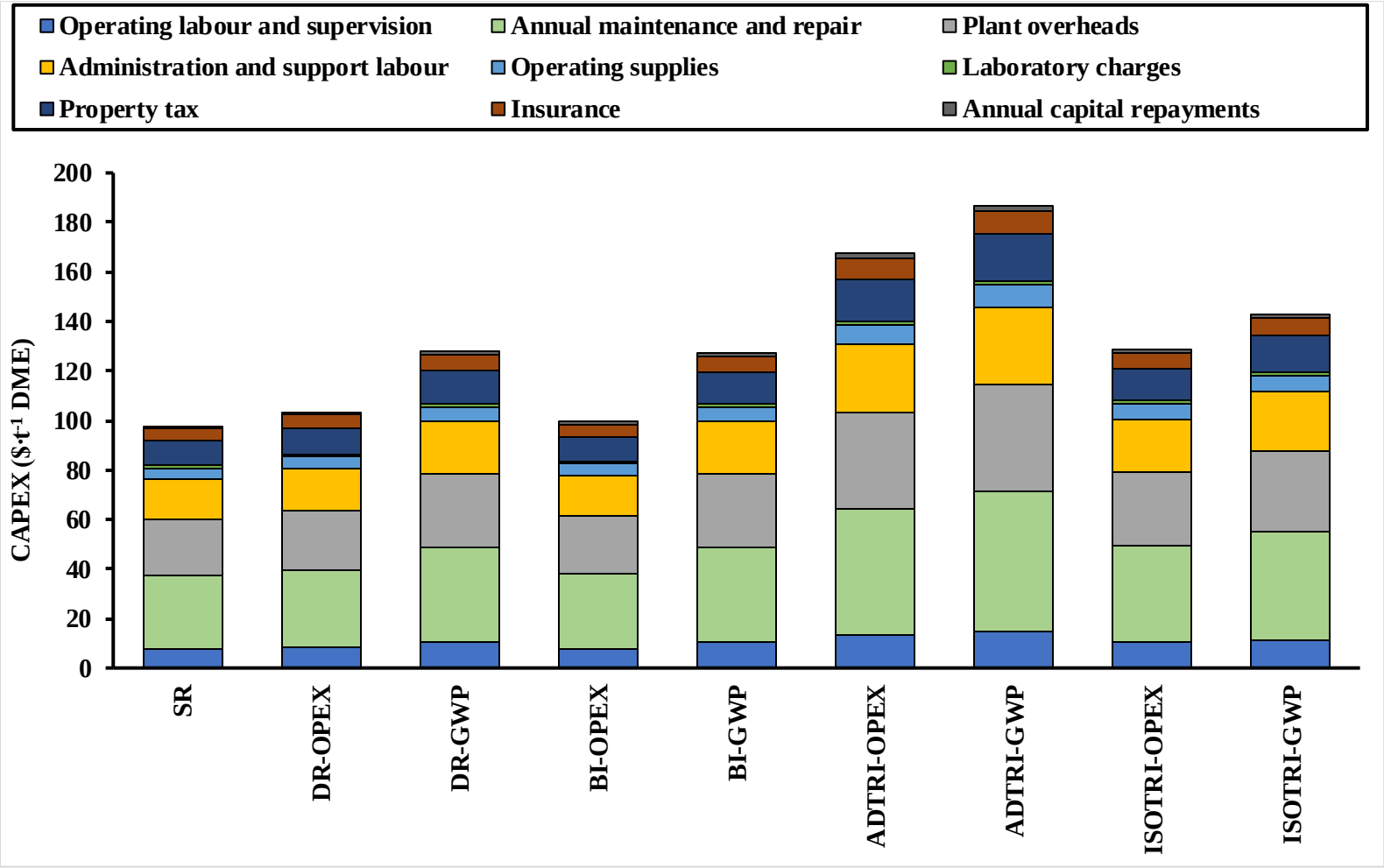

Figure 3.13. CAPEX breakdown for scenarios optimised after heat integration.

5.3 Global warming potential

Figure 3.14 and Figure 3.15 provide a breakdown of the GWP sources for each CCU scenarios before and after heat integration. Before heat integration, the purged flue gases are the greatest sources of GWP followed by the heating utility.

Before heat integration the GWP for the CCU scenarios studied were lower than that of the conventional SR scenario by 19.54% to 69.85%, ranging from 3.35 to 4.76 tCO_2-equivalent·t^{-1} DME. Although all dry and bi-reforming scenarios offer significantly higher overall CO_2 conversion compared to the tri-reforming scenarios, the GWP of the tri-reforming scenarios are lower. For example, whilst the BI-OPEX scenario has a CO_2 conversion of 86.16 %, the GWP is 40.3% greater than that of ADTRI-GWP, where CO_2 conversion is only 10.02% in the case of ADTRI-GWP. The increased CO_2 emissions, in the case of tri-reforming processes, are counteracted by the reduced utility requirements in the tri-reforming processes due to the exothermic nature of the tri-reforming reaction. There is a significant variation in the GWP depending on the optimisation objective, where optimisation based upon minimising global warming potential provides a 7.36% to 13.33% lower GWP.

After heat integration, the GWP for the CCU scenarios studied range from 2.2 to 3.27 tCO_2-eq·t^{-1} DME: 20.97% to 40.42% lower than before heat integration. GWP associated with heating requirements significantly decreases for all cases, indicating the significant benefits in optimising utility usage especially in terms of reducing the environmental impacts of a process. When compared to the SR scenario after heat integration, the GWP is 10.7% to 64.55% lower for the CCU scenarios studied.

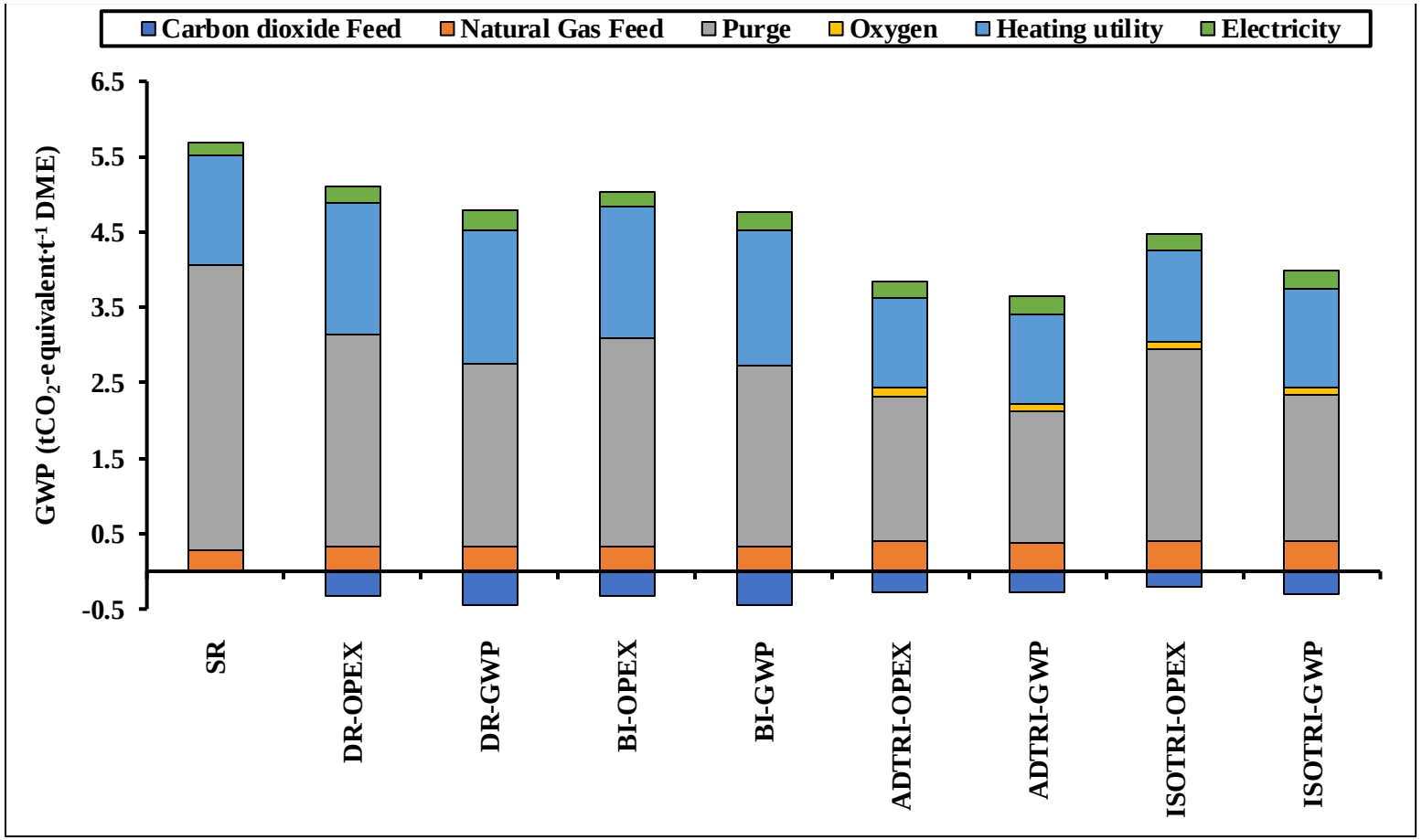

Figure 3.14. Breakdown of GWP sources for scenarios before heat integration.

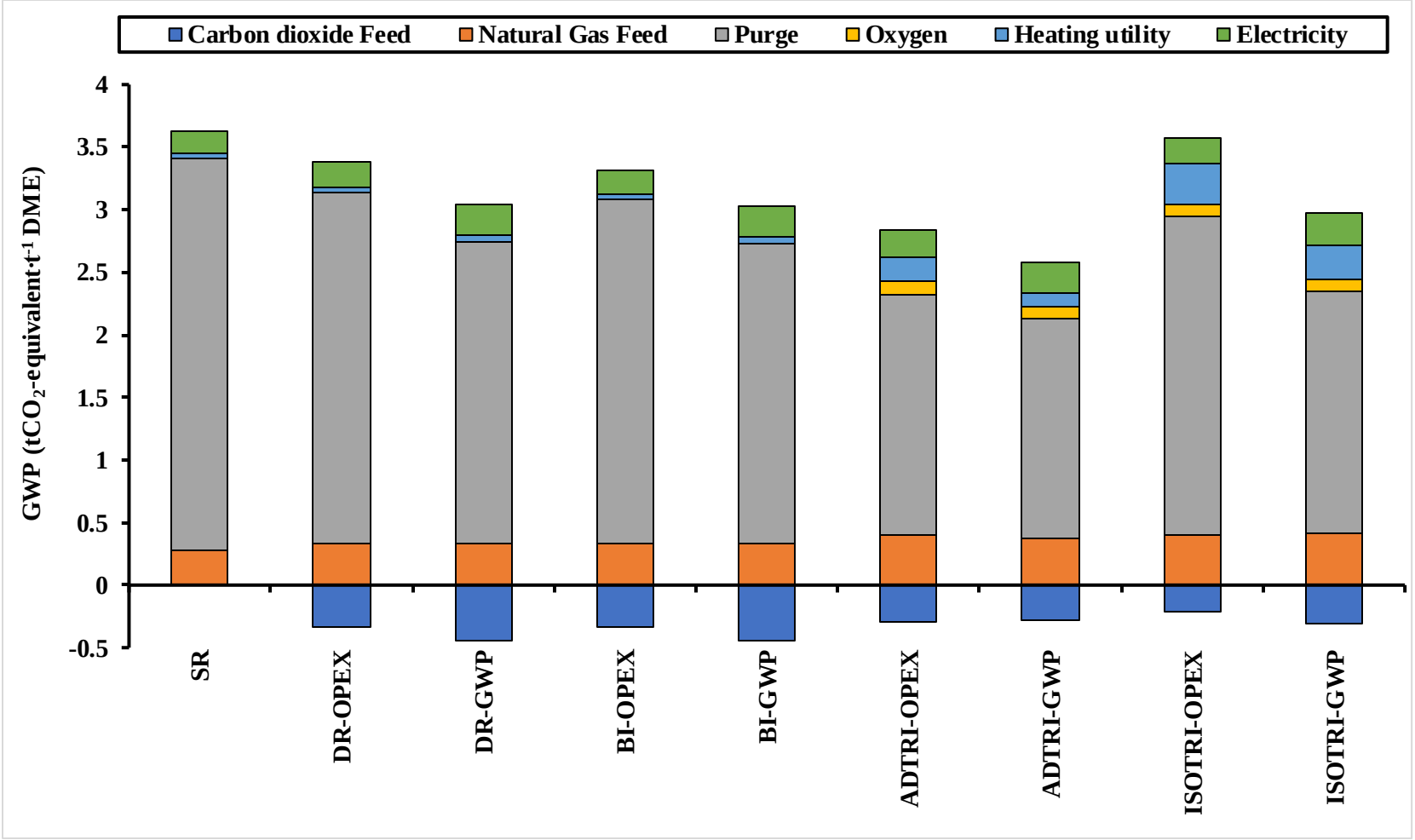

Figure 3.15. Breakdown of GWP sources for scenarios after heat integration

5.4 Cost of global warming potential reduction

The cost of global warming potential reduction (CGWP) is introduced as an economic metric to determine the cost of incorporating CCU technologies in relation to its capability to reduce GWP. This allows for a comparison with other CCU technologies as well as alternative GWP reduction strategies. As the CCU-based DME production processes reduce environmental impacts via a substitution of product, it is of importance a conventional route option is compared against.

The CGWP is determined via the division of the difference between the total production cost of the CCU process, $TPC_{DME,CCU}$, and conventional process $TPC_{DME,conv}$, by the difference between the GWP of the conventional process, $GWP_{DME,conv}$, and the CCU process, $GWP_{DME,CCU}$,

$$CGWP = \frac{TPC_{DME,CCU} - TPC_{DME,conv}}{GWP_{DME,conv} - GWP_{DME,CCU}}.$$

Figure 3.16 shows the CGWP of the CCU scenarios examined. The CGWP ranges from \$93.69 to \$581.23 t^{-1} CO_2-equivalent. The CGWP of the dry and bi-reforming cases are comparable whilst the CGWP of the tri-reforming scenarios are significantly higher. The scenarios optimised towards cost minimisation show lower CGWP than the ones optimised towards minimising GWP by 65.24% to 7.71%. The optimisation of the bi-reforming process displayed the lowest CGWP at \$93.69 t^{-1} CO_2-equivelant.

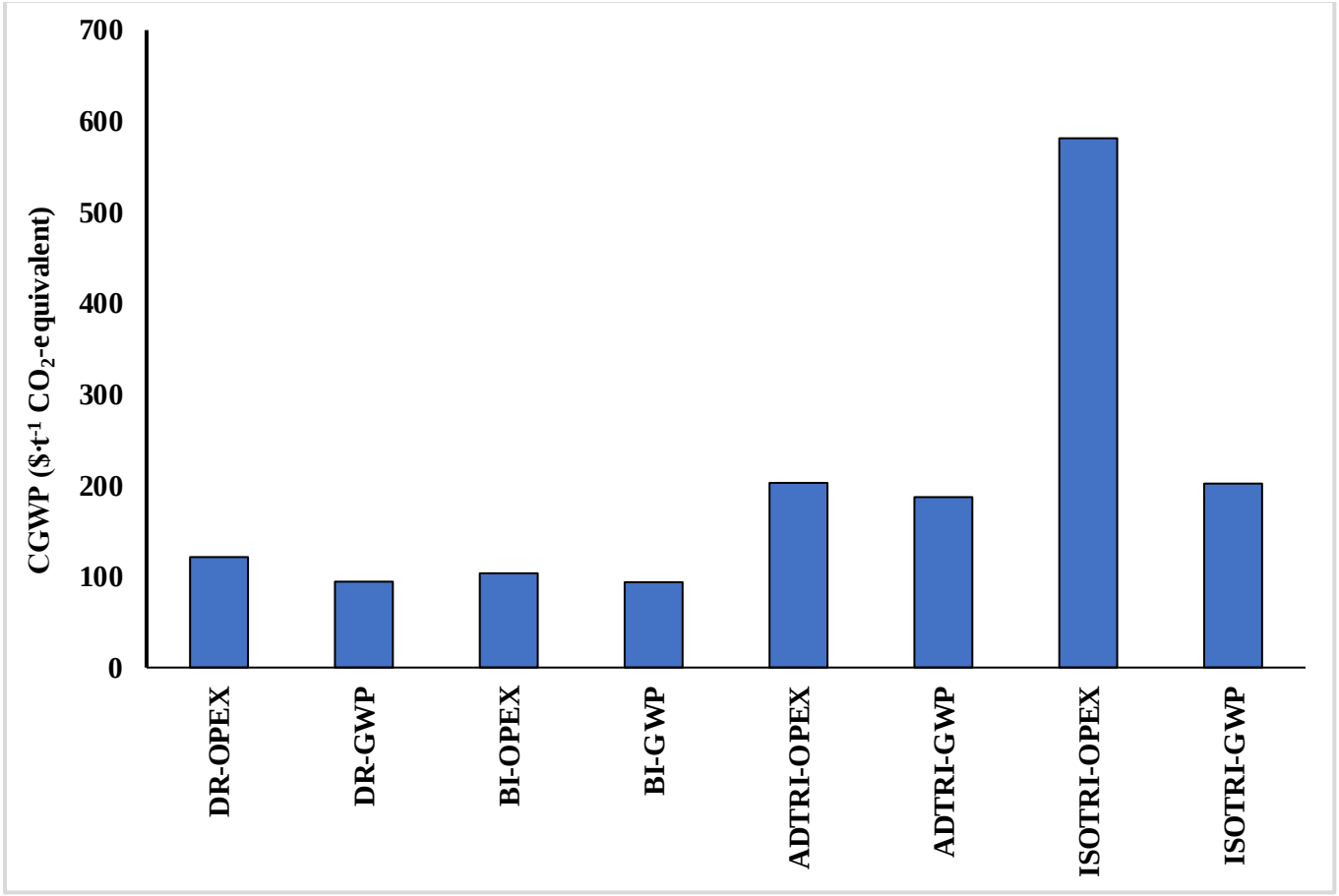

Figure 3.16. Cost of global warming potential reduction ($·t^{-1} CO_2-equivalent).

5.5 Minimum fuel selling price

Figure 3.17 shows the minimum fuel selling price (MFSP) for DME compared to diesel and liquified petroleum gas (LPG). The MFSP is the minimum sale price required to break-even. The MFSP of the scenarios studied ranges from 19.59% lower to 31.56% greater than the diesel selling price and 1.98% lower to 60.36% greater than LPG. The MFSP for the dry- and bi-reforming scenarios are lower than diesel whilst all tri-reforming scenarios are higher. In contrast, all CCU DME scenarios have greater MFSP than LPG.

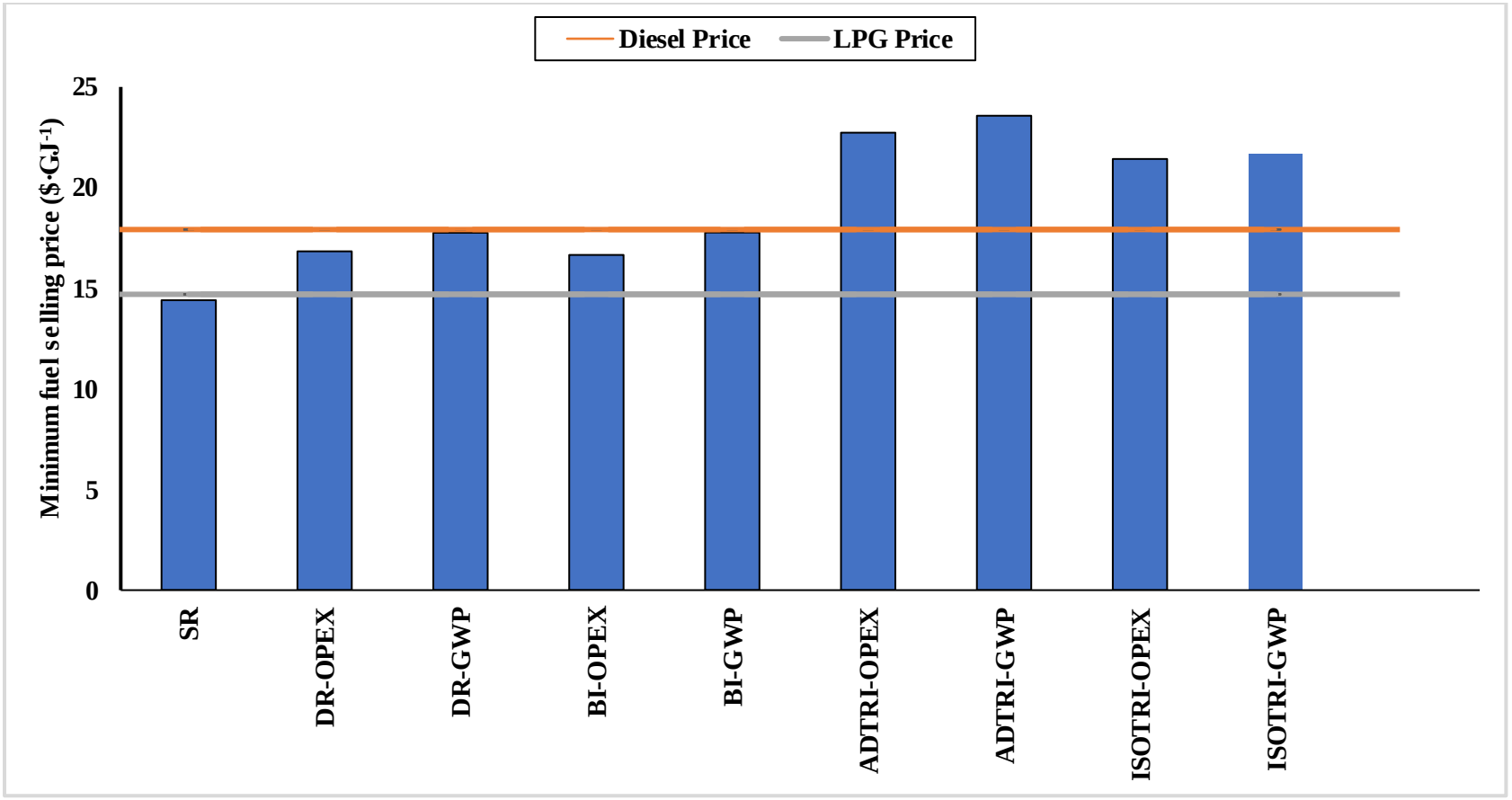

Figure 3.17. MFSP for DME scenarios in comparison to diesel ($17.92 GJ^{-1}) and LPG ($14.70 GJ^{-1}) [52] [53].

5.6 Sensitivity and uncertainty analysis

A Monte Carlo simulation is implemented using MATLAB to carry out a sensitivity analysis and uncertainty analysis. Using this is advantageous as it is probabilistic rather than deterministic; determining not only the effect of the input variables but also the probability for them to occur. This outlines the impact of key factors influencing the economic feasibility of the processes explored. The sensitivity analysis determines the effects of the parameters on total production cost individually whilst the uncertainty analysis determines the effects of all the parameters simultaneously. Sensitivity and uncertainty analysis are essential in outlining the robustness and reliability of the models, assumptions and methodology used.

The Monte Carlo simulation operates through an initial generation of pseudo-random numbers for the parameters studied that are confined to follow a probability distribution. From these probability distributions a random value is taken from each probability distributions generated. This is repeated a sufficient number of times to produce a resultant uncertainty distribution of the output. Parameters of significance to the total production cost of the DME production process and that have uncertainties present includes the cost of the feeds and utility, and the capital expenditure required for the building and setting up of the plant. The impact of the costs related to CO_2 feed, natural gas feed, the O_2 feed in the case of tri-reforming, CAPEX and utility costs are evaluated to determine the greatest impact to total DME production cost. For all parameters a higher and lower bound ranging from -20% to 30% of the base value are used and modelled as a triangular distribution with a sample size of $1x10^6$.

Table 3.16. Uncertainty input parameters examined and ranges for these parameters.

Parameter	Low value	Nominal	High value	Unit
Natural gas cost [54]	276	345	448.5	$\$\cdot t^{-1}$ *DME*
CO_2 cost	40.65	50.81	66.05	$\$\cdot t^{-1}$ *DME*
O_2 cost	48	60	78	$\$\cdot t^{-1}$ *DME*
CAPEX	-20%	See Table 3.15	+30%	$\$\cdot t^{-1}$ *DME*
Utility cost	-20%	See Table 3.15	+30%	$\$\cdot t^{-1}$ *DME*

The sensitivity analysis results presented in Figure 3.18 show that for all scenarios natural gas prices have the greatest impact on total production cost by a significant margin, for example it can be seen for BI-OPEX a 30% increase in natural gas cost increases total production cost by \$56.68 t^{-1} DME or an 11.73% increase from the base case. The impact of CAPEX and utility costs are similar, for example a 30% increase in CAPEX and utility cost for BI-OPEX increases total production cost by \$21.24 and \$18.80 t^{-1} DME respectively or a 4.4% and 3.9% increase from the base case respectively.Costs related to the carbon dioxide feed provide the lowest impact on the total DME production cost; for BI-OPEX, a 30% increase in CO_2 cost, a \$7.76 t^{-1} DME increase in total production cost is seen, 1.61% higher than the base case. This indicates that the source of CO_2 and capture technology have a limited effect on the production cost of CCU based DME production systems. Similarly, for the tri-reforming based scenarios oxygen feed cost has a low impact on production cost compared to other parameters; for ISOTRI-GWP, with a 30% increase in oxygen feed cost, an \$8.19 t^{-1} DME increase in total production cost is seen, 1.3% higher than the base case. This is due to the limited impact on total raw material cost from the CO_2 feed or oxygen feed as shown in Figure 3.9.

Even though natural gas prices have a high impact on total production cost, the effect of natural gas prices on plant economic uncertainty is limited as there is a high likeliness of correlation between natural gas prices and DME product sale price, as is present between methanol and natural gas prices in Europe [55]. This is because the costs of synthesised chemicals, such as methanol and DME, are a function of the main feed for their production.

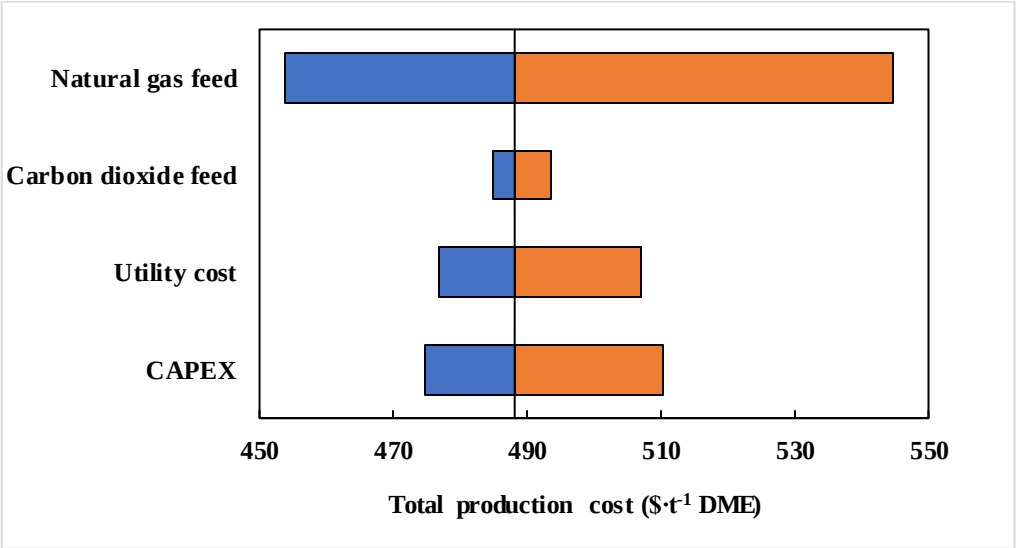

(i) DR-OPEX

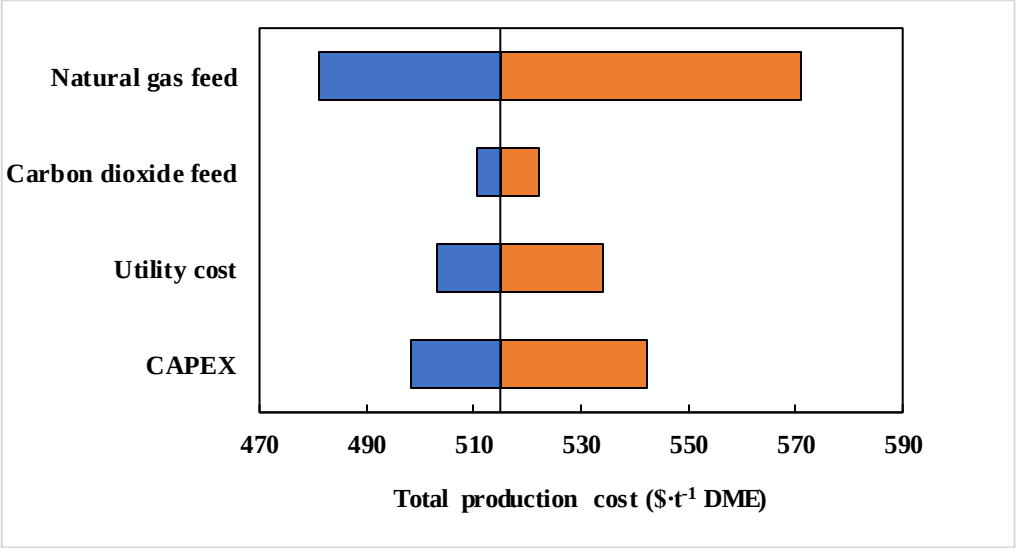

(ii) DR-GWP

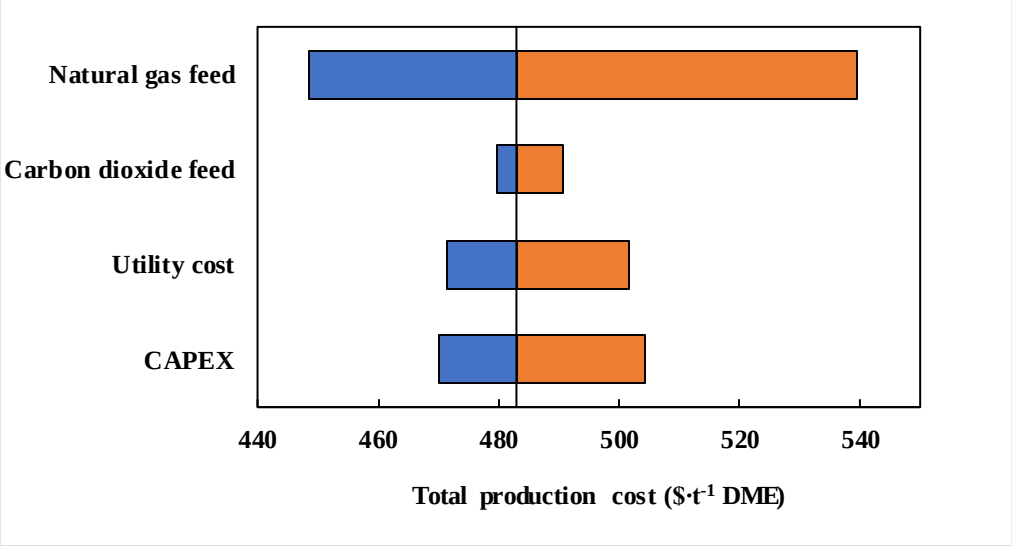

(iii) BI-OPEX

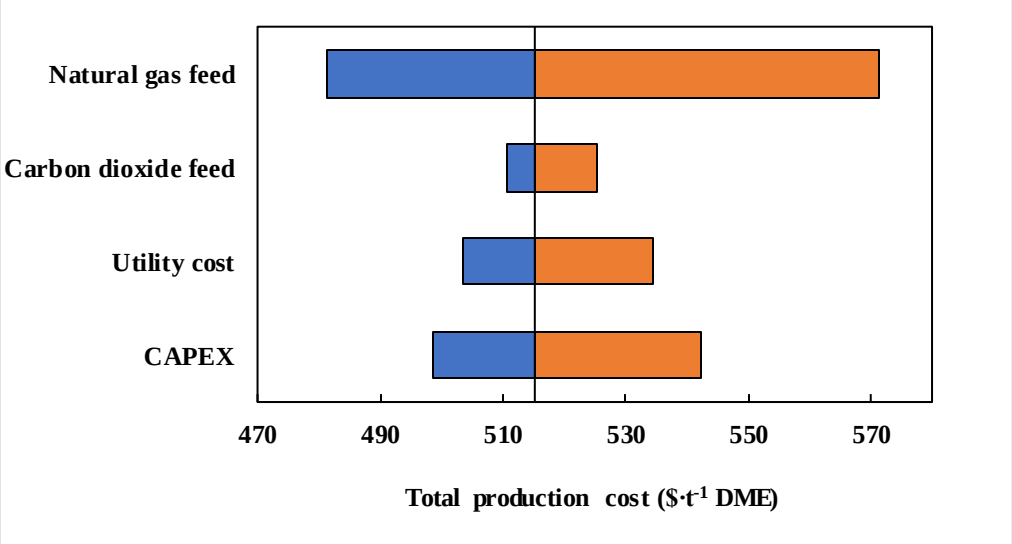

(iv) BI-GWP

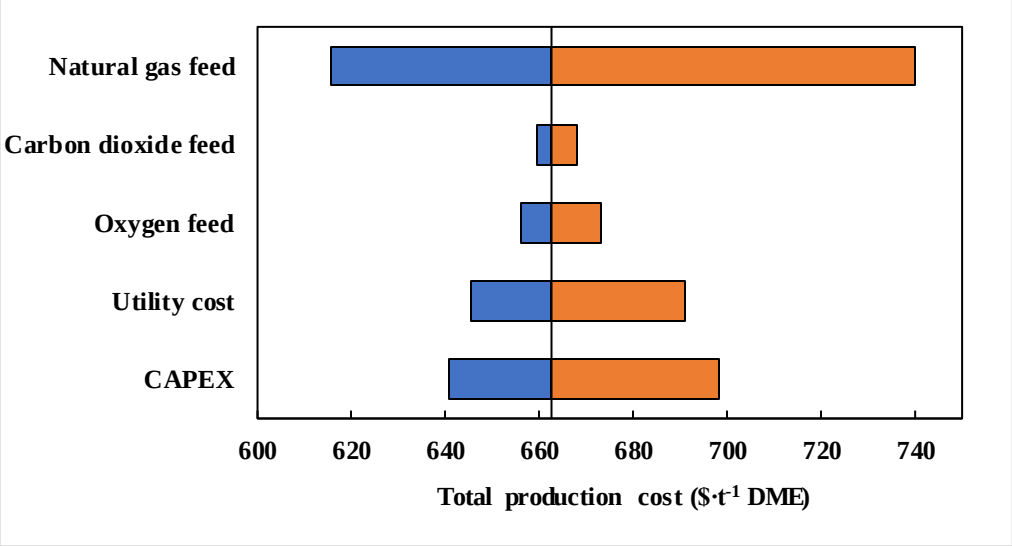

(v) ADTRI-OPEX

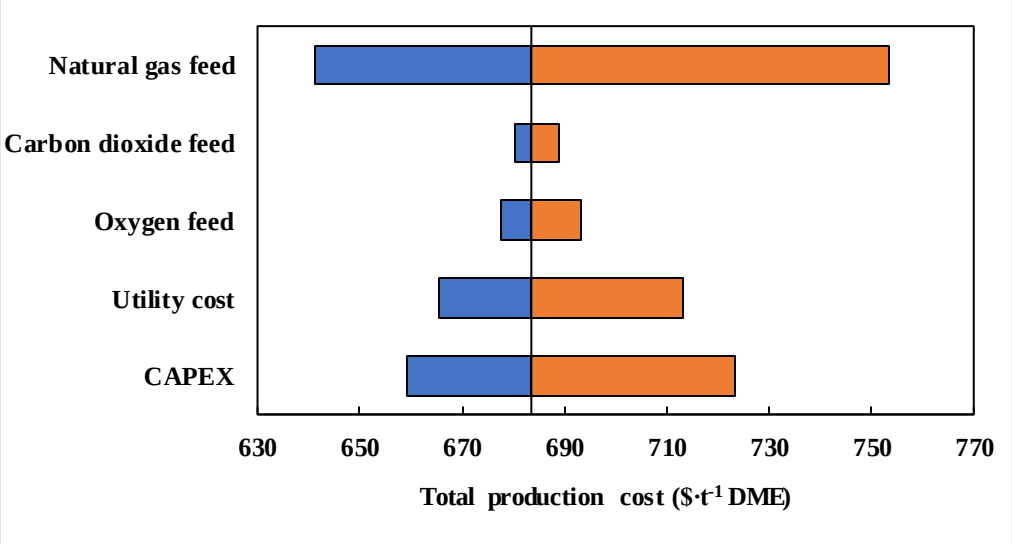

(vi) ADTRI-GWP

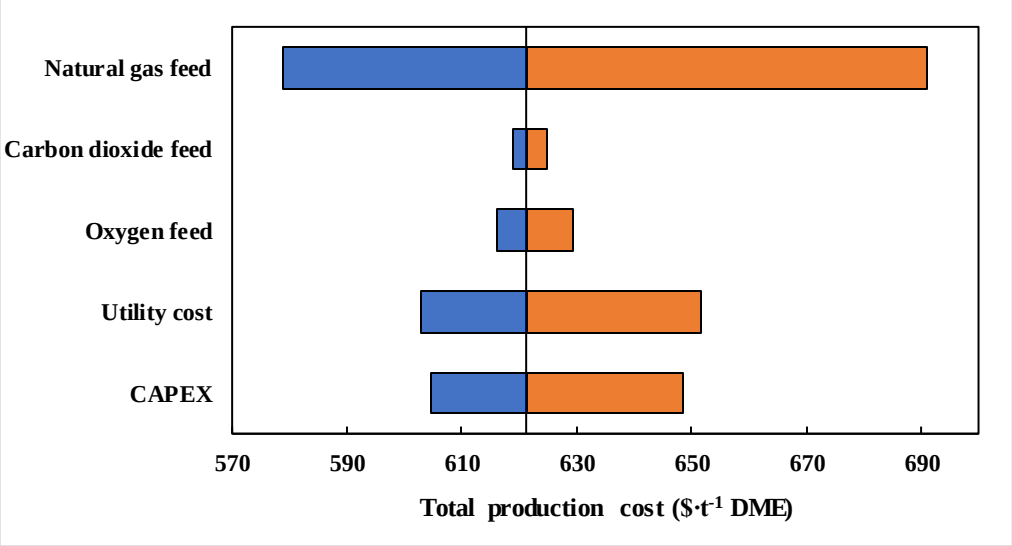

(vii) ISOTRI-OPEX

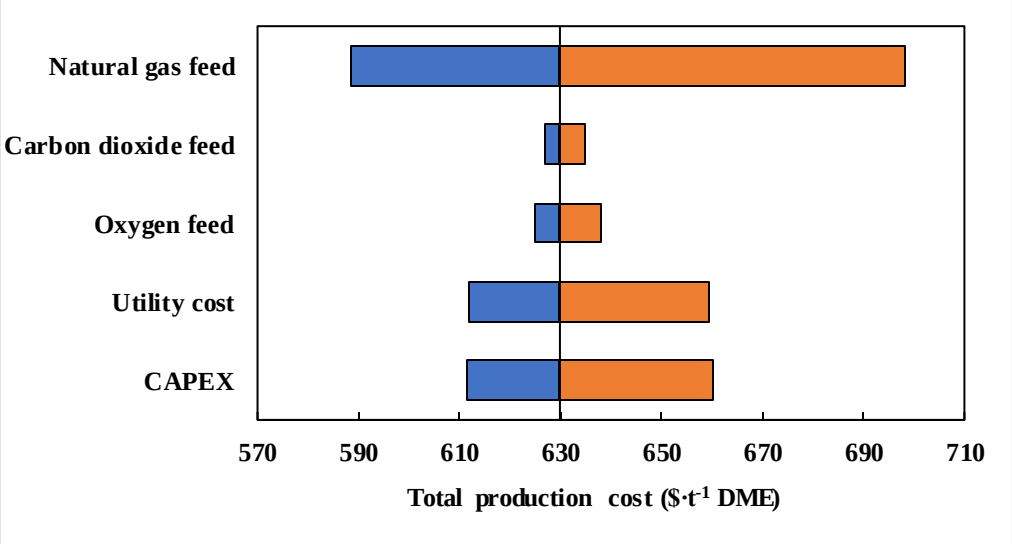

(viii) ISOTRI-GWP

Figure 3.18. Sensitivity analysis for CCU indirect DME production scenarios between a confidence interval of 5 to 95%.

The probability distribution for the uncertainty analysis of the CCU scenarios studied are shown in Figure 3.19. Providing an uncertainty analysis is an essential element of studying novel and low maturity technologies such as CCU. The uncertainty analysis provides an assessment of the risk of investment in the CCU scenarios studied and the level of confidence present in the calculated values from the techno-economic assessments conducted. The average values and standard deviation within a 90% confidence interval for the total production cost are outlined. The standard deviation in relation to the average ranges from $\pm$ 5.88% to $\pm$ 6.35%. Therefore for example, there is a 90% probability that the value for the total production cost for DR-OPEX lies between \$473.46 and \$535.02 t^{-1} DME. Wherein which if the sale price of DME is above \$535.02 t^{-1} DME, it is highly probable that the process is commercially viable.

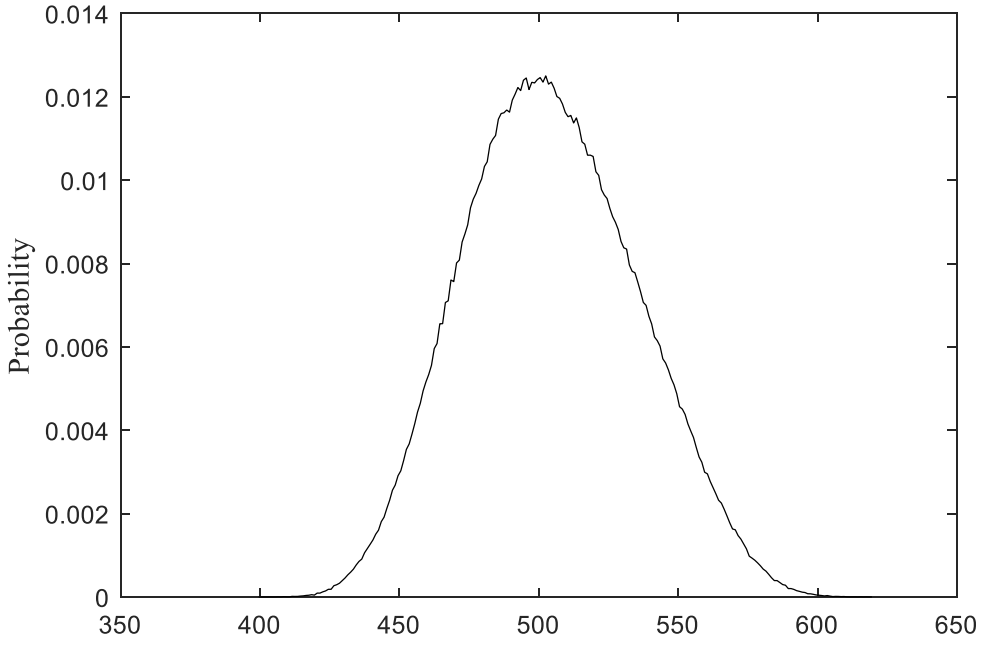

(i) DR-OPEX

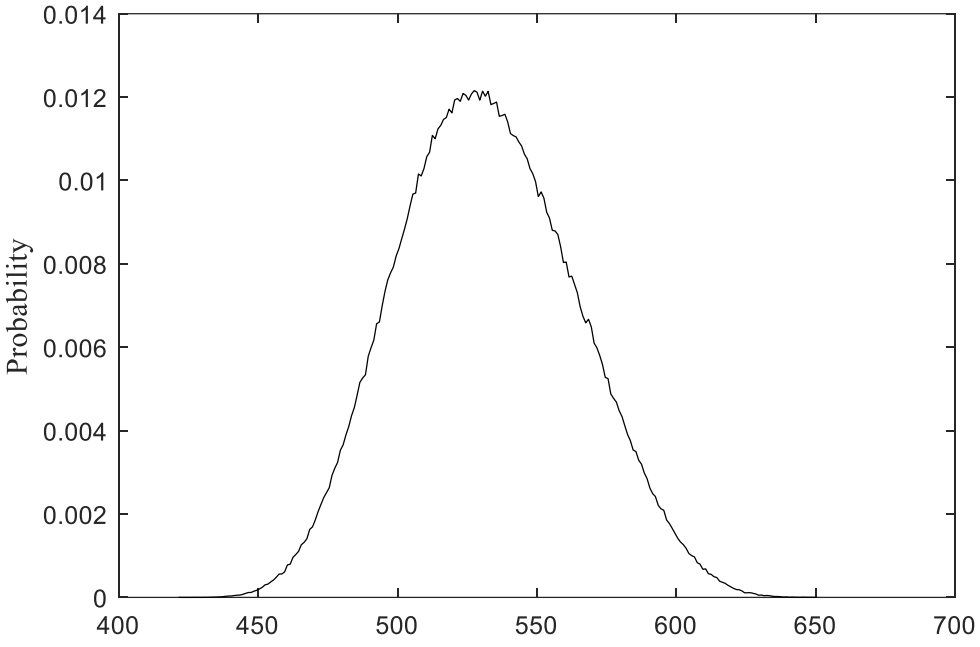

Average: 532.08 Standard Deviation:31.58

(ii) DR-GWP

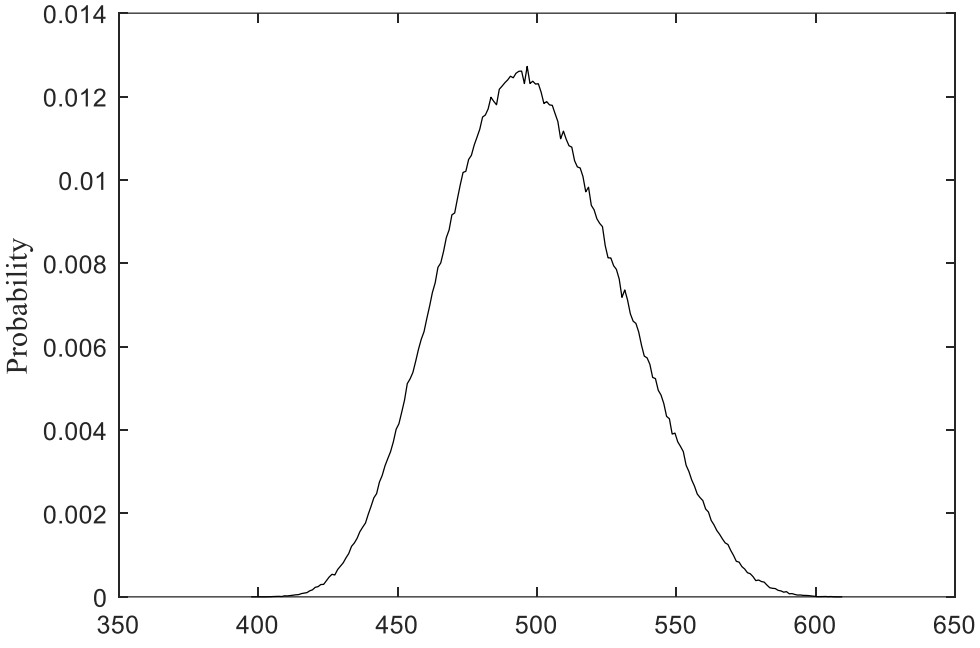

Average: 498.88 Standard Deviation:30.61

(iii) BI-OPEX

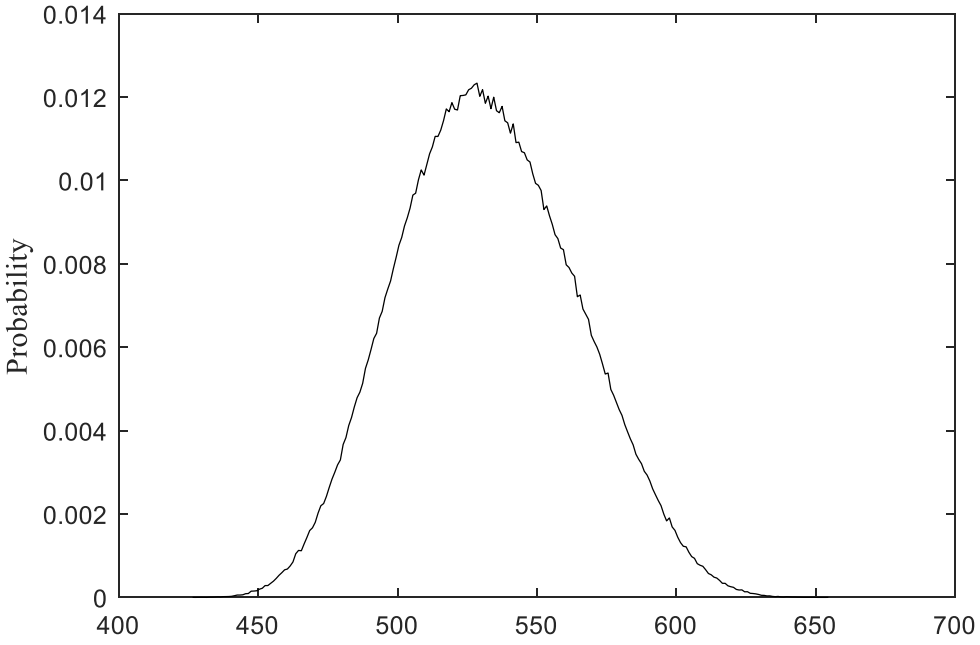

Average: 532.35 Standard Deviation:31.55

(iv) BI-GWP

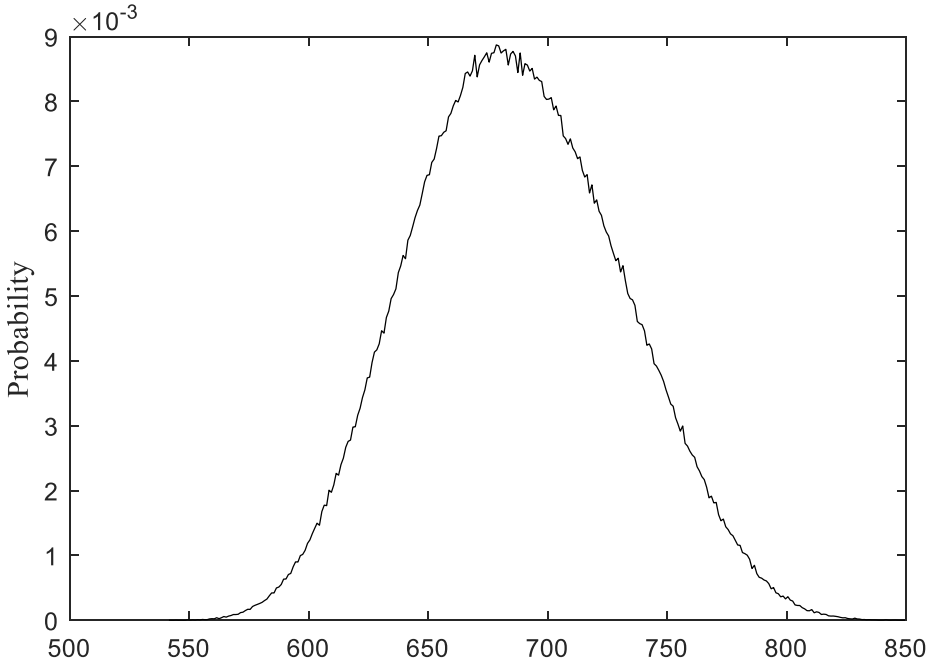

Average: 687.15 Standard Deviation:43.62

(v) ADTRI-OPEX

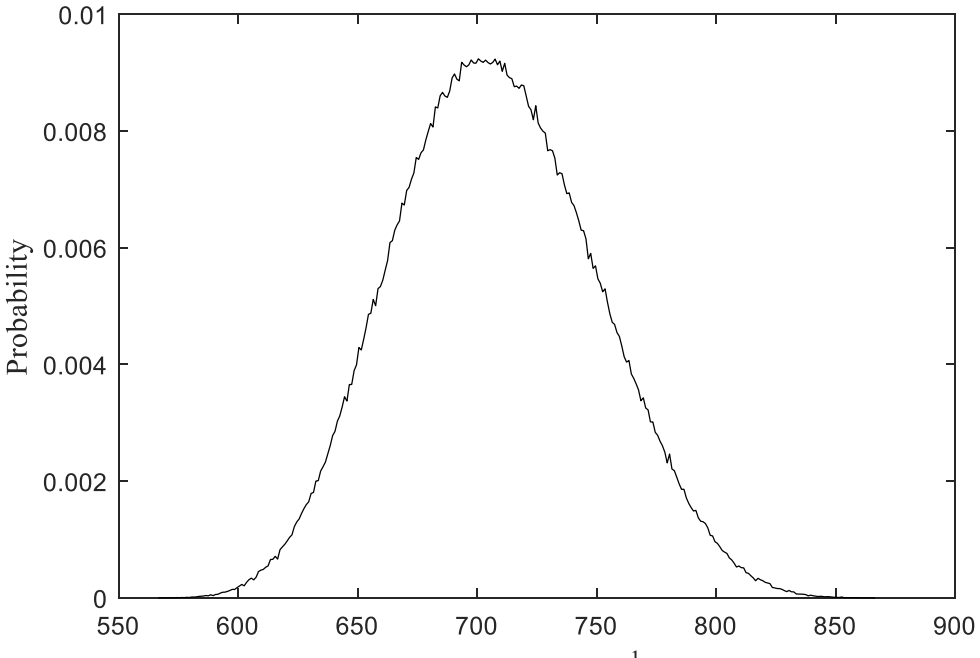

Average: 707.61 Standard Deviation:41.61

(vi) ADTRI-GWP

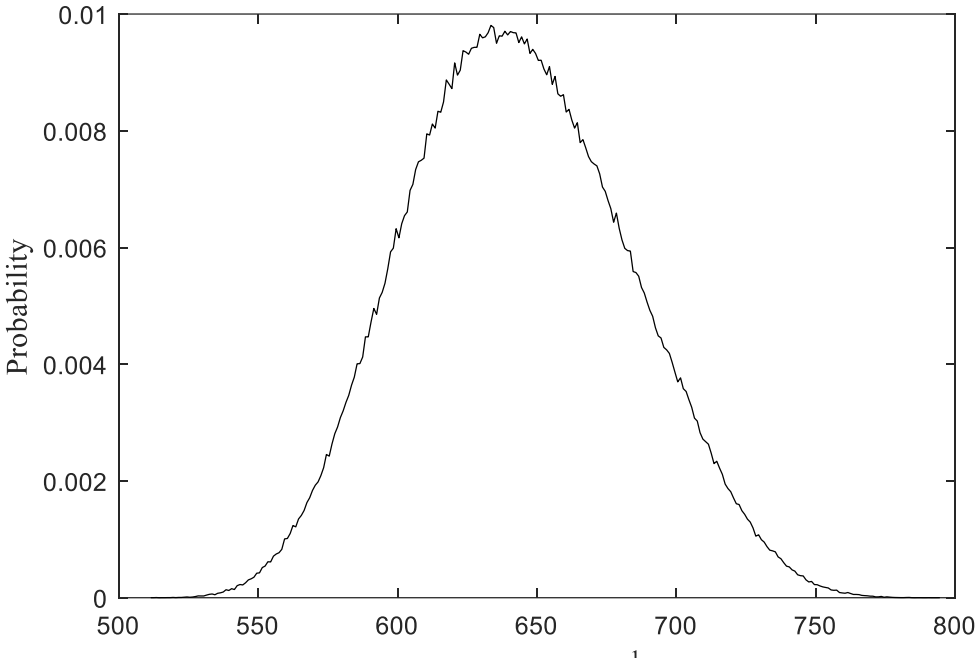

Average: 643 Standard Deviation:39.3

(vii) ISOTRI-OPEX

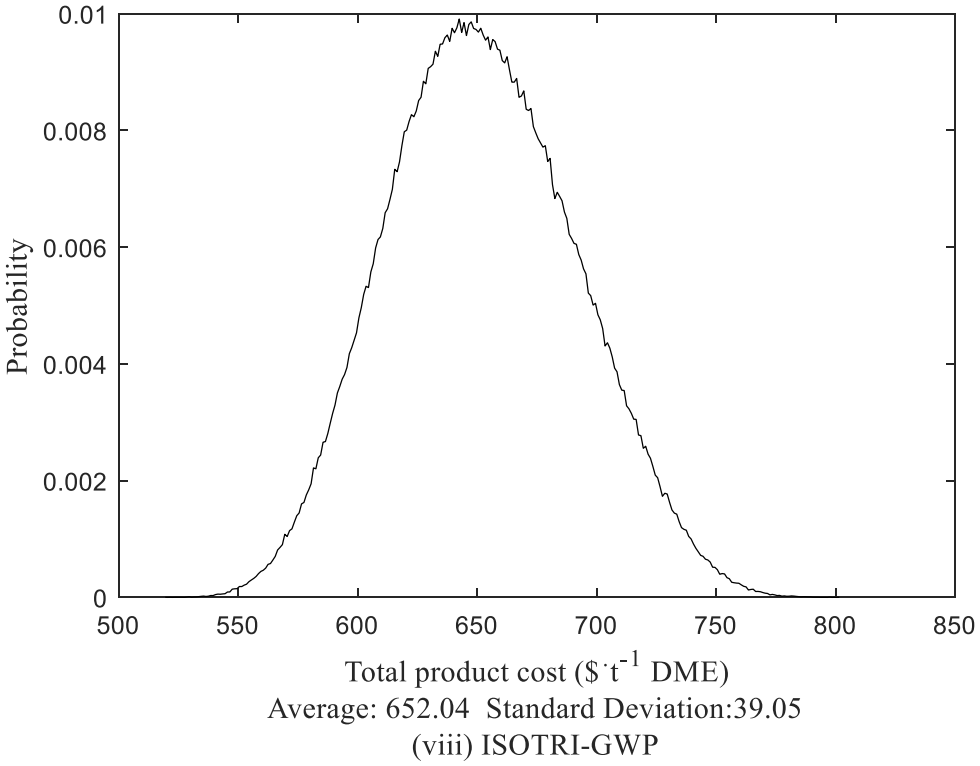

Figure 3.19.Uncertainty analysis for CCU indirect DME production scenarios.

6.0 Conclusion

CCU processes using a feed stock of CO_2 captured from a cement plant to produce DME indirectly from methanol dehydration were studied. Three alternative reforming technologies (dry-,bi- and tri-reforming) were modelled in Aspen Plus V12 and optimised using MATLAB towards minimising costs or minimising environmental impact. Subsequent heat integration was performed to complete a techno-economic and environmental assessment. A sensitivity and uncertainty analysis were completed using a Monte Carlo simulation. The CCU scenarios after initial optimisation showed a GWP ranging from 3.35 to 4.76 tonne CO_2-equivalent·t^{-1} DME and overall CO_2 conversions from -4.7% to 86.16%. ADTRI-GWP had the lowest GWP even though it had a CO_2 conversion of 10.02%. In contrast, DR-OPEX had an overall CO_2 conversion of 86.12% and a GWP of 4.76 tCO_2-equivalent·t^{-1} DME. The overall CO_2 conversion is a limited environmental impact indicator in comparison to GWP as it does not incorporate indirect CO_2 emissions and alternative greenhouse gases. The total production cost of the CCU scenarios ranged from $819.32 to

$970.87 tonne^{-1} DME, which is higher than the total production cost of conventional DME production scenario by 3.24% to 22%. Applying heat integration reduced the GWP and total production cost significantly. The GWP of the CCU scenarios were reduced to 2.2 – 3.27 tCO_2-equivalent·t^{-1} DME and the conventional DME production process to 3.62 tCO_2-equivalent·t^{-1} DME. ADTRI-GWP had the lowest GWP; 39.23% lower than the GWP of the conventional scenario. The total production cost was also reduced to $482.98 – 683.52 t^{-1} DME for the CCU scenarios and $417.78 t^{-1} DME for the conventional scenario. BI-OPEX had the lowest total production cost for the CCU scenarios, however this is still 15.6% greater than the total production cost for conventional DME production. In contrast ADTRI-GWP had the greatest total production cost at $683.52 tonne^{-1} DME; which is 41.52% greater than for conventional DME production.

The CGWP was introduced to allow for a performance indicator that outlines the link between the cost of the process in relation to the global warming potential reductions. The CGWP ranged from $93.69 to $581.23 t^{-1} CO_2-equivalent and BI-GWP had the lowest CGWP. In contrast, the tri-reforming scenarios had higher CGWP in comparison to the other reforming technologies even though, excluding ISOTRI-OPEX, they displayed lower GWP's than the other reforming technologies.

The MFSP for CCU scenarios ranged from $16.65 to $23.57 GJ^{-1}. These are 8.92% lower to 31.56% greater than the diesel selling price and 13.32% to 60.36% greater than LPG. The MFSP for the dry- and bi-reforming scenarios may be competitive compared to diesel as a fuel, however tri-reforming scenarios are significantly higher. However, this may be counteracted depending on the current value of carbon emission levy on diesel or a 'green' premium on the selling price of CCU tri-reforming synthesised DME.

The sensitivity analysis showed that natural gas had the largest impact on the total production cost followed by CAPEX and utility costs. The cost of CO_2 and

oxygen (for the tri-reforming scenarios) had a low impact on total production cost. The low impact of CO_2 and oxygen feed costs were due to their low impact on total raw material cost for the scenarios studied, whilst natural gas provided 83.11% to 92.2% of the total raw material cost for the CCU scenarios studied. The uncertainty analysis showed a standard deviation in relation to the average ranging from $\pm$ 5.88% to $\pm$ 6.35%.

From the scenarios studied, bi-reforming showed the greatest promise as an alternative to conventional steam reforming for the production of DME. For example, DME produced from bi-reforming is a commercially competitive alternative to diesel, with a MFSP of \$16.65 GJ^{-1} in comparison to diesel (\$17.92 GJ^{-1}).

References

[1] *M. R. F. K. G.R. Moradi, "The effects of partial substitution of Ni by Zn in LaNiO3 perovskite catalyst for methane dry reforming," Journal of CO2 Utilization, vol. 6, pp. 7-11, 2014.*

[2] *J. P. S. S.-W. S. F. E.G. Mahoney, "The effects of Pt addition to supported Ni catalysts on dry (CO2) reforming of methane to syngas," Journal of CO2 Utilization, vol. 6, pp. 40-44, 2014.*

[3] *C. S. Y. C. C. C. T. J. S. O. U. O. H. D. S. D.-V. N. V. S. Z. A. Hamidah Abdullah, "Recent Advances in CO2 Bi-Reforming of Methane for Hydrogen and Syngas Productions," in Chemo-Biological Systems for CO2 Utilization, CRC Press, 2020, p. 27.*

[4] *F. F.Yaripour, "Catalytic dehydration of methanol to dimethyl ether (DME) over solid-acid catalysts," Catalysis Communications, vol. 6, no. 2, pp. 147-152, 2005.*

[5] *G. O. S. S. R. Wouter Schakel, "Assessing the techno-environmental performance of CO2 utilization via dry reforming of methane for the production of dimethyl ether," Journal of CO2 Utilization, vol. 16, pp. 138-149, 2016.*

[6] *A. S. M. W. Mosleh Uddin, "Techno-economic and greenhouse gas emission analysis of dimethyl ether production via the bi- reforming pathway for transportation fuel," Energy, vol. 211, 2020.*

[7] *F. J. F. Javad Asadi, "Optimization of dimethyl ether production process based on sustainability criteria using a homotopy continuation method," Computers & Chemical Engineering, vol. 115, pp. 161-178, 2018.*

[8] *Y. J. B. Chirag Mevawala, "Techno-economic optimization of shale gas to dimethyl ether production processes via direct and indirect synthesis routes," Applied Energy, vol. 238, pp. 119-134, 2019.*

[9] *A. T.H.Fleisch, "Dimethyl ether: A fuel for the 21st century," Studies in Surface Science and Catalysis, vol. 107, pp. 117-125, 1997.*

[10] *A. BBE., "Dimethyl ether as an R12 replacement.," in Proc. IIF/IIR Gustav Lorentzen Conf., Oslo, Norway, 1998.*

[11] *S. A. G. M. S. T. e. a. A. A. Zharov, "Carbon dioxide and dimethyl ether mixture as a refrigerant for air conditioning systems for space ground-based infrastructure," in AIP Conference Proceedings 2171 , 120009, 2019.*

[12] *J. Yu, Y. Zhang, G. Jiang and Q. Kui, "An Experimental Study on Steady Flash Boiling Spray Characteristics of DME/Diesel Blended fuel," SAE 2010 World Congress & Exhibition, 2010.*

[13] *H. Salsing, V. Golovitchev and I. Denbratt, "Numerical Analysis of Combustion and Emissions Formation in a Heavy Duty DME Engine," SAE 2012 World Congress & Exhibition, 2012.*

[14] *K. R. G. P. M. S. R. Senthil, "Pollution Control Technique by Using CatalystCoated Alumina Ball Filter in a DI Diesel," International Journal of Applied Engineering Research, vol. 10, no. 38, 2015.*

[15] *D. Leed, "Spray Characteristics of DME-LPG Blended Fuel in a High-Pressure Diesel Injection System," Asia Pacific Automotive Engineering Conference, 2013.*

[16] *A.García-TrencoA.Vidal-MoyaA.Martínez, "Study of the interaction between components in hybrid CuZnAl/HZSM-5 catalysts and its impact in the syngas-to-DME reaction," Catalysis Today, vol. 179, no. 1, pp. 43-51, 2012.*

[17] J.-H. K.-J. P.-J.-S. J.-D. J. Kye Sang Yoo, "Influence of solid acid catalyst on DME production directly from synthesis gas over the admixed catalyst of Cu/ZnO/Al2O3 and various SAPO catalysts," Applied Catalysis A: General, vol. 330, pp. 57-62, 2007.

[18] Aspen Technology, "Aspen Plus User Guide," Aspen Technology, USA, 2000.

[19] M. Voldsund, R. Anantharaman, D. Berstad, G. Cinti, E. De Lena, M. Gatti, M. Gazzani and e. al., "CEMCAP framework for comparative techno-economic analysis of CO2 capture from cement plants - D3.2," CEMCAP, 2018.

[20] O. D. L. 2. R. 2. R. 1. V. 1.-F. P.-C. 3. B. 1. F. 1. A. 1. S. 3. G. 4. M. 3. a. Stefania Osk Gardarsdottir, "Comparison of Technologies for CO2 Capture from Cement Production—Part 2: Cost Analysis," Energies, 2019.

[21] Aspen Technology, "Aspen Physical Property System - Physical Property Methods," Burlington, USA, 2013.

[22] P. James R. Couper W. Roy Penney James R. Fair, Chemical Process Equipment - Selection and Design, Gulf Professional Publishing, 2009.

[23] HSE, "Pipelines and gas supply industry," HSE, [Online]. Available: https://www.hse.gov.uk/pipelines/faqs.htm#:~:text=Pipelines%20associated%20with%20gas%20terminals,some%20at%20over%20300%20bar.. [Accessed 02 09 2020].

[24] P. S. E. R. K. Altfeld, "Development of natural gas qualities in Europe," Gas Qual., vol. 152, pp. 544-550, 2011.

[25] J. S. G.S. Sandeep Alavandi, "Emerging and Existing Oxygen Production Technology Scan and Evaluation," 2018.

[26] M. S. Ahmad Reza Keshavarz, "Steam Prereforming of Natural Gas over Nanostructured Nickel/Magnesium Aluminate Spinel Catalysts: Effect of Support and Nickel Loading," Energy Technology, vol. 5, no. 4, pp. 629-636, 2017.

[27] B. P. W. K. J. H. Colin Rhodes, "Promotion of Fe3O4/Cr2O3 high temperature water gas shift catalyst," Catalysis Communications, vol. 3, no. 8, pp. 381-384, 2002.

[28] M. J.Skrzypek, "Kinetics of methanol synthesis over commercial copper/zinc oxide/alumina catalysts," Chemical Engineering Science, vol. 46, no. 11, pp. 2809-2813, 1991.

[29] F. Y. H. A. S. S. M. Mollavali, "Intrinsic kinetics study of dimethyl ether synthesis from methanol on γ-Al2O3 catalysts," Industrial Engineering Chemical Research, vol. 47, pp. 3265-3273, 2008.

[30] T. S. Christensen, "Adiabatic prereforming of hydrocarbons - an important step in syngas production," Applied Catalysis A: General, vol. 138, no. 2, pp. 285-309, 1996.

[31] H.Holm-Larsen, "CO2 reforming for large scale methanol plants - an actual case," Studies in Surface Science and Catalysis, vol. 136, pp. 441-446, 2001.

[32] C. Bartholomew and R. Farrauto, Fundamentals of Industrial Catalytic Process, 2nd ed, NJ, USA: Wiley Interscience:Hoboken, 2005.

[33] J. X. G. F. Froment, "Methane steam reforming, methanation and water-gas shift. I. Intrinsic kinetics," AIChE Journal, vol. 35, no. 1, pp. 88-96, 1989.

[34] H. L. Z. C. Z. Jianjun Guo, "Dry reforming of methane over nickel catalysts supported on magnesium aluminate spinels," Applied Catalysis A: General, vol. 273, no. 1-2, pp. 75-82, 2004.

[35] J. G. H. W. a. A. K. D. Zhang, "Kinetic Studies of Carbon Dioxide Reforming of Methane over Ni-Co/Al-Mg-O Bimetallic Catalyst," Industrial & Engineering Chemistry Research , vol. 48, pp. 677-684, 2009.

[36] J. T. a. S. A. P. Richardson, "Carbon Dioxide Reforming of Methane with Supported Rhodium," Applied Catalysis, vol. 61, pp. 293-309, 1990.

[37] M. B. A. T. D. T.-V. N. A. Sharanjit Singh, "Bi-reforming of methane on Ni/SBA-15 catalyst for syngas production: Influence of feed composition," International Journal of Hydrogen Energy, vol. 43, no. 36, pp. 17230-17243, 2018.

[38] M.-J. P. S.-C. B. K.-S. H. Y.-J. L. G. K. H.-G. P. K.-W. J. N. Park, "Modeling and optimization of the mixed reforming of methane: Maximizing CO2 utilization for non-equilibrated reaction," Fuel, vol. 115, pp. 357-365, 2014.

[39] C.-W. L. David L.Trimm, "The combustion of methane on platinum—alumina fibre catalysts—I: Kinetics and mechanism," Chemical Engineering Science, vol. 35, no. 6, pp. 1405-1413, 1980.

[40] E.V.Rebrov, "13 - Advances in water-gas shift technology: modern catalysts and improved reactor concepts," in Advances in Clean Hydrocarbon Fuel Processing, Woodhead Publishing Series in Energy, 2011, pp. 387-412.

[41] F. M. Giulia Bozzano, "Efficient methanol synthesis: Perspectives, technologies and optimization strategies," Progress in Energy and Combustion Science, vol. 56, pp. 71-105, 2016.

[42] A. S. M. B. K. Francesco Dalena, "Advances in Methanol Production and Utilization,Angelo Basile,Adolfo Iulianelli," membranes, 2018.

[43] J. C. S. E. R. R. Ana M. Ribeiro, "Syngas Stoichiometric Adjustment for Methanol Production and Co-Capture of Carbon Dioxide by Pressure Swing Adsorption," Separation Science and Technology , vol. 47, no. 6, pp. 850-866, 2012.

[44] J. S. D. B. W. W. R. Turton, Analysis, synthesis, and design of chemical processes, Prentice Hall , 2018.

[45] S. H. M. G. M. N. A. S. Y. Tavan, "From laboratory experiments to simulation studies of methanol dehydration to produce dimethyl ether - Part I: reaction kinetic study," Chemical Engineering and Processing: Process Intensification, vol. 73, pp. 144-150, 2013.

[46] M. W. B.T. Diep, "Thermodynamic equilibrium constants for the methanol-dimethyl ether-water system," Journal of Chemical and Engineering data, vol. 32, pp. 330-333, 1987.

[47] ASTM, "Active Standard ASTM D7901".

[48] M. Peters, K. Timmerhaus and R. West, Plant Design and Economics for Chemical Engineers, New York: McGraw Hilll, 2004.

[49] P. G.-G. H. E. M. C.-F. A. W. K. A. Ioanna Dimitriou, "Carbon dioxide utilisation for production of transport fuels: process and economic analysis," Energy & Environmental Science, vol. 8, no. 6, pp. 1775-1789, 2015.

[50] Mathworks, "actxserver," Mathworks, [Online]. Available: https://uk.mathworks.com/help/matlab/ref/actxserver.html.

[51] A. Neumaier, "Complete Search in Continuous Global Optimization and Constraint Satisfaction," in Acta Numerica, 13, Cambridge University Press, 2004, pp. 271-369.

[52] K. Marti, Stochastic Optimization Methods, Springer, 2008.

[53] ADHB, "Average fuel prices".

[54] MyLPGEU, "Chart of fuel prices in the UK," MyLPGEU, 01 July 2019. [Online]. Available: https://www.mylpg.eu/stations/united-kingdom/prices/. [Accessed 01 July 2019].

[55] Methanol Institute, "methanol-price-supply-demand," Methanol Institute, 2019.

[56] K. A. D. A. Mansur M.Masiha, "Price dynamics of natural gas and the regional methanol markets," Energy Policy, vol. 38, no. 3, pp. 1372-1378, 2010.

[57] GISTEMP Team, "GISS Surface Temperature Analysis (GISTEMP)," NASA Goddard Institute for Space Studies, 2018. [Online]. Available: https://data.giss.nasa.gov/gistemp/. [Accessed 29 04 2018].

[58] European commison, "European strategic long-term vision for a prosperous, modern, competitive and climate neutral economy," 2018.

[59] M. Sanjuán, C. Andrade, P. Mora and A. Zaragoza, "Carbon Dioxide Uptake by Cement-Based Materials: A Spanish Case Study," Applied Sciences, vol. 10, no. 1, p. 339, 2020.

[60] D. Elzinga, S. Bennett, D. Best, K. Burnard, P. Cazzola, D. D'Ambrosio, J. Dulac, A. Fernandez Pales, C. Hood, M. LaFrance and e. al., Energy Technology Perspectives 2015: Mobilising Innovation to Accelerate Climate Action, Paris, France: International Energy Agency (IEA) Publications, 2015.

[61] B. Diczfalusy, M. Wrake, K. Breen, K. Burnard, K. Cheung, J. Chiavari, F. Cuenot, D. D'Ambrosio, J. Dulac, D. Elzinga, L. Fulton, A. Gawel, S. Heinen, O. Ito, H. Kaneko, A. Koerner, S. McCoy, L. Munuera, U. Remme, C. Tam and T. Trigg, Energy Technology Perspectives 2012: Pathways to a Clean Energy, Paris: International Energy Agency, 2012.

[62] Close, "Carbon Capture, Utilization and Storage.," SETIS Magazine of the European Commission, 2016.

[63] IEA, "Putting CO2 to Use," 2019.

[64] W. K. W. L. J. L. P. Z. R. B. A. S. T. M. P. Markewitz, Energy Environ. Sci, vol. 5, no. 6, pp. 7281-7305, 2012.

[65] A Technical Basis for Carbon Dioxide Storage, CO2 Capture Project, 2009.

[66] A. S. J. M. M. H. J. H. J. G. P. Zapp, "Overall environmental impacts of CCS technologies—A life cycle approach," International Journal of Greenhouse Gas Control, vol. 8, pp. 12-21, 2012.

[67] A. D. A. A. M. Aresta, "Catalysis for the valorization of exhaust carbon: from CO2 to chemicals, materials, and fuels. technological use of CO2," Chemical reviews, vol. 114, no. 3, pp. 1709-1742, 2014.

[68] J. B. R. W. S. K. P. S. H.H. Khoo, "Carbon capture and utilization: Preliminary life cycle CO2, energy, and cost results of potential mineral carbonation," Energy Procedia, vol. 4, pp. 2494-2501, 20122.

[69] W. G. S. M. P. Jaramillo, "Life Cycle Inventory of CO2 in an Enhanced Oil Recovery System," Environmental Science and Technology, vol. 43, no. 21, pp. 8027-8032, 2009.

[70] M. G. M. Aresta, "Life cycle analysis applied to the assessment of the environmental impact of alternative synthetic processes. The dimethylcarbonate case: part 1," Journal of Cleaner Production, vol. 7, no. 3, pp. 181-193, 1999.

[71] U. H. J. W. M. W. J. e. a. Lee, "Well-to-Wheels Emissions of Greenhouse Gases and Air Pollutants of Dimethyl Ether from Natural Gas and Renewable Feedstocks in Comparison with Petroleum Gasoline and Diesel in the United States and Europe,," SAE International Journal of Fuels and Lubricants, vol. 9, no. 3, pp. 546-557, 2016.

Chapter 4 – Techno-economic and Environmental assessment of CCU MTO synthesis

Term	Acronym
Methanol-to-olefins	MTO
The Dalian Institute of Chemical Physics	DICP
Deep catalytic cracking	DCC
Dimethyl ether	DME
Methanol to propylene	MTP
Silicoaluminophosphate zeolite	SAPO
Fischer-Tropsch to olefins	FTO
Ethanol dehydration	ED
Greenhouse gas	GHG
Carbon capture and storage	CCS
Carbon capture and utilisation	CCU
Global warming potential	GWP
Redlich-Kwong-Soave	RK
Non-random two-liquid	NRTL
Water gas shift	WGS
Dry methane reforming	DMR
Total capital investment	TCI
Total direct costs	TDC
Total indirect costs	TIC
Fixed capital investment	FCI
Working capital	WC
Total capital investment	TCI
Fixed cost of production	FCP
Operating supervision	OS
Annual maintenance and repair costs	AMR
Variable costs of production	VCP

Annual capital repayment	ACR
capital expenditure	CAPEX
Life cycle assessments	LCA
Component object model	COM
Mixed integer non-linear programming	MILP
Mesh adaptive search	MADS
Aspen Energy Analyzer	AEA
Cost of global warming potential reduction	CGWP
Minimum fuel selling price	MFSP
Liquified petroleum gas	LPG

1.0 Introduction and gaps in knowledge

An option that may be incorporated as part of the solution to reduce global greenhouse gas emissions from cement production is the synthesis of lower olefins, including ethylene and propylene, through carbon capture and utilisation (CCU). The benefit of producing CCU based lower olefins is the considerable global demand they have, the global demand for propylene and ethylene is 120 MT yr^{-1} and 180 MT yr^{-1} respectively [1] [2]. Therefore, a significant portion of captured CO_2 may be incorporated to produce value-added products, substituting alternative fossil fuel-based synthesis of lower olefins such as the steam cracking of naphtha. Dry-reforming, bi-reforming and tri-reforming have been suggested as suitable options for CCU-based olefin synthesis [3] [4] [5].

Studies related to reforming based MTO processes have incorporated a CO_2 rich natural gas feed. Chen et al studied the dry-reforming process combined with the Fischer-Tropsch to olefins technology. A CO_2 rich natural gas stream sourced from the South China Sea was converted to high value-added linear alpha olefin products with a net CO_2 emission of 0.06 ton CO_2 per ton product; a carbon efficiency of 62.2 %; and a product cost of 8839 RMB per ton [6]. Alturki conducted a techno-economic study on the use of shale-derived natural gas in the US to produce olefins through a methanol intermediate. Syngas production through dry-reforming, partial oxidation, autothermal reforming and tri-reforming was combined with a methanol to olefin process. It was found that the dry-reforming process showed a 99.24% reduction in CO_2 at low syngas ratios [7].

Other techno-economic studies have focussed upon fossil fuel-based olefin production. Xing et al conducted a technoeconomic assessment of a coal to olefins plant (CTO) and a Fischer-Tropsch to olefins (FTO) plant. It was found that due to the lower olefin selectivity, the FTO total product cost was 17.46% higher than the CTO process [8]. Vincenzo completed a techno-economic assessment of olefin production from naptha and natural gas through oxidative coupling of methane and naptha steam cracking [9]. Man et al proposes a novel co-feed

process for coke oven gas assisted coal to olefin production [10]. It was found that energy efficiency was improved by 10%, reducing GHG emissions by 85% in comparison to conventional CTO processes. Furthermore, economic feasibility is achieved with a carbon tax greater than 150 CNY t^{-1} CO_2.

Previous studies related to CCU based olefin production have focussed on the use of renewable energy to produce H_2 for methanol synthesis through CO_2 hydrogenation. Rosental et al completed a cradle-to-gate life cycle assessment to produce olefins through a MTO process. The methanol was produced through CO_2 hydrogenation using CO_2 from direct air capture or amine scrubbing and H_2 from alkaline water electrolysis. Electricity was assumed to be supplied from offshore wind turbines. It was found that GHG emissions are reduced by 88-97% in comparison to conventional fossil-fuel based production routes [11]. Ioannou et al carried out a process optimisation to minimise total cost and global warming potential for ethylene production through a hybridisation of direct electrochemical synthesis and MTO synthesis with steam cracking. Methanol for the MTO process was produced using either hydrogen from steam methane reforming combined with carbon capture and storage or electrolytic hydrogen, with electricity supplied from a range of renewable sources. It was found that the carbon footprint of the CCU routes was improved by 236% when compared to fossil fuel-based ethylene [12].

Previous publications regarding CCU based olefins productions have incorporated methanol production through CO_2 hydrogenation assuming hydrogen production using electricity from renewable energy. Studies utilising syngas production from reforming technologies has implemented a shale-derived natural gas rather than using captured CO_2 as a feed. There is limited literature for the techno-economic assessment of CCU-based olefin production.

2.0 Olefins Background

Light olefins, such as ethylene and propylene, have considerable demand due to their presence as an essential feedstock to produce polymers and chemical intermediates. The traditional means of producing olefins is via the steam cracking of crude-oil based naphtha. However, alternatives such as the MTO process have been developed due to oil shortages. Another factor is the energy-intensive nature of the steam cracking process due to the high temperature requirements

The MTO production process is a major source of global methanol demand (an estimated 25% of global methanol demand in 2019 [13]). The MTO process operates through the dehydration of methanol, forming dimethyl ether initially, followed by the production of olefins through the repeated process of methylation and dealkylation of larger olefins. The MTO process is advantageous in comparison to the steam cracking process due to high light olefins selectivity, flexibility in ethylene-to-propylene ratio and the capability to operate at moderate temperatures [14]. Molecular sieve catalysts such as SAPO-34 have been developed to enable high selectivity for the MTO process [15]. The Dalian Institute of Chemical Physics (DICP) constructed and established the first coal-to-olefins plant in China based upon the MTO process in 2010, providing up to 80 wt% selectivity towards ethylene and propylene [16] [17]. This is significantly higher than for the case of steam cracking.

2.1 Olefin synthesis routes

2.1.1 Steam cracking

Steam cracking (SC) is an established and essential process in the petrochemical industry accounting for an estimated usage of 40% of the global hydrocarbon feedstock [18]. Steam cracking operates through a ’hot section’ and a ‘cold section’. The steam cracking process operates through the heating of hydrocarbon (naphtha, LPG or ethane) feed diluted with steam in a tubular reactor at temperatures above 800 °C [19]. To increase ethene yield the product gas is

quenched, preventing further reaction. Further cooling occurs via the injection of quench oil. This first section is considered the 'hot section'. In the 'cold section' the products are separated through fractional distillation. Propene is a by-product in this process.

2.1.2 Deep catalytic cracking and catalytic pyrolysis

Deep catalytic cracking (DCC) converts heavy oils into olefins. The main products are propylene with ethylene and C4-hydrocarbons as a by-product. DCC operates at a temperature of 530 to 560 °C. To further increase ethylene yield a catalytic pyrolysis unit is incorporated through a tubular cracking furnace, operating at a temperature of 580 to 640 °C. Alkanes present in the product gas are further converted in a second tubular cracking furnace to further increase olefin yield [20].

2.1.3 Propane dehydrogenation

Propylene is produced from propane derived from natural gas or petroleum. The endothermic dehydrogenation reaction occurs at a temperature of 500 to 680 °C and a pressure of 15-250 kPa [21].

$$C_3H_8 \leftrightarrow C_3H_6 + H_2$$

2.1.4 MTO Processes

In the initial step methanol is dehydrated to dimethyl ether (DME),

$$2CH_3OH \leftrightarrow CH_3OCH_3 + H_2O$$

followed by a series of dealkylation and methylation processes to olefins such as ethylene, propylene and butenes. By-products are also formed including methane, ethane, propane, heavy hydrocarbons and aromatics.

Four alternative MTO technologies are available: a) the UOP/Norsk Hydro MTO b) Dalian Institute of Chemical Physics (DICP) D-MTO and D-MTO-II c) Sinopec's S-MTO d) Luirgi Methanol to propylene (MTP).

The UOP/Norsk Hydro technology was developed by UOP (currently Honeywell UOP) in collaboration with Hydro and represents a majority of global olefins production capacity. It has a high selectivity of 75-80% for ethylene and propylene production from methanol using a silicoaluminophosphate zeolite (SAPO) based catalyst, SAPO-34 [22]. A methanol feed preheated to a gaseous phase is used in a low pressure fluidised bed reactor with a fluidised-bed regenerator. The reactor operates at temperatures ranging from 340 to 540 °C and a pressure of 0.1 to 0.3 MPa. The fluidised bed reactor is advantageous for an MTO reactor due to the frequent catalyst regeneration requirements and high reaction temperature. A reactor effluent including ethylene, propylene, water and heavy olefins is produced and cooled. In order to separate water and other impurities from the reactor effluent, a water quench system is employed. Further separation and purification is applied to separate the gaseous product from other by-products such as pentane and ethane. The UOP/Norsk Hydro technology is combined with an olefin cracking process developed by UOP and Total Petrochemicals to further increase propene and ethene selectivity [23].

The (DICP's MTO) D-MTO/D-MTO-II technology was developed by DICP and funded by Sinopec. A significant portion of MTO capacity in China is dominated by the D-MTO/D-MTO-II technology (70% of total capacity) [24].

The S-MTO technology, developed by SINOPEC, follows a similar production process as the UOP/Norsk Hydro technology. However, the process adopts a proprietary catalyst developed by SINOPEC. The reaction temperature used in the fluidised bed reactor is 340 to 540 °C and a pressure of 0.08 to 0.25 MPa. A 600 kt yr^{-1} S-MTO plant in Henan province, China is in operation with another three 1,800 kt yr^{-1} plants under design or construction [25].

For the Lurgi MTP technology the methanol feed is preheated to a temperature of 260 °C prior to entering a DME synthesis reactor. A methanol dehydration reaction using an acidic catalyst occurs in the DME synthesis reactor, converting ~75% of the methanol feed to DME and water whilst the rest remains unreacted. The reactor effluent is heated to ~470 °C and mixed with steam to be fed into the first of three parallel mixed bed MTP reactors. A H-ZSM-5 catalyst is used in the MTP reactor [26]. The initial reactor converts a significant portion of the DME reactor effluent (greater than ~99%), however the second and third MTP reactor units are used to further increase propylene yield. To aid in temperature control the DME reactor effluent is injected between each MTP reactor bed. Furthermore, olefin selectivity is increased through the recycling of by-products such as ethene and butene as well as condensate water.

2.1.5 Other olefin synthesis routes

Alternative methods of olefin synthesis include Fischer-Tropsch to olefins (FTO) and ethanol dehydration (ED). FTO synthesis operates through the conversion of syngas into hydrocarbons and oxygenates at high temperatures using a metal catalyst such as cobalt or nickel. The application of FTO is limited due to low selectivity towards olefins [27].

ED converts ethanol to ethylene through the process of dehydration at temperatures of 300 to 500 °C over catalysts such as activated alumina or supported phosphoric acid [28].

$$C_2H_5OH \leftrightarrow C_2H_4 + H_2O$$

3.0 Study outline

This Chapter aims to provide an assessment and comparison of techno-economic performance indicators and the global warming potential (GWP) of CCU MTO synthesis processes. MTO processes using one of the three CCU reforming technologies: dry methane reforming, bi-reforming and tri-reforming are compared to the use of steam reforming as the conventional MTO production technology. In a similar fashion to the CCU indirect DME synthesis scenarios discussed in Chapter 2, CO_2 captured using the oxyfuel capture technology from a cement manufacturing plant was used as the source of CO_2. An optimisation towards minimisation of operating costs and GWP for each reforming technology was completed. Further heat integration was conducted on all scenarios studied. The scenarios considered are shown in Table 4.1.

Table 4.1 Table outlining list of MTO production scenarios represented in this study.

Scenario	Reforming technology	Optimisation target
SR	Steam reforming	Operating Costs
DR-OPEX	Dry-reforming	Operating Costs
DR-GWP	Dry-reforming	GWP
BR-OPEX	Bi-reforming	Operating Costs
BR-GWP	Bi-reforming	GWP
ADTRI-OPEX	Adiabatic tri-reforming	Operating Costs
ADTRI-GWP	Adiabatic tri-reforming	GWP
ISOTRI-OPEX	Isothermal tri-reforming	Operating Costs
ISOTRI-GWP	Isothermal tri-reforming	GWP

4.0 Methodology

Similarly to Chapter 3, the scenarios studied were modelled and simulated on Aspen Plus V12 to produce mass and energy balances. MATLAB R2020b and the actxserver function, which allows the linking of Aspen Plus to MATLAB, were used to complete the optimisation of the scenarios. The Aspen Energy Analyser was used to conduct heat integration. From the optimised results, key techno-

economic performance indicators such as CO_2 conversion and olefin conversion factor were calculated. The total cost of production was also determined, accounting for capital and operating costs. Sensitivity and uncertainty analyses of parameters and their effect on process economics were completed.

4.1 System boundaries

This study aims to assess the economic and environmental impact of using CCU technologies incorporating CO_2 captured from a cement manufacturing plant including the costs and GWP of the capture, compression, and transport of the CO_2 from the cement plant. As in Chapter 3, appropriate system boundaries have been used to conduct the techno-economic and environmental assessment of the scenarios studies, as shown in Figure 4.1. The system boundaries were limited to the MTO production process, which includes methanol synthesis and the MTO process.

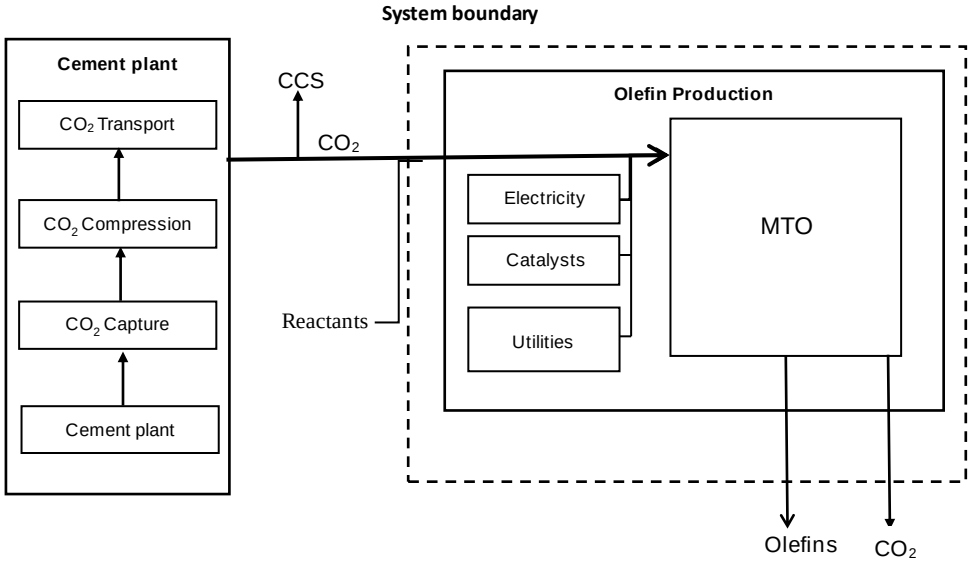

Figure 4.1 System boundary for the CCU and conventional olefins production scenarios. The CO_2 feed is only present in the CCU scenario.

4.2 Plant location and scale

Similarly to Chapter 3, a 1 $Mt.day^{-1}$ cement plant in the United Kingdom incorporating an oxyfuel capture unit was assumed. Production rate of the CCU process assumed an estimated 10% usage of captured CO_2 as a raw material. The

carbon capture unit used in the cement plant was an oxyfuel capture unit based upon the work by Gardarsdottir et al [29].

A summary of key plant characteristics is shown in Table 4.2.

Table 4.2 Cement plant location, capacity, and captured CO_2 data.

Plant location	United Kingdom
Production capacity (Mtonnes clinker yr^{-1})	1
Annual operating hours (hours)	8000
CO_2 capture technology	Oxyfuel
Clinker produced (t hr^{-1}) [29]	125
CO_2 captured (t hr^{-1}) [29]	99
Captured CO_2 to CCU (%)	10

4.3 Process outline

As shown in Figure 4.2, the processes modelled include a reforming section of either steam-, dry-, bi- or tri-reforming, a methanol synthesis section and a MTO section. CO_2 captured from the cement plant, natural gas, steam, and oxygen (in the case of tri-reforming) are fed to the reforming section. Syngas is produced in the reforming section which is used to produce methanol. The produced methanol is then used to produce olefins and other by-products in the MTO section.

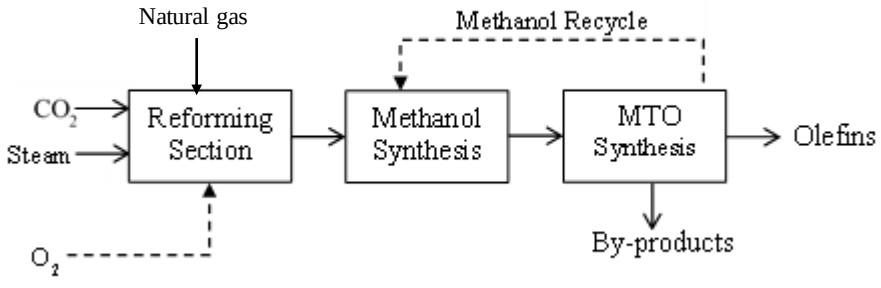

Figure 4.2 System boundary for the CCU and conventional olefins production scenarios. The CO_2 feed is only present in the CCU scenario.

4.4 Modelling assumptions

The properties used in this study are similar to what are used in Chapter 3. The MTO scenarios were modelled within Aspen Plus V12 under steady-state using the sequential modular mode. The RK-MHV2 model was used to determine physical and thermodynamic properties of high-pressure streams (>10bar) [30]. All other streams used the NRTL-RK model to estimate properties of the vapour phase. Tear streams, recycles and design specifications used the Broyden method for convergence.

The mechanical and isentropic efficiencies for compressors and gas turbines are 100% and 71.5% respectively. Pumps are assumed to operate at 70% pump efficiency with 80% driver efficiency.

High, medium and low-pressure steam turbines used isentropic efficiencies of 92%, 94% and 88% respectively [31]. A minimum approach temperature difference of 10 °C was used for heat transfer in the processes.

A summary of key units operating conditions and simulation assumptions are shown in Table 4.3.

Table 4.3 Summary of key units operating conditions and simulation approach for olefin production.

	Feedstocks
NG feed	NG pipeline system. 25 bar, 40 °C [32]; 88.71 mol% CH_4, 6.93 mol% C_2H_6, 1.25 mol% C_3H_8, 0.28 mol% n-C_4H_{10}, 0.05 mol% n-C_5H_{12}, 0.02 mol% n-C_6H_{14}, 0.82 mol% N_2, and 1.94 mol% CO_2 [33]
Steam feed	42 bar, 350 °C

Make up water feed	1 bar, 25 °C
Oxygen feed (tri-reforming)	80 bar, 25 °C; Air cryogenics [34]
	Reforming section
Pre-reformer	Gibbs reactor; Adiabatic; Catalyst: $Ni/MgAl_2O$
Reformer	Plug flow reactor; Number of tubes:439; Reactor length: 10m; Tube diameter:0.1m
Gas shift unit	Gibbs reactor; Adiabatic; Catalyst: Fe_2O_3/Cr_2O_3
	Methanol synthesis section
Methanol reactors	Four plug flow reactors in parallel; Adiabatic; Inlet temperature:250 °C; Inlet pressure:60 bar; Reactor length:2.6 m; Tube diameter:10m; Catalyst: $CuO/ZnO/Al_2O_3$
Methanol recovery unit	RadFrac equilibrium column; Condenser pressure: 1.36 bar; Pressure drop: 0.34 bar; Reflux ratio: 1.26; No. of stages:52;

	Feed stage:27
	MTO section
MTO reactor	Plug flow reactor; Adiabatic; Catalyst: SAPO-34
Quench Units	
QT1	RadFrac equilibrium column; Inlet temperature:150 °C; Inlet pressure:2.2 bar; Condenser pressure: 2 bar No. of stages: 3; Feed stage:2;
QT2	RadFrac equilibrium column; Inlet temperature:81 °C; Inlet pressure:2 bar; Condenser pressure: 1.5 bar No. of stages: 6; Feed stage:3;
High pressure column	RadFrac equilibrium column; Inlet temperature:14 °C; Inlet pressure:20 bar; Condenser pressure: 20 bar No. of stages: 35; Feed stages: Saturated vapour:11, Saturated liquid:14; Distillate olefins recovery: 99.9% Bottoms light component recovery: 99.9%

Low pressure column	RadFrac equilibrium column; Condenser pressure: 19 bar No. of stages: 48; Feed stages: 24; Distillate C3 recovery: 99.9% Bottoms C4/C5 recovery: 99.9%
Demethaniser	RadFrac equilibrium column; Condenser pressure: 30 bar No. of stages: 34; Feed stages: LPC distillate:1, Vapour:5, Liquid:19; Distillate methane recovery: 99% Bottoms C3 recovery: 97%
C2/C3 Splitter	RadFrac equilibrium column; Condenser pressure: 29 bar No. of stages: 38; Feed stages: 17; Distillate C2 recovery: 99.9% Bottoms C3 recovery: 99.9%
C2 column	RadFrac equilibrium column; Condenser pressure: 28 bar No. of stages: 60; Feed stages: 30; Ethylene recovery 99.9% Ethylene purity 99.9%
C3 column	RadFrac equilibrium column; Condenser pressure: 18 bar No. of stages: 195; Feed stages: 135;

Propylene recovery 99.9%

Propylene purity 99.9%

4.5 Reforming section

The reforming section used for the MTO study is the same as what was applied in in Chapter 3. Syngas is produced in the reforming section prior to further synthesis in the methanol section as shown in Figure 4.3. The reforming section incorporated an initial pre-reforming step of the natural gas feed using steam, prior to further mixing with the CO_2 feed and oxygen for the tri-reforming cases. Further syngas composition adjustment was conducted using a water gas shift reactor unit if required.

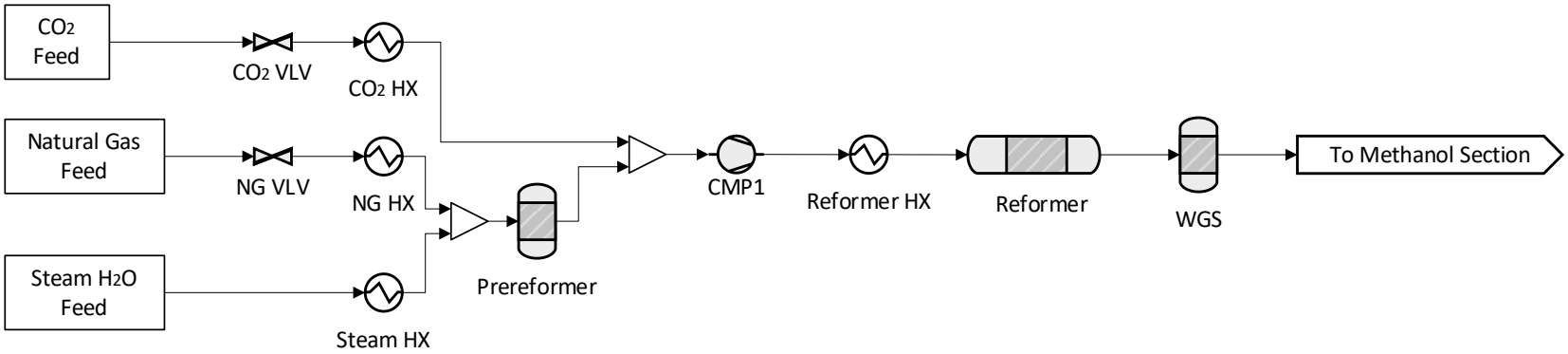

Figure 4.3. Flowsheet of reforming section.

The reformer operates through four alternative reforming technologies: (a) steam reforming, (b) dry-reforming, (c) bi-reforming, (d) and tri-reforming.

Table 4.4 Reforming technologies specifications.

Reforming technology	Catalyst	Pressure (bar)	Temperature (°C)
Steam reforming [47]	Ni/Al_2O_3	5-40	700-1000
Dry reforming [49] [50]	Ni-CO/Al-Mg-O	5-40	800-1000
Bi-reforming [52]	$Ni\text{-}CeO_2/MgAl_2O_4$	5-30	800-1100
Tri-reforming [47] [53]	Ni-based catalyst	5-30	800-1000

4.6 Methanol synthesis

Similarly to Chapter 3, methanol synthesis was completed through the conversion of syngas to methanol through the direct hydrogenation of CO and CO_2 using the ICI-synetix technology, as shown in Figure 4.4. A commercial $CuO/ZnO/Al_2O_3$ catalyst was used with a reactor inlet temperature of 250 °C and a pressure of 60 bar [35].

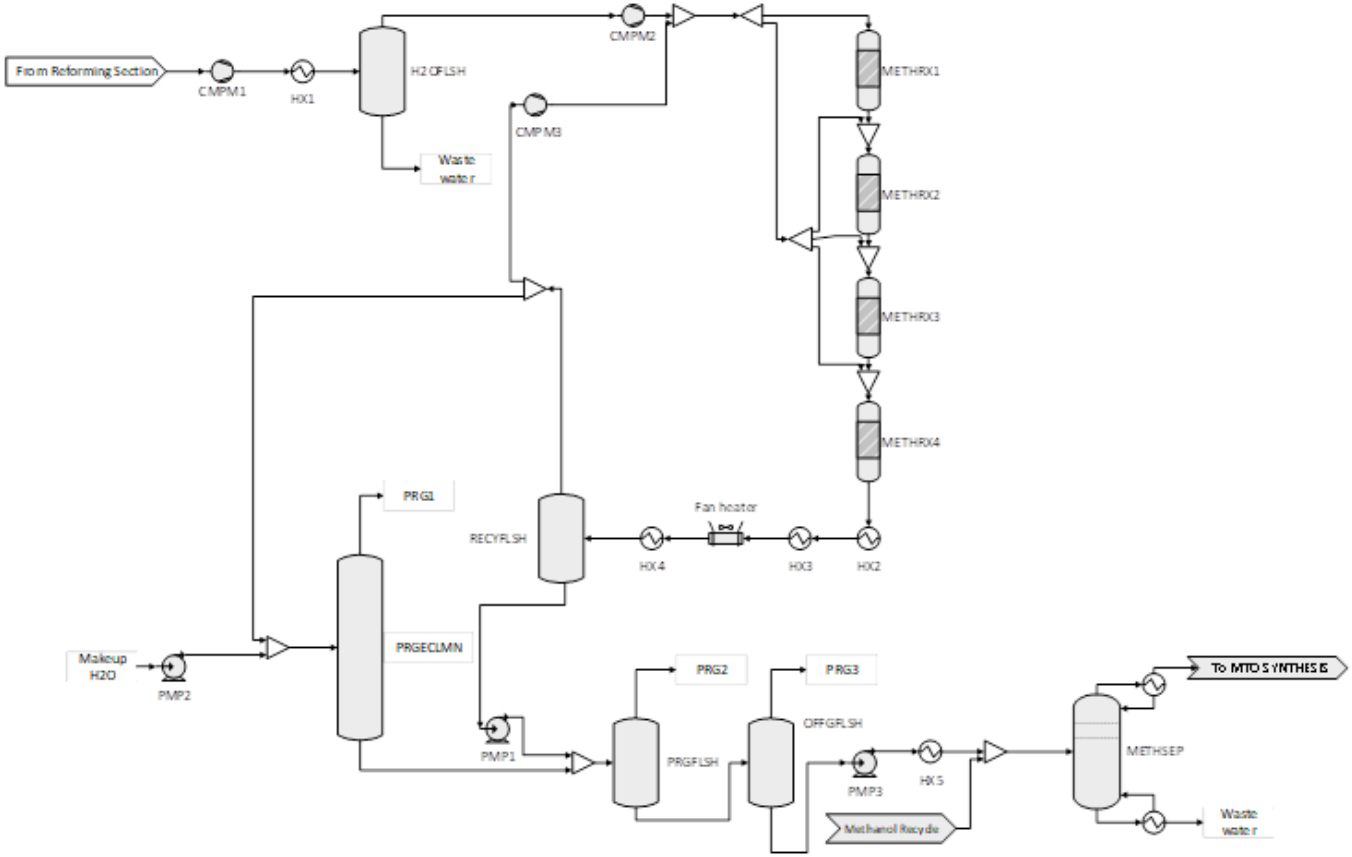

Figure 4.4. Flowsheet for methanol synthesis section.

4.7 MTO

The methanol feed into the MTO section was converted into products in a fluidised bed reactor. Catalysts fines were recovered and the deactivated catalyst was regenerated and recycled. Reactor effluent was transferred to a two-stage water quench system to separate particulates and reduce water content. Further separation was conducted to separate light components from heavy hydrocarbon by-products. The light components were then further separated to separate streams of the desired ethylene and propylene product.

4.7.1 Reactor

A fluidised bed reactor is used for the MTO reaction as it eases catalyst circulation as it allows for continuous catalyst regeneration via coke burning with air. Therefore, providing consistent catalyst activity and product composition. Additionally, a fluidised bed reactor offers the advantage of flexible operating conditions and increased opportunity for heat recovery, especially in the case of the exothermic MTO reaction.

Depending on the reaction condition used, an ethylene to propylene product ratio of 0.7 to 1.4 may be achieved. Varying the pressure and temperature will provide adjustment towards the desired product requirements. An increase in pressure results in a higher propylene ratio whilst increasing reaction temperature will increase the ethylene ratio. However, a decrease in olefin selectivity is also seen with increased temperature due to increased coke formation. Typical MTO reactor temperatures range between 400°C and 550°C, wherein which temperatures between 500°C to 520°C are used to favour ethylene production whilst temperatures between 350 °C and 475 °C are used to maximise propylene production [36]. A benefit of the MTO reaction is that a lower methanol partial pressure achieves an increase in light olefin selectivity. Hence, olefin yield is increased using a crude methanol feed containing up to 20 wt.% water, wherein which increasing water content increases ethylene yield [37]. Therefore, feed

composition and reaction operating conditions may be varied depending on market demand.

A lumped model kinetic expression using the DMTO catalyst from Ying et al was used, as provided in Appendix 2 [38].

$$2CH_3OH \leftrightarrow CH_3OCH_3 + H_2O \qquad \textit{Eqn.M1}$$

$$CH_3OCH_3 \leftrightarrow C_2H_4 + C_3H_6 + H_2O \qquad \textit{Eqn.M2}$$

$$CH_3OCH_3 + CH_2 \leftrightarrow C_2H_4 + CH_3OH \qquad \textit{Eqn.MTO1}$$

$$CH_3OCH_3 + CH_2 \leftrightarrow C_3H_6 + H_2O \qquad \textit{Eqn.MTO2}$$

The MTO reaction converts the methanol to methane, ethylene, propylene, propane, butylene, butadiene, butane and ethane.

4.7.2 Initial separation section

The vapour stream exiting the MTO reactor contains a high percentage of water as well as other particulates. Therefore, a two-stage water quench system is employed to separate the lighter hydrocarbon products from these particulates, and to reduce the water and heavy hydrocarbon content of the reactor effluent. A two-stage system is required due to the possible presence of trace acetic acid in the reactor product that may build-up in a conventional quench scheme, as shown in Figure 4.5.

To allow for heat recovery, the reactor effluent was initially passed through a heat exchanger prior to entering the first quench column. In the first quench column a quench water and neutralising agent stream was introduced at the top of the column. This allows for a hydrocarbon-rich vapour stream to exit the top of the tower, whilst a waste-water stream containing the particulates and heavy hydrocarbon by-products exits the bottom. Part of the waste-water stream may be recycled above the reactor effluent feed, whilst the remaining stream was treated to recover catalyst fines. Optimum operation parameters for the first quench

column includes an estimated 30-50% water content by weight in the overhead vapour stream; a 30%-47% by weight feed of quench water in comparison to the reactor effluent feed and a temperature less than 90 ˚C for the quench water [39]. Prior to entering the second quench column, the top product vapour was partially condensed to allow for further heat recovery and to reduce quench water requirements. A light olefin vapour product exits the top of the second quench column to allow for further separation. The column bottoms stream is a wastewater stream which in part is recycled back to the first quench column and another portion is heated and reintroduced to the second quench column. The remaining portion is further stripped to remove remaining small hydrocarbons which are transferred to the top vapour stream exiting the first quench column.

Furthermore, operation of the water quench columns is limited to temperatures of 95-115˚C as to allow the vapour temperature to remain above the dew point and minimise fouling due to the particulates present [40].

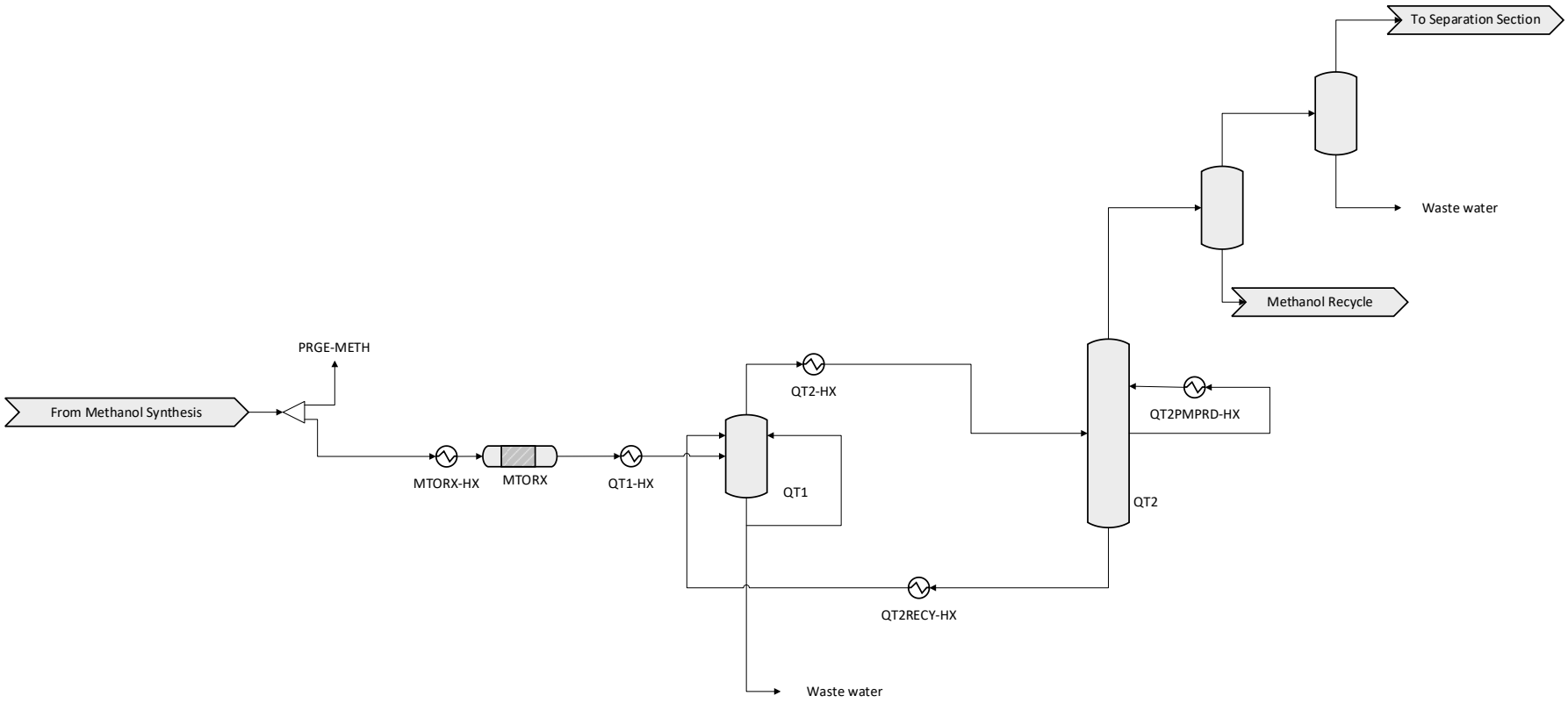

Figure 4.5. Flowsheet of methanol to olefin synthesis and quench unit configuration.

4.7.3 Second separation section

The light olefin product stream exiting the second quench tower is separated into three streams: a stream with light components such as H_2, CO and CH_4; a heavy hydrocarbon stream and a light hydrocarbon stream containing ethylene, propylene, ethane and propane to be sent to further separation. In this work, the separation process used followed the configuration adapted by Yu et al. from Wang et al. and is outlined in Figure 4.6 [41] [42].

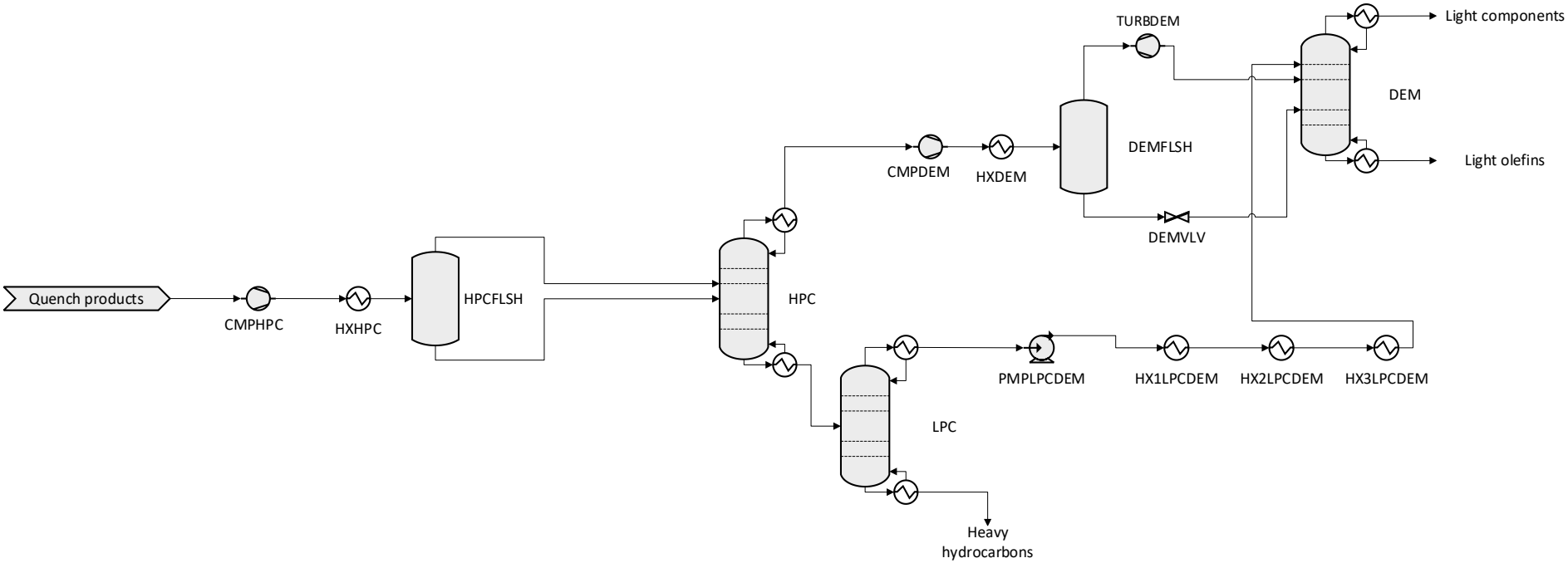

Figure 4.6. Flowsheet of second separation section for methanol to olefin synthesis section.

The configuration uses three columns, a high-pressure column (HPC), a low-pressure column (LPC) and a demethaniser (DEM). The light olefin stream exiting the second quench tower was initially compressed to the pressure of the HPC and further cooled for conversion to a partial vapor liquid which is separated to a saturated vapor, containing the light components (≤C2), and liquid stream, containing the heavy components (≥C3), in the HPC. The saturated liquid stream from the HPC is sent to the LPC to allow for C3 hydrocarbons to be extracted as a top product whilst the C4 and C5 products exit as the bottom product.

In order to minimise ethylene loss, the LPC distillate's pressure is increased and refrigerated to send to the top of the DEM. The saturated vapor product from the HPC is compressed and refrigerated to produce a partial vapor liquid which is separated into a vapor and liquid stream. The vapour stream is expanded and fed to the middle stage of the DEM, whilst the liquid stream is depressurised and fed to the DEM at a stage lower than the feed stage of the vapour stream.

The top product of the DEM is the stream containing the light components such as H_2, CO and CH_4 whilst the bottom product are the light hydrocarbon stream to be sent for further separation.

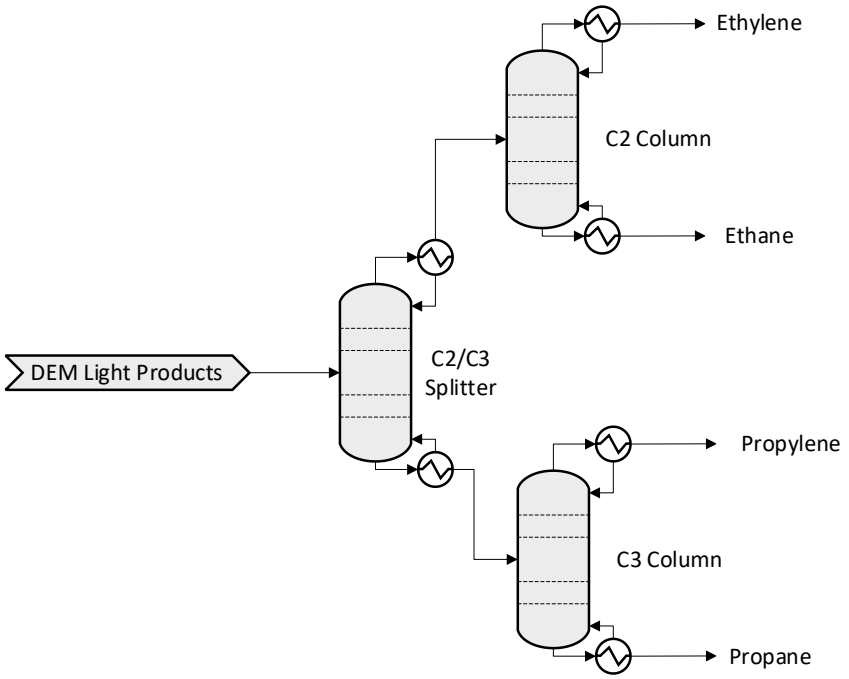

Figure 4.7. Flowsheet of the light olefin separation section for methanol to olefin synthesis.

The light hydrocarbon stream are separated through a configuration of three columns, an initial column separating C2 components from C3 components: a column separating the C2 components into ethylene and ethane and a column separating propylene from propane, as shown in Figure 4.7.

Table 4.5 Methanol to olefins separation section column specifications

Column	**Specification**	**Adjusted variables**
C2/C3 Splitter	Column top C2 recovery 99.9% Column bottom C3 recovery 99.9%	Reflux ratio Reboiler duty
C2 Column	Ethylene recovery 99.9% Ethylene purity 99.9%	Reflux ratio Reboiler duty
C3 Column	Propylene recovery 99.9% Propylene purity 99.9%	Reflux ratio Reboiler duty

4.8 Economic assessment

The assumptions used for the economic analysis are as outlined previously in Chapter 3:

- A plant located in the United Kingdom with a base year 2019 was assumed. This is used to provide purchased equipment and raw material costs and the product and by-product sale price.
- A 20-year plant economic life was assumed with an annual operating hour of 8000 hours.
- Purchased equipment costs were estimated with the Aspen Icarus database within Aspen Plus V12 using the Aspen Economic Analyser (AEA).
- Pumps were mapped as single stage centrifugal pumps and compressors as horizontal centrifugal compressors.
- Plant operation was assumed to be at 90% capacity.
- The cost of CO_2 assumes negligible compressions and transportation cost as the CCU plant was assumed to be in close vicinity to the cement plant with CO_2 capture. A cement plant with an oxyfuel capture unit on the work by Gardarsdottir et al provided the CO_2 feed cost [29].
- The costs of the catalysts were assumed to be negligible.
- It was assumed that there are 3 shifts per day with 3 operators per shift. Operator costs are $34 per operating hour and operating supervision costs were an estimated 15% of total operating labour costs.
- The loan interest rate was set at 10%.
- The TCI was calculated using purchased equipment cost and the factorial estimation method for a fluid processing plant as shown in Chapter 3.
- FCP was calculated as a factor of the FCI and the TCI as well as total operating labour cost as shown in Table 4.6.
- Raw material costs and product and by-product sale prices are constant and time independent throughout the plant's economic life. These are available in Appendix 2.
- Equipment, raw material and product and by-product sale prices price inflation were not considered.
- Government subsidies were not considered.

Table 4.6 Key economic variables and indicators.

Description	Variable	Value
Purchased equipment cost	PC	AEA
Fixed capital investment	FCI	TDC + TIC *where TDC are the total direct costs and TIC are the total indirect cost*
Total capital investment	TCI	FCI + WC *where WC is the working capital*
Fixed costs of production	FCP	Appendix
Raw material costs	RMC	$\sum_{i}^{i=x} \dot{m}_x \, cost_x$ ($ hr^{-1}) *where $\dot{m}_x$ is the mass flow rate of material x and $cost_x$ is the cost per unit x.*
Utility costs	UC	$\sum^{x} \dot{U}_x \, cost_x$ ($ hr^{-1}) *where $\dot{U}_x$ is the utility usage of utility x.*
Catalyst costs	C	Negligible
Variable cost of production	VCP	UC+RMC+C
Annualised capital repayment	ACR	$\frac{TCI \times r(1+r)^y}{(1+r)^y - 1}$ *where r is the interest rate and y is the plants economic life.*
Capital expenditure	CAPEX	$\frac{ACR + FCP}{(\dot{m}_{Propylene,out} + \dot{m}_{Ethylene,out}) \times OH}$

where $\dot{m}_{Propylene,out}$ is the mass flowrate ($t \cdot hr^{-1}$) of propylene product, $\dot{m}_{Ethylene,out}$ is the mass flowrate ($t \cdot hr^{-1}$) of ethylene product and OH is the annual operating hours.

Total production costs	TPC	$CAPEX + \frac{VCP}{(\dot{m}_{Propylene,out} + \dot{m}_{Ethylene,out}) \times OH}$

4.9 Environmental assessment

As in Chapter 3, an environmental assessment was conducted using the ISO 14044:2016 criteria and guidelines to conduct a life cycle assessment (LCA). The midpoint impact calculated was the GWP, providing the total impact of direct and indirect greenhouse gas emissions on global warming due to the process.

Assumptions used in the LCA includes:

- The 'Ecoinvent database' was used to provide the data for raw material and utility environmental impacts.
- The CO_2 feed was provided via oxyfuel carbon capture of CO_2 from a cement plant as outlined Gardarsdottir et al [29].
- Environmental impacts related to plant construction and catalyst production were not considered.

4.10 Process optimisation

The methodology used for process optimisation is as is provided in Chapter 3. Optimisation was completed using MATLAB R2020b and the actxserver function to link Aspen Plus V12 to MATLAB R2020b. As the optimisation objectives are mixed integer non-linear programming (MINLP) functions, to provide a global optimum the simulated annealing algorithm with a hybrid function of a pattern search was used. A complete poll through MADS NP1 and a genetic algorithm complete search at intervals of 10 iterations were used.

A FORTRAN calculator block within Aspen Plus V12 was used to calculate the objective functions. Two alternative optimisation targets where studied: (i) minimising total variable operating costs per tonne of olefins produced (ii) minimising GWP per tonne of olefins produced. In relation to these optimisation targets, two objective functions were used in this work: K (cost minimisation) and L (GWP minimisation).

4.10.1 Objective function K (cost minimisation)

The objective function, K, of minimising total variable operating costs, $T_{OC,MTO}$, per tonne of olefins produced, $F_{MTO,out}$, is provided below:

$$MIN: J = \frac{T_{OC,MTO}}{F_{MTO,out}}$$

where, the total variable operating costs, T_{OC}, are calculated as the sum of the total utilities cost, U_{cost}, and raw materials costs, RM_{cost}:

$$T_{OC,MTO} = RM_{cost} + U_{cost}$$

4.10.2 Objective function L (GWP minimisation)

The objective function, L, aims to minimise total GWP including from raw materials, utility requirements and greenhouse gas emission from the process, minimising the GWP per tonne of olefins produced:

$$Min: L = \frac{T_{GWP}}{F_{MTO,out}}.$$

The total GWP, T_{GWP}, is calculated from the sum of all sources outlined above:

$$T_{GWP} = \sum^{l} F_l \, i_{GWP,l} + \sum^{n} P_n \, i_{GWP,n} + \sum^{m} U_m \, i_{GWP,m}$$

where $i_{GWP,x}$ is the GWP per unit of x, F_l is the raw material requirements of, l, per tonne of olefins produced, P_n is the total amount of greenhouse gas , n, that exits the purge per tonne olefins produced and U_m is the utility, m, required per tonne of olefins produced.

4.10.3 Decision variables

The decision variables were selected within suitable ranges for the operation of the plant as shown in Table 4.7.

Table 4.7 Decision variables including lower and upper bounds used for optimisation.

Decision variable	Lower bound	Upper bound
Reformer heat exchanger temperature (°C)	800	1000
Reformer heat exchanger pressure (bar)	1	30
Natural gas heat exchanger temperature (°C)[a]	250	650
Natural gas heat exchanger pressure (bar)	1	30
Pre-reformer temperature (°C)	350	650
Pre-reformer pressure (bar)	1	30
Reformer exit stream ratio into water gas shift unit[b]	0	1
Natural gas feed mass flow ($tonnes.hr^{-1}$)	7	25
Steam feed mass flow ($tonnes.hr^{-1}$)	10	80
Oxygen feed mass flow ($tonnes.hr^{-1}$)[c]	1	20
Methanol recycle purge ratio (%)[d]	1	10
MTO reactor temperature (°C)	350	550
MTO reactor pressure (bar)	1	3

[a] For the adiabatic tri-reforming, exit temperature of reformer restricted to less than 1050 °C to limit catalyst deactivation.

[b] Water gas shift bypass option implemented via a splitter.

[c] For tri-reforming cases.

[d] Prior to the MTO section a purge for a portion of the recycled methanol is present.

4.11 Heat integration

The optimised scenario results were exported to the Aspen Energy Analyzer (AEA) for heat integration. A minimum approach temperature of 10 °C was used.

From the feasible iterations provided by AEA, the iteration with the lowest operating and annualised cost was selected.

5.0 Results

5.1. Technical performance indicators

The mass and energy balances of the optimised scenarios from Aspen Plus were used to calculate the overall CO_2 conversion for each CCU scenario:

$$Overall\ CO_2 conversion\ (\%) = \frac{\dot{m}_{CO_2,in} - \dot{m}_{CO_2,out}}{\dot{m}_{CO_2,in}},$$

where $\dot{m}_{CO_2,in}$ is the mass flowrate ($t \cdot hr^{-1}$) of CO_2 in the process feed stream coming from the cement CO_2 capture plant and $\dot{m}_{CO_2,out}$ is the mass flowrate of CO_2 ($t \cdot hr^{-1}$) in the output streams.

The olefins conversion factor was calculated to determine the amount of olefins produced per kg of feed CO_2:

$$Olefins\ conversion\ factor = \frac{\dot{m}_{Propylene,out} + \dot{m}_{Ethylene,out}}{\dot{m}_{CO_2,in}}.$$

5.1.1 Technical performance before heat integration

Table 4.8 shows key technical performance indicators for the CCU based olefins production scenarios. CO_2 conversion ranges from -4.5% to 71.79% for all six CCU scenarios. The tri-reforming scenarios have low CO_2 conversion values in comparison to the dry and bi-reforming scenarios. For example, BI-OPEX had a CO_2 conversion of 65.31% whilst CO_2 conversion for ADTRI-OPEX was 9.06%. A net increase of 4.5% CO_2 emissions was seen for ISOTRI-GWP. The lower tri-reforming scenarios CO_2 conversion values are due to the partial oxidation reaction (*Eqn.TR2)* in the tri-reformer and the increased natural gas feed requirements for the tri-reforming scenarios, increasing the total quantity of

reactant natural gas that converts to CO_2. For example, the natural gas feed for ISOTRI-OPEX was 70.93% greater than for BI-OPEX.

The total olefin production rate for the tri-reforming scenarios where significantly greater due to the increased total feed input for its production. For example, the total olefin production rate for ISOTRI-OPEX was 82.17% greater than for BI-OPEX.

Propylene provides a greater portion of the produced olefins for the scenarios optimised towards minimising operating costs than that were optimised to minimising GWP by 2.23% to 50.72%, as propylene has a greater selling price than ethylene. For example, the propylene represented 72.7% and 64.55% of the produced olefins for BI-OPEX and BI-GWP respectively.

The olefins conversion factors of the tri-reforming scenarios are higher than that of the dry and bi-reforming scenarios. ADTRI-OPEX has the highest olefins conversion factor at 2.78 tonne olefins t^{-1} CO_2. Olefin production rates for the tri-reforming scenarios are higher than that of the dry and bi-reforming scenarios due to the increased total feed.

The olefins conversion factor for the scenarios optimised towards minimising costs are 22.58% to 102.92% greater than for the scenarios optimised towards minimising GWP. An exception to this case are the isothermal tri-reforming scenarios wherein which the olefins conversion factor for ISOTRI-GWP was 15.86% higher than for ISOTRI-OPEX.

Table 4.8 Technical performance indicators for olefin production scenarios studied before heat integration and heat exchanger network optimisation.

		Conventional	Dry reforming		Bi-reforming		Adiabatic Tri-reforming		Isothermal Tri-reforming	
		SR	DR-OPEX	DR-GWP	BI-OPEX	BI-GWP	ADTRI-OPEX	ADTRI-GWP	ISOTRI-OPEX	ISOTRI-GWP
CO_2 Feed	$t \cdot t^{-1}$ ***Olefins***	-	1.31	1.61	0.81	1.44	0.36	0.73	0.44	0.38
Natural gas Feed	$t \cdot t^{-1}$ ***Olefins***	0.77	1.07	1.31	0.86	1.17	1.54	1.58	1.47	1.50
Steam water Feed	$t \cdot t^{-1}$ ***Olefins***	0.95	0.99	1.21	1.40	1.47	0.58	0.68	0.92	1.36
Make-up water	$t \cdot t^{-1}$ ***Olefins***	5.31	5.67	6.94	3.48	6.19	1.55	3.17	1.91	1.64
O_2 Feed	$t \cdot t^{-1}$ ***Olefins***	-	-	-	-	-	1.16	1.19	1.09	1.13
Olefin production rate	$t \cdot hr^{-1}$	12.47	7.06	5.76	11.50	6.46	25.84	12.63	20.95	24.46
Propylene production rate	$t \cdot hr^{-1}$	9.23	7.02	3.80	8.36	4.17	16.67	7.97	13.51	15.30
Ethylene production rate	$t \cdot hr^{-1}$	3.24	0.00	1.93	3.08	2.26	9.03	4.60	7.33	9.04
Propane production rate	$l \cdot hr^{-1}$	64.3	56.71	33.40	67.50	91.50	134.68	813.36	109.13	90.57
Ethane production rate	$l \cdot hr^{-1}$	0.02	0.09	143.90	0.12	168.26	710.35	385.16	576.21	714.36
Heating requirements	$GJ \cdot t^{-1}$ ***Olefins***	49.49	33.15	47.27	47.01	46.65	31.86	41.40	38.94	44.33
Cooling Requirements	$GJ \cdot t^{-1}$ ***Olefins***	40.03	30.97	35.20	38.03	35.41	34.87	38.50	35.83	39.07
Electricity requirements	$kWh \cdot t^{-1}$ ***Olefins***	1063.61	1189.65	1457.16	1010.38	1344.60	1538.96	1664.74	1287.20	1399.72
CO_2 conversion	*%*	-	71.77	71.79	65.31	60.36	9.06	30.63	3.64	-4.50
Olefins conversion factor	$tOlefins \cdot t^{-1}\ CO_2$	-	0.76	0.62	1.23	0.69	2.78	1.37	2.27	2.63

Heating utility requirements ranged from 31.86 to 47.27 $GJ \cdot t^{-1}$ olefins produced for the CCU scenarios. The tri-forming scenarios overall have lower heating requirements than the dry- and bi-reforming scenarios. This was due to the exothermic partial oxidation reaction (*Eqn.TR2)* which provides a portion of the required heating requirements in the reformer.

Electricity requirements ranged from 1010.38 to 1664.74 $kWh \cdot t^{-1}$ olefins. Scenarios optimised towards minimising GWP have higher electricity usage than the scenarios optimised towards minimising operating costs; 8.17% to 22.49% higher. For the conventional and the dry and bi-reforming scenarios, electricity usage inversely correlated significantly with the olefin production rate. However, the electricity requirement for the tri-reforming scenarios where overall greater due to significant increase in total raw material that require pumping.

From Figure 4.8 it can be seen that the majority of the heating requirements were supplied by natural gas. Natural gas provided 55.85% to 76.01% of the total heating utility requirements for the scenarios studied.

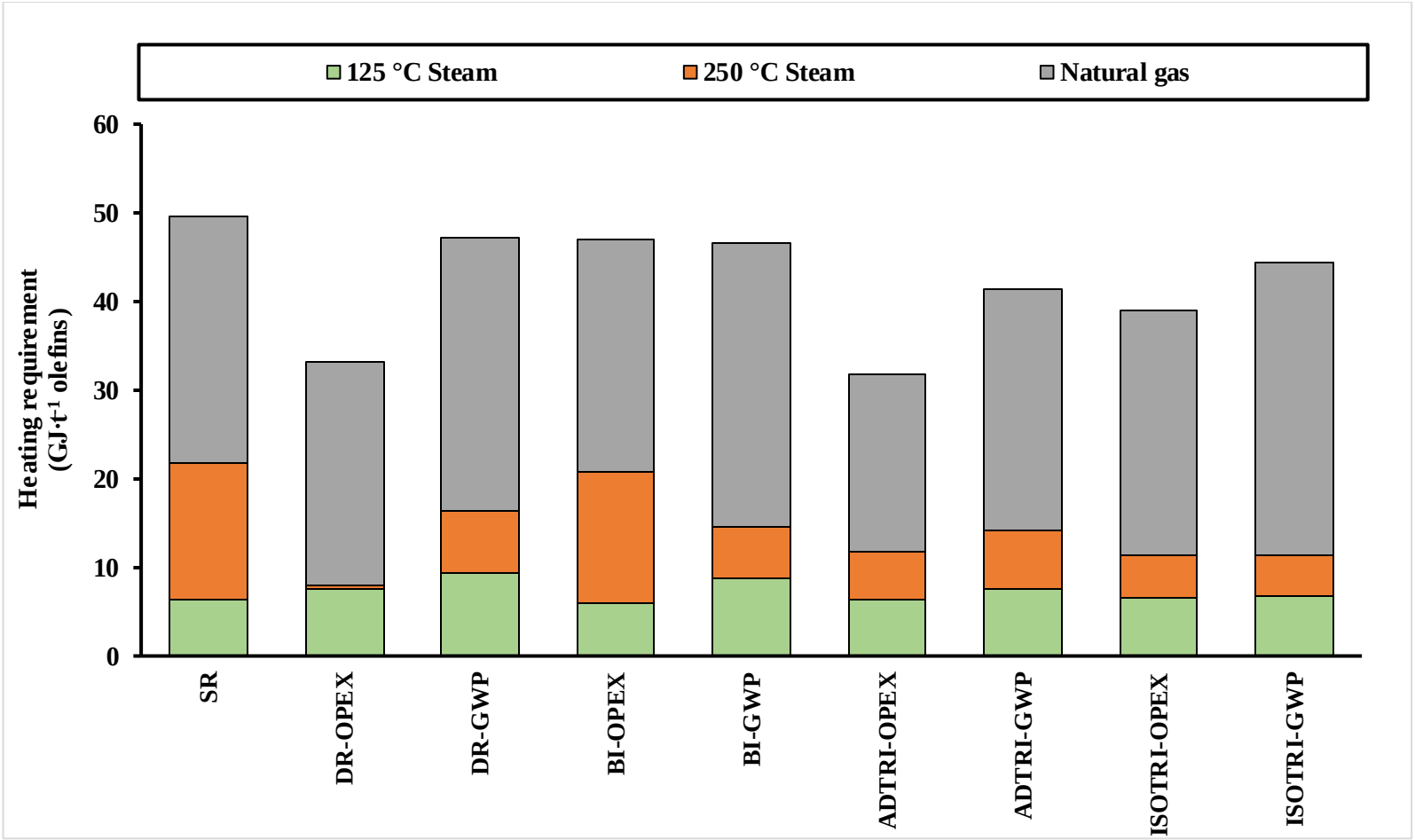

Figure 4.8. Heating utility breakdown for olefin production scenarios optimised before heat integration.

5.1.2 Technical performance after heat integration

Table 4.9 Technical performance indicators for olefin production scenarios studied after heat integration and heat exchanger network optimisation.

		Conventional	Dry reforming		Bi-reforming		Adiabatic Tri-reforming		Isothermal Tri-reforming	
		SR	DR-OPEX	DR-GWP	BI-OPEX	BI-GWP	ADTRI-OPEX	ADTRI-GWP	ISOTRI-OPEX	ISOTRI-GWP
CO_2 Feed	$t \cdot t^{-1}$ *Olefins*	-	1.31	1.61	0.81	1.44	0.36	0.73	0.44	0.38
Natural gas Feed	$t \cdot t^{-1}$ *Olefins*	0.77	1.07	1.31	0.86	1.17	1.54	1.58	1.47	1.50
Steam water Feed	$t \cdot t^{-1}$ *Olefins*	0.95	0.99	1.21	1.40	1.47	0.58	0.68	0.92	1.36
Make-up water	$t \cdot t^{-1}$ *Olefins*	5.31	5.67	6.94	3.48	6.19	1.55	3.17	1.91	1.64
O_2 Feed	$t \cdot t^{-1}$ *Olefins*	-	-	-	-	-	1.16	1.19	1.09	1.13
Olefin production rate	$t \cdot hr^{-1}$	12.47	7.06	5.76	11.50	6.46	25.84	12.63	20.95	24.46
Propylene production rate	$t \cdot hr^{-1}$	9.23	7.02	3.80	8.36	4.17	16.67	7.97	13.51	15.30
Ethylene production rate	$t \cdot hr^{-1}$	3.24	0.00	1.93	3.08	2.26	9.03	4.60	7.33	9.04
Propane production rate	$l \cdot hr^{-1}$	64.3	56.71	33.40	67.50	91.50	134.68	813.36	109.13	90.57
Ethane production rate	$l \cdot hr^{-1}$	0.02	0.09	143.90	0.12	168.26	710.35	385.16	576.21	714.36
Heating requirements	$GJ \cdot t^{-1}$ *Olefins*	4.95	2.31	3.93	2.53	4.14	3.19	2.94	7.66	7.06
Cooling Requirements	$GJ \cdot t^{-1}$ *Olefins*	4.00	3.13	2.80	3.85	2.73	3.49	5.35	2.77	4.04
Electricity requirements	$kWh \cdot t^{-1}$ *Olefins*	1063.61	1189.65	1457.16	1010.38	1344.60	1538.96	1664.74	1287.20	1399.72
CO_2 conversion	*%*	-	71.77	71.79	65.31	60.36	9.06	30.63	3.64	-4.50
Olefins conversion factor	$tOlefins \cdot t^{-1}$ CO_2	-	0.76	0.62	1.23	0.69	2.78	1.37	2.27	2.63

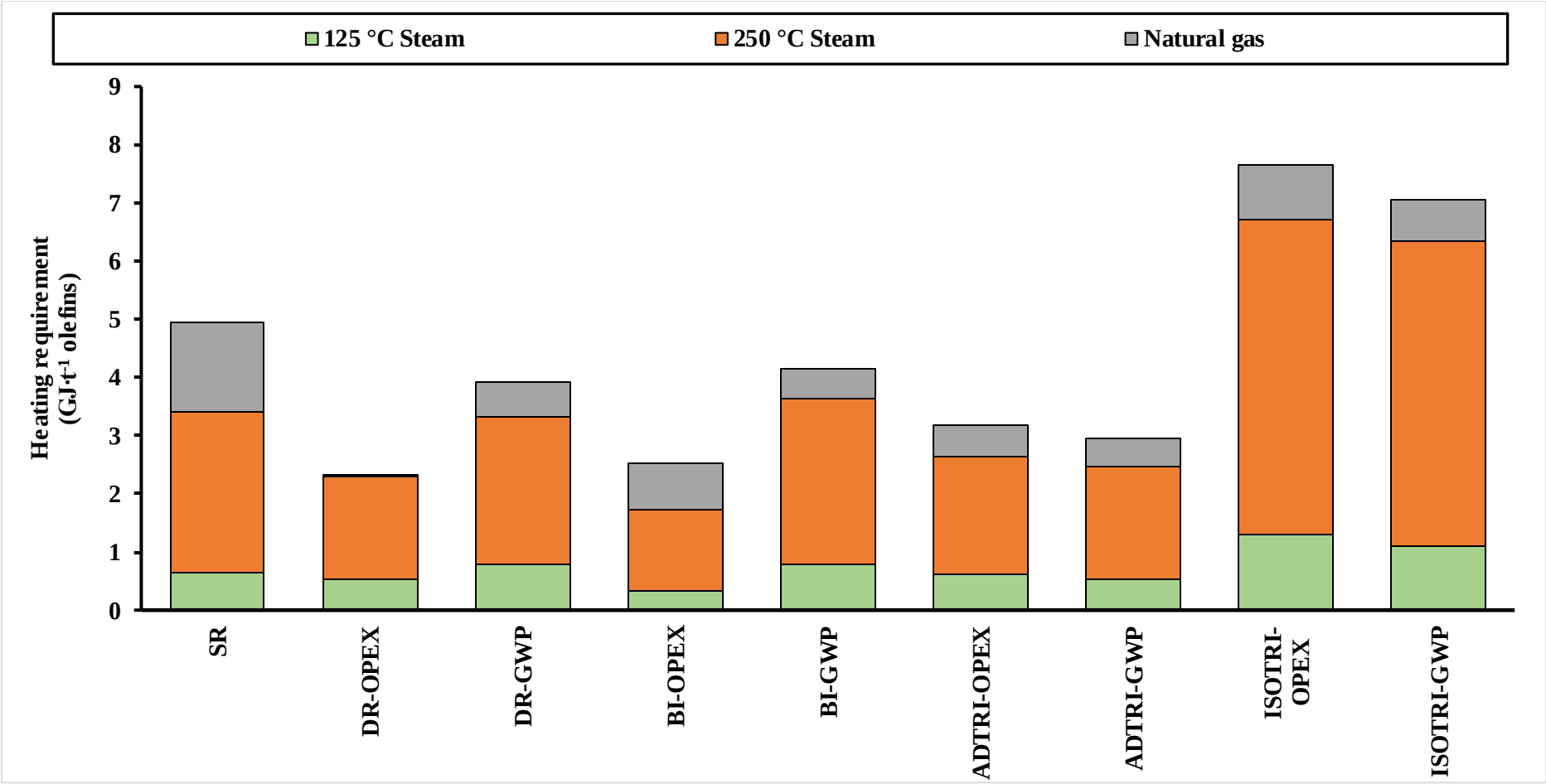

Figure 4.9. Heating utility breakdown for olefin production scenarios optimised after heat integration.

Table 4.9 and Figure 4.9 show that utility requirements are significantly lower with heat integration by 80.33% to 94.62%. The heating utility requirements range from 2.31 to 7.66 GJ tonne^{-1} olefins for the CCU scenarios studied. However, a significantly lower decrease in utility requirements was seen for the tri-reforming cases in comparison to the dry- and bi-reforming cases. This was due to the decreased availability of heat for integration in the tri-reforming cases.

5.2 Economic performance indicators

5.2.1 Economic performance before heat integration

The breakdown of the total production cost and other key economic performance indicators for the MTO scenarios studied are provided in Table 4.10. The total production cost of the CCU scenarios range from **$**1189.03 to **$**1540.48 t^{-1} olefins produced. In comparison to conventional MTO steam reforming-based synthesis, the CCU scenarios show an increased total production cost of 11.03% to 43.85%. BI-OPEX has the lowest production cost in comparison to the other CCU scenarios studied due to the lower material costs for this scenario.

The greatest portion of the total production cost for the conventional, dry- and bi-reforming scenarios are provided by the utility costs (41.13% to 52.23%). Conversely, for the tri-reforming scenarios, raw material costs contribute the majority of the total production cost (50.68% to 55.36%).

The CAPEX ranged from **$**103.24 and **$**291.57 tonne^{-1} olefins and its contribution to total production cost was 50.4% to 84.78% and 53.79% to 82.94% lower than material and utility costs, respectively.

All scenarios display negative profitability prior to heat integration, ranging from -**$**749.65 to -**$**262.97 per tonne of olefins with DR-GWP showing the greatest net loss.

Table 4.10. Key economic performance indicators for olefin production scenarios before heat integration

	Conventional	Dry reforming		Bi-reforming		Adiabatic Tri-reforming		Isothermal Tri-reforming	
	SR	**DR-OPEX**	**DR-GWP**	**BI-OPEX**	**BI-GWP**	**ADTRI-OPEX**	**ADTRI-GWP**	**ISOTRI-OPEX**	**ISOTRI-GWP**
Purchased equipment cost (M$)	39.418533	46.31	47.56	61.27	47.84	75.52	58.52	67.07	72.26
FCI (M$)	216.87939	254.79	261.68	337.09	263.19	415.50	321.99	369.03	397.58
Working capital (M$)	38.297085	44.99	46.21	59.52	46.47	73.37	56.86	65.16	70.21
CAPEX ($·$t^{-1}$ *Olefins)*	111.61	231.80	291.57	188.15	261.47	103.24	163.61	113.09	104.37
Total raw material cost ($·$t^{-1}$ *Olefins*)	306.0085	486.37	595.67	379.35	531.47	678.60	713.05	650.18	660.85
Total utility cost ($·$t^{-1}$ *Olefins)*	654.27	501.67	653.25	621.53	631.19	443.85	530.25	465.58	520.51
Total utility and material cost ($·$t^{-1}$ *Olefins)*	960.2785	988.04	1248.92	1000.88	1162.65	1122.45	1243.30	1115.76	1181.36
Total production cost ($·$t^{-1}$ *Olefins)*	1071.889	1219.84	1540.48	1189.03	1424.13	1225.69	1406.91	1228.86	1285.73
Revenue ($·$t^{-1}$ *Olefins)*	808.9152	856.95	790.84	803.06	789.27	787.89	794.42	787.85	783.77
Profit/Loss ($·$t^{-1}$ *Olefins)*	***-262.97***	***-362.89***	***-749.65***	***-385.97***	***-634.86***	***-437.80***	***-612.49***	***-441.01***	***-501.96***

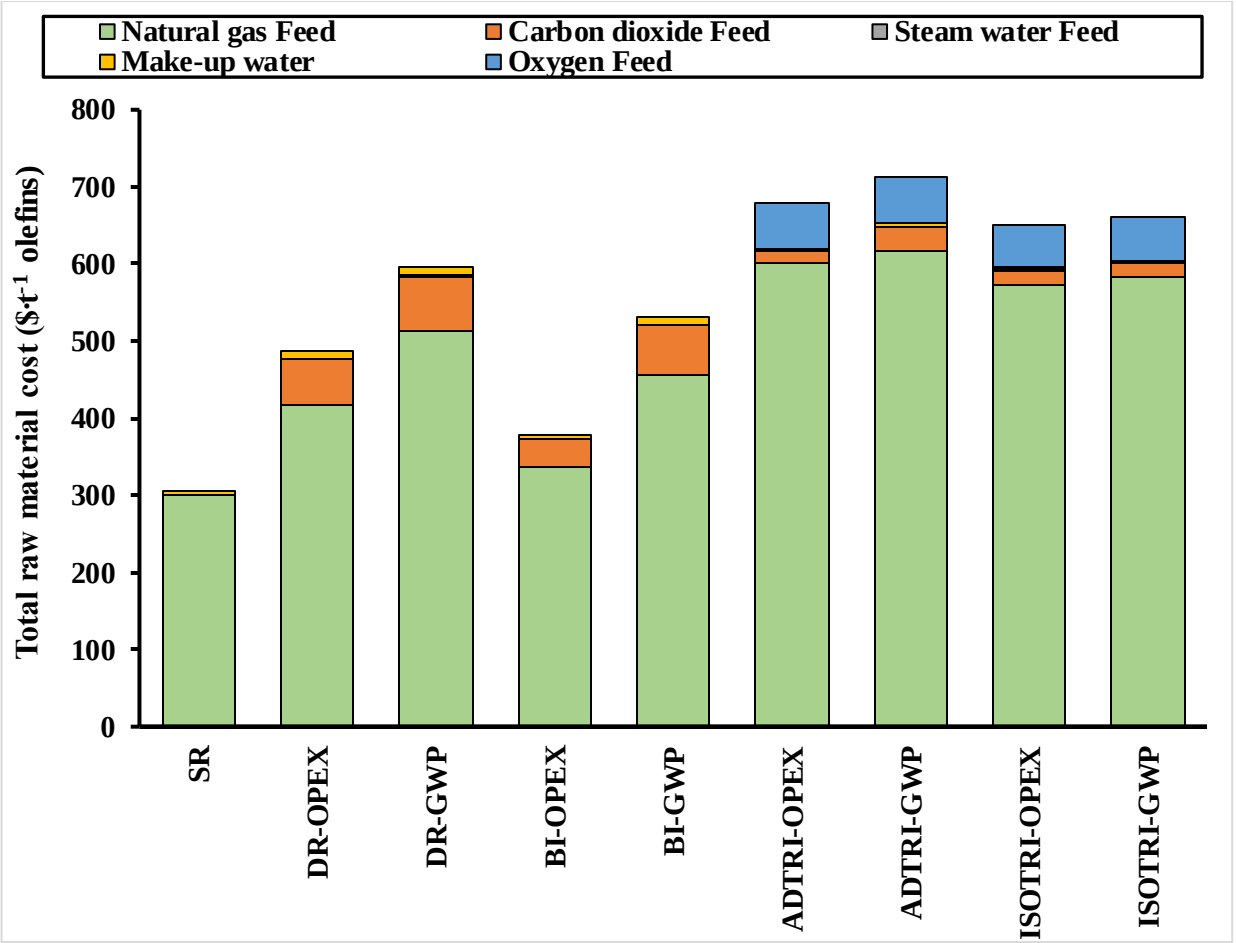

Figure 4.10. Breakdown of total raw material cost for olefin production scenarios studied before heat integration.

Figure 4.10 shows that for all scenarios studied costs related to the natural gas feed contribute the most to the total raw material cost. Natural gas represents 85.98% to 88.68% of the total raw material cost for the CCU scenarios and a significant 98.19% of the total raw material cost for the SR scenario. The total material cost for the scenarios optimised towards minimising total costs are 1.61% to 28.62% lower than for the scenarios optimised towards minimising GWP. This was due to the lower olefin production rate in the cases of optimising towards minimising GWP. Figure 4.11 shows that natural gas used for heating contributed the most to the total utility costs at 33.05% to 54.07% of the total cost. Similarly, the scenarios optimised towards minimising GWP had 1.55 % to 23.2% higher total utility costs than the scenarios optimised towards minimising total costs.

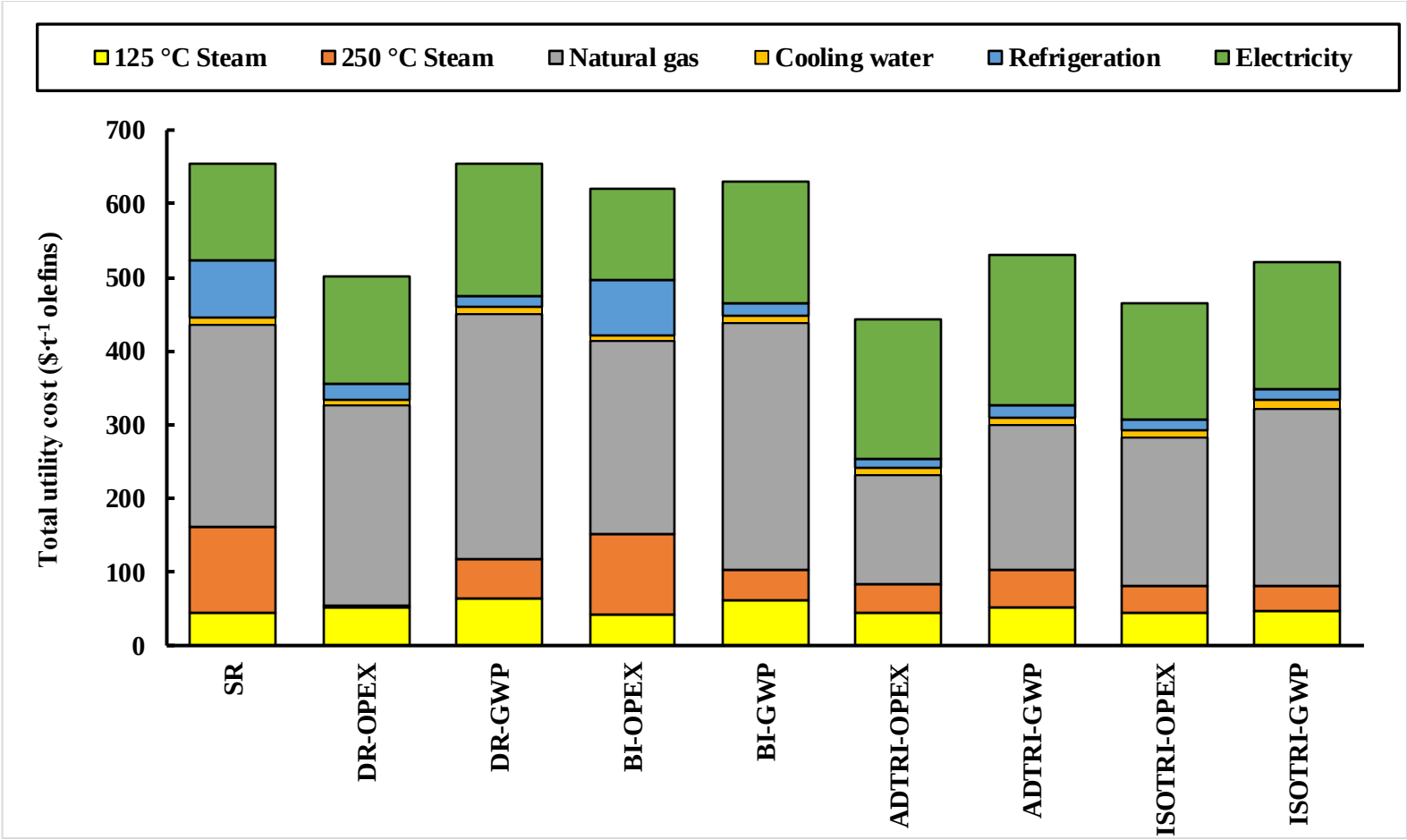

Figure 4.11. Breakdown of total utility cost for olefin production scenarios studied before heat integration.

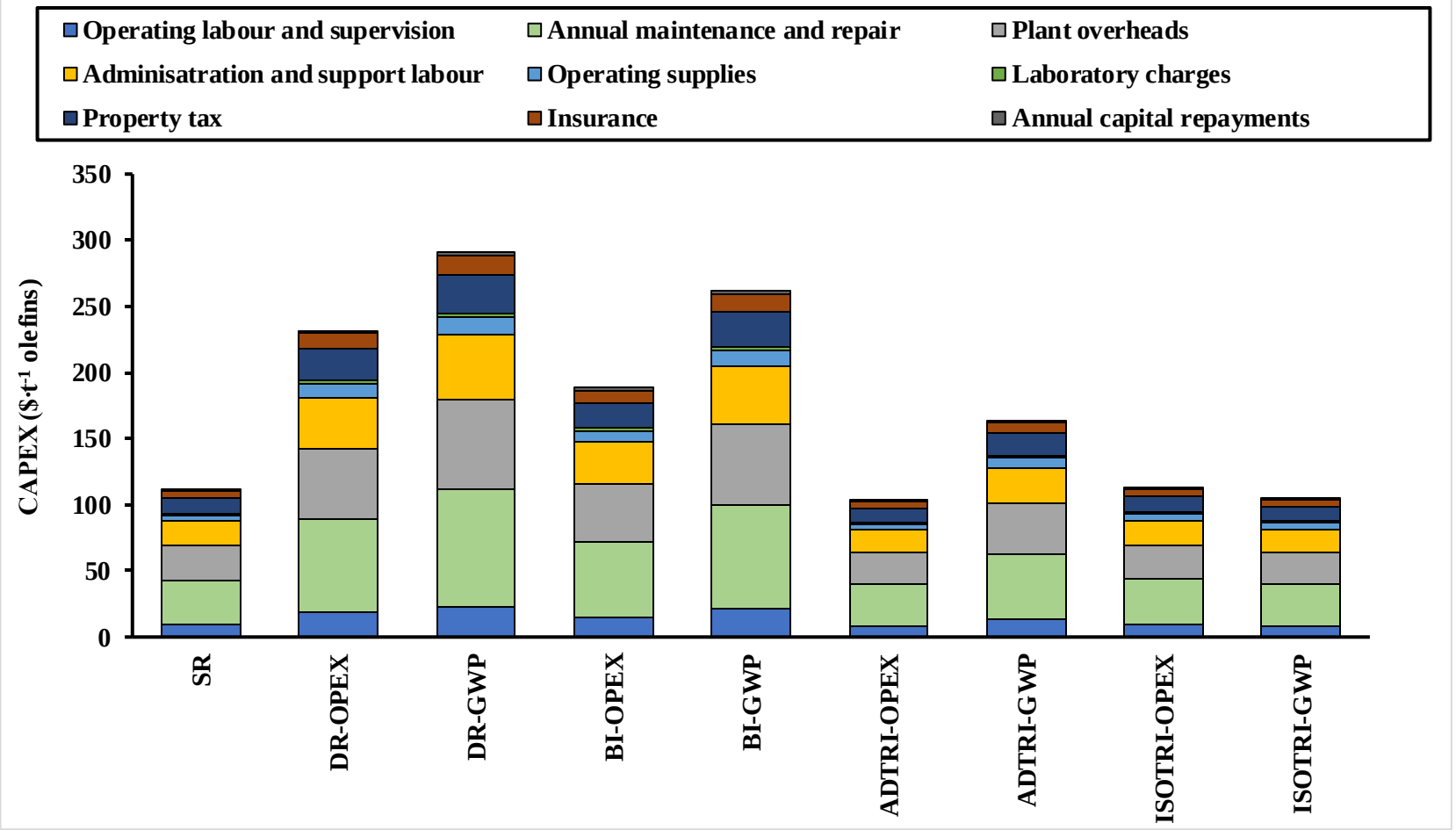

Figure 4.12. Breakdown of CAPEX for olefin production scenarios studied before heat integration.

5.2.2 Economic performance after heat integration

Table 4.11 shows the results of the economic analysis for the scenarios examined after heat integration was applied. Total production costs are reduced by 20.38% to 46.03% due to the reduction in total utility costs. The total utility costs after heat integration are reduced by 20.38% to 46.03% for the scenarios studied.

The material cost provides the greater portion of the total production cost for all scenarios, ranging from 52.9% to 69.56%. The raw material cost to utility cost ratio for the CCU scenarios are significantly higher than that of the conventional scenario. This ratio was 1.67 for the conventional scenario and 2.58 to 3.16 for the CCU scenarios. Furthermore, the raw material cost to utility cost ratio for the tri-reforming scenarios are greater than that of the dry and bi-reforming CCU scenarios. The material to utility cost ratio for the tri-reforming scenarios range from 2.92 to 3.16 and 2.45 to 2.83 for the dry and bi-reforming scenarios. This waas due to the lower total utility requirements for the tri-reforming cases, as the exothermic reaction provides a portion of the heating utility.

The CAPEX ranged from **$**68.59 and **$**243.13 tonne^{-1} olefins where in which a reduction in CAPEX was seen for all scenarios. The CAPEX after heat integration was reduced by 13.94% to 39.34% in comparison to before applying heat integration.

There was an increase in profit after heat integration, however all CCU scenarios remain negative except for BI-OPEX, which remains 47.6% lower than the conventional SR scenario.

Table 4.11. Key economic performance indicators for olefin production scenarios after heat integration

	Conventional	Dry reforming		Bi-reforming		Adiabatic Tri-reforming		Isothermal Tri-reforming	
	SR	**DR-OPEX**	**DR-GWP**	**BI-OPEX**	**BI-GWP**	**ADTRI-OPEX**	**ADTRI-GWP**	**ISOTRI-OPEX**	**ISOTRI-GWP**
Purchased equipment cost (M$)	31.53	39.85	39.66	54.66	39.35	60.42	50.21	40.68	49.23
FCI (M$)	173.50351	219.28	218.21	300.76	216.50	332.40	276.25	223.82	270.89
Working capital (M$)	30.637668	38.72	38.53	53.11	38.23	58.70	48.78	39.52	47.83
CAPEX ($·$t^{-1}$ *Olefins)*	89.288	199.49	243.13	167.87	215.09	82.59	140.37	68.59	71.11
Total raw material cost ($·$t^{-1}$ *Olefins*)	306.0085	486.37	595.67	379.35	531.47	678.60	713.05	650.18	660.85
Total utility cost ($·$t^{-1}$ *Olefins)*	183.168	172.01	218.52	154.99	206.38	214.75	229.64	215.86	226.20
Total utility and material cost ($·$t^{-1}$ *Olefins)*	489.18	658.38	814.19	534.34	737.84	893.35	942.69	866.04	887.05
Total production cost ($·$t^{-1}$ *Olefins)*	578.46	857.87	1057.32	702.21	952.93	975.94	1083.06	934.63	958.16
Revenue ($·$t^{-1}$ *Olefins)*	808.91	856.95	790.84	803.06	789.27	787.89	794.42	787.85	783.77
Profit/Loss ($·$t^{-1}$ *Olefins)*	*230.45*	*-0.91*	*-266.48*	*100.85*	*-163.66*	*-188.05*	*-288.64*	*-146.78*	*-174.40*

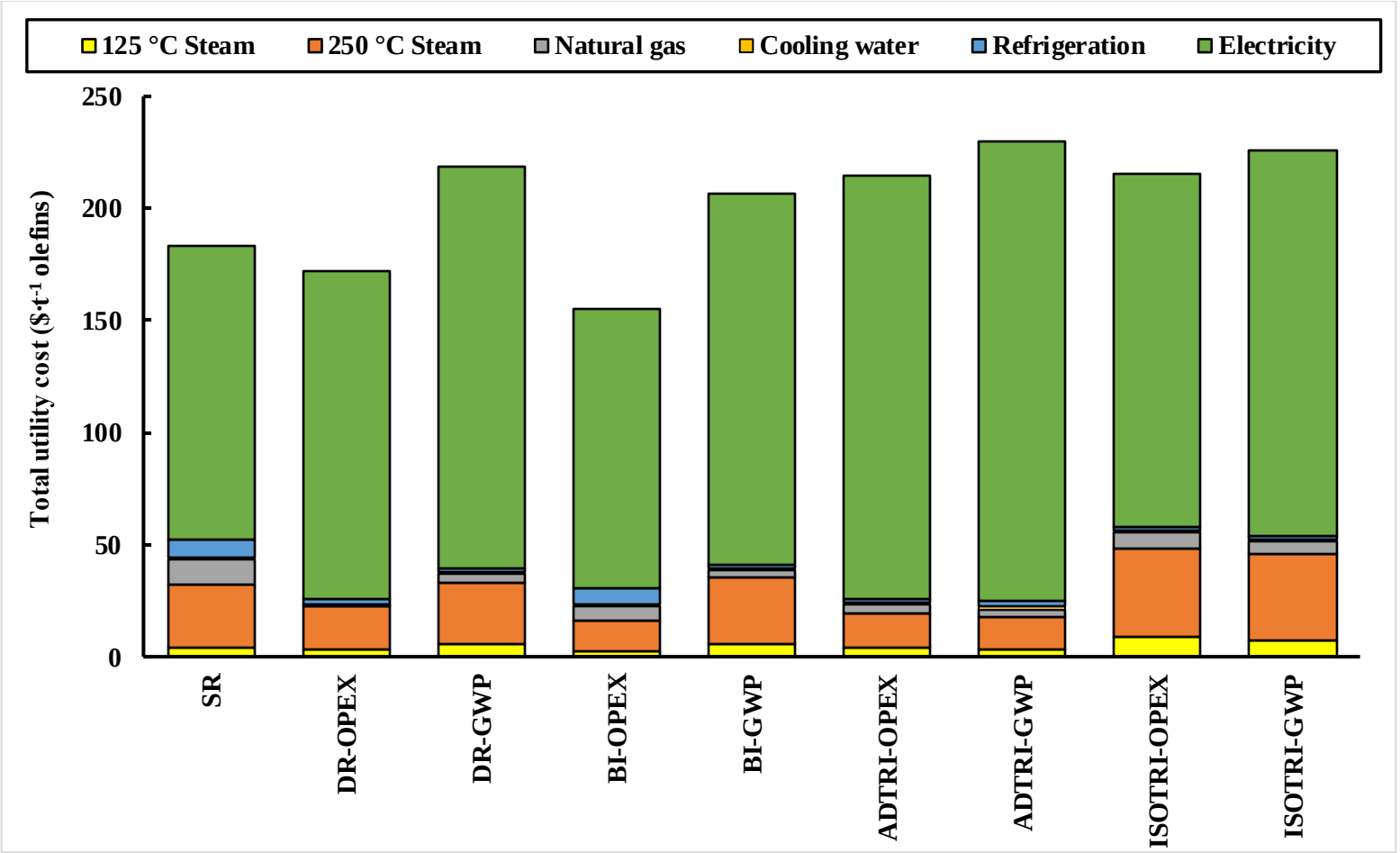

Figure 4.13. Breakdown of total utility cost for olefin production scenarios studied after heat integration.

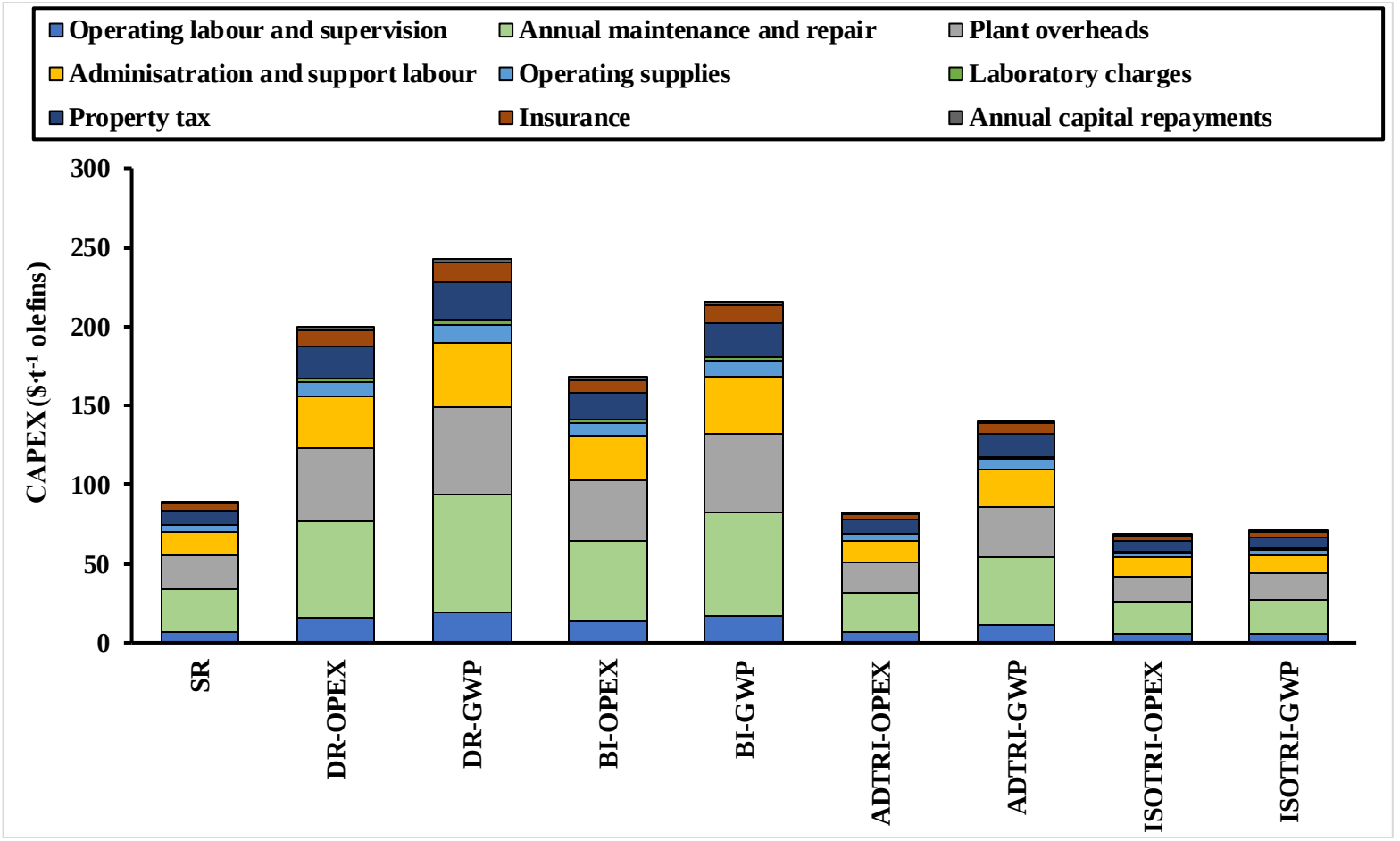

Figure 4.14. Breakdown of CAPEX for olefin production scenarios studied after heat integration.

5.3 Global warming potential

Figure 4.15 and Figure 4.16 provide a breakdown of the GWP sources for the scenarios studied before and after heat integration. Before applying heat integration, the majority of the GWP was due to the heating utility requirements, representing 39.04% to 67.17% of the total positive GWP sources for the scenarios studied. Before heat integration the GWP for the CCU scenarios studied were lower than that of the conventional SR scenario by 16.56% to 45.29%, ranging from 2.74 to 4.19 tCO_2-equivalent$\cdot t^{-1}$ olefins. The optimisation objective affects the GWP significantly as the scenarios optimised towards minimising environmental impact displayed significantly lower GWP values; 5.9% to 34.21% lower.

Although the tri-reforming scenarios have lower overall CO_2 conversion compared to the dry- and tri-reforming scenarios, this did not necessarily correlate with the GWP. For example, although the CO_2 conversion for ISOTRI-CST and BI-CST are 3.64% and 65.31% respectively, the GWP for ISOTRI-CST was 37.38% lower than that for BI-CST. The increase in CO_2 emissions in the tri-reforming processes was due to the increased natural gas requirements because of the presence of an oxygen feed. However, the effect on the GWP was limited by the exothermic nature of the tri-reforming reaction, reducing utility requirements in the reactor.

The GWP for the CCU scenarios studied after heat integration ranged from 0.26 to 1.75 tCO_2-eq$\cdot t^{-1}$ olefins, providing a decrease in GWP of 42.36% to 90.91%. Furthermore, in comparison to the conventional scenario with heat integration, the GWP for the CCU scenarios were 7.51% to 86.48% lower. After heat integration the tri-reforming scenarios overall displayed a lower GWP than the other CCU scenarios. For example, the GWP for DR-OPEX was 29.84% higher than that for ISOTRI-OPEX.

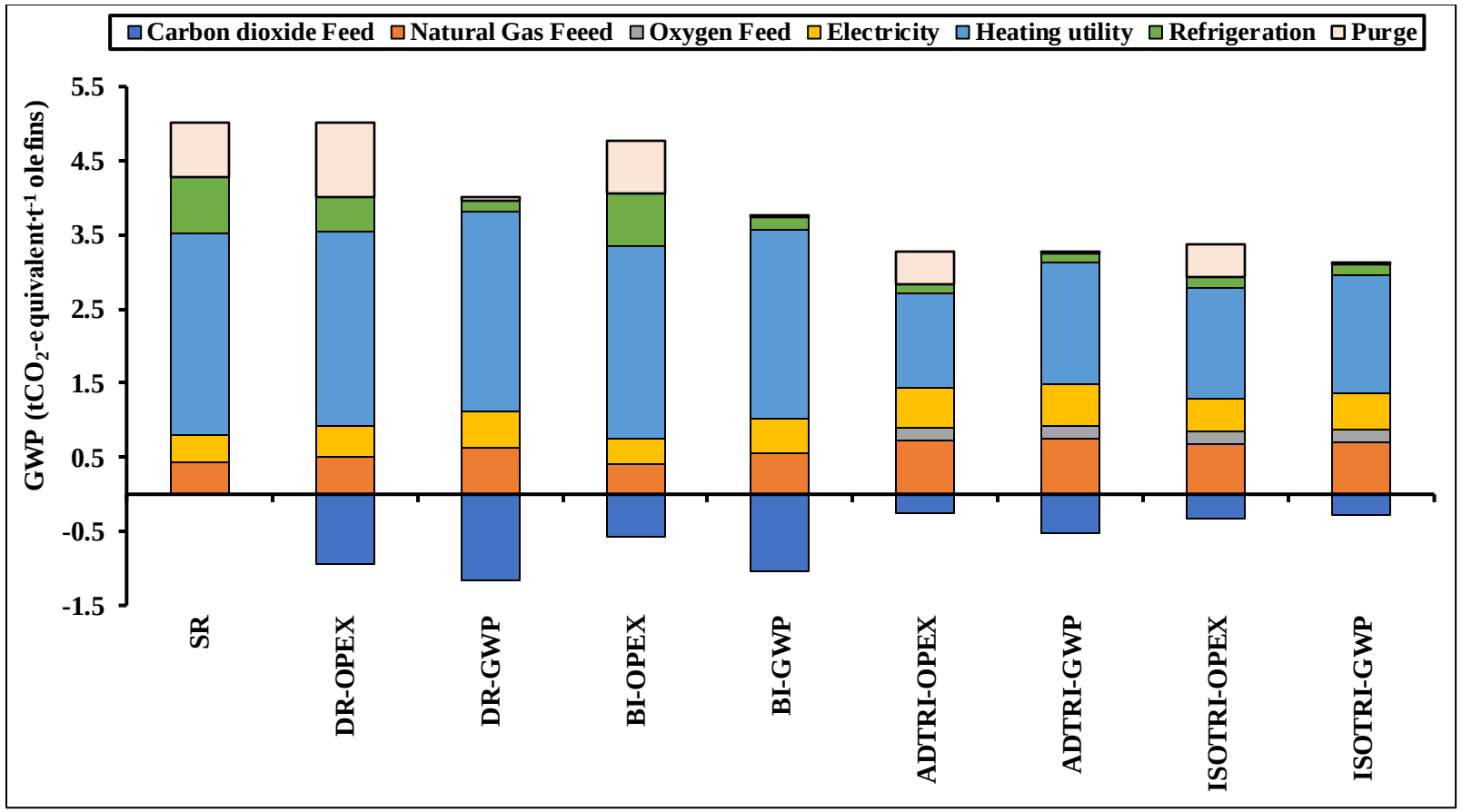

Figure 4.15. Breakdown of GWP sources for the MTO scenarios before heat integration.

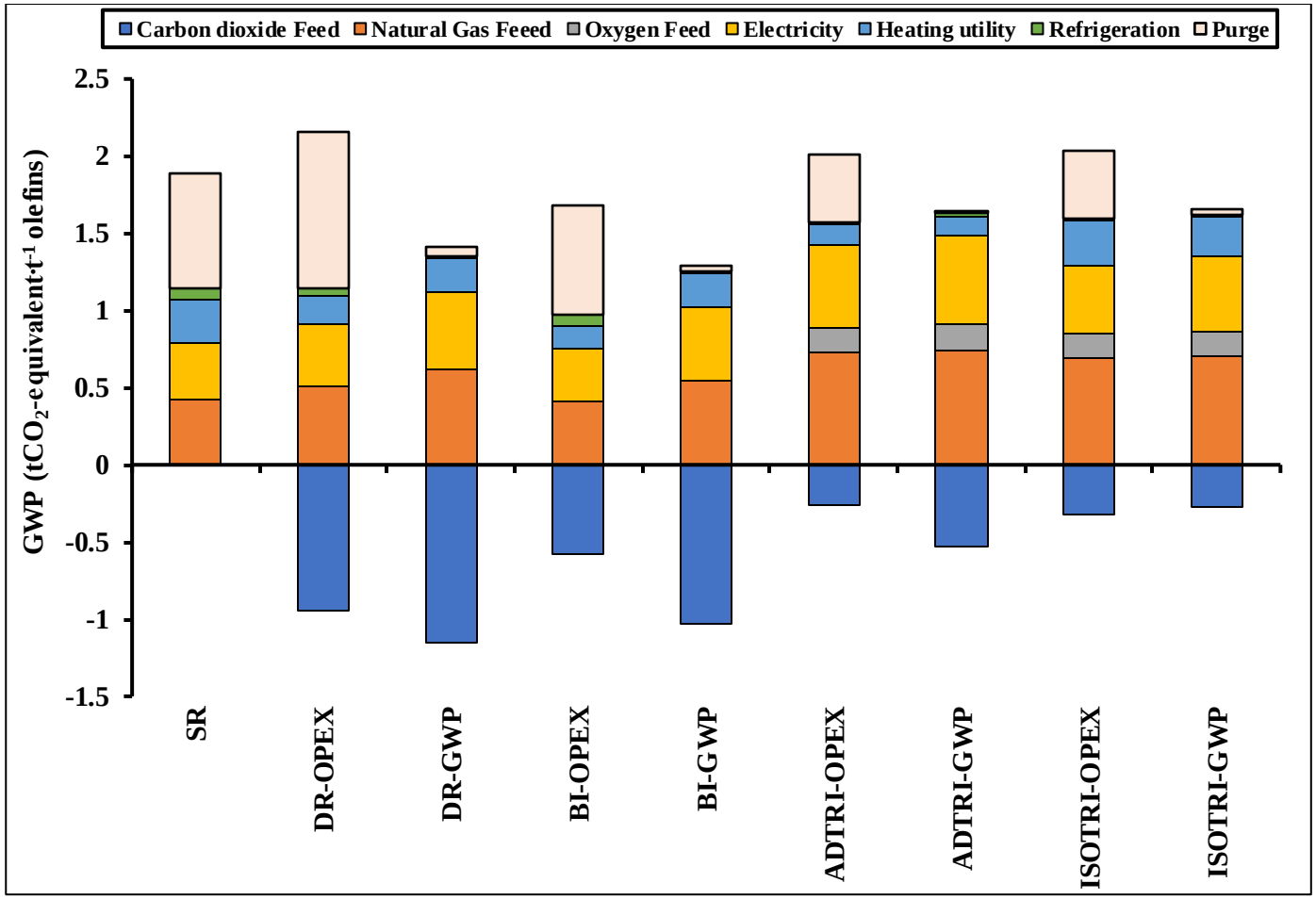

Figure 4.16. Breakdown of GWP sources for the MTO scenarios after heat integration.

5.4 Cost of global warming potential reduction

The cost of global warming potential reduction (CGWP) provides a metric to outline the economics of using a CCU technology in relation to the reduction in GWP it provides. The CCU-based scenarios studied reduce GWP through substitution of the olefin products that would otherwise be produced through conventional fossil fuel-based technologies.

Therefore, the CGWP for the CCU scenarios may be calculated by,

$$CGWP = \frac{TPC_{olefins,CCU} - TPC_{olefins,conv}}{GWP_{olefins,conv} - GWP_{olefins,CCU}}$$

where $TPC_{olefins,CCU}$ is the total production cost of the CCU process, $TPC_{olefins,conv}$ is the total production cost of conventional olefin production, $GWP_{olefins,conv}$ is the total GWP of conventional olefin production and $GWP_{olefins,CCU}$ is the total GWP of the CCU scenario.

The CGWP of the CCU scenarios studied are shown in Figure 4.17. The CGWP ranged from \$156.12 to \$2800.23 t^{-1} CO_2-equivalent. The CGWP of the tri-reforming scenarios were significantly greater than that for the dry and bi-reforming scenarios by 37.44% to 94.43%. The CGWP for the scenarios optimised towards minimising production cost for the tri-reforming and dry-reforming cases were significantly greater than that for the scenarios optimised towards minimising GWP by 28.31% to 76.69%. This is due to the difference in total raw material cost between the cost minimisation and the GWP minimisation scenario for the bi-reforming cases being greater than that for the other cases. The total material cost for BI-GWP was 40.1% higher than BI-OPEX in comparison to a 22.57% to 1.64% difference for the dry and tri-reforming cases. BI-OPEX displayed the lowest CGWP at \$156.12 per tonne CO_2-equivalent.

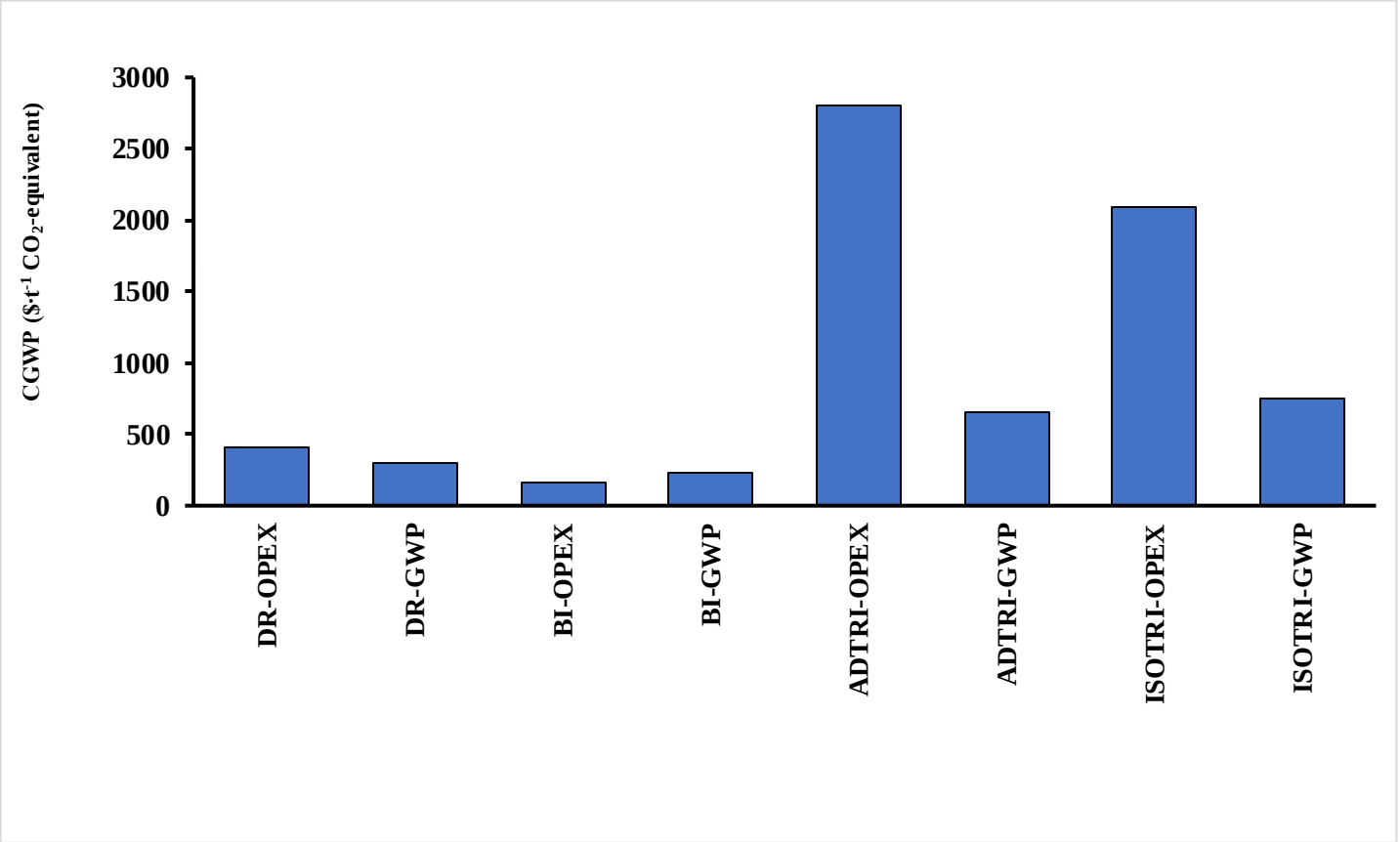

Figure 4.17. Cost of global warming potential for methanol to olefin synthesis scenarios.

5.5 Sensitivity and uncertainty analysis

A sensitivity and uncertainty analysis were conducted through a Monte Carlo simulation using MATLAB. The impact of key parameters that affect the total production cost of the olefin production process and their uncertainties are studied including the cost of feed materials, utility requirements and the capital expenditure needed. The costs related to CO_2 feed, natural gas feed, the O_2 feed (tri-reforming scenarios only), CAPEX and utilities usage are evaluated to determine the greatest impact of these parameters on the total olefin production cost.

The parameters are modelled using a triangular distribution with a sample size of $1x10^6$. A lower and higher bound from -20% to 30% of their base value are used. The selected uncertain parameters together with their value range are shown in Table 4.12.

Table 4.12. Uncertain input parameters examined and ranges for these parameters.

Parameter	Low value	Nominal	High value	Unit
Natural gas cost [36]	276	345	448.5	$\$\cdot t^{-1}$ *olefins*
CO_2 cost	40.65	50.81	66.05	$\$\cdot t^{-1}$ *olefins*
O_2 cost	48	60	78	$\$\cdot t^{-1}$ *olefins*
CAPEX	-20%	See Table 4.12	+30%	$\$\cdot t^{-1}$ *olefins*
Utility cost	-20%	See Table 4.12	+30%	$\$\cdot t^{-1}$ *olefins*

Figure 4.18 shows the sensitivity analyses for all the CCU scenarios. The price of natural gas has the greatest impact on total production cost for all scenarios. For example, it can be seen for DR-OPEX a 30% increase in natural gas cost increases total production cost by \$78.76 t^{-1} olefins or a 9.18% increase from the base case. However as there is a significant correlation between natural gas prices and the sale price of synthesised chemical such as olefins and methanol [37], the impact of uncertainty present in natural gas prices is limited as an increased natural gas price correlates heavily to an increased market value for olefins.

Utility costs and CAPEX also have a high impact on total production costs, especially for the dry and bi-reforming scenarios: for example, a 30% increase in CAPEX and utility cost for DR-OPEX increases total production cost by \$42.56 and \$36.70 t^{-1} olefins respectively or a 4.96% and 4.27% increase from the base case respectively.For the tri-reforming scenarios, CAPEX has a lower impact on total production costs, whereas the impact of the costs related to utility are higher: for example, a 30% increase in CAPEX and utility cost for ISOTRI-OPEX increases total production cost by \$14.62 and \$46.06 t^{-1} olefins respectively or a 1.56% and 4.93% increase from the base case respectively

The costs related to the CO_2 feed, including its capture, and transportation, have a low impact on total production cost for all scenarios; for DR-OPEX a 30% increase in CO_2 feed cost increases total production cost by \$14.20 t^{-1} olefins or a 1.66% increase from the base case. This indicates the limited impact of the capture technology and capture source on the economics of MTO CCU processes. Finally, the impact of oxygen feed cost is low for the tri-reforming scenarios examined: a 30% increase in oxygen cost for ISOTRI-OPEX increases total production cost by \$13.95 t^{-1} olefins or a 1.49% increase from the base case respectively. The limited impact of the CO_2 feed or oxygen feed is due to their low impact on total raw material cost as shown in Figure 4.10.

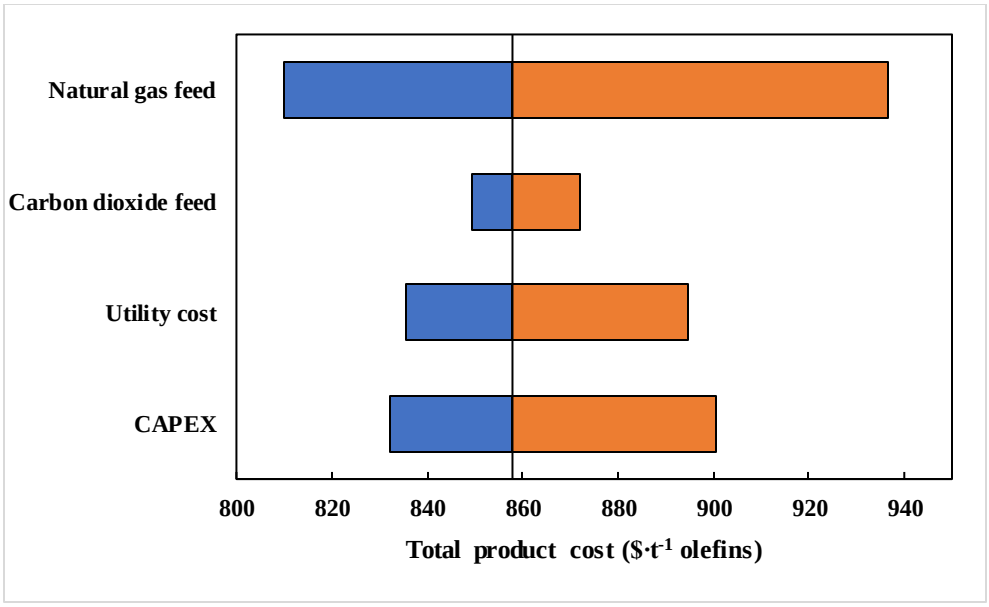

(i) DR-OPEX

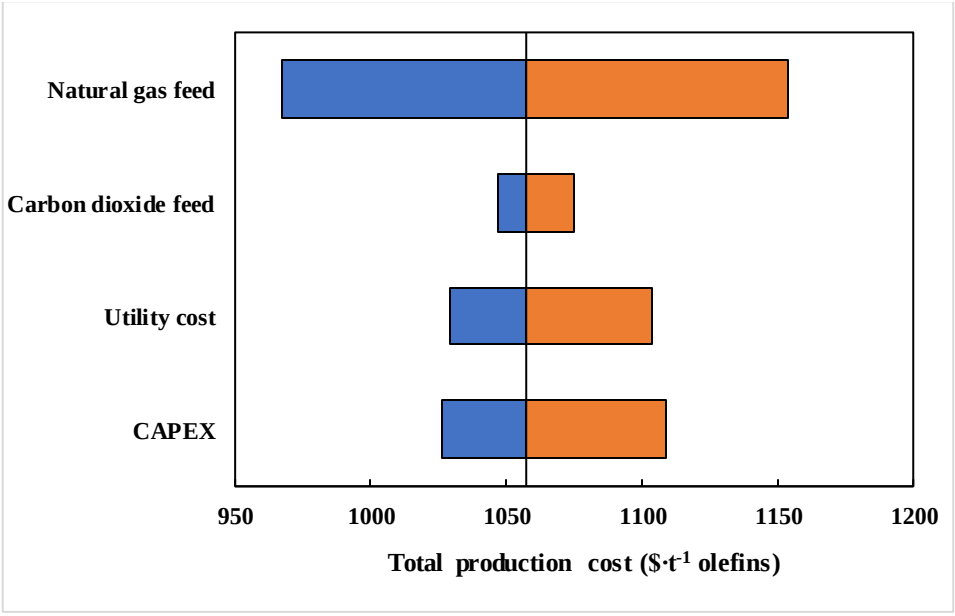

(ii) DR-GWP

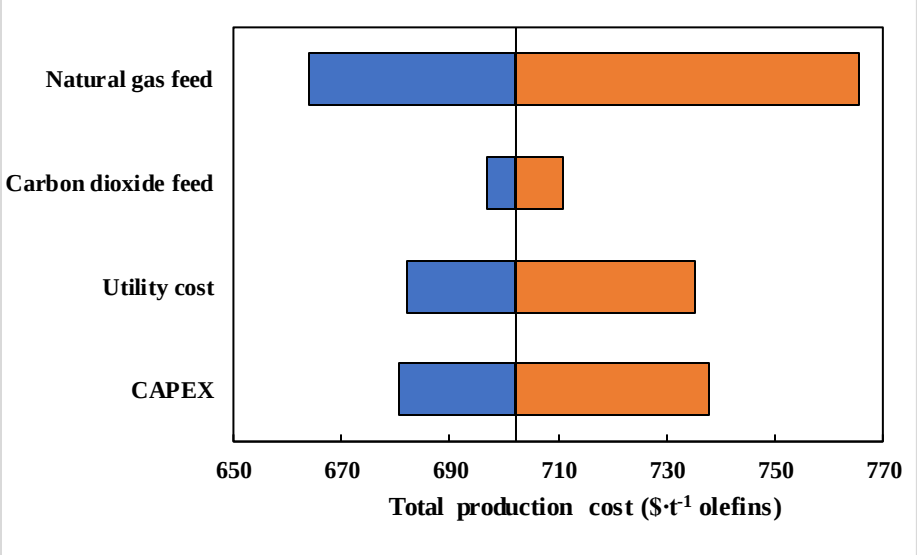

(iii) BI-OPEX

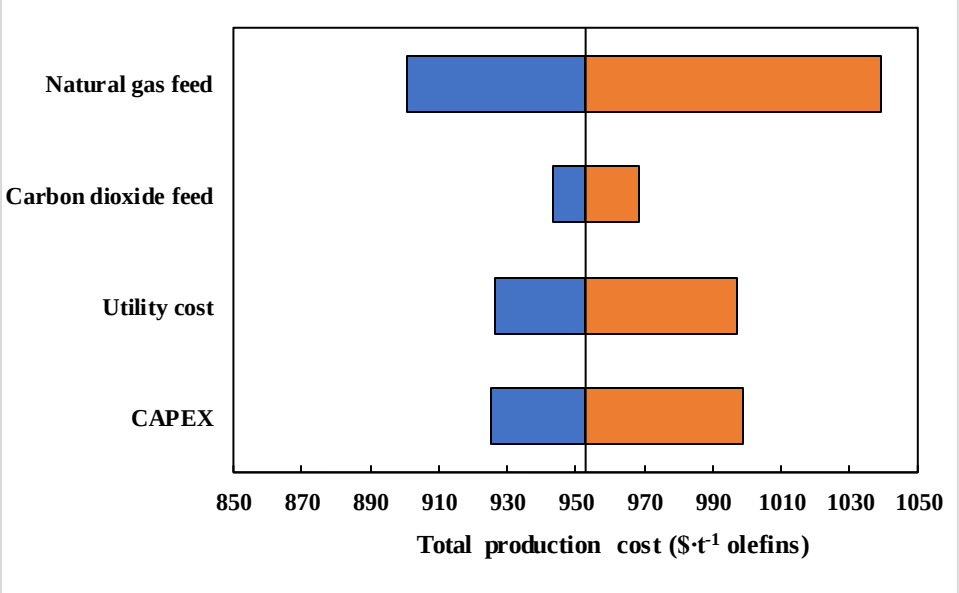

(iv) BI-GWP

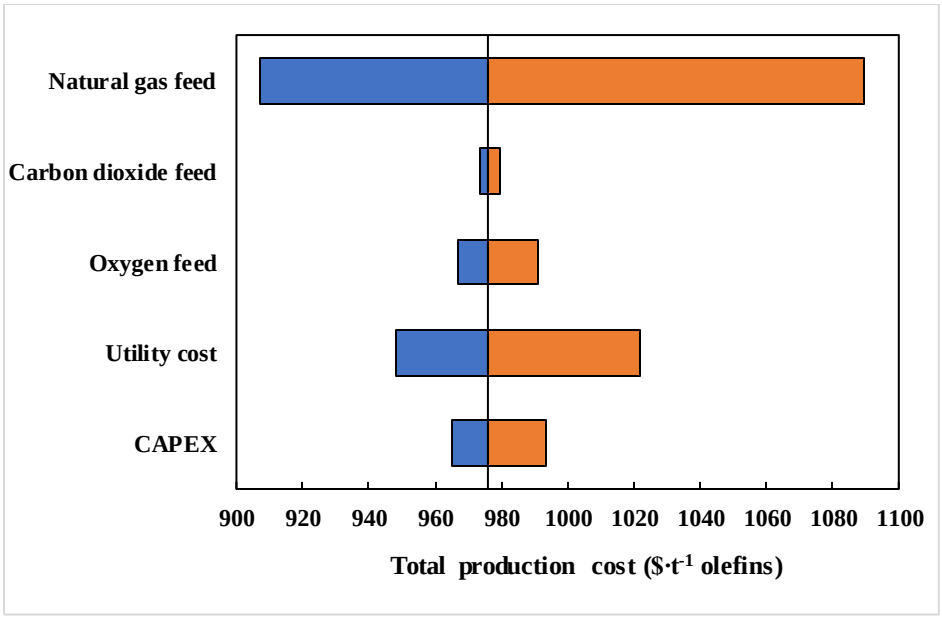

(v) ADTRI-OPEX

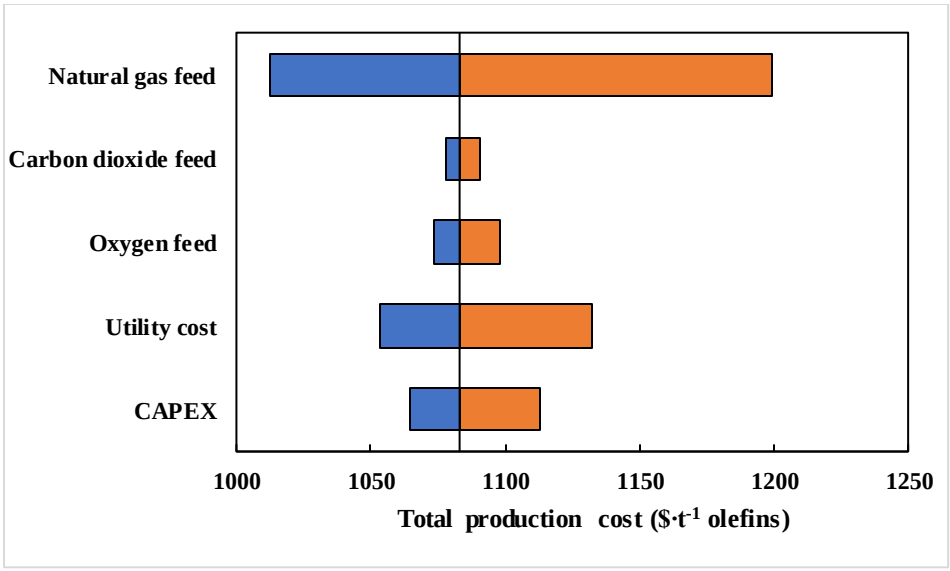

(vi) ADTRI-GWP

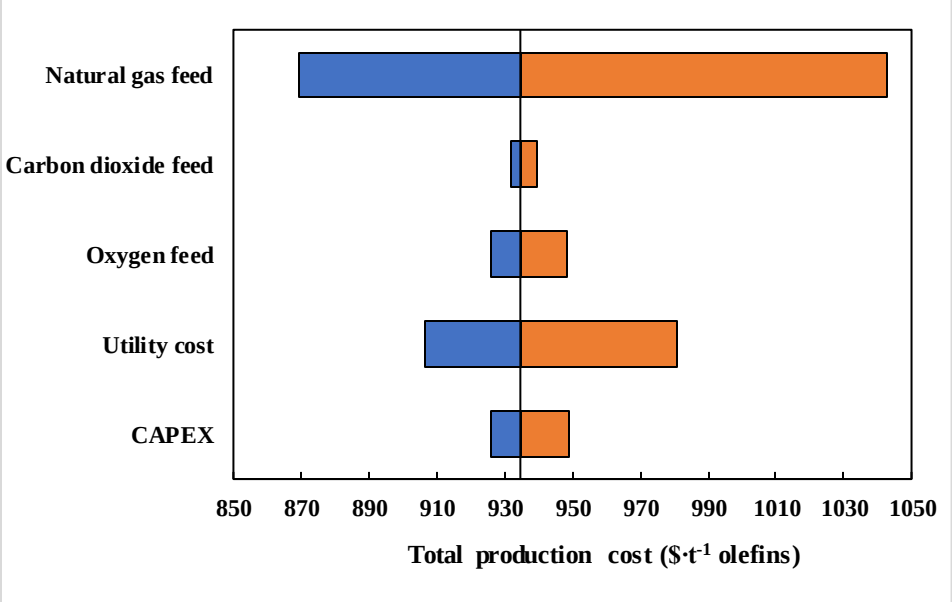

(vii) ISOTRI-OPEX

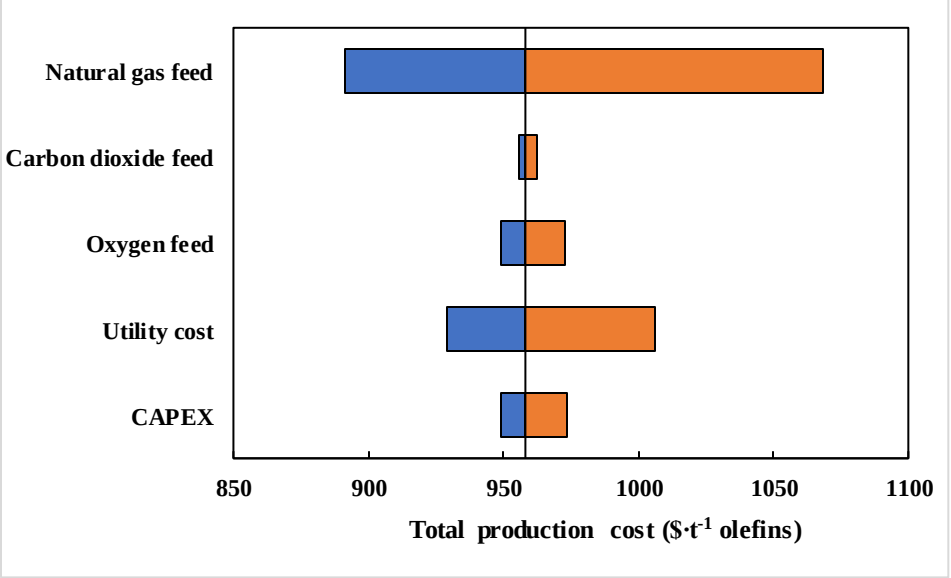

(viii) ISOTRI-GWP

Figure 4.18. Sensitivity analysis for CCU MTO scenarios between a confidence interval of 5 to 95%.

Figure 4.19 displays the probability distribution for the uncertainty analysis of the studied scenarios showing average values and standard deviation within a 90%

confidence interval. In relation to the average, the standard deviation ranges from $\pm$ 5.3 % to $\pm$ 5.97%. An uncertainty analysis provides a quantitative analysis of the risk associated with the investment into the scenario studied and commercial viability and the techno-economic analyses conducted. For example there is a 90% probability that the value for the total production cost for BI-OPEX is within the range of \$703.5 and \$780.90 t^{-1} olefins, which is below the estimated revenue of \$803.06 t^{-1} olefins, as shown in Table 4.11.

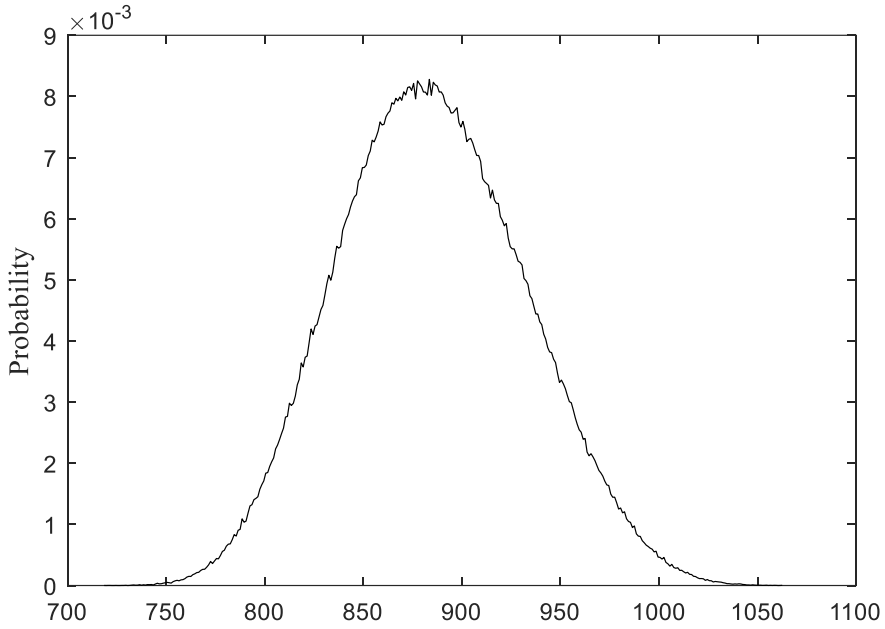

Average: 884.78 Standard Deviation:47.07

(i) DR-OPEX

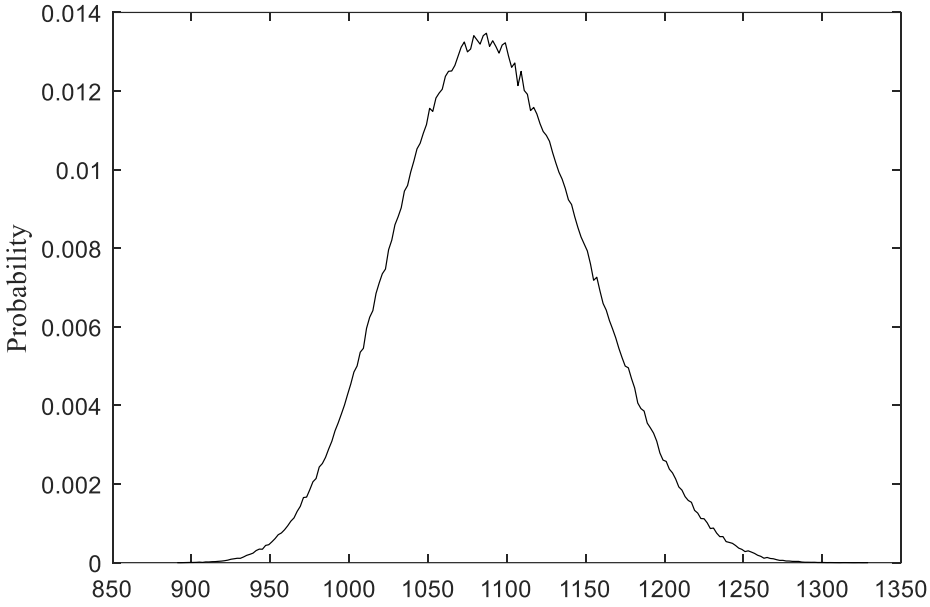

Average: 1090.66 Standard Deviation:57.92

(ii) DR-GWP

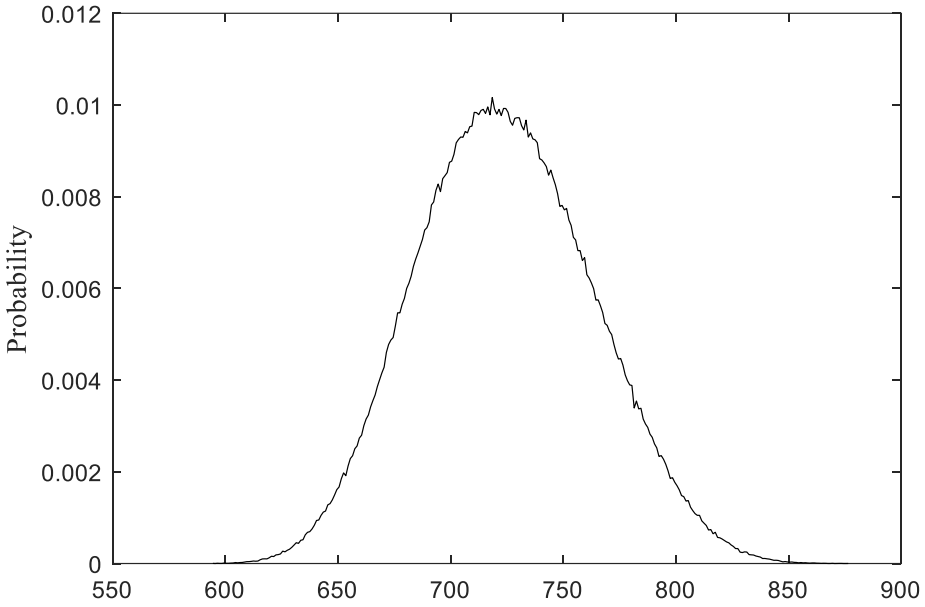

Average: 724.2 Standard Deviation:38.7

(iii) BI-OPEX

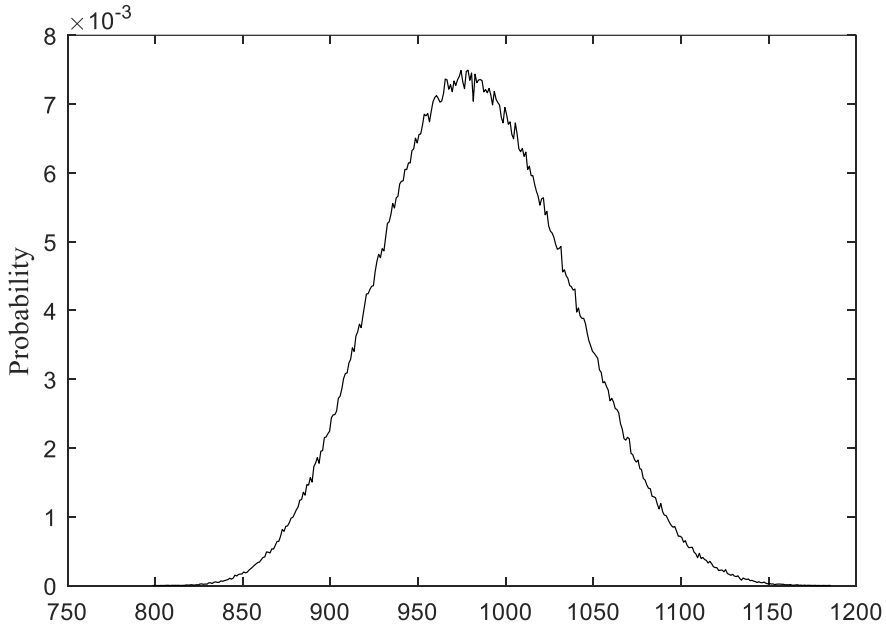

Average: 982.89 Standard Deviation:52.1

(iv) BI-GWP

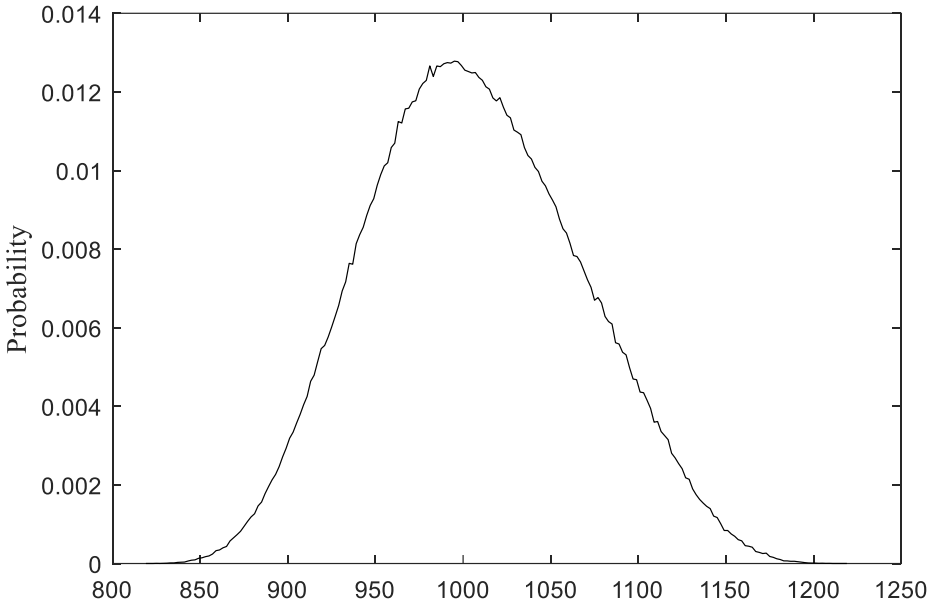

Average: 1006.38 Standard Deviation:59.97

(v) ADTRI-OPEX

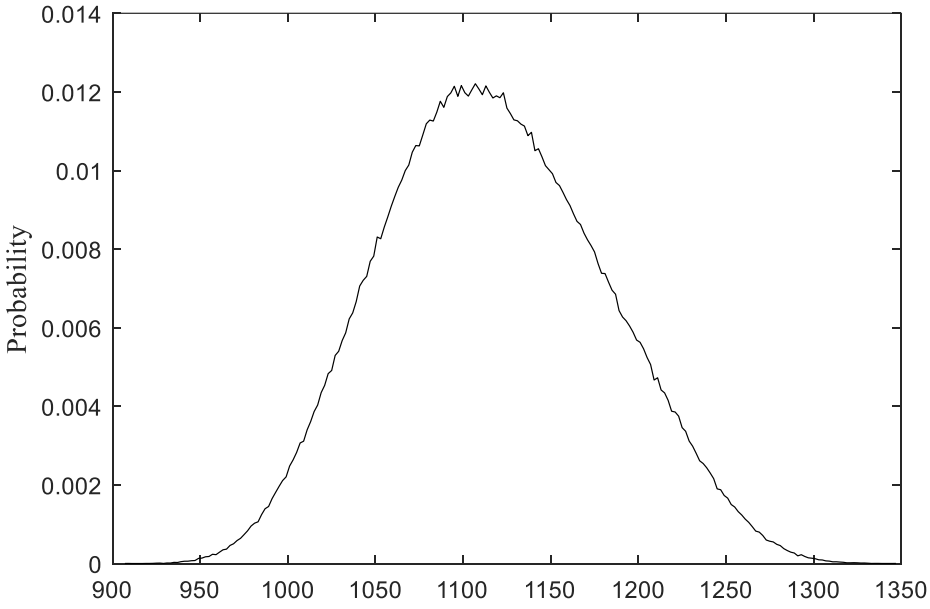

Average: 1117.11 Standard Deviation:63.02

(vi) ADTRI-GWP

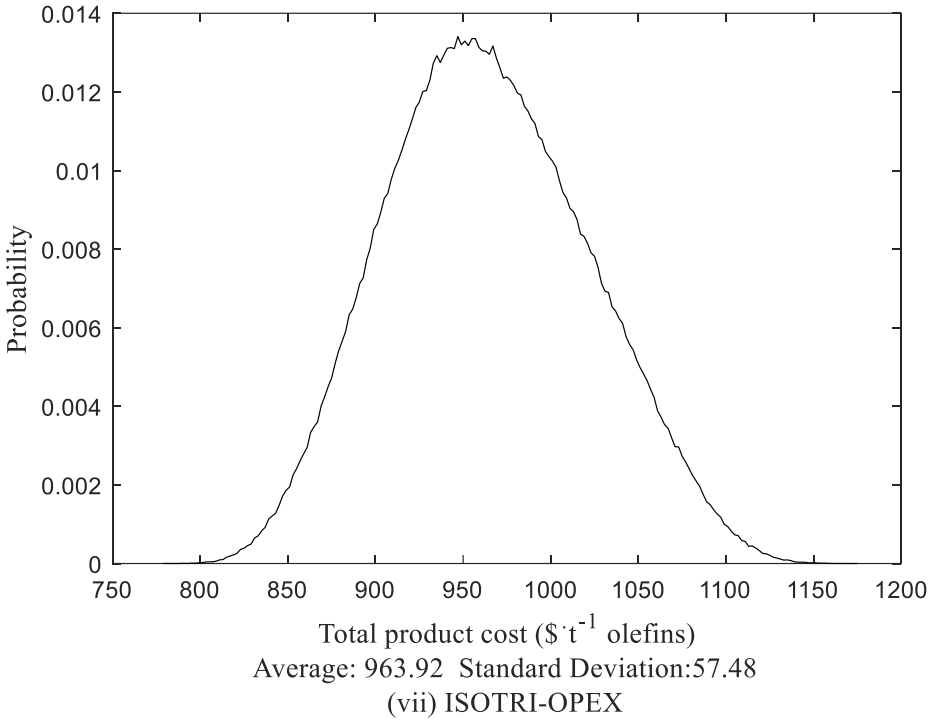

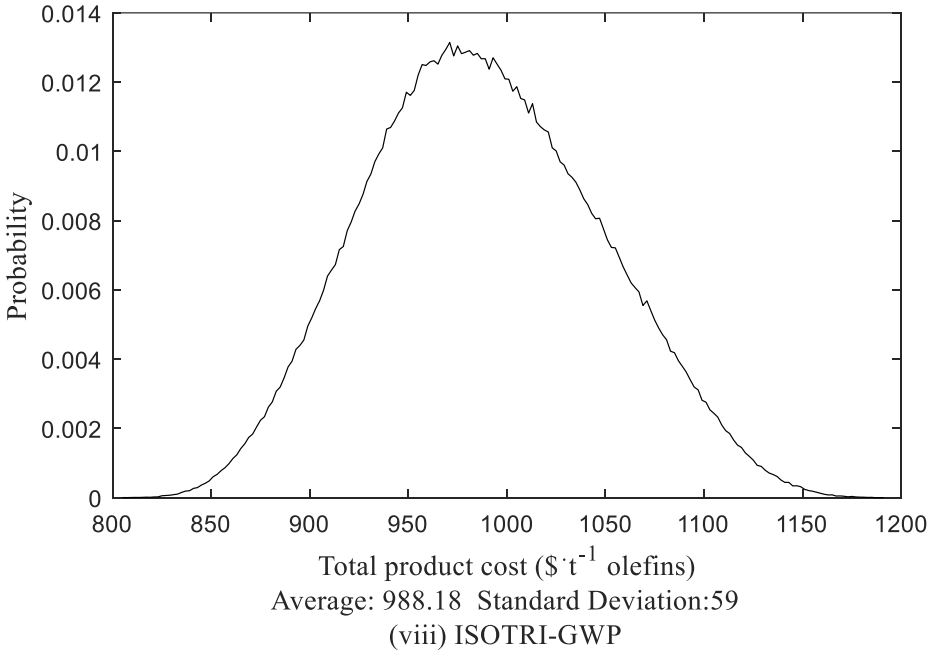

Figure 4.19. Uncertainty analysis for CCU MTO scenarios.

6.0 Conclusion

Six CCU MTO production scenarios have been studies using CO_2 captured froma cement plant with an oxyfuel capture system installed. Processes using dry, biand tri-reforming technologies were modelled in Aspen Plus V12 and optimised towards either minimising production costs or minimising environmental impact

using MATLAB. After optimisation heat integration was applied to allow for a techno-economic and environmental assessment to be conducted. A Monte Carlo simulation was used to complete a sensitivity and uncertainty analysis.

Before heat integration the CCU scenarios have a GWP ranging from 2.74 to 4.19 tCO_2-equivalent·t^{-1} olefins and CO_2 conversion ranged from -4.5% to 71.79%. In regard to the CCU scenarios, BI-GWP resulted in the lowest GWP whereas DR-CST had the highest. In comparison to the conventional MTO technology (i.e. steam reforming) a reduction in GWP of 16.56% to 45.29% was seen using the CCU scenarios. The total production cost of the CCU scenarios ranged from **$**1189.03 to **$**1540.48 tonne^{-1} olefins- which was 11.03% to 43.85% higher than the conventional MTO scenario. However, all scenarios before heat integration, including the conventional production, scenario resulted in negative profits, ranging from -**$**749.65 to -**$**262.97 tonne^{-1} olefins.

The total production cost and GWP for all scenarios were reduced by 20.38% to 46.03% and 42.36% to 90.91% respectively after heat integration was carried out. Specifically, the GWP for the CCU scenarios after heat integration ranged from 0.26 to 1.75 tCO_2-eq·t^{-1} olefins- which was 7.51% to 86.48% lower than the conventional production scenario. DR-GWP displayed the lowest GWP after heat integration. The total production cost for the CCU scenarios and conventional production scenario was reduced to **$**857.87 – 1083.06 t^{-1} olefins and **$**578.46 t^{-1} olefins respectively. This was due to the reduction of the total utility requirements and thus total utility cost by 20.38% to 46.03% for the scenarios studied. The profitability of the scenarios was increased through the application of heat integration. The profit for the CCU scenarios studied ranged from - **$**288.64 t^{-1} olefins to **$**100.85 t^{-1} olefins whilst the conventional production scenario had a profit of **$**230.45 t^{-1} olefins. The only profitable CCU scenario was BI-OPEX, however this was still 47.6% less profitable than the conventional scenario. This outlines the limitations that may be present in CCU technologies without suitable policies and regulations being incorporated to promote their use in comparison to conventional fossil fuel-based production technologies.

The CGWP is a performance indicator that links the reduction of GWP to the impact on economics provided by implementing CCU technology. The CGWP ranged from \$156.12 to \$2800.23 per tCO_2-equivalent where BI-OPEX had the lowest CGWP. The CGWP of the tri-reforming scenarios were significantly higher than the dry and bi-reforming scenarios.

The sensitivity analysis showed that natural gas had the largest impact on the total production cost for all CCU scenarios studied. For the dry and bi-reforming scenarios, CAPEX and utility costs had a high impact on total production cost. Comparatively, CAPEX has a lower impact than utility costs to total production cost for the tri-reforming scenarios. The impacts of costs related to the CO_2 feed and oxygen (for the tri-reforming scenarios) to total production cost was low. This was due to the low impact of costs related to the CO_2 feed and oxygen to total raw material cost for the CCU scenarios. The uncertainty analysis showed a standard deviation ranging from $\pm$ 5.3 % to $\pm$ 5.97% in relation to the average.

Bi-reforming based MTO synthesis showed the greatest potential for commercial feasibility as an alternative to conventional MTO synthesis.

References

[1] Statista, "Propylene demand and capacity worldwide from 2015 to 2022," [Online]. Available: https://www.statista.com/statistics/1246689/propylene-demand-capacity-forecast-worldwide/. [Accessed 21 24 2022].

[2] Statista, "Ethylene demand and production capacity worldwide from 2015 to 2022," [Online]. Available: https://www.statista.com/statistics/1246694/ethylene-demand-capacity-forecast-worldwide/. [Accessed 24 Jan 2022].

[3] M. R. F. K. G.R. Moradi, "The effects of partial substitution of Ni by Zn in LaNiO3 perovskite catalyst for methane dry reforming," *Journal of CO2 Utilization,* vol. 6, pp. 7-11, 2014.

[4] J. P. S. S.-W. S. F. E.G. Mahoney, "The effects of Pt addition to supported Ni catalysts on dry (CO2) reforming of methane to syngas," *Journal of CO2 Utilization,* vol. 6, pp. 40-44, 2014.

[5] C. S. Y. C. C. C. T. J. S. O. U. O. H. D. S. D.-V. N. V. S. Z. A. Hamidah Abdullah, "Recent Advances in CO2 Bi-Reforming of Methane for Hydrogen and Syngas Productions," in *Chemo-Biological Systems for CO2 Utilization*, CRC Press, 2020, p. 27.

[6] D. W. G. Y. T. S. W. Qianqian Chen, "Techno-economic evaluation of CO2-rich natural gas dry reforming for linear alpha olefins production," *Energy Conversion and Management,* vol. 205, no. 112348, 2020.

[7] A. Alturki, "Techno-Economic Analysis of a Process to Convert Methane to Olefins, Featuring a Combined Reformer via the Methanol Intermediate Product," *hydrogen,* vol. 3, pp. 1-27, 2022.

[8] S. Y. Y. Q. D. Xiang, "Techno-economic analysis and comparison of coal based olefins processes," *Energy Conversion and Management,* vol. 110, pp. 33-41, 2016.

[9] I. V. J. J. e. a. V. Spallina, "Techno-economic assessment of different routes for olefins production through the oxidative coupling of methane (OCM): advances in benchmark technologies," *Energy Conversion and Management,* vol. 154, pp. 244-261, 2007.

[10] S. Y. Z. Q. Yi Man, "Conceptual design of coke-oven gas assisted coal to olefins process for high energy efficiency and low CO2 emission," *Applied Energy,* vol. 133, pp. 197-205, 2014.

[11] T. F. a. A. L. Marian Rosental, "Life Cycle Assessment of Carbon Capture and Utilization for the Production of Large Volume Organic Chemicals," *Frontiers in Climate,* 2020.

[12] S. C. D. A. J. M. J. P.-R. G. G.-G. Iasonas Ioannou, "Hybridization of Fossil- and CO2-Based Routes for Ethylene Production using Renewable Energy," *ChemSusChem,* vol. 13, no. 23, pp. 6370-6380, 2020.

[13] MMSA , "MMSA MTO Coverage," MMSA , [Online]. Available: https://www.methanolmsa.com/mto/. [Accessed 01 January 2021].

[14] Y. W. M. Y. a. Z. L. Peng Tian, "Methanol to Olefins (MTO): From Fundamentals to Commercialization," *ACS Catalysis,* vol. 5, no. 3, p. 1922–1938, 2015.

[15] H. L. Z. G. W. Y. Juan Liang, "Characteristics and performance of SAPO-34 catalyst for methanol-to-olefin conversion," *Applied Catalysis,* vol. 64, pp. 31-40, 1990.

[16] Dalian Institute of Chemical Physics, "The 10th DMTO Plant Start-up: An Academic Success Story From Coal to Chemical Building Blocks," DICP, 20 April 2016. [Online]. Available: http://english.dicp.cas.cn/ns_17179/icn/201604/t20160420_162156.html. [Accessed 2021 01 01].

[17] Y. Z. a. W. Zhao, "Dalian Institute of Chemical Physics, Chinese Academy of Sciences," *National Science Review,* vol. 6, no. 4, pp. 843-853, 2019.

[18] V. Zacharopoulou and A. Lemonidou, "Olefins from biomass intermediates: A review.," *Catalysts* , vol. 8, no. 2, 20188.

[19] W. Posch, "3 - Polyolefins," in *Applied Plastics Engineering Handbook*, 2011, pp. 23-48.

[20] P. V. L. T. P. S. V. P. Doronin, "Effect of process conditions on the composition of products in the conventional and deep catalytic cracking of oil fractions," *Catalysis in Industry,* vol. 5, pp. 100-104, 2012.

[21] N. D. S. B. D Wolf, "Oxidative dehydrogenation of propane for propylene production — comparison of catalytic processes," *Chemical Engineering Science,* vol. 56, no. 2, pp. 713-719, 2001.

[22] D. S. P. a. J. K. Hurd, "FITT research: China's coal-to-olefins industry," Deutsche Bank, Hong Kong, 2014.

[23] J.-P. G. Michel Guisnet, "Methanol to Olefins (MTO) and Beyond," in *Zeolites For Cleaner Technologies*, London, Imperial College Press, 2002.

[24] M. R. Gogate, "Methanol-to-olefins process technology: current status and future prospects," *Petroleum Science and Technology,* no. 5, pp. 559-565, 2019.

[25] J. Z. M. Q. Y. Shiyan Chang, "Clean Coal Technologies in China: Current Status and Future Perspectives," *Engineering,* vol. 2, no. 4, pp. 447-459, 2016.

[26] M. M.Firoozi, "The effect of micro and nano particle sizes of H-ZSM-5 on the selectivity of MTP reaction," *Catalysis Communications,* vol. 10, no. 15, pp. 1582-1585, 2009.

[27] J. Z. W. S. X.-F. H. Zhengpai Zhang, "Promotional effects of multiwalled carbon nanotubes on iron catalysts for Fischer-Tropsch to olefins," *Journal of Catalysis,* vol. 365, pp. 71-85, 2018.

[28] Y. Y. Minhua Zhang, "Dehydration of Ethanol to Ethylene," *Industrial and Engineering Chemisty Research,* vol. 52, no. 28, p. 9505–9514, 2014.

[29] O. D. L. 2. R. 2. R. 1. V. 1.-F. P.-C. 3. B. 1. F. 1. A. 1. S. 3. G. 4. M. 3. a. Stefania Osk Gardarsdottir, "Comparison of Technologies for CO2 Capture from Cement Production—Part 2: Cost Analysis," *Energies,* 2019.

[30] Aspen Technology, "Aspen Physical Property System - Physical Property Methods," Burlington, USA, 2013.

[31] P. James R. Couper W. Roy Penney James R. Fair, Chemical Process Equipment - Selection and Design, Gulf Professional Publishing, 2009.

[32] HSE, "Pipelines and gas supply industry," HSE, [Online]. Available: https://www.hse.gov.uk/pipelines/faqs.htm#:~:text=Pipelines%20associated%20with%20gas%20terminals,some%20at%20over%20300%20bar.. [Accessed 02 09 2020].

[33] P. S. E. R. K. Altfeld, "Development of natural gas qualities in Europe," *Gas Qual.,* vol. 152, pp. 544-550, 2011.

[34] J. S. G.S. Sandeep Alavandi, "Emerging and Existing Oxygen Production Technology Scan and Evaluation," 2018.

[35] M. J.Skrzypek, "Kinetics of methanol synthesis over commercial copper/zinc oxide/alumina catalysts," *Chemical Engineering Science,* vol. 46, no. 11, pp. 2809-2813, 1991.

[36] L. Miller, "Oxygenate conversion reactor catalyst coolers". United States Patent No. US 8,062,599 B2., 2011.

[37] B. V. e. a. Vora, "Production of light olefins from natural gas.," *Studies in Surface Science and*

Catalysis, vol. 136, pp. 537-542, 2001.

[38] X. Y. Y. C. L. L. Lei Ying, "A seven lumped kinetic model for industrial catalyst in DMTO process," *Chemical Engineering Research and Design,* vol. 100, pp. 179-191, 2015.

[39] J. J. H. N. M. P. &. L. J. D. R. Beech, "Process for handling catalyst from an oxygenate to olefin reaction.". United States Patent US 7,119,241 B2., 2006.

[40] H. e. a. Wang, "Method for purifying quench water and scrubbing water from MTO by mini-hydrocyclone and apparatus used for same.". China Patent US 8,083,951 B2, 2011.

[41] I.-L. C. Bor-Yih Yu, "Design and Optimization of the Methanol-to-Olefin Process. Part I: Steady-State Design and Optimization," *Chemical Engineering & Technology,* vol. 39, no. 12, pp. 2293-2303, 2016.

[42] X. P. H. Z. S. Wang.China Patent CN Patent 201010203557, 2010 .

[43] Methanol Institute, "methanol-price-supply-demand," Methanol Institute, 2019.

[44] K. A. D. A. Mansur M.Masiha, "Price dynamics of natural gas and the regional methanol markets," *Energy Policy,* vol. 38, no. 3, pp. 1372-1378, 2010.

[45] T. A. A. R. J. a. M. G. Boden, "Global, Regional,and National Fossil-Fuel CO2 Emissions, Carbon Dioxide Information Analysis Centre," Global, Regional,and National Fossil-Fuel CO2 Emissions, Carbon Dioxide Information Analysis Centre, [Online]. Available: https://cdiac.ess-dive.lbl.gov/trends/emis/meth_reg.html. [Accessed 22 May 2019].

[46] "Natural gas prices," Our World, 01 June 2019. [Online]. Available: https://ourworldindata.org/grapher/natural-gas-prices. [Accessed 01 June 2019].

[47] J. S. G.S. Sandeep Alavandi, "Emerging and Existing Oxygen Production Technology Scan and Evaluation," Gas Technology Institute, 2018.

Chapter 5 – CCU policy and comparison of CCU technologies

Term	Acronym
International Panel on Climate Change	IPCC
Fifth Assessment Report	AR5
Carbon capture and storage	CCS
International Energy Agency	IEA
World Economic Forum	WEF
Greenhouse gas	GHG
Carbon capture and utilisation	CCU
Life cycle assessment	LCA
Natural gas	NG
Dimethyl ether	DME
Methanol to olefins	MTO
Cost of global warming potential reduction	CGWP

1.0 Carbon capture and utilisation policy

After the Paris agreement came into effect in 2020, updated international policy regarding global climate change issues was formulated. The International Panel on Climate Change (IPCC) conducted the Fifth Assessment Report (AR5) and concluded that limiting global average temperature rise to below 2 ℃ is unachievable without the introduction of carbon capture and storage (CCS) [1]. It was recommended by the International Energy Agency (IEA) that incorporating an estimated 9% implementation of CCS is required [2].

The World Economic Forum (WEF) emphasised that a circular economy approach to greenhouse gas (GHG) emissions is required. This is conducted through a closing of the carbon circle by capturing the emitted GHG and using them to further improve economics [3]. CCU can significantly contribute to the reduction of greenhouse gas emissions as part of a comprehensive strategy to producing a low carbon circular economy [4].

Due to the accessibility to inexpensive natural gas, there is an increased availability of low-cost commodity chemicals that may be produced from natural gas such as ethylene. This has hindered the commercial competitivity of alternative methods of production [5].

CCU technologies offers the opportunity to address and counter act some of the limitations provided by CCS technologies including the selection and preparation of suitable sites for CO_2 storage.

A major restriction that is present in the development of a suitable policy framework for CCU technologies is the trend to incorporate CCU as a subcategory of CCS, as both require the initial incorporation of CO_2 capture technology. This hinders its capability for further advancement as there is a

tendency to examine and assess the CCU technologies to standards similar to CCS technologies. CCU technologies are outlined as an alternative to CCS rather than a parallel solution, as part of an overarching strategy. Therefore, to address stakeholder concerns and develop suitable policy instruments regarding CCU, there needs to be a greater separation and acknowledgement of the differences and assessment requirements between CCS and CCU.

The main limiting factor for greater industrial implementation of CCU is the increased costs when compared with conventional production pathways. This may include the requirement for renewable energy to allow for the use of hydrogen as an energy carrier, which is incorporated in many CCU technologies.

A range of possible options are present for the incorporation of CCU into a carbon reduction credit system and characterisation in government policy consideration. This includes only considering CCU technologies that provides sufficient evidence that incorporating this technology displaces CO_2 from a fossil fuel origin. Furthermore, there may be only consideration for CCU technologies that provide permanent abatement of CO_2 emissions. However, in this case there requires a consideration to the time period that equates to permanent abatement, from 100 years to 10,000 years.

Currently, the United Kingdom does not provide any carbon reduction credits for CCU. This assumes that captured CO_2 from a process is emitted to the atmosphere rather than permanently or temporarily abated. The potential for investment towards CCU technologies is improved through the decrease in uncertainty regarding CCU technologies in terms of applicative policies and support provided. This may be improved through the outline of key criteria and benchmarks that needs to be achieved by a CCU technology. These may include a life cycle assessment (LCA) proving the capability to abate captured

CO_2 for a defined period or proof of significant reduction in impact towards climate change.

Strategies such as the introduction of carbon pricing offers the opportunity for CCU technologies to garner commercial feasibility. Alternatively, the fossil fuel sources of raw material that is being displaced through the use of CCU may be targeted for increased carbon levy and taxes to increase competitiveness of CCU technologies in the UK market.

To this end two alternate policy regulations and market decisions are studied:

1. A carbon levy on the natural gas (NG) feed assuming a 100% discount for CCU technologies, to estimate the required carbon levy for the CCU technologies to be commercially competitive in comparison to the conventional processes.
2. Applying a 'green' premium on the sale price of the product

Table 5.1 shows that CCU indirect dimethyl ether (DME) synthesis processes overall have a lower carbon levy requirement in comparison to the CCU methanol to olefins (MTO) processes. In both technologies the BI-OPEX provide the greatest competitiveness compared to the conventional production process requiring a carbon levy of \$94.49 and \$ 160.71 t^{-1} NG for the indirect DME synthesis and MTO synthesis respectively. These values are higher than the carbon price support rates in the United Kingdom by 78.05% and 202.83%. Furthermore, these are only applied for natural gas used in energy production and only an 86% discount is available for climate change agreement holders [6]. However, applying an increased carbon levy on natural gas has social considerations regarding its impact on consumer energy prices.

Table 5.1 Breakdown of required 'green' premium and carbon levy for CCU indirect DME synthesis and CCU MTO synthesis scenarios.

Indirect DME synthesis

		DR-OPEX	DR-GWP	BI-OPEX	BI-GWP	ADTRI-OPEX	ADTRI-GWP	ISOTRI-OPEX	ISOTRI-GWP
Carbon levy	**($ t^{-1} NG)**	101.97	140.78	94.49	141.22	354.78	385.13	294.83	307.41
'Green' premium	**%**	13.22	23.52	11.21	23.64	94.04	98.45	71.69	74.65

Methanol to olefin synthesis

		DR-OPEX	DR-GWP	BI-OPEX	BI-GWP	ADTRI-OPEX	ADTRI-GWP	ISOTRI-OPEX	ISOTRI-GWP
Carbon levy	**($ t^{-1} NG)**	362.87	621.90	160.71	486.32	516.21	655.32	462.56	493.12
'Green' premium	**%**	79.83	163.50	24.96	117.00	146.39	193.34	125.88	136.91

2.0 Techno-economic comparison of studied CCU scenarios

Table 5.2 shows a comparison of the two CCU technologies studied in Chapter 3 and 4: indirect DME synthesis and MTO synthesis. Table 5.2 shows that the cost of global warming potential reduction (CGWP) for the DME synthesis scenarios are lower than that of the olefin production scenarios. Furthermore, that bi-reforming provides the greatest commercial feasibility in comparison to the other CCU reforming technologies studied. The GWP for the olefin scenarios are significantly lower than the DME scenarios due to the increased total production rate of the MTO scenarios. However, the electricity requirements for the MTO scenarios are higher due to the increased complexity of the separation process for the MTO process, increasing the number of processing units and pumping requirements.

Table 5.2 Techno-economic comparison of CCU indirect DME synthesis and CCU MTO synthesis scenarios.

Product	Method	Direct CO_2 emission (t)	CO_2 efficiency (%)	Electricity requirements *($kWh \cdot t^{-1}$ product)*	Heating requirements *($GJ \cdot t^{-1}$ product)*	Cooling requirements *($GJ \cdot t^{-1}$ product)*	CGWP ($\$ \cdot t^{-1}$ CO_2-equivalent)	GWP (tCO_2-equivalent $\cdot t^{-1}$ product)
Dimethyl ether	Indirect reforming using dry-reforming	0.071 to 0.2	70.10 to 86.12	583.34 to 692.40	0.66 to 0.79	2.09 to 2.61	94.31 to 121.31	2.54 to 3
	Indirect reforming using bi-reforming	0.071 to 0.2	70.09 to 86.16	583.45 to 692.40	0.51to 0.85	2.04 to 2.61	93.69 to 103.49	2.48 to 2.96
	Indirect reforming using tri-reforming	0.35 to 0.46	-4.70 to 10.02	585.94 to 747.05	1.90 to 5.28	4.44 to 8.62	187.14 to 581.23	2.2 to 3.27
Olefins	MTO using dry-reforming	0.37 to 0.45	71.77 to 71.79	1189.65 to 1457.16	2.31 to 3.93	2.80 to 3.13	292.82 to 408.43	0.26 to 1.21
	MTO using bi-reforming	0.28 to 0.57	60.36 to 65.31	1010.38 to 1344.60	2.53 to 4.14	2.73 to 3.85	156.12 to 229.69	0.26 to 1.10
	MTO reforming using tri-reforming	0.33 to 0.51	-4.5 to 30.63	1287.20 to 1664.74	2.94 to 7.66	2.77 to 5.35	652.87 to 2800.23	1.25 to 2.02

References

[1] IPCC, “AR5 Climate Change,” IPCC, 2014.

[2] IEA, “The Role of CO2 Storage,” 2019.

[3] World Resour. Forum, “Seven Messages about the Circular Economy and Climate Change.,” 2019. [Online]. Available: https://ovam.vlaanderen.be/. [Accessed 19 07 2022].

[4] World Economic Forum, “Annual Report 2019-2020,” 2019.

[5] W. Garcia, “The European Chemical Industry perspective,” IEA Global Industry Dialogue, Expert Review Workshop, Paris, 2013.

[6] Gov.uk, “Environmental taxes, reliefs and schemes for businesses,” [Online]. Available: https://www.gov.uk/green-taxes-and-reliefs/climate-change-levy. [Accessed 01 June 2022].

Chapter 6 – Conclusions and recommendations

Term	Acronym
Global warming potential	GWP
Dimethyl ether	DME
Carbon capture and utilisation	CCU
Cost of global warming potential reduction	CGWP
Methanol to olefins	MTO

Conclusions

- After optimisation and heat integration the GWP for the DME CCU scenarios studied ranged from 2.2 to 3.27 tCO_2-equivalent·t^{-1} DME, where ADTRI-GWP had the lowest GWP: 39.23% lower than the GWP of the conventional scenario.
- After optimisation and heat integration the total production cost for the DME CCU scenarios studied ranged from **$**482.98 – 683.52 t^{-1} DME, where BI-OPEX had the lowest total production cost: 15.6% higher than the total production cost of the conventional scenario.
- The CGWP for the DME CCU scenarios studied ranged from $93.69 to $581.23 per tCO_2-equivelant where BI-GWP had the lowest CGWP.
- The minimum fuel selling price for the DME CCU scenarios studied ranged from $16.65 to $23.57 GJ^{-1}.
- After optimisation and heat integration the GWP for the MTO CCU scenarios studied ranged from to 0.26 to 1.75 tCO_2-eq·t^{-1} olefins, where BI-GWP had the lowest GWP: 86.48% lower than the conventional scenario.
- After optimisation and heat integration the total production cost for the MTO CCU scenarios studied ranged from **$**857.87 – 1083.06 t^{-1} olefins with a profit or loss of - **$**288.64 t^{-1} olefins to **$**100.85 t^{-1} olefins; where BI-OPEX had the lowest total production cost: 47.6% greater than the total production cost of the conventional scenario.
- The CGWP for the MTO CCU scenarios studied ranged from $156.12 to $2800.23 per tCO_2-equivelant where BI-OPEX had the lowest CGWP
- The carbon levy needed for the DME CCU scenarios and MTO CCU scenarios are $94.49 to $385.13 t^{-1} NG and $160.71 to $655.32 t^{-1} NG respectively.
- The ‘green’ premium required for the DME CCU scenarios and MTO CCU scenarios are 11.21% to 98.45% and 24.96% to 193.34% respectively.

- From the studied CCU pathways, bi-reforming provides the greatest opportunity for commercial feasibility in applying CCU.

Due to the low technology maturity of the CCU-based reforming technologies studied and high capital expenditure required, there is uncertainty present in their economic and environmental performance indicators. This limits stakeholder confidence in commercial feasibility and exposure to emission regulations such as the Emissions Trading Scheme (ETS).

The UK governments has displayed support to CCUS projects through supply-side contract models such as Contract for Difference [1] , allocating a portion of the risk to itself. However, these have focussed upon projects that display permanent geological storage of CO_2. In the near term, the development of first-of-a-kind CCU plants will require government grants and subsidies to incentivise further deployment. However due to the unsustainable nature of subsidy-based support, legislations and regulations such as market-based incentives for decarbonisation are required. Examples includes the expansion and accommodation of CCU processes to the ETS. Accounting for the permeance of CO_2 abatement provided by the CCU process may be accounted and be included through the introduction of partial credits that may be allocated based upon the leakage rate of the captured CO_2.

Recommendations for future works

The recommendations resulting from the work reported in this thesis are as follows:

- A cradle to gate analysis has been considered for the scenarios studied. The expansion of the system boundary to a cradle to grave analysis, incorporating the end use of the CCU products, provides a greater understanding for the ability of the CCU technology to provide CO_2 emission abatement.

- With regard to the possible uses of DME as a transport fuel, conducting a well to wheel analysis life cycle assessment for DME compared to conventional diesel and gasoline vehicles would provide an assessment of the effectiveness of CCU based DME as an alternative to fossil fuel-based fuels. This may also be compared to electrical vehicles.
- DME may also be produced through a direct process; conducting a techno-economic assessment on the direct DME process including CCU-based direct DME synthesis could provide insights on the economic feasibility of this route.
- Alternatively, a multi-objective optimisation may have been conducted rather than targeting each optimisation objective individually. Developing a pareto front provides the ability to outline the trade-offs between the two objectives studies in greater detail.
- For olefin production the steam reforming methanol to olefins (MTO) process was considered as the conventional process, however there are alternative conventional olefin production methods that have significant industrial usage such as methanol to propylene and naptha cracking. To provide an improved analysis these alternative pathways should be studied and compared to.
- Optimisation of the processes towards minimising costs were limited towards the variable costs including material and utility costs; this does not consider capital expenditure required for equipment costs. Incorporating capital costs requirements to the objective function would provide improved results.
- Optimisation was carried out prior to heat integration. Although there is difficulty in the completion of a comprehensive heat integration for each iteration in terms of feasibility and computation costs; incorporating a pinch analysis determining the minimum heating and cooling demand may be possible. Including heat integration to the objective function and optimisation process would provide improved results.
- The economic analysis completed determined total production costs for the CCU products. The addition of investment feasibility performance

indicators, such as return on investment and net present value, can provide improved conclusions to the commercial feasibility of the CCU processes.

References

[1] Department for Business, Energy & Industrial Strategy, "Contracts for Difference," 14 December 2022. [Online].

Appendix

List of Tables

List of Figures

Appendix 1

This appendix provides required supplementary information for the methodology applied in Chapter 3.

Section A.1.1

This section provides the kinetic equations and parameters for the kinetic models used in this study.

$$k_i = A_i \exp\left(\frac{B_i}{RT}\right),$$

$$K_i = A_i \exp\left(\frac{B_i}{RT}\right)$$

where R is the molar gas constant (8.314 $J.mol^{-1}K^{-1}$).

Appendix 1.A. Kinetic equations and parameters for dry-reforming

$$CH_4 + CO_2 \leftrightarrow 2CO + 2H_2 \qquad r_{DMR,1} = \frac{k_{DMR,1}\left(K_{CO_2,dmr1}K_{CH_4,dmr1}p_{CO_2}p_{CH_4} - \frac{1}{K_{eq,DMR,1}}(p_{CO}p_{H_2})^2\right)}{\left(1 + K_{CO_2,dmr1}p_{CO_2} + K_{CH_4,dmr1}p_{CH_4}\right)^2} \qquad \text{(A.DMR1)}$$

$$CO_2 + H_2 \leftrightarrow CO + H_2O \qquad r_{DMR,2} = \frac{k_{DMR,2}(K_{CO_2,dmr2}K_{H_2,dmr2}p_{CO_2}p_{H_2} - \frac{1}{K_{eq,DMR,2}}(p_{CO}p_{H_2})^2)}{\left(1 + K_{CO_2,dmr2}p_{CO_2} + K_{H_2,dmr2}p_{H_2}\right)^2} \qquad \text{(A.DMR2)}$$

Table A.1 Parameters values for the kinetic model of dry-reforming *[1] [2]*.

$k_{DMR,1}$(molkg^{-1} s^{-1})	$A_{DMR,1}$	1.29 x 10^6
	$B_{DMR,1}$	-102065
$k_{DMR,2}$(molkg^{-1} s^{-1})	$A_{DMR,2}$	0.35 x 10^6
	$B_{DMR,2}$	-81030
$K_{CO_2,dmr1}$ (bar^{-1})	$A_{CO_2,dmr1}$	2.61 x 10^{-2}
	$B_{CO_2,dmr1}$	-37641
$K_{CH_4,dmr1}$ (bar^{-1})	$A_{CH_4,dmr1}$	2.61 x 10^{-2}
	$B_{CH_4,dmr1}$	40684
$K_{CO_2,dmr2}$ (bar^{-1})	$A_{CO_2,dmr2}$	0.5771
	$B_{CO_2,dmr2}$	9262
$K_{H_2,dmr2}$ (bar-1)	$A_{H_2,dmr2}$	1.494
	$B_{H_2,dmr2}$	6025

$$K_{eq,DMR,1} = 6.78 \times 10^{14} \exp\left(-\frac{259{,}660}{RT}\right)$$

$$K_{eq,DMR,2} = 56.4971 \exp\left(-\frac{36{,}580}{RT}\right)$$

Appendix 1.B. Kinetic equations and parameters for bi-reforming

$$CH_4 + CO_2 \leftrightarrow 2CO + 2H_2$$

$$r_{BR,1} = \frac{k_{BR,1}\left(f_{CO_2} f_{CH_4} - \frac{1}{K_{eq,BR,1}}(f_{CO} f_{H_2})^2\right)}{\left(1 + K_{CO_2,BR} f_{CO_2}\right)\left(1 + K_{CH_4,BR} f_{CH_4} + K_{CO,BR} f_{CO}\right)} \quad \text{(B.BRM.1)}$$

$$H_2O + CH_4 \leftrightarrow CO + 3H_2$$

$$r_{BR,2} = \frac{\frac{k_{BR,2}}{f_{H_2}^{2.5}}\left(f_{H_2O} f_{CH_4} - \frac{1}{K_{eq,BR,2}} f_{CO} f_{H_2}^{3}\right)}{\left(1 + K_{H_2,BR} f_{H_2} + K_{CH_4,BR} f_{CH_4} + K_{CO,BR} f_{CO} + K_{H_2O,BR}\frac{f_{H_2O}}{f_{H_2}}\right)^2} \quad \text{(B.BRM.2)}$$

$$2H_2O + CH_4 \leftrightarrow CO + 4H_2$$

$$r_{BR,3} = \frac{\frac{k_{BR,3}}{f_{H_2}^{3.5}}\left(f_{H_2O}^{2} f_{CH_4} - \frac{1}{K_{eq,BR,3}} f_{CO} f_{H_2}^{4}\right)}{\left(1 + K_{H_2,BR} f_{H_2} + K_{CH_4,BR} f_{CH_4} + K_{CO,BR} f_{CO} + K_{H_2O,BR}\frac{f_{H_2O}}{f_{H_2}}\right)^2} \quad \text{(B.BRM.3)}$$

$$CO + H_2O \leftrightarrow CO_2 + H_2$$

$$r_{BR,4} = \frac{\frac{k_{BR,4}}{f_{H_2}}\left(f_{H_2O}\ \ f_{CO} - \frac{1}{K_{eq,BR,4}} f_{CO_2} f_{H_2}\ \ \right)}{\left(1 + K_{H_2,BR} f_{H_2} + K_{CH_4,BR} f_{CH_4} + K_{CO,BR} f_{CO} + K_{H_2O,BR}\frac{f_{H_2O}}{f_{H_2}}\right)^2} \quad \text{(B.BRM.4)}$$

Table A.2. Parameters values for the kinetic model of bi-reforming *[3]*.

$\boldsymbol{k_{BR,1}}$ (mol.Pa^{-2}.gcat^{-1}.h^{-1})	$\boldsymbol{A_{BR,1}}$	2.91 x 10^{-7}
	$B_{BR,1}$	234851
$\boldsymbol{k_{BR,2}}$ (mol.Pa$^{0.5}$.gcat^{-1}.h^{-1})	$A_{BR,2}$	4.72 x 10^{6}
	$B_{BR,2}$	232477
$\boldsymbol{k_{BR,3}}$ (mol.Pa$^{0.5}$.gcat^{-1}.h^{-1})	$A_{BR,3}$	1.89 x 10^{3}
	$B_{BR,3}$	267760
$\boldsymbol{k_{BR,4}}$ (mol.Pa^{-1}.gcat^{-1}.h^{-1})	$A_{BR,4}$	1.06 x 10^{-3}
	$B_{BR,4}$	71537
$\boldsymbol{K_{CO_2,BR}}$ (Pa^{-1})	$A_{CO_2,BR}$	5.97 x 10^{-7}
	$B_{CO_2,BR}$	52670
$\boldsymbol{K_{CO,BR}}$ (Pa^{-1})	$A_{CO,2}$	8.23 x 10^{-10}
	$B_{CO,2}$	70650
$\boldsymbol{K_{H_2,BR}}$ (Pa^{-1})	$A_{H_2,2}$	6.12 x 10^{-14}
	$B_{H_2,2}$	82900
$\boldsymbol{K_{CH_4,BR}}$ (Pa^{-1})	$A_{CH_4,2}$	6.65 x 10^{-9}
	$B_{CH_4,2}$	38280
$\boldsymbol{K_{H_2O,BR}}$	$A_{H_2O,2}$	1.77 x 10^{5}
	$B_{H_2O,2}$	-88680

$$\ln K_{eq,BR,2} = 2.48 - \frac{22920.6}{T} + 7.19 \ln T - 2.95 \times 10^{-3} T$$

$$\ln K_{eq,BR,4} = -12.11 - \frac{5318.69}{T} + 1.01 \ln T + 1.14 \times 10^{-4} T$$

$$K_{eq,BR,3} = K_{eq,BR,2} K_{eq,BR,4}$$

$$K_{eq,BR,1} = \frac{K_{eq,BR,2}}{K_{eq,BR,4}}$$

Appendix 1.C. Kinetic equations and parameters for tri-reforming

$$H_2O + CH_4 \leftrightarrow CO + 3H_2$$

$$r_{TRI,1} = \frac{\frac{0.07k_{TRI,1}}{P_{H_2}^{2.5}}\left(P_{H_2O}P_{CH_4} - \frac{1}{K_{eq,TRI,1}}P_{CO}P_{H_2}^{3}\right)}{\left(1 + K_{CH_4,TRI1}P_{CH_4} + K_{CO,TRI}P_{CO} + K_{H_2,TRI}P_{H_2} + K_{H_2O,TRI}\frac{P_{H_2O}}{P_{H_2}}\right)^2} \quad \text{(C.TRI.1)}$$

$$2H_2O + CH_4 \leftrightarrow CO_2 + 4H_2$$

$$r_{TRI,2} = \frac{\frac{0.06k_{TRI,2}}{P_{H_2}^{3.5}}\left(P_{H_2O}^{2}P_{CH_4} - \frac{1}{K_{eq,TRI,2}}P_{CO_2}P_{H_2}^{4}\right)}{\left(1 + K_{CH_4,TRI1}P_{CH_4} + K_{CO,TRI}P_{CO} + K_{H_2,TRI}P_{H_2} + K_{H_2O,TRI}\frac{P_{H_2O}}{P_{H_2}}\right)^2} \quad \text{(C.TRI.2)}$$

$$H_2O + CO \leftrightarrow CO_2 + H_2$$

$$r_{TRI,3} = \frac{\frac{0.7k_{TRI,3}}{P_{H_2}}\left(P_{H_2O}P_{CO} - \frac{1}{K_{eq,TRI,3}}P_{CO_2}P_{H_2}\right)}{\left(1 + K_{CH_4,TRI1}P_{CH_4} + K_{CO,TRI}P_{CO} + K_{H_2,TRI}P_{H_2} + K_{H_2O,TRI}\frac{P_{H_2O}}{P_{H_2}}\right)^2} \quad \text{(C.TRI.3)}$$

$$CH_4 + 2O_2 \leftrightarrow CO_2 + 2H_2O$$

$$r_{TRI,4} = \frac{0.05k_{TRI,4a}P_{CH_4}P_{O_2}}{\left(1 + K_{CH_4,TRI2}P_{CH_4} + K_{O_2,TRI}P_{H_2}\right)^2} + \frac{0.05k_{TRI,4b}P_{CH_4}P_{O_2}}{\left(1 + K_{CH_4,TRI2}P_{CH_4} + K_{O_2,TRI}P_{H_2}\right)^2} \quad \text{(C.TRI.4)}$$

Table A. 3. Parameters values for the kinetic model of tri-reforming [42] *[4]*.

$\boldsymbol{k_{TRI,1}}$ (mol.bar$^{0.5}$.kgcat^{-1}.s^{-1})	$\boldsymbol{A_{TRI,1}}$ $B_{TRI,1}$ (J.mol^{-1})	1.17 x 10^{15} 240100
$\boldsymbol{k_{TRI,2}}$ (mol.bar$^{0.5}$.kgcat^{-1}.s^{-1})	$A_{TRI,2}$ $B_{TRI,2}$ (J.mol^{-1})	2.83 x 10^{14} 243900
$\boldsymbol{k_{TRI,3}}$ (mol.bar^{-1}.kgcat^{-1}.s^{-1})	$A_{TRI,3}$ $B_{TRI,3}$ (J.mol^{-1})	5.43 x 10^{5} 67130
$\boldsymbol{k_{TRI,4a}}$ (mol.bar^{-2}.kgcat^{-1}.s^{-1})	$A_{TRI,4a}$ $B_{TRI,4a}$ (J.mol^{-1})	8.11 x 10^{5} 86000
$\boldsymbol{k_{TRI,4b}}$ (mol.bar^{-2}.kgcat^{-1}.s^{-1})	$A_{TRI,4b}$ $B_{TRI,4b}$ (J.mol^{-1})	6.82 x 10^{5} 86000
$\boldsymbol{K_{CH_4,TRI1}}$ (bar^{-1})	$A_{CH_4,TRI1}$ $B_{CH_4,TRI1}$ (J.mol^{-1})	6.65 x 10^{-4} -38280
$\boldsymbol{K_{CO,TRI}}$ (bar^{-1})	$A_{CO,TRI}$ $B_{CO,TRI}$ (J.mol^{-1})	8.23 x 10^{-5} -70650
$\boldsymbol{K_{H_2,TRI}}$ (bar^{-1})	$A_{H_2,TRI}$ $B_{H_2,TRI}$ (J.mol^{-1})	6.12 x 10^{-9} -82900
$\boldsymbol{K_{H_2O,TRI}}$	$A_{H_2O,TRI}$ $B_{H_2O,TRI}$ (J.mol^{-1})	1.77 x 10^{5} 88680
$\boldsymbol{K_{CH_4,TRI2}}$ (bar^{-1})	$A_{CH_4,TRI2}$ $B_{CH_4,TRI2}$ (J.mol^{-1})	1.26 x 10^{-1} -27300
$\boldsymbol{K_{O_2,TRI}}$ (bar^{-1})	$A_{O_2,4}$ $B_{O_2,4}$ (J.mol^{-1})	7.87 x 10^{-7} -92800

$$K_{eq,TRI,1} = \exp\left(\frac{-26830}{T} + 30.114\right)$$

$$K_{eq,TRI,3} = \exp\left(\frac{4400}{T} - 4.036\right)$$

$$K_{eq,TRI,2} = K_{eq,TRI,1} K_{eq,TRI,3}$$

Appendix 1.D Kinetic equations and parameters for steam reforming

$$CH_4 + H_2O \leftrightarrow CO + 3H_2$$

$$r_{SR,1} = \frac{\frac{k_{SR,1}}{p_{H_2}^{2.5}}\left(p_{H_2O}p_{CH_4} - \frac{1}{K_{eq,SR,1}}p_{CO}p_{H_2}^{3}\right)}{\left(1 + K_{H_2,SR}p_{H_2} + K_{CH_4,SR}p_{CH_4} + K_{CO,SR}p_{CO} + K_{H_2O,SR}\frac{p_{H_2O}}{p_{H_2}}\right)^2} \quad \text{(D.SR1)}$$

$$CO + H_2O \leftrightarrow CO_2 + H_2$$

$$r_{SR,2} = \frac{\frac{k_{SR,2}}{p_{H_2}}\left(p_{H_2O}\ \ p_{CO} - \frac{1}{K_{eq,SR,2}}p_{CO_2}p_{H_2}\ \ \right)}{\left(1 + K_{H_2,SR}p_{H_2} + K_{CH_4,SR}p_{CH_4} + K_{CO,SR}p_{CO} + K_{H_2O,SR}\frac{p_{H_2O}}{p_{H_2}}\right)^2} \quad \text{(D.SR2)}$$

$$CH_4 + 2H_2O \leftrightarrow CO_2 + 4H_2$$

$$r_{SR,3} = \frac{\frac{k_{SR,3}}{p_{H_2}^{3.5}}\left(p_{H_2O}^{2}p_{CH_4} - \frac{1}{K_{eq,SR,3}}p_{CO}p_{H_2}^{4}\right)}{\left(1 + K_{H_2,SR}p_{H_2} + K_{CH_4,SR}p_{CH_4} + K_{CO,SR}p_{CO} + K_{H_2O,SR}\frac{p_{H_2O}}{p_{H_2}}\right)^2} \quad \text{(D.SR3)}$$

Table A.4. Parameters values for the kinetic model of steam reforming [42].

$k_{SR,1}$(molkg^{-1} s^{-1})	$A_{SR,1}$	4.225 x 10^{-15}
	$B_{SR,1}$	28879
$k_{SR,2}$(molkg^{-1} s^{-1})	$A_{SR,2}$	1.955 x 10^{6}
	$B_{SR,2}$	28879
$k_{SR,3}$(molkg^{-1} s^{-1})	$A_{SR,3}$	1.02 x 10^{5}
	$B_{SR,3}$	29336
$K_{CO,SR}$	$A_{CO,SR}$	8.23 x 10^{-5}
	$B_{CO,SR}$	−8497.7
$K_{CH_4,SR}$	$A_{CH_4,SR}$	6.65 x 10^{-4}
	$B_{CH_4,SR}$	−4604.3
$K_{H_2,SR}$	$A_{H_2,SR}$	6.12 x 10^{-9}
	$B_{H_2,SR}$	−9971.13
$K_{H_2O,SR}$	$A_{H_2O,SR}$	1.77 x 10^{5}
	$B_{H_2O,SR}$	10666.35

$$K_{eq,SR,1}(bar^2) = 1.01325^2 \exp\left(-\frac{53717 - 60.25T}{1.987T}\right)$$

$$K_{eq,SR,2} = \exp\left(-\frac{8514 + 7.11T}{1.987T}\right)$$

$$K_{eq,SR,3}(bar^2) = 1.01325^2 \exp\left(-\frac{45203 - 52.54T}{1.987T}\right)$$

Appendix 1.E Kinetic equations and parameters for methanol synthesis

$$CO_2 + 3H_2 \leftrightarrow CH_3OH + H_2O$$

$$r_{meth,1} = \frac{k_{meth,1} P_{CO_2} P_{H_2} \left(1 - \frac{1}{K_{eq,meth}} \frac{P_{H_2O} P_{CH_3OH}}{{P_{H_2}}^3 P_{CO_2}}\right)}{\left(1 + K_{H_2O,meth1} \frac{P_{H_2O}}{P_{H_2}} + K_{H_2,meth} {P_{H_2}}^{0.5} + K_{H_2O,meth2} P_{H_2O}\right)^3} \quad \text{(E.METH.1)}$$

$$-$$

$$r_{meth,2} = \frac{k_{meth,2} P_{CO_2} \left(1 - \frac{1}{K_{eq2,meth}} \frac{P_{H_2O} P_{CH_3OH}}{{P_{H_2}}^3 P_{CO_2}}\right)}{\left(1 + K_{H_2O,meth1} \frac{P_{H_2O}}{P_{H_2}} + K_{H_2,meth} {P_{H_2}}^{0.5} + K_{H_2O,meth2} P_{H_2O}\right)} \quad \text{(E.METH.2)}$$

Table A.5.Parameters values for the kinetic model of methanol synthesis *[5]*.

$k_{meth,1}$(kmolkg^{-1} s^{-1})	$A_{meth,1}$	1.07
	$B_{meth,1}$	40,000
$k_{meth,2}$(kmolkg^{-1} s^{-1})	$A_{meth,2}$	1.22 x 10^{10}
	$B_{meth,2}$	−98,084
$K_{H_2O,meth1}$	$A_{H_2O,meth1}$	3453.38
	$B_{H_2O,meth1}$	–
$K_{H_2O,meth2}$(atm^{-1})	$A_{H_2O,meth2}$	6.62 x 10^{-11}
	$B_{H_2O,meth2}$	124,119
$K_{H_2,meth}$(atm$^{-0.5}$)	$A_{H_2,meth}$	0.499
	$B_{H_2,meth}$	17,197

$$K_{eq,meth} = \exp\left(\frac{3066}{T} - 10.592\right)$$

$$K_{eq2,meth} = \exp\left(-\frac{2073}{T} + 2.029\right)$$

Appendix 1.F Kinetic equations and parameters for DME synthesis

$$2CH_3OH \leftrightarrow CH_3OCH_3 + H_2O$$

$$r_{DME} = \frac{k_{DME} P_{CH_3OH} - \frac{k_{DME}}{K_{eq,DME}} \frac{P_{H_2O} P_{CH_3OCH_3}}{P_{CH_3OH}}}{\left(1 + K_{H_2O,DME} P_{H_2O} + K_{CH_3OH} P_{CH_3OH}{}^{0.5}\right)^4} \quad \text{(F.DME.1)}$$

Table A.6.Parameters values for the kinetic model of methanol synthesis *[6] [7]*.

k_{DME}(kmolkg^{-1} s^{-1})	A_{DME}	4328.76
	B_{DME}	2544.16
$K_{H_2O,DME}$	$A_{H_2O,DME}$	0.085
	$B_{H_2O,DME}$	42,151.98
K_{CH_3OH}(bar^{-1})	A_{CH_3OH}	0.046
	B_{CH_3OH1}	35,280.46

$$K_{eq,DME} = \exp\left(\frac{2835.2}{T} + 1.675 \ln T - 2.39 \times 10^{-4} - 13.36\right)$$

Section A.1.2

This section covers the economic and technological assumptions used in this study.

Table A.7.Raw material and utility prices.

<u>Feed</u>		
CO_2 [8]	50.81	\$/tonne
Natural gas [9]	345	\$/tonne
Demineralized water	1.06	\$/tonne
O_2 (Air cryogenics) [10]	60	\$/tonne
Catalysts	negligible	
<u>Utility</u>		
125 °C Steam	6.88	\$/GJ
175 °C Steam	7.27	\$/GJ
250 °C Steam	7.5	\$/GJ
2000 °C Fired Heater	18.75	\$/GJ
Heating Oil	12.3	\$/GJ
Cooling water	0.03	\$/m^3

Electricity	0.123	$/kWh

Table A.8. GWP of materials present in mass balance.

Material	GWP	
CO_2 [8]	-0.719	kg CO_2-eq/kg
Natural gas [9]	0.529	kg CO_2-eq/kg
O_2 (Air cryogenics) [10]	0.146	kg CO_2-eq/kg
CH_4	28	kg CO_2-eq/kg
H_2	0.233	kg CO_2-eq/kg

Table A.9. Reactor catalyst characteristics.

Reactor	Steam-,dry- and bi-reforming	Tri-reforming	Methanol	DME
Catalyst density ($kg_{cat}\,m^{-3}$)	2396.965	1562.5	1100	2141
Bed voidage	0.605	0.605	0.33	0.4
Catalyst diameter (mm)	17.4131	17.4131	6	10

Appendix 2

This appendix provides required supplementary information for the methodology applied in Chapter 4.

Section A.2.1

This section provides the kinetic equations and parameters for the kinetic models used in this study.

For kinetic equations and parameters related to the reforming and methanol synthesis section, refer to Appendix 1.A, 1.B, 1.C, 1.D, 1.E, 1.F.

Appendix 2.A

$$CH_3OH + H_2 \rightarrow CH_4 + H_2O \qquad r_1 = \frac{k_1 C_{MEOH} d_1}{(1 + K_{H20} C_{H20})} \qquad \text{(A.MTO1)}$$

$$CH_3OH \rightarrow 0.5C_2H_4 + H_2O \qquad r_2 = \frac{k_2 C_{MEOH} d_2}{(1 + K_{H20} C_{H20})} \qquad \text{(A.MTO2)}$$

$$CH_3OH \rightarrow \frac{1}{3}C_3H_6 + H_2O \qquad r_3 = \frac{k_3 C_{MEOH} d_3}{(1 + K_{H20} C_{H20})} \qquad \text{(A.MTO3)}$$

$$CH_3OH + H_2 \rightarrow \frac{1}{3}C_3H_6 + H_2O \qquad r_4 = \frac{k_4 C_{MEOH} d_4}{(1 + K_{H20} C_{H20})} \qquad \text{(A.MTO4)}$$

$$CH_3OH \rightarrow \frac{1}{4}C_4H_8 + H_2O \qquad r_5 = \frac{k_5 C_{MEOH} d_5}{(1 + K_{H20} C_{H20})} \qquad \text{(A.MTO5)}$$

$$CH_3OH \rightarrow \frac{1}{5}C_5H_{10} + H_2O \qquad r_6 = \frac{k_6 C_{MEOH} d_6}{(1 + K_{H20} C_{H20})} \qquad \text{(A.MTO6)}$$

$$CH_3OH + H_2 \rightarrow \frac{1}{2}C_2H_6 + H_2O \qquad r_7 = \frac{k_7 C_{MEOH} d_7}{(1 + K_{H20} C_{H20})} \qquad \text{(A.MTO7)}$$

$$CH_3OH \rightarrow \frac{1}{6}C_6H_{12} + H_2O \qquad r_8 = \frac{k_8 C_{MEOH} d_8}{(1 + K_{H20} C_{H20})} \qquad \text{(A.MTO8)}$$

$$CH_3OH \rightarrow CO + 2H_2 \qquad r_9 = \frac{k_9 C_{MEOH} d_9}{(1 + K_{H20} C_{H20})} \qquad \text{(A.MTO9)}$$

$$CO + H_2O \rightarrow CO_2 + H_2 \qquad r_{10} = \frac{k_9 C_{H2O} C_{CO}}{(1 + K_{H20} C_{H20})} \qquad \text{(A.MTO10)}$$

Table A.10. Parameters values for the kinetic model of methanol to olefins synthesis *[11]*.

k_1(molg^{-1} min^{-1})	A_1	7.327
	B_1	6549.8
d_1	C_1	0.06
k_2(molg^{-1} min^{-1})	A_2	11.633
	B_2	7150.0
d_2	C_2	0.14
k_3(molg^{-1} min^{-1})	A_3	9.064
	B_3	5023.5
d_3	C_3	0.21
k_4(molg^{-1} min^{-1})	A_4	9.064
	B_4	2804.2
d_4	C_4	0.20
k_5(molg^{-1} min^{-1})	A_5	5.34
	B_5	3069.2
d_5	C_5	0.24
k_6(molg^{-1} min^{-1})	A_6	0.020
	B_6	1064.8
d_6	C_6	0.27
k_7(molg^{-1} min^{-1})	A_7	−0.450
	B_7	1064.8
d_7	C_7	0.27
k_8(molg^{-1} min^{-1})	A_8	9.702
	B_8	6410.8
d_8	C_8	0.31

k_9(molg^{-1} min^{-1})	A_9	17.098
	B_9	13591.5
d_9	C_9	0.06
k_{10}(molg^{-1} min^{-1})	A_{10}	24.229
	B_{10}	14313.2

where

$$k_i = \exp\left(A_i - \frac{B_i}{T}\right),$$

$$d_i = \frac{1}{1 + 9\exp\left(2C_c - 15.6\right)} \exp\left(-C_c C_i\right)$$

where C_c is the coke content.

Section A.2.2

This section covers the economic and technological assumptions used in this study.

Table A.11.Raw material, product and utility prices.

Feed		
CO_2 [8]	50.81	$/tonne
Natural gas [9]	345	$/tonne
Demineralized water	1.06	$/tonne
O_2 (Air cryogenics) [10]	60	$/tonne
Catalysts	negligible	
Product		
Ethylene [12]	660	$/tonne
Ethane [13]	0.0475	$/ l
Propylene [13]	860	$/tonne
Propane [15]	0.156	$/ l
Utility		
125 °C Steam	6.88	$/GJ
250 °C Steam	7.5	$/GJ
2000 °C Fired Heater	18.75	$/GJ
Cooling water	0.03	$/$m^3$
Electricity	0.123	$/kWh
Refrigeration	5.88	$/GJ

Table A.12. GWP of materials present in mass balance.

Material	**GWP**	
CO_2 [8]	-0.719	kg CO_2-eq/kg
Natural gas [9]	0.529	kg CO_2-eq/kg
O_2 (Air cryogenics) [10]	0.146	kg CO_2-eq/kg
CH_4	28	kg CO_2-eq/kg
H_2	0.233	kg CO_2-eq/kg

Table A.13. Reactor catalyst characteristics.

Reactor	Steam-,dry- and bi-reforming	Tri-reforming	Methanol	MTO
Catalyst density ($kg_{cat}\,m^{-3}$)	2396.965	1562.5	1100	1220
Bed voidage	0.605	0.605	0.33	0.6
Catalyst diameter (mm)	17.4131	17.4131	6	-
Catalyst surface area ($m^2\,g^{-1}$)	-	-	-	263.55

Appendix 3

This appendix provides a breakdown of the results for Chapter 3 and Chapter 4.

Table A.14. Heating utility (GJ·t^{-1} DME) breakdown before heat integration for DME scenarios.

	SR	DR-OPEX	DR-GWP	BI-OPEX	BI-GWP	ADTRI-OPEX	ADTRI-GWP	ISOTRI-OPEX	ISOTRI-GWP
125 °C Steam	4.32201583	5.174655549	5.61037988	5.17694751	5.659134366	7.346188646	5.123683383	4.769697718	5.123683383
175 °C Steam	2.14668681	2.571013511	2.58498259	2.57131981	2.564427442	0.900974402	2.578564376	2.576244295	2.578564376
250 °C Steam	1.23470277	1.475483676	1.37500578	1.47893753	1.372605278	1.726927954	1.467792605	1.54050175	1.467792605
Heating oil	2.53103196	3.034359134	2.78533989	3.03169172	3.032783522	3.190074587	2.875843179	2.873427437	2.875843179
Natural gas	12.9571703	15.54588571	15.4310188	15.5202166	15.35984695	7.589644793	7.775604471	7.530774646	7.775604471

Table A.15. Heating utility (GJ·t^{-1} DME) breakdown after heat integration for DME scenarios.

	SR	DR-OPEX	DR-GWP	BI-OPEX	BI-GWP	ADTRI-OPEX	ADTRI-GWP	ISOTRI-OPEX	ISOTRI-GWP
Natural gas	0.44137374	0.368855824	0.43959345	0.28751467	0.4075546	1.06011882	0.745697348	2.062393369	1.738782272
Heating oil	0.08621717	0.071995965	0.07934779	0.05616261	0.091567964	0.445588456	0.275799604	0.786922723	0.643096644
125 °C Steam	0.04205896	0.035008668	0.03917068	0.02739757	0.041442678	0.241216668	0.140764497	0.421884964	0.328228085
175 °C Steam	0.07312482	0.061002205	0.07364008	0.0470414	0.077427023	0.125847776	0.247289921	0.705535539	0.576619097
250 °C Steam	0.14722531	0.122778584	0.15982654	0.09590384	0.170864623	1.026112954	0.491372359	1.306239186	1.145759133

Table A.16. Raw material costs ($\$\cdot t^{-1}$ DME) breakdown for DME scenarios.

	SR	DR-OPEX	DR-GWP	BI-OPEX	BI-GWP	ADTRI-OPEX	ADTRI-GWP	ISOTRI-OPEX	ISOTRI-GWP
Oxygen Feed	0	0	0	0	0	43.44558169	40.27296063	34.36916442	34.31907957
Make-up water	1.5462951	1.72742237	2.69697889	1.72544098	2.395222453	1.487397351	1.525956609	0.99616875	1.411550892
Steam water Feed	0.9002403	1.006779909	1.2350651	1.00562511	1.102027232	0.675064078	0.702127274	0.53129	0.653671219
Natural gas Feed	244.743465	273.2902564	320.774513	272.976787	286.221551	300.454654	297.8521047	301.8489766	295.006489
Carbon dioxide Feed	0	20.39554136	31.8634431	20.3721472	28.43119929	15.79855458	18.01685081	11.81440027	16.80204937

Table A.17. Utility costs ($\$\cdot t^{-1}$ DME) breakdown for DME scenarios before heat integration.

	SR	DR-OPEX	DR-GWP	BI-OPEX	BI-GWP	ADTRI-OPEX	ADTRI-GWP	ISOTRI-OPEX	ISOTRI-GWP
Electricity	60.4123914	72.68531959	74.85614678	72.44581136	81.67601996	75.87380383	91.6867228	77.70058419	93.43160834
Cooling water	5.621473077	6.777079132	6.005773702	6.741371507	6.588546548	6.982832096	7.610117756	7.27723805	7.47468467
Natural gas	245.4214426	295.2794216	255.2754707	293.7655713	276.1983258	127.4952253	151.8820987	152.2312217	154.7725595
Heating Oil	31.42446222	37.8084202	30.22710286	37.64367331	35.77498042	35.15419413	36.85033737	38.1037882	37.5510434
250 °C Steam	9.317329077	11.21016775	9.098692774	11.19729037	9.872787952	11.60397223	11.46824904	12.45621995	11.68650073
175 °C Steam	15.73745611	18.93455962	16.58079106	18.87088869	17.87959627	5.868377738	19.52915921	20.19222899	19.90081768
125 °C Steam	29.97544551	36.06503213	34.05602218	35.9553935	37.33974307	45.28159466	36.72331515	35.37871896	37.42219476

Table A.18. Utility costs ($\$\cdot t^{-1}$ DME) breakdown for DME scenarios after heat integration.

	SR	DR-OPEX	DR-GWP	BI-OPEX	BI-GWP	ADTRI-OPEX	ADTRI-GWP	ISOTRI-OPEX	ISOTRI-GWP
Electricity	35.86933936	77.5197	79.401	79.215	78.384	92.69	107.73	74.09	84.328
Cooling water	0.38661875	1.540220868	2.295226298	0.8649	1.0178	7.934783332	5.998335503	8.879225036	7.377571915
Natural gas	27.093	6.777079132	6.005773702	5.95	8.049	21.756	16.392	39.754	31.23
Heating Oil	3.471807654	0.957	0.913	0.763	1.0425	1.98	2.1077	5.273	4.0166
250 °C Steam	1.032705764	0.284	0.275	0.2268	0.2877	0.241216668	0.140764497	0.421884964	0.328228085
175 °C Steam	1.7404278	0.479	0.501	0.382	0.521	1.001	2.1077	5.273	4.0166
125 °C Steam	3.316100672	0.913	1.029	0.7283	1.088	7.727	3.935	9.23889	7.553

Table A.19. CAPEX costs ($\$\cdot t^{-1}$ DME) breakdown for DME scenarios before heat integration.

	SR	DR-OPEX	DR-GWP	BI-OPEX	BI-GWP	ADTRI-OPEX	ADTRI-GWP	ISOTRI-OPEX	ISOTRI-GWP
Annual capital repayments	1.4851	1.6297	1.8805	1.6236	1.8738	1.4544	1.5618	1.2642	1.489
Insurance	7.57401	8.31147	9.59055	8.28036	9.55638	7.41744	7.96518	6.44742	7.5939
Property tax	14.99951	16.45997	18.99305	16.39836	18.92538	14.68944	15.77418	12.76842	15.0389
Laboratory charges	1.4851	1.6297	1.8805	1.6236	1.8738	1.4544	1.5618	1.2642	1.489
Operating supplies	6.83146	7.49662	8.6503	7.46856	8.61948	6.69024	7.18428	5.81532	6.8494
Administration and support labour	24.80117	27.21599	31.40435	27.11412	31.29246	24.28848	26.08206	21.11214	24.8663
Plant overheads	34.30581	37.64607	43.43955	37.50516	43.28478	33.59664	36.07758	29.20302	34.3959
Annual maintenance and repair	45.14704	49.54288	57.1672	49.35744	56.96352	44.21376	47.47872	38.43168	45.2656
Operating labour and supervision	11.8808	13.0376	15.044	12.9888	14.9904	11.6352	12.4944	10.1136	11.912

Table A.20. CAPEX costs ($\$\cdot t^{-1}$ DME) breakdown for DME scenarios after heat integration.

	SR	DR-OPEX	DR-GWP	BI-OPEX	BI-GWP	ADTRI-OPEX	ADTRI-GWP	ISOTRI-OPEX	ISOTRI-GWP
Annual capital repayments	0.9768	1.0325	1.2763	0.9956	1.2718	1.6739	1.8671	1.2872	1.4279
Insurance	4.98168	5.26575	6.50913	5.07756	6.48618	8.53689	9.52221	6.56472	7.28229
Property tax	9.86568	10.42825	12.8963	10.05556	12.84518	16.90639	18.85771	13.00072	14.42179
Laboratory charges	0.9768	1.0325	1.2763	0.9956	1.2718	1.6739	1.8671	1.2872	1.4279
Operating supplies	4.49328	4.7495	5.87098	4.57976	5.85028	7.69994	8.58866	5.92112	6.56834
Administration and support labour	16.31256	17.24275	21.31421	16.62652	21.23906	27.95413	31.18057	21.49624	23.84593
Plant overheads	22.56408	23.85075	29.48253	22.99836	29.37858	38.66709	43.13001	29.73432	32.98449
Annual maintenance and repair	29.69472	31.388	38.79952	30.26624	38.66272	50.88656	56.75984	39.13088	43.40816
Operating labour and supervision	7.8144	8.26	10.2104	7.9648	10.1744	13.3912	14.9368	10.2976	11.4232

Table A.21. GWP breakdown (tCO_2-equivalent·t^{-1} DME) breakdown for DME scenarios before heat integration.

	SR	DR-OPEX	DR-GWP	BI-OPEX	BI-GWP	ADTRI-OPEX	ADTRI-GWP	ISOTRI-OPEX	ISOTRI-GWP
Electricity	0.169115497	0.203867581	0.245649127	0.202588551	0.246010111	0.214606274	0.233891161	0.203493055	0.257048385
Heating Utility	1.459842578	1.761524032	1.793712334	1.748789427	1.803386225	1.182969021	1.186049855	1.226953141	1.303478923
Oxygen	0	0	0	0	0	0.109227637	0.088258842	0.093247801	0.096997222
Purge	3.786698448	2.80236998	2.411597378	2.756399963	2.396380519	1.923263161	1.759569665	2.540379898	1.933782094
Natural gas Feed	0.274343478	0.331156753	0.329497239	0.328644322	0.329817896	0.40243662	0.370761923	0.402605565	0.40747052
Carbon dioxide Feed	0	-0.334687496	-0.448658687	-0.332148233	-0.445980421	-0.289909523	-0.286112356	-0.21558148	-0.314439924

Table A.22. GWP breakdown (tCO_2-equivalent·t^{-1} DME) breakdown for DME scenarios after heat integration.

	SR	DR-OPEX	DR-GWP	BI-OPEX	BI-GWP	ADTRI-OPEX	ADTRI-GWP	ISOTRI-OPEX	ISOTRI-GWP
Electricity	0.169115497	0.203867581	0.245649127	0.202588551	0.246010111	0.214606274	0.233891161	0.203493055	0.257048385
Heating Utility	0.05	0.041487272	0.049775024	0.032366767	0.053162165	0.183902548	0.120713517	0.335640802	0.281474145
Oxygen	0	0	0	0	0	0.109227637	0.088258842	0.093247801	0.096997222
Purge	3.786698448	2.80236998	2.411597378	2.756399963	2.396380519	1.923263161	1.759569665	2.540379898	1.933782094
Natural gas Feed	0.274343478	0.331156753	0.329497239	0.328644322	0.329817896	0.40243662	0.370761923	0.402605565	0.40747052
Carbon dioxide Feed	0	-0.334687496	-0.448658687	-0.332148233	-0.445980421	-0.289909523	-0.286112356	-0.21558148	-0.314439924

Table A.23. Material balance for DME scenarios.

		Conventional	Dry reforming		Bi-reforming		Adiabatic Tri-reforming		Isothermal Tri-reforming	
		SR	DR-OPEX	DR-GWP	BI-OPEX	BI-GWP	ADTRI-OPEX	ADTRI-GWP	ISOTRI-OPEX	ISOTRI-GWP
Input										
CO_2 Feed	$t \cdot hr^{-1}$	-	10.28	10.30	10.24	10.22	11.23	10.24	10.26	10.36
Natural gas Feed	$t \cdot hr^{-1}$	13.86	15.52	11.68	15.45	11.60	24.06	19.08	29.55	20.51
Steam water Feed	$t \cdot hr^{-1}$	17.07	19.15	15.06	19.07	14.95	16.72	15.06	17.42	15.21
Make-up water	$t \cdot hr^{-1}$	29.32	32.86	32.89	32.71	32.50	36.20	32.73	32.66	32.85
O_2 Feed	$t \cdot hr^{-1}$	-	-	-	-	-	19.02	15.26	19.90	14.11
Output										
DME	$t \cdot hr^{-1}$	20.08	20.16	15.37	20.07	15.26	22.91	20.08	31.10	22.05
H_2O	$t \cdot hr^{-1}$	20.00	22.44	18.35	22.34	18.21	20.34	18.33	20.68	18.50
CO_2	$t \cdot hr^{-1}$	1.94	1.43	3.08	1.42	3.06	10.35	9.21	10.75	9.33
CH_4	$t \cdot hr^{-1}$	0.06	0.06	0.05	0.06	0.05	0.09	0.08	0.10	0.08
H_2	$t \cdot hr^{-1}$	0.15	0.15	0.12	0.15	0.12	0.23	0.20	0.24	0.21

Table A.24. Material balance for MTO scenarios.

		Conventional	Dry reforming		Bi-reforming		Adiabatic Tri-reforming		Isothermal Tri-reforming	
		SR	DR-OPEX	DR-GWP	BI-OPEX	BI-GWP	ADTRI-OPEX	ADTRI-GWP	ISOTRI-OPEX	ISOTRI-GWP
Input										
CO_2 Feed	$t \cdot hr^{-1}$	-	9.25	9.27	9.32	9.30	9.30	9.22	9.22	9.29
Natural gas Feed	$t \cdot hr^{-1}$	9.60	7.55	7.55	9.89	7.56	39.79	19.96	30.80	36.69
Steam water Feed	$t \cdot hr^{-1}$	11.85	6.99	6.97	16.10	9.50	14.99	8.59	19.27	33.27
Make-up water	$t \cdot hr^{-1}$	66.22	40.03	39.97	40.02	39.99	40.05	40.04	40.01	40.11
O_2 Feed	$t \cdot hr^{-1}$	-	-	-	-	-	29.97	15.03	22.84	27.64
Output										
Olefins	$t \cdot hr^{-1}$	20.08	20.16	15.37	20.07	15.26	22.91	20.08	31.10	22.05
Propylene	$t \cdot hr^{-1}$	9.23	7.02	3.8	8.36	4.17	16.67	7.97	13.51	15.3
Ethylene	$t \cdot hr^{-1}$	3.24	0	1.93	3.08	2.26	9.03	4.6	7.33	9.04
Propane	$l \cdot hr^{-1}$	64.3	56.71	33.4	67.5	91.5	134.68	813.36	109.13	90.57
Ethane	$l \cdot hr^{-1}$	0.02	0.09	143.9	0.12	168.26	710.35	385.16	576.21	714.36
H_2O	$t \cdot hr^{-1}$	18.47	10.99	5.76	11.50	6.46	25.84	12.63	20.95	24.46
CO_2	$t \cdot hr^{-1}$	3.54	2.61	10.97	20.10	13.49	18.99	12.59	23.28	37.28
CH_4	$t \cdot hr^{-1}$	0.06	0.03	2.62	3.23	3.69	8.46	6.40	8.88	9.71
H_2	$t \cdot hr^{-1}$	0.14	0.08	0.03	0.05	0.03	0.08	0.06	0.08	0.09

Table A.25. Heating utility (GJ·t^{-1} olefins) breakdown before heat integration for MTO scenarios.

	SR	DR-OPEX	DR-GWP	BI-OPEX	BI-GWP	ADTRI-OPEX	ADTRI-GWP	ISOTRI-OPEX	ISOTRI-GWP
Natural gas	27.64349	25.2	30.86	26.26	32.1	20.18	27.17	27.58	32.98
250 °C Steam	15.52414	0.38	7.1	14.75	5.7	5.38	6.77	4.79	4.51
175 °C Steam	6.323585	7.58	9.3	6.01	8.85	6.3	7.46	6.57	6.83

Table A. 26. Heating utility (GJ·t^{-1} olefins) breakdown after heat integration for MTO scenarios.

	SR	DR-OPEX	DR-GWP	BI-OPEX	BI-GWP	ADTRI-OPEX	ADTRI-GWP	ISOTRI-OPEX	ISOTRI-GWP
Natural gas	1.552414	0.03	0.59	0.79	0.51	0.54	0.48	0.94	0.72
250 °C Steam	2.764349	1.76	2.56	1.42	2.85	2.02	1.93	5.43	5.26
125 °C Steam	0.632359	0.53	0.77	0.32	0.79	0.63	0.53	1.29	1.09

Table A.27. Raw material costs ($·t^{-1} olefins) breakdown for MTO scenarios.

	SR	DR-OPEX	DR-GWP	BI-OPEX	BI-GWP	ADTRI-OPEX	ADTRI-GWP	ISOTRI-OPEX	ISOTRI-GWP
Oxygen Feed	0	0	0	0	0	58.01	59.36	54.35	56.74
Make-up water	4.701017	9.11	11.16	5.59	9.95	2.49	5.09	3.07	2.63
Steam water Feed	0.839467	0.88	1.07	1.24	1.3	0.51	0.6	0.81	1.2
Natural gas Feed	300.468	418.44	512.48	336.98	456.94	601.76	615.64	572.43	583.57
Carbon dioxide Feed	0	57.94	70.96	35.55	63.27	15.82	32.36	19.52	16.72

Table A.28. Utility costs ($·t^{-1} olefins) breakdown for MTO scenarios before heat integration.

	SR	DR-OPEX	DR-GWP	BI-OPEX	BI-GWP	ADTRI-OPEX	ADTRI-GWP	ISOTRI-OPEX	ISOTRI-GWP
Electricity	130.8234	146.33	179.23	124.28	165.39	189.29	204.76	158.33	172.17
Refrigeration	78.94616	20.92	14.68	75	18.01	14.43	15.09	14.44	15.24
Cooling water	7.981049	8.22	9.81	7.58	9.71	9.73	10.78	10.01	10.94
Natural gas	276.5821	271.24	332.27	262.74	334.42	146.73	197.53	201.65	241.31
250 °C Steam	116.4311	2.82	53.28	110.6	42.77	40.35	50.75	35.96	33.83
125 °C Steam	43.50626	52.13	63.98	41.33	60.91	43.33	51.33	45.2	47.02

Table A.29. Utility costs ($\$\cdot t^{-1}$ olefins) breakdown for MTO scenarios after heat integration.

	SR	DR-OPEX	DR-GWP	BI-OPEX	BI-GWP	ADTRI-OPEX	ADTRI-GWP	ISOTRI-OPEX	ISOTRI-GWP
Electricity	130.8233709	146.3266	179.230194	124.2765	165.3857	189.2917018	204.7625	158.326103	172.1657
Refrigeration	7.894615746	2.115986	1.16834172	7.599013	1.386254	1.442981919	2.096944	1.11855306	1.574818
Cooling water	0.79810491	0.831879	0.7809811	0.768221	0.747152	0.972541163	1.497534	0.77525336	1.130985
Natural gas	11.64310643	0.196623	4.42557344	5.960519	3.793439	4.034756647	3.604444	7.07392155	5.389548
250 °C Steam	27.65820934	18.9031	27.5975435	14.15922	29.66268	14.6729186	14.02933	39.6714498	38.44829
125 °C Steam	4.350626481	3.633249	5.31422632	2.22724	5.40234	4.332551975	3.645861347	8.8916969	7.492286

Table A.30. CAPEX costs ($\$\cdot t^{-1}$ olefins) breakdown for MTO scenarios before heat integration.

	SR	DR-OPEX	DR-GWP	BI-OPEX	BI-GWP	ADTRI-OPEX	ADTRI-GWP	ISOTRI-OPEX	ISOTRI-GWP
Annual capital repayments	1.116235743	2.318	2.9161	1.882	2.615	1.032526	1.6363	1.13104	1.044
Insurance	5.692794774	11.823	14.87186	9.5968	13.337	5.26587342	8.345114	5.768284	5.3235
Property tax	11.26683307	23.4	29.4335	18.99	26.39	10.421896	16.5161	11.4162	10.54
Laboratory charges	1.116235743	2.318	2.9161	1.882	2.615	1.032526	1.6363	1.13104	1.044
Operating supplies	5.133587049	10.662	13.41098	8.6541	12.027	14.7486025	7.525367	5.201661	4.8006
Administration and support labour	18.64025751	38.71	48.6958	31.42	43.67	17.242363	27.3249	18.8874	17.43
Plant overheads	25.78067874	53.54	67.3495	43.46	60.4	23.847301	37.7921	26.1225	24.11
Annual maintenance and repair	33.93356659	70.476	88.64806	57.205	79.497	31.3887771	49.74349	34.38354	31.732
Operating labour and supervision	8.929885945	18.55	23.3284	15.05	20.92	8.2602045	13.0904	9.0483	8.351

Table A.31. CAPEX costs ($\$\cdot t^{-1}$ olefins) breakdown for MTO scenarios after heat integration.

	SR	DR-OPEX	DR-GWP	BI-OPEX	BI-GWP	ADTRI-OPEX	ADTRI-GWP	ISOTRI-OPEX	ISOTRI-GWP
Annual capital repayments	0.892988595	1.995143	2.4315957	1.678904	2.151162	0.826000448	1.40387072	0.68598342	0.711186
Insurance	4.554235819	10.17521	12.4011217	8.5624	10.97091	4.212596724	7.15973123	3.49851083	3.627046
Property tax	9.013466455	20.13816	24.5435456	16.94618	21.71296	8.337315143	14.1701045	6.92403978	7.178429
Laboratory charges	0.892928465	1.995008	2.43143197	1.678791	2.151017	0.825944829	1.40377619	0.68593723	0.711139
Operating supplies	4.10686909	9.175695	11.1829497	7.721309	9.893229	3.798790022	6.45642518	3.15484935	3.270759
Administration and support labour	14.91220601	33.31731	40.6057325	28.0308	35.9227	13.79355674	23.4435351	11.4553827	11.87625
Plant overheads	20.62454299	46.07999	56.1603478	38.77612	49.68342	19.07737888	32.4239215	15.8435333	16.42563
Annual maintenance and repair	27.14685327	60.65234	73.9205093	51.03869	65.39531	25.11041363	42.6776699	20.853896	21.62007
Operating labour and supervision	7.143908756	15.96114	19.4527656	13.43123	17.20929	6.608003586	11.2309658	5.48786737	5.689492

Table A.32. GWP breakdown (tCO_2-equivalent·t^{-1} olefins) breakdown for MTO scenarios before heat integration.

	SR	DR-OPEX	DR-GWP	BI-OPEX	BI-GWP	ADTRI-OPEX	ADTRI-GWP	ISOTRI-OPEX	ISOTRI-GWP
Purge	0.748866067	1.01	0.06	0.71	0.04	0.44	0.02	0.44	0.04
Refrigeration	0.750390474	0.46	0.14	0.71	0.17	0.14	0.14	0.14	0.14
Heating utility	2.722610718	2.62	2.69	2.59	2.55	1.28	1.63	1.49	1.6
Electricity	0.36896772	0.41	0.51	0.35	0.47	0.53	0.58	0.45	0.49
Oxygen Feed	0	0	0	0	0	0.17	0.17	0.16	0.17
Natural Gas Feed	0.425927595	0.5	0.62	0.4	0.55	0.722	0.74	0.69	0.7
Carbon dioxide Feed	0	-0.94	-1.16	-0.58	-1.03	-0.26	-0.528	-0.32	-0.27

Table A.33. GWP breakdown (tCO_2-equivalent·t^{-1} olefins) breakdown for MTO scenarios after heat integration.

	SR	DR-OPEX	DR-GWP	BI-OPEX	BI-GWP	ADTRI-OPEX	ADTRI-GWP	ISOTRI-OPEX	ISOTRI-GWP
Purge	0.7488661	1.01	0.06	0.71	0.04	0.44	0.02	0.44	0.04
Refrigeration	0.075039	0.05	0.01	0.07	0.01	0.01	0.02	0.01	0.01
Heating utility	0.2722611	0.18	0.22	0.14	0.23	0.13	0.12	0.29	0.25
Electricity	0.3689677	0.41	0.51	0.35	0.47	0.53	0.58	0.45	0.49
Oxygen Feed	0	0	0	0	0	0.17	0.17	0.16	0.17
Natural Gas Feed	0.4259276	0.5	0.62	0.4	0.55	0.722	0.74	0.69	0.7
Carbon dioxide Feed	0	-0.94	-1.16	-0.58	-1.03	-0.26	-0.528	-0.32	-0.27

Appendix 4

This appendix provides the MATLAB code used.

Figure A.1. MATLAB code for linking Aspen Plus V12 to MATLAB.

```
function Objective=Optim(variables)
global Aspen

Aspen = actxserver('Apwn.Document.38.0')
Aspen.invoke('InitFromArchive2',['File Name'])% File to be optimised
Aspen.Visible = 0;
Aspen.SuppressDialogs = 1;
variables %Show current variables
Aspen.Reinit;
Aspen.Tree.FindNode("variable 1 path").Value = variables(1);
Aspen.Tree.FindNode("variable 2 path").Value = variables(2);
...

Aspen.Engine.Run2(1) %Run the simulation.
time = 1;
Error = 0; %Error
while Aspen.Engine.IsRunning == 1
pause(0.5);
time = time+1;
if time>=1000 % Max simulation time control
Error = 1;
Aspen.Engine.Stop
end
end
if Error == 0
obj1= Aspen.Tree.FindNode("path to objective function 1 value").Value %Objective 1
obj2= Aspen.Tree.FindNode("path to objective function 2 value").Value %Objective 2
else
Objective = 2e9 %Give objective infinite value if error
end
Aspen.Close;
Aspen.Quit;
end
```

Figure A.2. MATLAB code for sensitivity analysis.

```
% Fixed base
NGBase=345
O2Base=60
CO2Base=50.81

% Inputs
NG=;
O2=;
CO2=;
TotMatcost=;
TotUticost=;
CAPEX=;

a = CAPEX*0.8; m = CAPEX; b = CAPEX*1.3; % sensitivity analysis parameter lb,nominal, ub (input) e.g. CAPEX
N = 1000000;                             % Number of samples (input)

% Values
NGcst=NGBase;
CO2cst=CO2Base;
O2cst=O2Base;

% Sensitivity analysis inputs
pd = makedist('Triangular',a,m,b);
T = random(pd,N,1);  % Create probability distribution object#
CAPEX=T % Changeto variable#


% Array creation
Cost=[];
[Cost]= (TotMatcost-NG*NGBase-CO2*CO2Base-O2*O2Base)+(NG*NGcst+CO2*CO2cst+O2*O2cst)+CAPEX+TotUticost; % Total cost
Cost=[Cost;Cost];

```

```
% Outputs
% histogram/boxplot
%figure;hist(Cost);figure;boxplot(Cost);
%mean
mCost=mean(Cost)
%SD
SDCost=std(Cost)
%quantile 5%,10% 25%,50%,75%,90%,95%
q = quantile(Cost,[0 0.05 0.1 0.25 0.50 0.75 0.9 0.95 1])
```

FigureA.3. MATLAB code for uncertainty analysis.

```
% Fixed base
NGBase=;
O2Base=;
CO2Base=;

% Inputs
NG=;
O2=;
CO2=;
TotMatcost=;
TotUticost=;
CAPEX=;

N = 1000000;            % Number of samples (input)

% Uncertainty analysis inputs

% NG
a = 0.8*NGBase; m = NGBase; b = 1.3*NGBase; % parameter lb,nominal, ub (input)
```

```
pd = makedist('Triangular',a,m,b);
T = random(pd,N,1);  % Create probability distribution object#
NGcst=T; % Change to variable#
% O2
a = 0.8*O2Base; m = O2Base; b = 1.3*O2Base; % parameter lb,nominal, ub (input)
pd = makedist('Triangular',a,m,b);
T = random(pd,N,1);  % Create probability distribution object#
O2cst=T; % Change to variable#
% CO2
a = 0.8*CO2Base; m = CO2Base; b = 1.3*CO2Base; % parameter lb,nominal, ub (input)
pd = makedist('Triangular',a,m,b);
T = random(pd,N,1);  % Create probability distribution object#
CO2cst=T; % Changeto variable#
% UTIL
a = 0.8*TotUticost; m = TotUticost; b = 1.3*TotUticost; % parameter lb,nominal, ub (input)
pd = makedist('Triangular',a,m,b);
T = random(pd,N,1);  % Create probability distribution object#
TotUticost=T; % Change to variable#
% CAPEX
a = 0.8*CAPEX; m = CAPEX; b = 1.3*CAPEX; % parameter lb,nominal, ub (input)
pd = makedist('Triangular',a,m,b);
T = random(pd,N,1);  % Create probability distribution object#
CAPEX=T % Change to variable#

% Array creation
Cost=[];
    [Cost]= (TotMatcost-(NG*NGBase+CO2*CO2Base+O2*O2Base))+(NG*NGcst+CO2*CO2cst+O2*O2cst)+CAPEX+TotUticost;
    Cost=[Cost;Cost];

% Outputs
% histogram/boxplot
%figure;hist(Cost);figure;boxplot(Cost);
%mean
mCost=round(mean(Cost),2)
%SD
SDCost=round(std(Cost),2)
```

```
%quantile 5%,10% 25%,50%,75%,90%,95%
q = quantile(Cost,[0.05 0.1 0.25 0.50 0.75 0.9 0.95])
%figure
%h = histogram(Cost, 'Normalization', 'probability');
[values, edges] = histcounts(Cost, 'Normalization', 'probability');
centers = (edges(1:end-1)+edges(2:end))/2;
figure
set(gcf,'color','w');
plot(centers, values, 'k-')
str = "Total product cost ($^.t^-^1 olefins)";
str = str +  newline + "Average: " +string (mCost) + "  Standard Deviation:"+string (SDCost)+ newline +""
xlabel(str,'FontSize',12,'FontName','Times New Roman')
ylabel('Probability','FontSize',12,'FontName','Times New Roman')
%figure
%h = histogram(Cost, 'Normalization', 'probability');
%hold on
%plot(centers, values, 'k-')
%x=0:0.001:1;
%plot(x,quantile(Cost,[x]))
```

Appendix 5

This appendix provides an example of the technical and economic assessment methodology used.

For DME DR-OPEX scenario:

Optimisation

The function Objective was developed as shown in Figure A.*4*.

Figure A.4. MATLAB code for linking Aspen Plus V12 to MATLAB for DME DR-OPEX scenario.

```
function Objective=Optim(variables)
global Aspen

Aspen = actxserver('Apwn.Document.38.0')
Aspen.invoke('InitFromArchive2',['DME.bkp'])% File to be optimised
Aspen.Visible = 0;
Aspen.SuppressDialogs = 1;
variables %Show current variables
Aspen.Reinit;
Aspen.Tree.FindNode("\Data\Blocks\HX-REFOR\Input\TEMP").Value = variables(1);
Aspen.Tree.FindNode("\Data\Blocks\HX-REFOR\Input\PRES").Value = variables(2);
Aspen.Tree.FindNode("\Data\Blocks\CMP1\Input\PRES").Value = variables(2);
Aspen.Tree.FindNode("\Data\Blocks\HX-NG\Input\TEMP").Value = variables(3);
Aspen.Tree.FindNode("\Data\Blocks\HX-NG\Input\PRES").Value = variables(4);
Aspen.Tree.FindNode("\Data\Blocks\PRE-REFO\Input\TEMP").Value = variables(5);
Aspen.Tree.FindNode("\Data\Blocks\PRE-REFO\Input\PRES").Value = variables(6);
Aspen.Tree.FindNode("\Data\Blocks\HX-DME\Input\TEMP").Value = variables(7);
Aspen.Tree.FindNode("\Data\Blocks\HX-DME\Input\PRES").Value = variables(8);
Aspen.Tree.FindNode("\Data\Blocks\PMPDME\Input\PRES").Value = variables(8);
Aspen.Tree.FindNode("\Data\Blocks\RWGSBYP\Input\FRAC\BYP").Value = variables(9);
Aspen.Tree.FindNode("\Data\Streams\NG-FEED\Input\TOTFLOW\MIXED").Value = variables(10);
Aspen.Tree.FindNode("\Data\Streams\STEAM\Input\TOTFLOW\MIXED").Value = variables(11);
Aspen.Tree.FindNode("\Data\Streams\METHPRG\Input\TOTFLOW\MIXED").Value = variables(12);...
```

```
24.
25. Aspen.Engine.Run2(1) %Run the simulation.
26. time = 1;
27. Error = 0; %Error
28. while Aspen.Engine.IsRunning == 1
29. pause(0.5);
30. time = time+1;
31. if time>=1000 % Max simulation time control
32. Error = 1;
33. Aspen.Engine.Stop
34. end
35. end
36. if Error == 0
37. TOTCSTUTIL= Aspen.Tree.FindNode("\Data\Streams\GWP\Input\TOTCSTUTIL\MIXED").Value
38. TOTMATCOST= Aspen.Tree.FindNode("\Data\Streams\GWP\Input\TOTMATCOST\MIXED").Value
39. obj1= TOTMATCOST+TOTCSTUTIL %Objective 1
40. obj2= Aspen.Tree.FindNode("\Data\Streams\GWP\Input\TOTFLOW\MIXED").Value %Objective 2
41. else
42. Objective = 2e9 %Give objective infinite value if error
43. end
44. Aspen.Close;
45. Aspen.Quit;
46. end
```

The optimisation algorithm is run on the function developed through the code shown in Figure A.5.

Figure A.5. MATLAB code for optimisation of DME DR-OPEX scenario.

```
% Pass fixed parameters to objfun
x = [1000,15,650,15,650,15,360,25,1,25,80,0.1]
lb = [800,1,250,1,350,1,160,1,0,7,10,0.01]
ub = [1000,30,650,30,650,30,360,50,1,25,80,0.1]

objfun = @(variables)Objective(x,a);


% Set nondefault solver options
options = optimoptions("patternsearch","SearchFcn","searchga",...
    "UseCompleteSearch",true,"PollMethod","MADSPositiveBasisNp1",...
    "UseCompletePoll",true);
lb = [800,1,250,1,350,1,160,1,0,7,10,0.01]
ub = [1000,30,650,30,650,30,360,50,1,25,80,0.1]
% Solve
[solution,objectiveValue] = patternsearch(objfun,x,[],[],[],[],repmat(-Inf,...
    size(x)),Inf(size(x)),[],options);

% Clear variables
clearvars objfun options
```

Technical performance indicators

DME production rate (from mass balance) = 20.08 t/hr

CO_2 Feed (from mass balance) = 10.2408 t/hr

NG Feed (from mass balance) = 15.4616 t/hr

Steam water Feed (from mass balance) = 19.076 t/hr

Make-up water Feed (from mass balance) = 32.7304 t/hr

CO_2 conversion

CO_2 Feed (from mass balance) = 10.2408 t/hr

CO_2 exit from purge (from mass balance) = 1.42142304 t/hr

CO_2 conversion = 1 - (1.421423/10.2408) = 0.8612 (86.12%)

DME conversion factor

DME production rate (from mass balance) = 20.08 t/hr

CO_2 Feed (from mass balance) = 10.2408 t/hr

DME conversion factor = 20.08/10.2408 = 1.9607 tDME/tCO_2

Economics

Purchased equipment cost (PC): through Aspen Icarus Database = 11.25M

Fixed Capital Investment = PC*5.04 = 56.7 M$

Working Capital (with 10% contingency) = PC*0.89*1.1 = 44.99 M$

CAPEX = 162.97 $/tDME

Fortran block used to calculate total material cost is provided in Figure A.*6*.

Figure A.6. Fortran block to calculate total material cost for DME DR-OPEX scenario.

```
1.  CSTCO2=CO2IN*50.81
2.  CSTNG=NGIN*345
3.  O2IN=O2IN*60
4.  CSTSTM=STMIN*1.06
5.
6.  TOTMATCOST=CSTCO2+CSTNG+O2IN+CSTSTM
```

In order to allow the transfer of the value to MATLAB, the value calculated for TOTMATCOST is transferred to the flowrate of a free stream TOTMATCOST.

Total raw material cost = 296.42 $/tDME

Fortran block used to calculate total utility cost is provided in Figure A.*7*.

Figure A.7. Fortran block to calculate total utility cost for DME DR-OPEX scenario.

```
1.  TOTCSTUTIL=TOTCST125+TOTCST250+TOTCSTNGUTIL+TOTCSTELEC+TOTCSTREFRIG
```

In order to allow the transfer of the value to MATLAB, the value calculated for TOTCSTUTIL is transferred to the flowrate of a free stream TOTMATCOST.

Total utility cost = 478.76 $/tDME

Total production cost = CAPEX + Total raw material cost +Total utility cost = 938.15 $/tDME

Global warming potential

Fortran block used to calculate GWP is provided in Figure A.*8*. The values of the GWP of the utilities are calculated within Aspen Plus and transferred to the Fortran block.

Figure A.8. Fortran block to calculate the GWP for DME DR-OPEX scenario.

```
1.  GWPCO2=CO2IN*-0.719
2.  GWPNG=NGIN*0.529
3.  GWPO2=O2IN*0.146
4.  PRGTOT=PRGCH4*28+PRGH2*0.23+PRGCO2
5.  TOTEMUTIL=TOTEM125+TOTEM250+TOTEMNG+TOTEMELEC+TOTEMREFRIG
6.  TOTEM=GWPCO2+GWPNG+GWPO2+PRGTOT+TOTEMUTIL
7.  EM=TOTEM/TOTDME
```

In order to allow the transfer of the value to MATLAB, the value calculated for EM is transferred to the flowrate of a free stream GWP.

References

[1] J. G. H. W. a. A. K. D. Zhang, "Kinetic Studies of Carbon Dioxide Reforming of Methane over Ni-Co/Al-Mg-O Bimetallic Catalyst," *Industrial & Engineering Chemistry Research* , vol. 48, pp. 677-684, 2009.

[2] J. T. a. S. A. P. Richardson, "Carbon Dioxide Reforming of Methane with Supported Rhodium," *Applied Catalysis,* vol. 61, pp. 293-309, 1990.

[3] M.-J. P. S.-C. B. K.-S. H. Y.-J. L. G. K. H.-G. P. K.-W. J. N. Park, "Modeling and optimization of the mixed reforming of methane: Maximizing CO2 utilization for non-equilibrated reaction," *Fuel,* vol. 115, pp. 357-365, 2014.

[4] C.-W. L. David L.Trimm, "The combustion of methane on platinum—alumina fibre catalysts—I: Kinetics and mechanism," *Chemical Engineering Science,* vol. 35, no. 6, pp. 1405-1413, 1980.

[5] M. J.Skrzypek, "Kinetics of methanol synthesis over commercial copper/zinc oxide/alumina catalysts," *Chemical Engineering Science,* vol. 46, no. 11, pp. 2809-2813, 1991.

[6] F. Y. H. A. S. S. M. Mollavali, "Intrinsic kinetics study of dimethyl ether synthesis from methanol on γ-Al2O3 catalysts," *Industrial Engineering Chemical Research,* vol. 47, pp. 3265-3273, 2008.

[7] M. W. B.T. Diep, "Thermodynamic equilibrium constants for the methanol-dimethyl ether-water system," *Journal of Chemical and Engineering data,* vol. 32, pp. 330-333, 1987.

[8] O. D. L. 2. R. 2. R. 1. V. 1.-F. P.-C. 3. B. 1. F. 1. A. 1. S. 3. G. 4. M. 3. a. Stefania Osk Gardarsdottir, "Comparison of Technologies for CO2 Capture from Cement Production—Part 2: Cost Analysis," *Energies,* 2019.

[9] "Natural gas prices," Our World, 01 June 2019. [Online]. Available: https://ourworldindata.org/grapher/natural-gas-prices. [Accessed 01 June 2019].

[10] J. S. G.S. Sandeep Alavandi, "Emerging and Existing Oxygen Production Technology Scan and Evaluation," Gas Technology Institute, 2018.

[11] X. Y. Y. C. L. L. Lei Ying, "A seven lumped kinetic model for industrial catalyst in DMTO process," *Chemical Engineering Research and Design,* vol. 100, pp. 179-191, 2015.

[12] statista, [Online]. Available: https://www.statista.com/statistics/1170573/price-ethylene-forecast-globally/. [Accessed 10 10 2019].

[13] barchart, [Online]. Available: https://www.barchart.com/futures/quotes/JC0X20/price-history/historical. [Accessed 10 10 2019].

[14] STATISTA, [Online]. Available: https://www.statista.com/statistics/1170576/price-propylene-forecast-globally/. [Accessed 10 10 2019].

[15] TRADING ECONOMICS, [Online]. Available: https://tradingeconomics.com/commodity/propane. [Accessed 10 10 2019].

[16] L. D. M. V. C. D. B. E. Y. Benguerba, "Modelling of methane dry reforming over Ni/Al2O3 catalyst in a fixed-bed catalytic reactor," *Reaction Kinetics, Mechanisms and Catalysis,* pp. 114, pages109–119, 2015.